UNED Escuela de Doctorado

# Tesis Doctoral

2015

# Top-down and Bottom-up Approaches to Discrete Diffusion Models

Jaime Arturo de la Torre Rodríguez

Master Universitario en Física de Sistemas Complejos

Programa de doctorado en Ciencias

Director: Dr. Pep Español Garrigós


Doctoral dissertation presented at the Doctoral School in the National University of Distance Education.

| | |
|---|---|
| Title: | Top-down and Bottom-up Approaches to Discrete Diffusion Models |
| Author: | Jaime Arturo de la Torre Rodríguez, M. Sc. in Physics of Complex Systems. |
| Director: | Dr. Pep Español Garrigós. |

Tesis doctoral presentada en la Escuela de Doctorado de la Universidad Nacional de Educación a Distancia.

| | |
|---|---|
| Título: | Acercamientos arriba-abajo y abajo-arriba para modelos de difusión discreta. |
| Autor: | Jaime Arturo de la Torre Rodríguez, Máster Universitario en Física de Sistemas Complejos. |
| Director: | Dr. Pep Español Garrigós. |

# Acknowledgments

A DISSERTATION CANNOT BE COMPLETED until you mention all the people who have helped (directly or not) to its completion. Not only scientists who contributed to make the work possible, but also people who encouraged you to keep pushing [1] and made these years a pleasant journey.

To my family, because without their support in the every-day life, from the very first moment, I would have never been here. For their patience and their love. And for being always with me in the distant.

I would like to thank to J. A. Castilla, my first Physic's teacher at high school, who discovered me the principles of Physics and their beauty. To A. Córdoba, M. C. Lemos, and J. C. García-Vázquez, from the University of Seville, who introduced me into the world of Complex Systems. I would like to show special gratitude to P. Español, my thesis supervisor, who gave me the opportunity of doing this research which ends now. Not only did he teach me physics, but he also taught me how Science should be done, and how to grow up as a scientist. This work would have never been possible without his continuous help and patiente. To A. Donev, with whom I spent three months at the New York University. Without his help I would be still waiting for the simulations to be completed. He really contributed to boost this work and I would like to recognize his effort. I would also like to thank the external reviewers who have read this dissertation for their unestimable contributions. And the proofreaders who have fixed many of the typos and grammar unconsistencies.

Also, my apreciation to the colleagues of the Department of Fundamental Physics at UNED. They treated me as one member of the team since the very first day I appeared there. To my coworkers in the different subjects I have

been teaching, because they covered me in the last stages of this dissertation. To the people from room 226 in the Faculty of Science, because they have been great coworkers whom with I spent plenty of good moments. To the gang of the cafeteria, just because all the discussions, arguments, laughs, parties, and moments of truly happiness. To the people who accompanied me during these years, from Algeciras, from Seville, and from Madrid.

To the ones that participated in some way in that last crazy week in Miraflores. To those burguers at 2am when everything else was closed. To the conversations until dawn. To those nights at the roofs of Madrid. To all of you who were there in the Coco the year 2014. To the one who was here at the beginning of this journey. To the one who stayed with me during the journey. To the one who was here at the end. To those taxi rides at dawn. To the brunches in-and-out on weekends. To the ones with whom I lived adventures times. To the one who fed me, who supported me, who encorauged me not to give up.

To Blizzard, to id Software, to LucasArts. To reddit, meneame, and twitter. To Joshua Bartlet, to Michael Scott, to John Constantine. To all the fictional characters that makes me laugh and feel alive.

To all the moments that I cannot forget and the ones that I cannot remember. For the record. Thank you. To all of you that have been part of my life in these times.

# Contents

# Listing of figures

# Abstract

This dissertation discusses the formulation of *discrete* models for diffusion of Brownian particles. We will describe the evolution of a *discrete* set of concentration variables given by the number of Brownian particles per unit volume around a given region. The discrete concentration is defined in terms of a set of basis functions localized around nodes of a mesh. These local functions describe how the number of Brownian particles contribute to each node. The evolution equation for the discrete concentration field takes the form of a Stochastic Differential Equation (SDE). One of the aim of this dissertation is the study of the continuum limit of this equation.

Two approaches will be followed in order to obtain the SDE. The first one starts from a microscopic description in terms of the position and velocities of all the particles that constitute the colloidal suspension. By using the Theory of Coarse-Graining (ToCG), we derive the equation governing the evolution of the discrete concentration field. This will be referred to as the Bottom-up approach. The second approach starts from a continuum diffusion equation that is discretized with numerical analysis techniques. This will be called the Top-down approach. Interestingly, and fortunately, both approaches lead to the same deterministic dynamics for the discrete concentration, under suitable approximations.

We will study two possibilities for the basis functions set that are used to define the discrete concentration variables. In both cases, the basis functions are defined on top of the Delaunay triangulation. The first set of basis functions is given directly by a standard finite element basis functions (a pyramid with support on the triangular mesh in $2D$). This basis set turns out to be valid for

regular grids. The second set, termed as *conjugate* finite elements, is given by a linear combination of the Delaunay finite elements. We show that this second basis functions set is superior for irregular grids and has a second order of convergence, as oposed to the finite element basis function.

The SDE for the discrete concentration variables allow us to discuss the general theme of how to introduce thermal fluctuations in a Partial Differential Equation (PDE), of which the diffusion equation is a primary example. The continuum limit of such SDE should produce a Stochastic Partial Differential Equation (SPDE). We show that for the models considered in this dissertation which are all of them in $1D$, the continuum limit exists. In general, for $D > 1$ the continuum limit of the models considered here does not exist. The coarse-graining point of view in the present dissertation sheds further light to this problem, and gives the naive physicist answer: one should be aware that the models used usually limit the cell size by physical conditions, and the existence of a continuumm limit for the selected models should not be of concern when considering thermal fluctuations.

# Resumen

Esta tesis doctoral discute la formulación de modelos *discretos* para la difusión de partículas Brownianas. Describiremos la evolución de un conjunto *discreto* de variables dado por el número de partículas Brownianas por unidad de volumen alrededor de una región. La concentración discreta se define en términos de un conjunto de funciones base localizadas alrededor de los nodos de una determinada malla. Estas funciones locales describen cómo las partículas Brownianas contribuyen a cada nodo. La ecuación de evolución para el campo de concentración discreto toma la forma de una ecuación diferencial estocástica (SDE). Uno de los propósitos de esta tesis es el estudio del límite continuo de esta ecuación.

Se seguirán dos procedimientos para obtener la ecuación diferencial estocástica. El primero de ellos comienza con una descripción microscópica en términos de las posiciones y las velocidades de todas las partículas que constituyen la suspensión coloidal. Utilizando la Teoría del *Coarse-Graining* (ToCG) obtendremos la ecuación que gobierna la evolución del campo discreto de concentraciones. A este procedimiento lo llamaremos el acercamiento abajo-arriba. El segundo procedimiento comienza con una ecuación de difusión en el espacio continuo que discretizaremos mediante técnicas de análisis numérico. Lo llamaremos acercamiento arriba-abajo. Interesante y afortunadamente, ambos acercamientos convergen a la misma dinámica determinista para la concentración discreta bajo ciertas aproximaciones.

También estudiaremos dos posibilidades para el conjunto de funciones base que serán usadas para definir las variables de concentración discreta. En ambos casos las funciones base se definen en términos de la triangulación de Delau-

nay. El primero de los conjuntos de funciones base está dado directamente por un elemento finito convencional (como, por ejemplo, una pirámide con soporte en la red triangular para el caso bidimensional). Este conjunto base es válido para redes regulares. El segundo conjunto, denominado de elementos finitos *conjugados*, está dado por una combinación lineal de los elementos finitos de Delaunay. En contraposición al conjunto formado por elementos finitos, mostraremos como este segundo conjunto de funciones base es superior en redes irregulares y tiene un orden de convergencia 2.

La ecuación diferencial estocástica para las variables de concentración discreta nos permite discutir cómo introducir fluctuaciones térmicas en una Ecuación en Derivadas Parciales (PDE), de las que la ecuación de difusión es un ejemplo paradigmático. En el límite continuo, estas ecuaciones diferenciales estocásticas deben ser equivalentes a una Ecuación Estocástica en Derivadas Parciales (SPDE). Mostraremos que para los modelos considerados en esta tesis doctoral, todos ellos en una dimensión, el límite continuo existe. En general, para $D > 1$, el límite continuo de los modelos considerados no existe. El punto de vista de la teoría del *Coarse-Graining* en esta tesis doctoral arroja algo de luz sobre este problema y aporta una respuesta física naíf: los modelos que habitualmente se usan limitan el tamaño de las celdas discretas debido a las condiciones físicas del problema y, por tanto, la existencia de un límite continuo para estos modelos no debe preocuparnos cuando consideramos fluctuaciones térmicas.

To all of you who patiently waited to its completion.

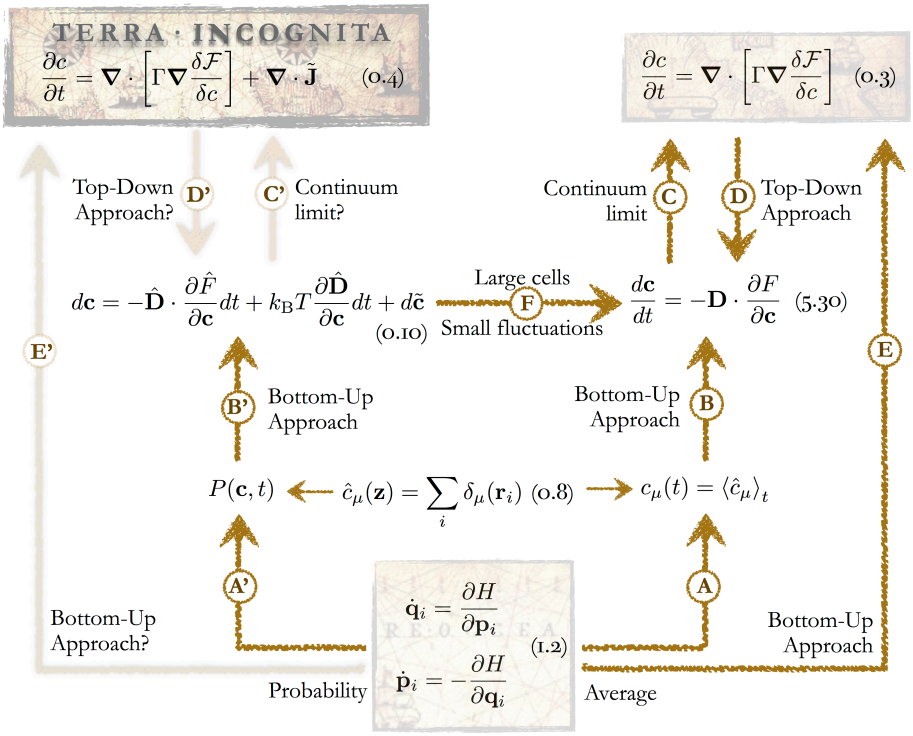
TERRA · INCOGNITA
$\frac{\partial c}{\partial t} = \nabla \cdot \left[ \Gamma \nabla \frac{\delta \mathcal{F}}{\delta c} \right] + \nabla \cdot \tilde{\mathbf{J}}$ (0.4)
$\frac{\partial c}{\partial t} = \nabla \cdot \left[ \Gamma \nabla \frac{\delta \mathcal{F}}{\delta c} \right]$ (0.3)
Top-Down Approach?
D'
C'
Continuum limit?
Continuum limit
C
D
Top-Down Approach
$d\mathbf{c} = -\hat{\mathbf{D}} \cdot \frac{\partial \hat{F}}{\partial \mathbf{c}} dt + k_B T \frac{\partial \hat{\mathbf{D}}}{\partial \mathbf{c}} dt + d\tilde{\mathbf{c}}$ (0.10)
Large cells
F
Small fluctuations
$\frac{d\mathbf{c}}{dt} = -\mathbf{D} \cdot \frac{\partial F}{\partial \mathbf{c}}$ (5.30)
E'
E
B'
Bottom-Up Approach
Bottom-Up Approach
B
$P(\mathbf{c}, t)$ $\hat{c}_\mu(\mathbf{z}) = \sum_i \delta_\mu(\mathbf{r}_i)$ (0.8) $c_\mu(t) = \langle \hat{c}_\mu \rangle_t$
A'
A
Bottom-Up Approach?
$\dot{\mathbf{q}}_i = \frac{\partial H}{\partial \mathbf{p}_i}$
$\dot{\mathbf{p}}_i = -\frac{\partial H}{\partial \mathbf{q}_i}$ (1.2)
Bottom-Up Approach
Probability
Average

# 0 Introduction

Many countries have standards for the minimum fat levels in dairy products. In the U.S., for example, whole milk has to contain at least 3.25 % fat. [2] The rest of the milk is a water-based fluid that contains dissolved carbohydrates, proteins and minerals.[3] The water-based fluid is made of particles from 1 Å to 3 Å of length, while the fatty acids that compound the butterfat are mostly triglycerides of size from 0.2 $\mu$m to 15 $\mu$m. Milk is an example of a *colloidal suspension*, a substance compounded by dispersed insoluble particles (the fatty acids) suspended throughout a fluid (the water-based fluid).[i] Other similar examples of colloids are ink or blood. Dust and fog are also colloids, made of particles immersed not into liquids but into gases.

In 1827, while studying the structure of the pollen, R. Brown found what he called a *vivid motion* in grains of pollen of about 7 $\mu$m in length immersed into

[i] In this dissertation, it is customary to name the insoluble particles as *colloidal particles*. The fluid is frequently called *solvent particles* or, simply, *solvent*. The colloidal suspension is called indistinguishably *suspension*, or *thermodynamical system*, or simply *system*.

water. [4] The motion consisted not only on a change in the relative positions of the grains (apparently erratic), but also on a change of shape of the grains. From his subsequent experiments he concluded that he found "the supposed constituent or elementary Molecules of organic bodies". Further experiments showed that those "Molecules" appeared in both organic and inorganic matter. The motion arose neither from currents in the fluid in which the molecules were immersed into, nor from the gradual evaporation of the fluid, nor from the interaction between molecules. He thought that the movement belonged to the particles themselves.

In 1905, by using the molecular-kinetic theory [5], Einstein showed that dissolved molecules and suspended particles are identical in their behavior at great dilution. [6] Einstein's Theory of Brownian Motion explains the movement of the pollen. The molecules that Brown described did not move by themselves but because of the collisions with the particles that compound the fluid (see Fig. 1). Einstein's Theory, and experiments carried out by Perrin *et al.* [7], finally established the evidence of the atomistic behavior of Nature.

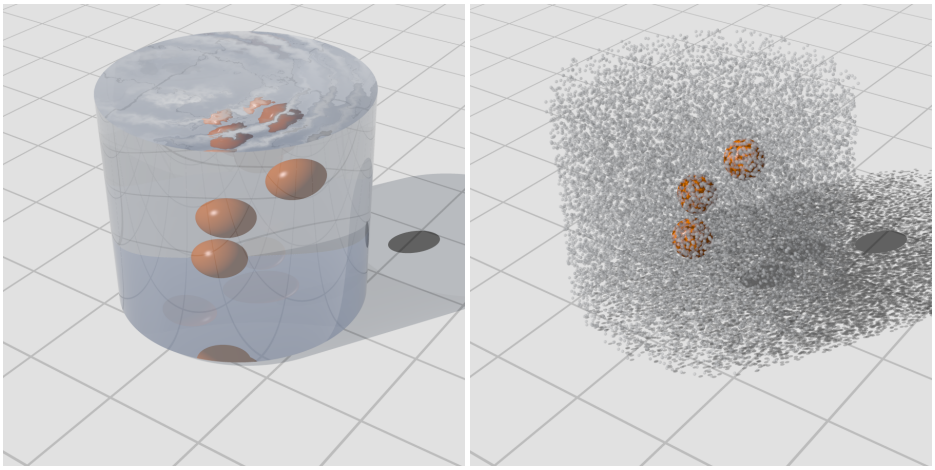

**Figure 1:** Einstein proved that dissolved molecules and suspended particles have an identical behavior for dilute suspensions. The motion of the colloidal particles (depicted in orange) is due to the collisions with the particles of the fluid.

In this atomistic vision, the laws of Classical Mechanics can be used to predict the time evolution of the constituents of a colloidal suspension[ii]. Formally, we would need to provide the initial positions and velocities of *all* the particles that constitute the suspension in order to predict the subsequent evolution of the system. [8] Let us recover the milk example. One cubic millimeter of whole milk has roughly $n \sim 10^{20}$ molecules of water and $N \sim 10^{16}$ molecules of fatty acids. There are as much as $6(n + N)$ initial conditions to be specified[iii] and $6(n + N)$ equations of motion to be solved. We shall conclude that finding a solution for the position and the velocities of all the particles at any time is unfeasible from an analytical point of view.

Discarded the analytical solution for the evolution equations, we may use a computer to obtain an approximate expression for the positions and velocities of the particles of the suspension. The basic idea is to discretize the time in small intervals (called time steps) and to evaluate the position and velocity of *every* particle at *every* time step. The procedure of performing numerical simulations to obtain approximate solutions of the evolution laws is called Molecular Dynamics (MD). Typically for a fluid, there are as many as $10^{20}$ collisions per second. [9] A realistic MD simulation of the colloidal suspension would need a time step much smaller than the typical collision time. The position of a colloidal particle evolves in a time scale of $10^{-3}$ seconds. [10] Therefore, we need more than $10^{17}$ evaluations of the position and the velocity of *every* particle in the colloidal suspension just to obtain a small displacement of a colloidal particle. To sum up, the dynamic equations of a colloidal suspension are impossible to solve, neither analytically, nor computationally, even for such a small size of one cubic millimeter.

The description given in the previous paragraph, which takes into account the positions and velocities of *all* the particles in the colloidal suspension, is called the *microscopic level of description*. This microscopic description is highly detailed, as it allows one (in principle) to recover, at any time, the exact state (position and velocity) of any particle that belongs to the colloidal suspension.

[ii] Quantum Mechanics is not required at the range of typical temperatures and masses in colloidal suspensions.

[iii] In $3D$, each particle needs three Cartesian coordinates and three components for the velocity to be fully described by Hamilton's equations.

Sometimes, we may be interested only in partial (coarser) information. For example, we may just want to know the positions of the colloidal particles at a given time, regardless of the positions or momenta of the solvent particles. Or we could be interested in the total number of colloidal particles. This would be the coarsest level of description, called the *macroscopic level of description*. Between the micro- and the macro- levels, there are many other levels of description. The retained amount of information (in the form of what degrees of freedom are retained) defines the level of description. Hereinafter, we will use indistinguishably the terms *degrees of freedom*, *relevant variables* or *coarse grained variables* to refer the set of variables retained in a given level of description. The neglected information is usually incorporated into the evolution equation for the relevant variables as dissipative and stochastic terms. The selection of the appropriate coarse-grained variables relies on the presence of a separation of time scales between the retained variables and the neglected ones.

Let us discuss in more detail the different levels of description. The microscopic level of description is also called the level of *Classical Mechanics*. It is fully deterministic and the evolution equations are given by Hamilton's equations. To describe a colloidal suspension at this level of description, we need the positions and momenta of all the particles. That is, the positions and momenta of the $n$ fluid particles (given by $\{\mathbf{q}_i, \mathbf{p}_i; i = 1, \dots, n\}$) and the corresponding positions and momenta of the $N$ colloidal particles (given by $\{\mathbf{Q}_j, \mathbf{P}_j; j = 1, \dots, N\}$). A coarser level of description is given by *Hydrodynamics*. At this level, the solvent dynamics is modeled through hydrodynamic variables, i.e., a set of fields of mass, momentum and energy $\{\rho, \mathbf{g}, e\}$ that couple to the colloidal particles $\{\mathbf{Q}_j, \mathbf{P}_j\}$. In the *Fokker-Planck* level of description [11], the state of the system is given by the set $\{\mathbf{Q}_j, \mathbf{P}_j\}$. The *Smoluchowski* level of description [12] is characterized by the positions of the colloidal particles $\{\mathbf{Q}_j\}$. The eliminated degrees of freedom takes the form of stochastic terms that appear in the evolution equation for the relevant variables. For example, the evolution equation for colloidal particles like the ones that Brown described can be written in modern terms as

$$d\mathbf{Q}_j = \sigma d\boldsymbol{\mathcal{W}}_j \,, \tag{0.1}$$

where $\sigma \triangleq \sqrt{2k_{\mathrm{B}}TD}$ is a friction coefficient[iv] and $d\boldsymbol{\mathcal{W}}_j$ is a set of independent increments of the Wiener process (i.e. random Gaussian numbers). The bigger the $\sigma$ coefficient, the larger the displacement of the colloidal particles at every time step. At high temperature, for example, it is expected that the colloidal particles move a larger distance than at low temperature. Eq. (0.1) reflects the erratic motion originally described by Brown in his experiments with grains of pollen. Fig. 2 shows the position of a colloidal particle that moves according to Eq. (0.1). It is appreciable the random displacement of the particle at every time step.

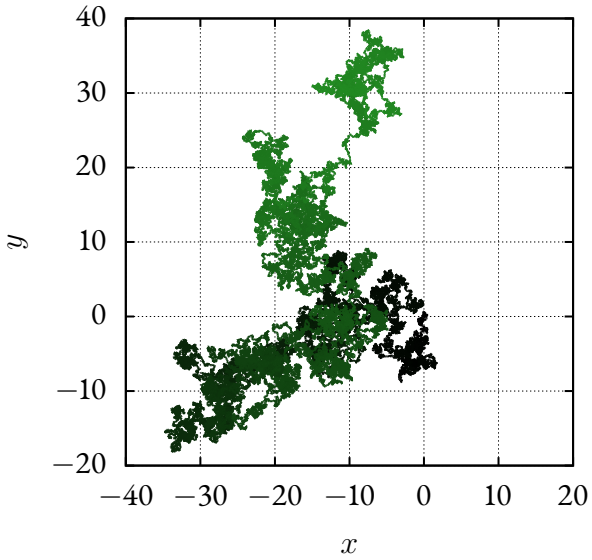


**Figure 2:** Brown described in his experiments that the grains moved erratically throughout the fluid. The picture shows a simulation of Eq. (0.1) for the motion of a colloidal particle projected in the $XY$ plane. The color gradient shows the temporal evolution from the starting position at $(0, 0, 0)$ (black) to the final position (green) after $T$ time steps.

A coarser description can be assumed if we are interested in the number of

[iv] In the friction coefficient, $k_{\mathrm{B}}$, $T$ and $D$ are some constant that we will define later on. See Appendix H for the definition of every symbol.

colloidal particles in a region of the space around a point $\mathbf{r}$. The *Fick* level of description [13] is characterized by choosing as relevant variable the concentration field $c(\mathbf{r}, t)$. At this level of description we know how many particles are in a region, but not which one is exactly where. For a dilute suspension in which there is no interaction between the colloidal particles, the evolution equation for the relevant variables takes the form of

$$\frac{\partial c}{\partial t}(\mathbf{r}, t) = D\nabla^2 c(\mathbf{r}, t)\,, \tag{0.2}$$

where $D$ is the diffusion coefficient. This equation is a particular example of the more general diffusion equation

$$\frac{\partial c}{\partial t}(\mathbf{r}, t) = \boldsymbol{\nabla} \cdot \left[\Gamma(c(\mathbf{r}, t))\boldsymbol{\nabla}\frac{\delta \mathcal{F}}{\delta c(\mathbf{r}, t)}[c(\mathbf{r}, t)]\right]\,. \tag{0.3}$$

where $\Gamma(c)$ is a mobility coefficient and $\mathcal{F}[c]$ is a free energy functional[v]. The equation (0.3) has become the focus of DDFT for the study of the dynamics of colloidal suspensions. [14–17] The partial differential equation (0.3) is paradigmatic in that it captures two essential features of a non equilibrium system. On one hand, being in divergence form, it conserves the number of particles

$$N = \int d\mathbf{r}\, c(\mathbf{r}, t) = \text{constant}\,.$$

On the other hand, it fulfills the H-theorem because the time derivative of $\mathcal{F}[c]$ is always negative provided that the mobility $\Gamma(c)$ is positive.

The non-linear diffusion equation (0.3) has been generalized in order to describe thermal fluctuations. In this case, one writes

$$\frac{\partial c}{\partial t}(\mathbf{r}, t) = \boldsymbol{\nabla} \cdot \left[\Gamma(c(\mathbf{r}, t))\boldsymbol{\nabla}\frac{\delta \mathcal{F}}{\delta c(\mathbf{r}, t)}[c(\mathbf{r}, t)]\right] + \boldsymbol{\nabla} \cdot \tilde{\mathbf{J}}(\mathbf{r}, t)\,, \tag{0.4}$$

[v] It is a matter of simple calculation to obtain, for a dilute suspension in which the free energy functional takes the form of an ideal gas, the particular Eq. (0.2) from Eq. (0.3).

where, following the pioneering work of Landau and Lifshitz [18], noise in a conservative PDE is introduced as the divergence of a random flux. The stochastic mass flux $\tilde{\mathbf{J}}(\mathbf{r},t)$ is related to the mobility as follows

$$\tilde{\mathbf{J}}(\mathbf{r},t) = \sqrt{2k_{\mathrm{B}}T\Gamma(c)}\boldsymbol{\mathcal{W}}(\mathbf{r},t)\,, \tag{0.5}$$

which obviously requires that $\Gamma(c) > 0$. Here, $\boldsymbol{\mathcal{W}}(\mathbf{r},t)$ is again a random Gaussian number[vi]. The covariance of the stochastic mass flux is proportional to the mobility coefficient, a result known as the Fluctuation Dissipation Theorem (FDT), The stochastic term (0.5) ensures that the probability distribution for the concentration field is given by

$$P^{\mathrm{eq}}[c] = \frac{1}{\mathcal{Z}}\exp\left\{-\frac{\mathcal{F}[c]}{k_{\mathrm{B}}T}\right\}\,, \tag{0.6}$$

where the partition function $\mathcal{Z}$ normalizes the probability distribution. Fluctuating equations of the form (0.4) have been considered in the Dynamic Density Functional Theory (DDFT) literature [17], where a debate on its physical meaning has arisen (see Ref. [19] for a review). Eq. (0.4) has been used for the description of phase separation [20] and critical phenomena, where it is known as Model B in the terminology of Ref. [21].

Despite the formal similarity between (0.3) and (0.4), they are very different kinds of equations, not only because one is deterministic and the other stochastic. From a purely mathematical point of view, the very existence of an equation like (0.4) or a functional like (0.6) is a delicate point, due to the fact that the term $\boldsymbol{\mathcal{W}}(\mathbf{r},t)$ and the field itself $c(\mathbf{r},t)$ are very irregular objects [22, 23]. For example, in the Ginzburg-Landau free energy model to be discussed later on in this dissertation, the partition function $\mathcal{Z}$ in Eq. (0.6) has a proper continuum limit in $1D$ but it is divergent in $D > 1$, a phenomenon known as *ultraviolet catastrophe*. In this latter case, renormalization group techniques have been used in order to recover a continuum limit. [24–28] A rigorous mathematical analysis of the renormalization of SPDEs near the critical point has been conducted recently. [29, 30] Alternatively, one may regularize the equation by introducing a physical coarse-graining length. This may take the form

[vi] Formally, a white noise in space and time.

of regularization of the noise, e.g. replacing white noise with colored noise, or regularization of nonlinear terms [31].

The non-linear diffusion equation (0.3) can be obtained from microscopic principles by using the Theory of Coarse Graining (ToCG), as shown in Ref. [32]. One chooses as relevant variable the empirical or instantaneous concentration

$$\hat{c}_{\mathbf{r}}(\mathbf{z}) \triangleq \sum_i \delta(\mathbf{r} - \mathbf{r}_i) \,, \tag{0.7}$$

where $\mathbf{z}$ is the microscopic state of the system and $\mathbf{r}_i$ is the position of the $i$-th colloidal particle. The ToCG allows to obtain an exact equation for the ensemble average $c(\mathbf{r}, t)$ of $\hat{c}_{\mathbf{r}}(\mathbf{z})$, where the average is over the solution of the microscopic Liouville equation. The resulting exact equation is non-local in space and in time. Under the assumption that the concentration evolves very slowly as compared with any other variable in the system, the exact integro-differential equation becomes an approximate local in time equation. A further approximation in which the space non-locality of the dissipative kernel is neglected, leads to Eq. (0.3). [32] The average $c(\mathbf{r}, t)$ is just the probability density of finding (any) one colloidal particle (i.e. its center of mass) at the point $\mathbf{r}$ of space. The free energy functional $\mathcal{F}[c]$ and the mobility $\Gamma(c)$ have both expressions in terms of the Hamiltonian dynamics of the underlying system.[32]

Instead of using the relevant variables (0.7) we may use the number of colloidal particles per unit volume at the mesh node $\mathbf{r}_\mu$ as input for the ToCG. These relevant variables are

$$\hat{c}_\mu(\mathbf{z}) \triangleq \sum_i \delta_\mu(\mathbf{r}_i) \,. \tag{0.8}$$

The function $\delta_\mu(\mathbf{r})$ is assumed to be localized around the mesh node $\mathbf{r}_\mu$ and, therefore, the function $\hat{c}_\mu(\mathbf{z})$ counts the number of colloidal particles that are around $\mathbf{r}_\mu$. Different functional form have been proposed for $\delta_\mu(\mathbf{r})$ in the context of the Theory of Coarse-Graining for discrete hydrodynamics, ranging from a function defined in terms of a finite number of Fourier modes [33] to the characteristic function of the Voronoi cell around $\mathbf{r}_\mu$ (divided by the volume of the cell) [34]. As we have discussed in Ref. [35], the resulting dynamic

equations are not well behaved for the Voronoi cells. Motivated by Ref. [35], in this dissertation we study different proposals for the basis function. [36, 37]

The physical justification of the SPDE (0.4) is a sensible issue. The first question to address is the physical meaning to be assigned to the symbol $c(\mathbf{r}, t)$ in Eq. (0.4). It cannot be "the probability density of finding a colloidal particle at $\mathbf{r}$ at time $t$" as in Eq. (0.3), because in (0.4) $c(\mathbf{r}, t)$ is an intrinsically stochastic field and cannot be a "fluctuating probability". Except for non-interacting Brownian walkers, Eq. (0.4) cannot be understood as an equation governing the dynamics of the spiky field (0.7), and even in that case, (0.4) can only be interpreted formally. [38] There has been a lot of debate about the meaning of fluctuating equations in the field of DDFT. [19]

Clearly, in order to speak about "fluctuations in the number of particles per unit volume" one needs to use the variables (0.8) as relevant variables and consider the time dependent probability distribution $P(\mathbf{c}, t)$ that the phase functions $\hat{c}_\mu(\mathbf{z})$ in (0.8) take particular values $\mathbf{c}$. As will be seen later, it is possible to obtain an exact integro-differential equation for $P(\mathbf{c}, t)$ with the ToCG. After the assumption of clear separation of time scales between the evolution of the concentration and any other variable in the system, one obtains the following Fokker-Planck equation that governs $P(\mathbf{c}, t)$

$$\frac{\partial P}{\partial t}(\mathbf{c}, t) = \frac{\partial}{\partial \mathbf{c}} \cdot \left\{ \hat{\mathbf{D}}(\mathbf{c}) \cdot \left[ \frac{\partial \hat{F}}{\partial \mathbf{c}}(\mathbf{c}) P(\mathbf{c}, t) + k_\mathrm{B} T \frac{\partial}{\partial \mathbf{c}} P(\mathbf{c}, t) \right] \right\} . \quad (0.9)$$

The Ito stochastic differential equation (SDE) corresponding to the FPE (0.9) is

$$d\mathbf{c}(t) = -\hat{\mathbf{D}}(\mathbf{c}) \cdot \frac{\partial \hat{F}}{\partial \mathbf{c}}(\mathbf{c}) dt + k_\mathrm{B} T \frac{\partial}{\partial \mathbf{c}} \cdot \hat{\mathbf{D}}(\mathbf{c}) dt + d\tilde{\mathbf{c}}(t) , \quad (0.10)$$

where the term proportional to $k_\mathrm{B}T$ is a reflection of the Ito stochastic interpretation of this SDE. Here $d\tilde{\mathbf{c}}$ is a linear combination of Wiener processes that has the covariance structure

$$\left\langle d\tilde{c}_\mu(t) d\tilde{c}_\nu(t) \right\rangle = 2 k_\mathrm{B} T \hat{D}_{\mu\nu}(\mathbf{c}) \delta_{\mu\nu} dt .$$

The ToCG is extremely useful as it gives the structure of the equations (0.3) and (0.10), but it remains formal because the microscopic expressions for the

objects appearing in these equations $\mathcal{F}[c]$, $\hat{F}(\mathbf{c})$ and $\Gamma(c)$, $\hat{\mathbf{D}}(\mathbf{c})$ are too complex to be evaluated explicitly. In this dissertation we will discuss different *models* for these quantities, inspired by both the Bottom-up microscopic approach and the Top-down numerical analysis approach.

The transition from the discrete world ($\hat{\mathbf{D}}(\mathbf{c})$, $\hat{F}(\mathbf{c})$) to a continuum notation ($\Gamma(c)$, $\mathcal{F}[c]$) is usual in the literature, [34, 39–41] but it is not exempt of potential problems. The natural question to ask is whether a sequence of equations like (0.10), with a given model for the free energy functional $\hat{\mathcal{F}}[c]$ has a "continuum limit" as we increase the resolution, in such a way that a proper meaning can be given to an equation like (0.4).

This dissertation is structured as follows. In Chapter 1 we review the Theory of Coarse-Graining that allows us to derive the dynamics of generic coarse-grained (CG) variables starting from the microscopic dynamics of the system. By assuming a separation of scales between the CG variables and the rest of variables, we obtain a Fokker-Planck Equation for the time evolution of the probability for the mesoscopic variables. We also obtain the equivalent Stochastic Differential Equation for the evolution of the coarse grained variables themselves.

In Chapter 2 we particularize the SDE obtained in the previous chapter to the case of a diffusion problem, obtaining Eq. (0.10). We define as coarse grained variable the discrete concentration field (0.8). The discretization definition uses a basis function $\delta_\mu(\mathbf{r})$ that is left unspecified. The two objects that enter into the SDE (the free energy function and the dissipative matrix) are written in terms of those generic basis functions. In Chapter 3 we specify as basis functions $\delta_\mu(\mathbf{r})$ the finite element $\psi_\mu(\mathbf{r})$ with support on the Delaunay triangulation. The free energy and the dissipative matrix are approximated to simple expressions in Chapter 4. With these particular models for the free energy and the dissipative matrix, we perform numerical simulations of the SDE (0.10) by using an explicit Predictor-Corrector Euler scheme. We extract static and dynamic properties for Gaussian models of the free energy with a state-dependent dissipative matrix, and compare them successfully with the direct "microscopic" simulation of independent Brownian particles.

In the INTERLUDE we suggest a generalization of the discretization procedure to the case of irregular lattices. We propose a conjugate finite element defined as a linear combination of the finite element $\psi_\mu(\mathbf{r})$ basis function. With this idea, in CHAPTER 5 we use the conjugate finite elements to discretize the deterministic and continuum diffusion equation (0.3), obtaining a deterministic discrete equation for the evolution of the coarse grained variables. We note that when the cells are large and contain many particles, fluctuations are neglected and the SDE (0.10) becomes deterministic. In this limit, the microscopically derived (0.10) and the discretization of the continuum equation coincide. In CHAPTER 6 we obtain the SDE (0.10) for discrete diffusion by using the conjugate finite element. This SDE (0.10) is a discrete version of the continuum SPDE (0.4) for diffusion. Finally, in CHAPTER 7 we consider the Ginzburg-Landau non-linear model for the free energy, and a state-independent dissipative matrix. With these models, we solve numerically the discrete SDE (0.10). We extract, static and dynamic properties, and we show numerically the existence of a continuum limit in $1D$.

# 1

# The Bottom-Up Approach

Where we review a general way to describe a system at a coarse level, starting from microscopic principles.

## 1.1. Introduction

In the Introduction we mentioned that a system can be described at different levels of description. Each level is in between two limits, the microscopic level where its state variables follow Hamilton's equations, and the macroscopic level described by Thermodynamics. All the intermediate mesoscopic levels have less information that the microscopic level but more information that the macroscopic one. The lack of information at mesoscopic levels is described in probabilistic terms leading to stochastic differential equations for the coarse-grained or relevant variables. In this chapter, we review the Theory of Coarse-Graining (ToCG) whose main objective is to derive the dynamics of the CG variables starting from the Liouville equation for the microscopic probability

density. The ToCG allows one to obtain a dynamical description of a system with much less information that the microscopic description. [10] By coarse-graining, fast variables are neglected and only slow variables remains in the description of the physical system. Two main advantages arise in the new description: i) the number of degrees of freedom is much smaller and, therefore, the computational cost for solving the evolution equations is reduced, and ii) it is possible to explore much larger time scales.

After the foundational work by Gibbs on Equilibrium Statistical Mechanics [42], Einstein[6], Onsager [43], and Kirkwood [44] made crucial contributions to Non-Equilibrium Statistical Mechanics. The Theory of Coarse-Graining, which is another name for the latter, was formulated by Green [45, 46] in its present form. Zwanzig [47] and Mori [48] used projection operators to re-derive the Theory. Many others have contributed to the formulation of coarse-graining. [49] Starting from the microscopic Liouville equation for the probability density in the phase space, projection operator techniques allow one to obtain the evolution equations for the coarse grained variables. This evolution equation is a closed integro-differential equation for the probability distribution of the CG variables. When there exists a clear separation of time scales between the eliminated variables and the coarse grained variables, relevant variables "forget" their past quickly, and their future evolution depend only on their present state. This description is said to be *Markovian*. Under the Markovian approximation, the integro-differential equation for the probability distribution becomes a Fokker-Planck Equation (FPE) for the probability distribution of CG variables. This is, in the Markovian approximation, the dynamics of CG variables is modeled as a diffusion process in the space of CG variables [45, 46].

The dynamics of a diffusion process can be described either by its FPE or by a Stochastic Differential Equation (SDE) which is mathematically equivalent to the former. Solving numerically a multidimensional FPE, which is a PDE, is in general a daunting task. However, we are usually interested in averages of functions of the relevant variables and not in the full probability distribution. In such cases, the numerical solution of the SDE is sufficient to obtain these averages, and at a much reduced cost.[50]

In this chapter, we will obtain the SDE for the CG variables starting from the

microscopic dynamics of the system. This chapter is a summary of Ref. [10].

## 1.2. The Theory of Coarse-Graining

In the present section, we will rewrite the Liouville equation for the probability density $\rho(\mathbf{z}, t)$

$$\frac{d\rho}{dt}(\mathbf{z}, t) = \frac{\partial \rho}{\partial t}(\mathbf{z}, t) + i\mathcal{L}\rho(\mathbf{z}, t) = 0\,, \tag{1.1}$$

where $\mathbf{z}$ summarizes all the positions and momenta of the system. For example, in a colloidal suspension with $n$ solvent particles and $N$ colloidal particles, $\mathbf{z} \equiv \{\mathbf{q}_i, \mathbf{p}_i, \mathbf{Q}_j, \mathbf{P}_j; i = 1, \ldots, n; j = 1, \ldots, N\}$. The operator $i\mathcal{L}$ in (1.1) is the Liouville operator defined by

$$i\mathcal{L} \triangleq -\frac{\partial H}{\partial \mathbf{z}} \mathbf{L}_0 \frac{\partial}{\partial \mathbf{z}}\,,$$

and $\mathbf{L}_0$ is the simplectic matrix given by the blocks

$$\mathbf{L}_0 = \begin{pmatrix} 0 & \mathbf{1} \\ -\mathbf{1} & 0 \end{pmatrix}\,.$$

The Liouville equation states that the volume of the phase space is conserved by a Hamiltonian dynamics. For Hamiltonian systems, the evolution equation for the $n + N$ particles is given by the Hamilton's equations [51]

$$\dot{\mathbf{z}} = \mathbf{L}_0 \frac{\partial H}{\partial \mathbf{z}}\,. \tag{1.2}$$

To solve the set of first order differential equations (1.2), we need to specify the initial condition $\mathbf{z}_0$ of all the particles that belong to the system. Formally, given a vector $\mathbf{z}_0$ with the initial state in the phase space, the solution of Hamilton's equations at time $t$ will be $\mathbf{z}(\mathbf{z}_0, t) = \mathcal{T}_t \mathbf{z}_0$, where we introduced the evolution operator $\mathcal{T}_t$ that satisfies the following properties:

$$\begin{aligned} \mathcal{T}_0 &= \mathbf{1}\,, \\ \mathcal{T}_t \mathcal{T}_{t'} &= \mathcal{T}_{t+t'}\,. \end{aligned}$$

For colloidal suspensions like the ones we mentioned in the INTRODUCTION, the number of variables that enter into (1.2) is extremely large, and we cannot solve neither analytically nor computationally the set of equations (1.2). For that reason, instead of focusing in the evolution equation for the variables in the microscopic level of description, we will focus on the evolution of CG variables at a coarser (mesoscopic) level. The CG variables are phase functions and denoted by $\mathbf{X}(\mathbf{z})$ so that $\mathbf{X}(\mathbf{z}) \equiv \left\{X_\mu(\mathbf{z}); \mu = 1 \ldots, M\right\}$, usually with $M \ll N$ [i].

The coarse grained $\mathbf{X}(\mathbf{z})$ variables evolve, as a consequence of their dependence on $\mathbf{z}$, as follows

$$\begin{aligned}\frac{d\mathbf{X}}{dt}(\mathbf{z}) &= \frac{d\mathbf{X}}{dt}(\mathcal{T}_t\mathbf{z}_0) = \frac{\partial \mathbf{X}}{\partial \mathbf{z}}(\mathcal{T}_t\mathbf{z}_0)\frac{\partial \mathbf{z}}{\partial t} = \frac{\partial \mathbf{X}}{\partial \mathbf{z}}(\mathcal{T}_t\mathbf{z}_0)\dot{\mathbf{z}} = \frac{\partial \mathbf{X}}{\partial \mathbf{z}}(\mathcal{T}_t\mathbf{z}_0)\mathbf{L}_0\frac{\partial H}{\partial \mathbf{z}} \\ &= i\mathcal{L}\mathbf{X}(\mathcal{T}_t\mathbf{z}_0) = i\mathcal{L}\mathbf{X}(\mathbf{z})\,. \end{aligned} \tag{1.3}$$

Formally, the solution of (1.3) is given by

$$\mathbf{X}(\mathcal{T}_t\mathbf{z}_0) = \exp\left\{i\mathcal{L}t\right\}\mathbf{X}(\mathbf{z}_0)\,, \tag{1.4}$$

where the exponential operator can be formally defined through its Taylor expansion

$$\exp\left\{i\mathcal{L}t\right\} \triangleq 1 + i\mathcal{L}t + \frac{1}{2!}(i\mathcal{L}t)^2 + \frac{1}{3!}(i\mathcal{L}t)^3 + \ldots\,.$$

Equation (1.4) gives the exact solution for the coarse grained variables in terms of the microscopic solution $\mathcal{T}_t\mathbf{z}_0$. Note, however, that it is not a closed form equation for $\mathbf{X}(\mathbf{z})$. From the knowledge of the initial mesoscopic value of $\mathbf{X}(\mathbf{z}_0)$ we cannot predict the evolution of $\mathbf{X}(\mathbf{z})$. Suppose that we know exactly the value of $\mathbf{x}_0 = \mathbf{X}(\mathbf{z}_0)$ at a initial time $t = 0$. There are many different $\mathbf{z}_0$ that give the same $\mathbf{x}_0$, but we do not know which is the actual initial microstate. The evolution of the coarse grained variables will be different depending on the initial unknown microstate. Therefore, knowing the initial value $\mathbf{x}_0$ of the CG variables configuration is not sufficient to predict the value

[i] Note the use of Greek indices for labeling variables at the coarse level, while the microscopic variables are labeled with Latin indices.

at later times. All what can be known about $\mathbf{X}(\mathbf{z})$ is the *probability* of finding the mesoscopic variables at a given point of the space of CG variables.

Formally, given the probability density of the microstates $\rho(\mathbf{z}, t)$, the probability of finding the mesoscopic variables $\mathbf{X}(\mathbf{z})$ at a given configuration $\mathbf{x}$ at a time $t$ is given by

$$\begin{aligned} P(\mathbf{x}, t) &= \int d\mathbf{z}\, \delta(\mathbf{X}(\mathbf{z}) - \mathbf{x}) \rho(\mathbf{z}, t) \\ &= \int d\mathbf{z}\, \delta(\mathbf{X}(\mathcal{T}_t \mathbf{z}) - \mathbf{x}) \rho(\mathbf{z}, 0)\,. \end{aligned} \tag{1.5}$$

Here, we have used that the solution of the Liouville equation is $\rho(\mathbf{z}, t) = \rho(\mathcal{T}_{-t}\mathbf{z}, 0)$ and we have made the change of variable $\mathcal{T}_t \mathbf{z} \to \mathbf{z}$. Equation (1.5) displays the time dependence of the macroscopic probability as due to the microscopic dynamics. Our aim is to obtain a closed differential equation for $P(\mathbf{x}, t)$. As a first step, though, we need to specify the initial ensemble $\rho(\mathbf{z}, 0)$ that appears in (1.5).

We assume that we know what is the mesoscopic distribution $P(\mathbf{x}, 0)$ at a time $t = 0$. This is the only available information that we have about the microscopic state. It is obvious that this is not enough to fix the functional form of the microscopic initial ensemble $\rho(\mathbf{z}, 0)$ because many different ensembles can give the same $P(\mathbf{x}, 0)$, according to Eq. (1.5). We need a method to obtain the *least biased* guess for the initial ensemble given the mesoscopic information $P(\mathbf{x}, 0)$. The Principle of Maximum Entropy introduced by Jaynes [52] is such a method and we will use it in order to find the initial ensemble $\rho(\mathbf{z}, 0)$. Jaynes [52], after the seminal work by Gibbs [42], introduced the entropy functional defined as

$$S[\rho] \triangleq -k_{\mathrm{B}} \int d\mathbf{z}\, \rho(\mathbf{z}) \ln \frac{\rho(\mathbf{z})}{\rho^{\mathrm{eq}}(\mathbf{z})}\,,$$

Here, $k_{\mathrm{B}}$ is the Boltzmann's constant and $\rho^{\mathrm{eq}}(\mathbf{z})$ is the equilibrium stationary probability density. By maximizing this functional under the restriction given in Eq. (1.5) (for $t = 0$) we obtain the least biased initial ensemble compatible with the mesoscopic information $P(\mathbf{x}, 0)$. The entropy functional that takes

into account the restriction (1.5) *and* the normalization condition is

$$\mathcal{I}[\rho(\mathbf{z})] \triangleq -k_{\mathrm{B}} \int d\mathbf{z}\, \rho(\mathbf{z},0) \ln \frac{\rho(\mathbf{z},0)}{\rho^{\mathrm{eq}}(\mathbf{z})} + \int d\mathbf{z}\, \lambda(\mathbf{z}) P(\mathbf{x},0) + \mu \int d\mathbf{z}\, P(\mathbf{x},0)\,,$$

where $\lambda(\mathbf{z})$ and $\mu$ are two Lagrange multipliers that enforce the restrictions

$$\begin{aligned} \int d\mathbf{z}\, \rho(\mathbf{z}) &= 1\,, \\ \int d\mathbf{z}\, \delta(\mathbf{X}(\mathbf{z}) - \mathbf{x}) \rho(\mathbf{z}) &= P(\mathbf{x},0)\,, \end{aligned} \tag{1.6}$$

respectively. The maximum of $\mathcal{I}[\rho(\mathbf{z})]$ will be the one that satisfies

$$\frac{\delta \mathcal{I}[(\mathbf{z})]}{\delta \rho(\mathbf{z})} = -k_{\mathrm{B}} \ln \frac{\rho(\mathbf{z})}{\rho^{\mathrm{eq}}(\mathbf{z})} - 1 + \mu + \lambda(\mathbf{X}(\mathbf{z})) = 0\,,$$

that is

$$\rho(\mathbf{z},0) = \rho^{\mathrm{eq}}(\mathbf{z}) \exp\left\{\lambda(\mathbf{X}(\mathbf{z}))\right\} \exp\left\{\mu - 1\right\}\,. \tag{1.7}$$

The constraints (1.6) imply, respectively,

$$\begin{aligned} \exp\left\{\mu - 1\right\} &= \frac{1}{\int d\mathbf{z}\, \rho^{\mathrm{eq}}(\mathbf{z}) \exp\left\{\lambda(\mathbf{X}(\mathbf{z}))\right\}}\,, \\ \exp\left\{\lambda(\mathbf{X}(\mathbf{z}))\right\} &= \frac{P(\mathbf{x},0)}{\int d\mathbf{z}\, \rho^{\mathrm{eq}}(\mathbf{z}) \delta(\mathbf{X}(\mathbf{z}) - \mathbf{x})} \frac{1}{\int d\mathbf{z}\, \rho^{\mathrm{eq}}(\mathbf{z}) \exp\left\{\lambda(\mathbf{X}(\mathbf{z}))\right\}} \\ &= \frac{P(\mathbf{x},0)}{P^{\mathrm{eq}}(\mathbf{x})} \exp\left\{1 - \mu\right\}\,, \end{aligned} \tag{1.8}$$

where we define the equilibrium measure of the region of phase space compatible with the state $\mathbf{x}$ as

$$P^{\mathrm{eq}}(\mathbf{x}) \triangleq \int d\mathbf{z}\, \delta(\mathbf{X}(\mathbf{z}) - \mathbf{x}) \rho^{\mathrm{eq}}(\mathbf{z})\,. \tag{1.9}$$

Introducing (1.7) into (1.8) we obtain the probability density at $t = 0$ as [53]

$$\rho(\mathbf{z}, 0) = \rho^{\text{eq}}(\mathbf{z}) \frac{P(\mathbf{X}(\mathbf{z}), 0)}{P^{\text{eq}}(\mathbf{X}(\mathbf{z}))} \,. \tag{1.10}$$

We now introduce a crucial quantity in the Theory of Coarse-Graining, which is the *relevant ensemble* $\overline{\rho}(\mathbf{z}, t)$. This is the least biased ensemble which is compatible with the mesoscopic probability $P(\mathbf{x}, t)$ at time $t$. This ensemble does not satisfy the Lioville equation but has the virtue to reproduce the mesoscopic information encoded in $P(\mathbf{x}, t)$. The form of the relevant ensemble is obtained again from the Principle of Maximum Entropy and it is given by

$$\begin{aligned} \overline{\rho}(\mathbf{z}, t) &\triangleq \rho^{\text{eq}}(\mathbf{z}) \frac{P(\mathbf{X}(\mathbf{z}), t)}{P^{\text{eq}}(\mathbf{X}(\mathbf{z}))} \\ &= \rho^{\text{eq}}(\mathbf{z}) \int d\mathbf{x}\, \delta(\mathbf{X}(\mathbf{z}) - \mathbf{x}) \frac{P(\mathbf{x}, t)}{P^{\text{eq}}(\mathbf{x})} \,, \end{aligned} \tag{1.11}$$

We may check that, indeed, the relevant ensemble reproduces the mesoscopic probability

$$\begin{aligned} \overline{P}(\mathbf{x}, t) &= \int d\mathbf{z}\, \delta(\mathbf{X}(\mathbf{z}) - \mathbf{x}) \overline{\rho}(\mathbf{z}, t) \\ &= \int d\mathbf{z}\, \delta(\mathbf{X}(\mathbf{z}) - \mathbf{x}) \rho^{\text{eq}}(\mathbf{z}) \frac{P(\mathbf{X}(\mathbf{z}), t)}{P^{\text{eq}}(\mathbf{X}(\mathbf{z}))} \\ &= P(\mathbf{x}, t) \,. \end{aligned} \tag{1.12}$$

Note that the relevant ensemble (1.11) can be expressed in terms of the real ensemble (solution of the Liouville equation) as follows

$$\begin{aligned} \overline{\rho}(\mathbf{z}, t) &= \rho^{\text{eq}}(\mathbf{z}) \int d\mathbf{x}\, \delta(\mathbf{X}(\mathbf{z}) - \mathbf{x}) \frac{P(\mathbf{x}, t)}{P^{\text{eq}}(\mathbf{x})} \\ &= \rho^{\text{eq}}(\mathbf{z}) \int d\mathbf{x}\, \delta(\mathbf{X}(\mathbf{z}) - \mathbf{x}) \frac{1}{P^{\text{eq}}(\mathbf{x})} \int d\mathbf{z}'\, \delta(\mathbf{X}(\mathbf{z}') - \mathbf{x}) \rho(\mathbf{z}', t) \\ &= \mathcal{P}^{\dagger} \rho(\mathbf{z}, t) \,, \end{aligned} \tag{1.13}$$

where we introduce the projection operator $\mathcal{P}^\dagger$

$$\mathcal{P}^\dagger \cdots = \rho^{\mathrm{eq}}(\mathbf{z}) \int d\mathbf{x}\, \delta(\mathbf{X}(\mathbf{z}) - \mathbf{x}) \frac{1}{P^{\mathrm{eq}}(\mathbf{x})} \int d\mathbf{z}'\, \delta(\mathbf{X}(\mathbf{z}') - \mathbf{x}) \cdots .$$

We say that the (idempotent[ii]) projection operator $\mathcal{P}^\dagger$ *projects the microscopic dynamics into the mesoscopic dynamics.* It is useful to introduce the irrelevant part of the real ensemble as the difference between the real ensemble (obeying Liouville's equation) and the relevant one, that is,

$$\delta\rho(\mathbf{z}, t) \triangleq \rho(\mathbf{z}, t) - \overline{\rho}(\mathbf{z}, t) = \mathcal{Q}^\dagger \rho(\mathbf{z}, t)\,,$$

where we define the complementary projection operator $\mathcal{Q}^\dagger \triangleq 1 - \mathcal{P}^\dagger$. Because the initial ensemble (1.10) is of the relevant form (1.11) at $t = 0$, the irrelevant part vanishes at $t = 0$

$$\delta\rho(\mathbf{z}, 0) = 0\,. \tag{1.14}$$

In what follows, we aim at obtaining a closed equation for the relevant ensemble. Because the relevant ensemble is determined by the probability $P(\mathbf{x}, t)$ (as shown in (1.11)) this will turn out to be a closed equation for $P(\mathbf{x}, t)$ itself. By noting that the projection operator does not depend on time, the derivative of the irrelevant part is obtained by directly using the Liouville equation (1.1), i.e.,

$$\frac{\partial \delta\rho}{\partial t}(\mathbf{z}, t) = -\mathcal{Q}^\dagger i\mathcal{L}\rho(\mathbf{z}, t) = -\mathcal{Q}^\dagger i\mathcal{L}\overline{\rho}(\mathbf{z}, t) - \mathcal{Q}^\dagger i\mathcal{L}\delta\rho(\mathbf{z}, t)\,. \tag{1.15}$$

The formal solution of (1.15) (as can be seen by taking the time derivative) is

$$\begin{aligned}\delta\rho(\mathbf{z}, t) = \exp\left\{-\mathcal{Q}^\dagger i\mathcal{L}t\right\} \delta\rho(\mathbf{z}, 0) \\ - \int_0^t dt'\, \exp\left\{-\mathcal{Q}^\dagger i\mathcal{L}(t - t')\right\} \mathcal{Q}^\dagger i\mathcal{L}\overline{\rho}(\mathbf{z}, t') \\ = -\int_0^t dt'\, \exp\left\{-\mathcal{Q}^\dagger i\mathcal{L}(t - t')\right\} \mathcal{Q}^\dagger i\mathcal{L}\overline{\rho}(\mathbf{z}, t')\,,\end{aligned}$$

[ii] As a projection operator $\mathcal{P}^\dagger\mathcal{P}^\dagger \equiv \mathcal{P}^\dagger$.

where we used the property (1.14) in the last step. With this information, the time derivative of the relevant distribution (1.13) is

$$\frac{\partial\overline{\rho}}{\partial t}(\mathbf{z},t) = \mathcal{P}^\dagger \frac{\partial\rho}{\partial t}(\mathbf{z},t) = -\mathcal{P}^\dagger i\mathcal{L}\rho(\mathbf{z},t)\,,$$

where we used the Liouville equation in the last step. By noting that $\mathcal{P}^\dagger + \mathcal{Q}^\dagger = 1$, the time derivative turns into

$$\begin{aligned}\frac{\partial\overline{\rho}}{\partial t}(\mathbf{z},t) &= -\mathcal{P}i\mathcal{L}(\mathcal{P}^\dagger\rho + \mathcal{Q}^\dagger\rho)\\ &= -\mathcal{P}^\dagger i\mathcal{L}\overline{\rho}(\mathbf{z},t) - \mathcal{P}^\dagger i\mathcal{L}\delta\rho(\mathbf{z},t)\\ &= -\mathcal{P}^\dagger i\mathcal{L}\overline{\rho}(\mathbf{z},t)\\ &\qquad + \int_0^t dt'\,\mathcal{P}^\dagger i\mathcal{L}\exp\left\{-\mathcal{Q}^\dagger i\mathcal{L}(t-t')\right\}\mathcal{Q}^\dagger i\mathcal{L}\overline{\rho}(\mathbf{z},t')\,.\end{aligned}$$

This is an integro-differential closed-form equation for the probability density $\overline{\rho}(\mathbf{z},t')$. The corresponding equation for the probability distribution, $P(\mathbf{x},t)$, which is equivalent to $\overline{P}(\mathbf{x},t)$ as shown in (1.12), can be obtained through (1.5) as

$$\begin{aligned}\frac{\partial P}{\partial t}(\mathbf{x},t) &= \int d\mathbf{z}\,\delta(\mathbf{X}(\mathbf{z})-\mathbf{x})\frac{\partial\overline{\rho}}{\partial t}(\mathbf{z},t)\\ &= -\int d\mathbf{z}\,\delta(\mathbf{X}(\mathbf{z})-\mathbf{x})i\mathcal{P}^\dagger\mathcal{L}\rho^{\mathrm{eq}}(\mathbf{z})\frac{P(\mathbf{X}(\mathbf{z}),t)}{P^{\mathrm{eq}}(\mathbf{X}(\mathbf{z}))}\\ &\qquad + \int_0^t dt'\int d\mathbf{z}\,\delta(\mathbf{X}(\mathbf{z})-\mathbf{x})i\mathcal{P}^\dagger\mathcal{L}\exp\left\{-i\mathcal{Q}^\dagger\mathcal{L}(t-t')\right\}\\ &\qquad\qquad \times i\mathcal{Q}^\dagger\mathcal{L}\rho^{\mathrm{eq}}(\mathbf{z})\frac{P(\mathbf{X}(\mathbf{z}),t)}{P^{\mathrm{eq}}(\mathbf{X}(\mathbf{z}))}\,,\end{aligned} \tag{1.16}$$

or, in a more convenient form,

$$\begin{aligned}\frac{\partial P}{\partial t}(\mathbf{x},t) &= \int d\mathbf{x}'\,\mathcal{V}(\mathbf{x},\mathbf{x}')\frac{P(\mathbf{x}',t)}{P^{\mathrm{eq}}(\mathbf{x}')}\\ &\qquad + \int_0^t dt'\int d\mathbf{x}'\,\mathcal{D}(\mathbf{x},\mathbf{x}',t-t')\frac{P(\mathbf{x}',t)}{P^{\mathrm{eq}}(\mathbf{x}')}\,,\end{aligned} \tag{1.17}$$

where we defined the following quantities

$$\begin{aligned}
\mathcal{V}(\mathbf{x},\mathbf{x}') &\triangleq -\int d\mathbf{z}\,\Psi_{\mathbf{x}}(\mathbf{z}) i\mathcal{P}^{\dagger}\mathcal{L}\rho^{\mathrm{eq}}(\mathbf{z})\Psi_{\mathbf{x}'}(\mathbf{z})\,,\\
\mathcal{D}(\mathbf{x},\mathbf{x}',\tau) &\triangleq \int d\mathbf{z}\,\Psi_{\mathbf{x}}(\mathbf{z}) i\mathcal{P}^{\dagger}\mathcal{L}\exp\left\{-i\mathcal{Q}^{\dagger}\mathcal{L}\tau\right\} i\mathcal{Q}^{\dagger}\mathcal{L}\rho^{\mathrm{eq}}(\mathbf{z})\Psi_{\mathbf{x}'}(\mathbf{z})\,,\\
\Psi_{\mathbf{x}}(\mathbf{z}) &\triangleq \delta(\mathbf{X}(\mathbf{z})-\mathbf{x})\,. \qquad (1.18)
\end{aligned}$$

Equation (1.17) with the definitions (1.18) is an integro-differential non local equation for $P(\mathbf{x},t)$. Let us simplify this equation by introducing a projection operator $\mathcal{P}$ (adjoint[iii] of $\mathcal{P}^{\dagger}$) in such a way that when we apply it to a function $F(\mathbf{z})$ of the mesostate, it gives

$$\mathcal{P}F(\mathbf{z}) = \langle F\rangle^{\mathbf{X}(\mathbf{z})} = \int d\mathbf{x}\ \langle F\rangle^{\mathbf{x}}\,\delta(\mathbf{X}(\mathbf{z})-\mathbf{x})\,,$$

where the conditional average is defined as

$$\langle F\rangle^{\mathbf{x}} \triangleq \frac{1}{P^{\mathrm{eq}}(\mathbf{x})}\int d\mathbf{z}\,\rho^{\mathrm{eq}}(\mathbf{z})\delta(\mathbf{X}(\mathbf{z})-\mathbf{x})F(\mathbf{z})\,.$$

The projection operator $\mathcal{P}$ (and its complementary $\mathcal{Q}\triangleq 1-\mathcal{P}$) satisfy for any functions $A$ and $B$ of the phase space:

$$\begin{aligned}
\int d\mathbf{z}\,A(\mathbf{z})\mathcal{P}B(\mathbf{z}) &= \int d\mathbf{z}\,B(\mathbf{z})\mathcal{P}^{\dagger}A(\mathbf{z})\,,\\
\int d\mathbf{z}\,A(\mathbf{z})\mathcal{Q}B(\mathbf{z}) &= \int d\mathbf{z}\,B(\mathbf{z})\mathcal{Q}^{\dagger}A(\mathbf{z})\,.
\end{aligned}$$

therefore they are adjoints of $\mathcal{P}^{\dagger}$ and $\mathcal{Q}^{\dagger}$, respectively. In addition to this, the projection over $\Psi_{\mathbf{x}}(\mathbf{z})$ obeys

$$\begin{aligned}
\mathcal{P}\Psi_{\mathbf{x}}(\mathbf{z}) &= \Psi_{\mathbf{x}}(\mathbf{z})\,,\\
\mathcal{Q}\Psi_{\mathbf{x}}(\mathbf{z}) &= 0\,.
\end{aligned}$$

[iii] Given an operator $\mathcal{A}$, its adjoint operator $\mathcal{A}^{\dagger}$ is the one that satisfies $(\mathcal{A}x,y)=(x,\mathcal{A}^{\dagger}y)$, with the usual definition of the scalar product $(A,B)\triangleq\int d\mathbf{r}\,A(\mathbf{r})B(\mathbf{r})$.

A nice property about the operators $\mathcal{P}$, $\mathcal{P}^\dagger$, $\mathcal{Q}$ and $\mathcal{Q}^\dagger$ is that they allow the equilibrium distribution to travel from left to right as follows

$$\begin{aligned}
\int d\mathbf{z}\, \rho^{\mathrm{eq}}(\mathbf{z}) A(\mathbf{z}) \mathcal{P} B(\mathbf{z}) &= \int d\mathbf{z}\, \rho^{\mathrm{eq}}(\mathbf{z}) B(\mathbf{z}) \mathcal{P} A(\mathbf{z}) \,, \\
\int d\mathbf{z}\, A(\mathbf{z}) \mathcal{Q}^\dagger \rho^{\mathrm{eq}}(\mathbf{z}) B(\mathbf{z}) &= \int d\mathbf{z}\, \rho^{\mathrm{eq}}(\mathbf{z}) A(\mathbf{z}) \mathcal{Q} B(\mathbf{z}) \,, \\
\int d\mathbf{z}\, A(\mathbf{z}) i\mathcal{L} \rho^{\mathrm{eq}}(\mathbf{z}) B(\mathbf{z}) &= \int d\mathbf{z}\, \rho^{\mathrm{eq}}(\mathbf{z}) A(\mathbf{z}) i\mathcal{L} B(\mathbf{z}) \,.
\end{aligned}$$

These relations allow us to rewrite both $\mathcal{V}(\mathbf{x}, \mathbf{x}')$ and $\mathcal{D}(\mathbf{x}, \mathbf{x}', \tau)$ as

$$\begin{aligned}
\mathcal{V}(\mathbf{x}, \mathbf{x}') &= \int d\mathbf{z}\, \rho^{\mathrm{eq}}(\mathbf{z}) \Psi_{\mathbf{x}'}(\mathbf{z}) i\mathcal{L} \Psi_{\mathbf{x}}(\mathbf{z}) \,, \\
\mathcal{D}(\mathbf{x}, \mathbf{x}', \tau) &= -\int d\mathbf{z}\, \rho^{\mathrm{eq}}(\mathbf{z}) (\mathcal{Q} i\mathcal{L} \Psi_{\mathbf{x}'}(\mathbf{z})) \exp\left\{-\mathcal{Q} i\mathcal{L} \tau\right\} (\mathcal{Q} i\mathcal{L} \Psi_{\mathbf{x}}(\mathbf{z})) \,.
\end{aligned}$$

By using the Liouville equation to the "delta" function $\Psi_{\mathbf{x}}(\mathbf{z})$

$$i\mathcal{L}\Psi_{\mathbf{x}}(\mathbf{z}) = -\frac{\partial \Psi_{\mathbf{x}}}{\partial t}(\mathbf{z}) = -\dot{X}_\mu \frac{\partial \Psi_{\mathbf{x}}}{\partial X_\mu}(\mathbf{z}) = i\mathcal{L} X_\mu \frac{\partial \Psi_{\mathbf{x}}}{\partial x_\mu}(\mathbf{z}) \,,$$

we finally have the following simplified exact expressions

$$\begin{aligned}
\mathcal{V}(\mathbf{x}, \mathbf{x}') &= -\frac{\partial}{\partial x_\mu} \delta(\mathbf{x} - \mathbf{x}') v_\mu(\mathbf{x}) P^{\mathrm{eq}}(\mathbf{x}) \,, \\
\mathcal{D}(\mathbf{x}, \mathbf{x}', \tau) &= -\frac{\partial}{\partial x_\mu} \frac{\partial}{\partial x_\nu} P^{\mathrm{eq}}(\mathbf{x}') K_{\mu\nu}(\mathbf{x}, \mathbf{x}', \tau) \,,
\end{aligned} \tag{1.19}$$

where we define a drift term $v_\mu(\mathbf{x})$ and a memory kernel $K_{\mu\nu}(\mathbf{x}, \mathbf{x}', \tau)$ as

$$\begin{aligned}
v_\mu(\mathbf{x}) &\triangleq \left\langle i\mathcal{L} X_\mu \right\rangle^{\mathbf{x}} \\
K_{\mu\nu}(\mathbf{x}, \mathbf{x}', \tau) &\triangleq \frac{1}{P^{\mathrm{eq}}(\mathbf{x}')} \int d\mathbf{z}\, \rho^{\mathrm{eq}}(\mathbf{z}) (\mathcal{Q} \Psi_{\mathbf{x}'}(\mathbf{z}) i\mathcal{L} X_\nu(\mathbf{z})) \exp\left\{-\mathcal{Q} i\mathcal{L} \tau\right\} \\
&\qquad \times (\mathcal{Q} \Psi_{\mathbf{x}}(\mathbf{z}) i\mathcal{L} X_\mu(\mathbf{z})) \,.
\end{aligned}$$

To sum up, with the previous definitions, the evolution of the probability distribution (1.16) turns into

$$\frac{\partial P}{\partial t}(\mathbf{x},t) = -\frac{\partial}{\partial x_\mu} v_\mu(\mathbf{x}) P(\mathbf{x},t) + \int_0^{t'} dt' \int d\mathbf{x}'\, P^{\mathrm{eq}}(\mathbf{x}') \frac{\partial}{\partial X_\mu} K_{\mu\nu}(\mathbf{x},\mathbf{x}',t-t') \frac{\partial}{\partial X_\nu} \frac{P(\mathbf{x}',t')}{P^{\mathrm{eq}}(\mathbf{x}')} \,. \tag{1.20}$$

This equation (1.20) is a closed equation for the probability distribution that has been obtained *without any approximation*. Both the drift term and the memory kernel are defined formally in microscopic terms as integrals over all the microstates. The explicit obtention of those quantities is usually very difficult and modelling assumptions are required.

## 1.3. Separation of time scales and the Fokker-Planck equation

The integro-differential equation (1.20) is an exact formal equation that is untractable. We discuss now the Markovian approximation that renders this equation in the form of a memoryless differential equation. The Markovian assumption considers that the relevant variables have a time scale much larger than the time scale in which the memory kernel (1.19) decays. If this is true, during the time in which the memory kernel $K_{\mu\nu}(\mathbf{x},\mathbf{x}',\tau)$ is different from zero, the relevant variables $\mathbf{x}$ have hardly changed. Therefore we may approximate

$$\int_0^t dt'\, K_{\mu\nu}(\mathbf{x},\mathbf{x}',t-t') P(\mathbf{x}',t') \approx P(\mathbf{x}',t) \int_0^\infty dt'\, K_{\mu\nu}(\mathbf{x},\mathbf{x}',t') \,.$$

Due to the quick decay of the kernel, we extend the integral up to infinite without losing generality. With this approximation, the memory kernel (1.19) becomes

$$K_{\mu\nu}(\mathbf{x},\mathbf{x}',\tau) = \left\langle (i\mathcal{L}X_\nu - \langle i\mathcal{L}X_\nu\rangle^{\mathbf{x}}) \exp\left\{\mathcal{Q}i\mathcal{L}\tau\right\} (i\mathcal{L}X_\mu - \left\langle i\mathcal{L}X_\mu\right\rangle^{\mathbf{x}}) \right\rangle^{\mathbf{x}} \times \delta(\mathbf{x}-\mathbf{x}') \,, \tag{1.21}$$

i.e., it becomes diagonal in the space of the coarse grained variables. Substitution of this kernel (1.21) into (1.20) becomes

$$\frac{\partial P}{\partial t}(\mathbf{x},t) = -\frac{\partial}{\partial X_\mu} v_\mu(\mathbf{x}) P(\mathbf{x},t) + k_\mathrm{B} \frac{\partial}{\partial X_\mu} P^\mathrm{eq}(\mathbf{x}) D_{\mu\nu}(\mathbf{x}) \frac{\partial}{\partial X_\nu} \frac{P(\mathbf{x},t)}{P^\mathrm{eq}(\mathbf{x})} , \tag{1.22}$$

where we have defined the *dissipative matrix*

$$D_{\mu\nu}(\mathbf{x}) \triangleq \frac{1}{k_\mathrm{B}} \int_0^\infty dt' \, K_{\mu\nu}(\mathbf{x}, \mathbf{x}', t') .$$

Equation (1.22) is a *Fokker-Planck equation* (FPE) for the probability density of the mesoscopic variables $\mathbf{x} = \mathbf{X}(\mathbf{z})$. Note that this equation is completely determined by objects that can be computed in principle in the microscopic scale and, therefore, allows one to obtain the mesoscopic dynamics from microscopic principles. In fact, all the quantities involved in the FPE are defined microscopicaly

$$\begin{aligned}
P^\mathrm{eq}(\mathbf{x}) &= \int d\mathbf{z} \, \rho^\mathrm{eq}(\mathbf{z}) \delta(\mathbf{X}(\mathbf{z}) - \mathbf{x}) , \\
D_{\mu\nu}(\mathbf{x}) &= \frac{1}{k_\mathrm{B}} \int_0^\infty dt' \, \left\langle (i\mathcal{L}X_\nu - v_\nu(\mathbf{x})) \exp\left\{\mathcal{Q} i\mathcal{L} t'\right\} (i\mathcal{L}X_\mu - v_\mu(\mathbf{x})) \right\rangle^\mathbf{x} , \\
v_\mu(\mathbf{x}) &= \left\langle i\mathcal{L}X_\mu \right\rangle^\mathbf{x} , \\
\langle \cdots \rangle^\mathbf{x} &= \frac{1}{P^\mathrm{eq}(\mathbf{x})} \int d\mathbf{z} \, \rho^\mathrm{eq}(\mathbf{z}) \delta(\mathbf{X}(\mathbf{z}) - \mathbf{x}) \cdots .
\end{aligned} \tag{1.23}$$

Note that the equilibrium solution of (1.22) is precisely $P^\mathrm{eq}(\mathbf{x})$ given in (1.23). The dissipative matrix is given in terms of the time integral of a time-correlation function of the random force. This is a general result refered as a *Green-Kubo relation* for the dissipative matrix (or matrix of transport coefficients) [46, 54].

It is convenient to introduce the *thermodinamic potential*

$$\phi(\mathbf{x}) \triangleq k_\mathrm{B} \ln P^\mathrm{eq}(\mathbf{x}) .$$

Here, $\phi(\mathbf{x})$ could be either an entropy $S(\mathbf{x})$ or an equivalent free energy function $F(\mathbf{x})$, depending on whether the total energy of the system is included or

not in the list of relevant variables $\mathbf{x}$. If not, then $\phi(\mathbf{x})$ is a free energy. The FPE (1.22) in terms of the free energy is

$$\frac{\partial P}{\partial t}(\mathbf{x},t) = \frac{\partial}{\partial X_\mu}\left[-v_\mu(\mathbf{x}) + D_{\mu\nu}(\mathbf{x})\frac{\partial F}{\partial X_\nu}(\mathbf{x})\right] P(\mathbf{x},t) + k_{\mathrm{B}}T\frac{\partial}{\partial X_\mu}D_{\mu\nu}(\mathbf{x})\frac{\partial P}{\partial X_\nu}(\mathbf{x},t)\,. \quad (1.24)$$

It is matter of substitution to chech that that the equilibrium probability distribution is given by the Gibbs-Boltzmann's probability distribution,

$$P^{\mathrm{eq}}(\mathbf{X}(\mathbf{z})) \propto \exp\left\{-\frac{F(\mathbf{X}(\mathbf{z}))}{k_{\mathrm{B}}T}\right\}\,, \quad (1.25)$$

## 1.4. From the FPE to a SDE

The Fokker-Planck Equation (1.24) is a closed form equation for the probability distribution of the coarse grained variables. Such equation gives the probability distribution that the relevant variables $\mathbf{X}(\mathbf{z})$ take the particular values $\mathbf{x}$. Note that the FPE (1.24) is an $M$-dimensional Partial Differential Equation. Even for a small number of relevant variables the numerical resolution of the FPE (1.24) is unpractical. Such numerical resolution requires a grid in an $M$-dimensional space, and the required number of grid points scales exponentially with $M$. However, we are usually not interested in finding the full probability distribution but, instead, require the evaluation of averages of functions of the CG variables. In this case, it is sufficient to simulate the corresponding Stochastic Differential Equation (SDE) for the evolution of the CG variables. The computational cost in this case scales linearly with the number $M$ of variables.

There is a well known relationship between the FPE (1.24) and a mathematically equivalent Stochastic Differential Equation. [50] Let us consider a stochastic vector $\mathbf{x}(t) = \{x_\mu(t); \mu = 1,\ldots,M\}$ that obeys an Ito Stochastic Differential Equation (SDE) written as

$$d\mathbf{x} = \mathbf{a}(\mathbf{x},t)dt + \mathbf{B}(\mathbf{x},t)d\boldsymbol{\mathcal{W}}(t)\,. \quad (1.26)$$

Here, $\mathbf{a}$ is a $M$-dimensional vector, $\mathbf{B}$ a $M \times M$ matrix, and $d\boldsymbol{\mathcal{W}}(t) \in \mathbb{R}^M$ is a $M$-variable vector whose $\mu$-th component is an independent increment of the Wiener process

$$d\mathcal{W}_\mu(t) \triangleq \Delta\mathcal{W}_\mu(t) = \mathcal{W}_\mu(t+dt) - \mathcal{W}_\mu(t)\,.$$

The Wiener increments are uncorrelated in the following sense

$$d\mathcal{W}_\mu(t)d\mathcal{W}_\nu(t') = \delta_{\mu\nu}dt\,.$$

As indicated in Ref. [50], the FPE mathematically identical to the SDE (1.26) is

$$\frac{\partial P}{\partial t}(\mathbf{x},t) = -\frac{\partial}{\partial X_\mu}a_\mu(\mathbf{x})P(\mathbf{x},t) + \frac{1}{2}\frac{\partial^2}{\partial X_\mu X_\nu}B_{\mu\sigma}(\mathbf{x})B^T_{\sigma\nu}(\mathbf{x})P(\mathbf{x},t)\,.$$

Note that the FPE (1.24) can be rearranged as

$$\frac{\partial P}{\partial t}(\mathbf{x},t) = -\frac{\partial}{\partial X_\mu}\left[v_\mu(\mathbf{x}) - D_{\mu\nu}(\mathbf{x})\frac{\partial F}{\partial X_\nu}(\mathbf{x}) + k_\mathrm{B}T\frac{\partial D_{\mu\nu}}{\partial X_\nu}(\mathbf{x})\right]P(\mathbf{x},t) + \frac{1}{2}\frac{\partial^2}{\partial X_\mu X_\nu}2k_\mathrm{B}TD_{\mu\nu}(\mathbf{x})P(\mathbf{x},t)\,,$$

so that we may identify

$$\begin{aligned}\mathbf{a}(\mathbf{x}) &\equiv \mathbf{v}(\mathbf{x}) - \mathbf{D}(\mathbf{x})\frac{\partial F}{\partial \mathbf{x}}(\mathbf{x}) + k_\mathrm{B}T\frac{\partial \mathbf{D}}{\partial \mathbf{x}}(\mathbf{x})\,,\\ \mathbf{B}(\mathbf{x}) &\equiv \sqrt{2k_\mathrm{B}T\mathbf{D}(\mathbf{x})}\,.\end{aligned}$$

and then the SDE equivalent to the FPE (1.24) is

$$d\mathbf{x} = \left\{\mathbf{v}(\mathbf{x}) - \mathbf{D}(\mathbf{x})\frac{\partial F}{\partial \mathbf{x}}(\mathbf{x}) + k_\mathrm{B}T\frac{\partial \mathbf{D}}{\partial \mathbf{x}}(\mathbf{x})\right\}dt + \mathbf{B}(\mathbf{x})d\boldsymbol{\mathcal{W}}(t)\,, \quad (1.27)$$

The matrix $\mathbf{B}(\mathbf{x})$ satisfies

$$\mathbf{B}(\mathbf{x})\mathbf{B}^T(\mathbf{x}) = 2k_\mathrm{B}T\mathbf{D}(\mathbf{x})\,. \quad (1.28)$$

which is the celebrated Fluctuation-Dissipation Theorem [55]. This theorem says that the amplitude of the noise is determined by the dissipation matrix. The physical meaning attributed to this theorem is that in order for the SDE to reproduce the correct Gibbs-Boltzmann equilibrium distribution (1.25) the noise and the dissipation need to be in balance, according to (1.28).

As a final remark, note that there are many different SDE that give the same FPE. All these SDE (1.26) have a matrix $\mathbf{B}$ which gives the same $\mathbf{B}\mathbf{B}^T$ product. That is, a SDE with a matrix $\mathbf{B}' = \mathbf{B}\mathbf{O}$, where $\mathbf{O}$ is an arbitrary orthogonal matrix, such that

$$\mathbf{B}'\mathbf{B}'^T = \mathbf{B}\mathbf{B}^T \,,$$

corresponds to exactly the same FPE.

## 1.5. Summary

In this chapter we have obtained two types of equations that govern the evolution of a set of generic coarse grained variables in a mesoscopic level of description. The first equation, written as a FPE (1.24), is an evolution equation for the probability of finding the CG variables in a given point of the CG space. The validity of the FPE (1.24) needs a separation of time scales between the relevant variables $\mathbf{X}(\mathbf{z})$ and the memory kernel $K_{\mu\nu}(\mathbf{x}, \mathbf{x}', \tau)$. If this assumption is fulfilled, the closed-form equation for the probability of the coarse grained variables (given in (1.20)) can be approximated by a Fokker-Planck Equation (1.24).

The second equation that we have obtained is the SDE (1.27) for the evolution of the coarse grained variables. Both the FPE (1.24) and the SDE (1.27) are equivalent equations, but the latter is more suited for numerical simulations. The SDE (1.27) allows one to obtain average values of functions of the CG variables, which is all we are interested in, usually.

This chapter has shown how to describe the evolution of a mechanical system in a coarse grained level of description, provided that there is a separation of scales between the typical time scale of the probability distribution and that of the memory kernel. This assumption is usually fulfilled in many cases, and

it will be taken for granted in the next chapters. Up to now, we set a formal mechanism to obtain the evolution equation for the coarse grained variables, but we need to specify the functional form of the dissipative matrix and the free energy.

The generic SDE (1.27) obtained in this chapter is the basis of the Bottom-Up approach to diffusion in this dissertation.

*Excursus.* The Theory of Coarse-Graining can be applied to a wide range of physical problems to obtain evolution equations for a set of relevant variables much lower than the total number of variables involved in the microscopic description. Although it does not contribute directly to the line of this dissertation, we have used the Theory of Coarse-Graining in order to understand constraints. [56] It is quite usual in Molecular Dynamics simulations to introduce constraints whenever stiff potentials leading to high frequency motions appear. Care should be taken, though, because the dynamics and the statistics of a constrained system is different from those of an unconstrained one. On the contrary, if we do not use constraints but we neglect the fast degrees of freedom by using a coarse graining procedure, we may add the eliminated degrees of freedom as thermal fluctuations. This scheme has the advantage of preserving the correct statistics. [56]

For the sake of maintaining a coherent structure in this dissertation, we have decided not to continue the work on constraints. The interested reader may find more information in Ref. [56].

# 2

# The Bottom-Up Approach for Discrete Diffusion

Where we particularize the CG variables to be a set of discrete concentration variables.

## 2.1. Introduction

In Chapter 1 we presented a general framework that allows one to obtain, from microscopic principles, the Fokker-Planck Equation (1.24) for the probability of the CG variables. We also presented the equivalent Stochastic Differential Equation for the evolution of the coarse variables themselves (1.26). The only assumption is that the CG variables are slow compared with the decay time of the random forces which are, then, modelled as white noise. In the present chapter, we will use this framework in a specific example: an infinitely dilute colloidal suspension, i.e., a system of non-interacting Brownian

particles.

The continuum hypothesis allows one to formulate coarse grained field theories. [57] However, there are many situations in which it is necessary to work with a discrete version of the continuum theory. An obvious example is when one is interested in numerical solution of the continuum equations. Another example arises whenever we need to introduce thermal fluctuations, reflecting the underlying molecular structure of the system. A popular way to introduce thermal fluctuations in a field theory is to introduce stochastic terms and transform the governing Partial Differential Equation (PDE) into a Stochastic Partial Differential Equation (SPDE). This was pioneered by Landau and Lifshitz formulation of fluctuating hydrodynamics [18]. However, we have pointed out in the INTRODUCTION that there are a number of subtleties that make preferable to work directly with a discrete theory, [58] for which all problems disappear. [59] There has been a great effort in the numerical implementation of thermal fluctuations in continuum hydrodynamics, [60–63]. The present chapter is a first step towards the introduction of thermal fluctuations in transport equations in a physically and numerically sensible ways.

Another area where discrete version of a continuum-theory is necessary appears when devising hybrids algorithms for the simulation of systems with separate length and time scales. For example, in a system there may be regions of space in which full atomic detail is necessary (like in the docking of a protein or at the tip of a crack in a brittle material) and other regions where a more coarse-grained (and cheaper) description like hydrodynamics or elasticity can be used . The coupling of different levels of description is an interesting area with intense research [64–66] and requires a good understanding of the process of coarse-graining. In this way, microscopically motivated discretizations of continuum hydrodynamics models have been proposed in the past years. [32] The coarse-graining procedure leads to thermodynamically consistent discretizations and it accommodates the presence of thermal fluctuations in a way consistent with statistical mechanics.

In this chapter, we will consider one of the simplest systems displaying transport and thermal fluctuations which is a diffusing colloidal system. In this Chapter, we will assume that the system is made of $N$ non-interacting Brownian particles floating in a quiescent fluid. In latter Chapters we will consider

models with interacting Brownian particles. We will construct a coarse-grained theory of diffusion by seeding the space with a set of $M$ nodes and defining a set of discrete concentration variables at each node. We will particularize the general expressions given in CHAPTER I to this particular selection of CG variables. The resulting coarse grained dynamics of the discrete concentration variables is given by a set of stochastic differential equations that can be understood, as we will show, as a discretization of a fluctuating diffusion equation.

## 2.2. COARSE-GRAINED VARIABLES

The bottom level of description for a colloidal system is characterized by the microscopic state $\mathbf{z} = \{\mathbf{r}_i, \mathbf{p}_i, \mathbf{R}_j, \mathbf{P}_j; i = 1, \dots, n; j = 1, \dots, N\}$, i.e. the collection of positions and momenta of the $n$ solvent particles and the $N$ Brownian particles. We choose as the top level of description one in which the coarse variables $\mathbf{X}(\mathbf{z})$ are a set of *discrete* concentration of particles variables. We seed a space of total volume $V_T$ with $M$ discrete points (nodes). The $\mu$-th node is located at $\mathbf{r}_\mu$. The discrete concentration field $c_\mu$ at a node $\mu$ is defined as the number of Brownian particles per unit volume in the region that surround that node.

Specifically,

$$\hat{c}_\mu(\mathbf{z}) \triangleq \sum_j^N \delta_\mu(\mathbf{R}_j)\,. \tag{2.1}$$

Here, $\delta_\mu(\mathbf{r})$ is a function localized around $\mathbf{r}_\mu$ that counts the number of Brownian particles per unit volume that are in the vicinity of $\mathbf{r}_\mu$. The specific functional form of $\delta_\mu(\mathbf{r})$ that describes how each Brownian particle contributes to the concentration of node $\mu$ will be left unspecified until later chapters. We will refer to the collection of all $\delta_\mu(\mathbf{r})$ as the set of basis functions. The only required property for these $\delta_\mu(\mathbf{r})$ functions is

$$\sum_\mu V_\mu \delta_\mu(\mathbf{r}) = 1\,, \tag{2.2}$$

for any $\mathbf{r}$. Here, $V_\mu$ is a volume associated to the node $\mu$, that depends on the particular definition of $\delta_\mu(\mathbf{r})$. The property (2.2) ensures that no matter the microscopic state $\mathbf{z}$, the correct number $N$ of Brownian particles in the system is conserved, that is

$$\sum_\mu V_\mu \hat{c}_\mu(\mathbf{z}) = N \,.$$

We may translate the general FPE in CHAPTER 1 to the case that the relevant variables are the concentration. If $P(\mathbf{c},t)$ is the probability of being in a specific configuration $\mathbf{c} = \left\{c_\mu; \mu = 1,\ldots,M\right\}$ at time $t$ , then it obeys the Fokker-Planck equation (1.24) [35]

$$\frac{\partial P}{\partial t}(\mathbf{c},t) = \frac{\partial}{\partial c_\mu}\left[-\hat{v}_\mu(\mathbf{c}) + \hat{D}_{\mu\nu}(\mathbf{c})\frac{\partial \hat{F}}{\partial c_\nu}(\mathbf{c})\right] P(\mathbf{c},t) + k_\mathrm{B}T\frac{\partial}{\partial c_\mu}\hat{D}_{\mu\nu}(\mathbf{c})\frac{\partial P}{\partial c_\nu}(\mathbf{c},t)\,. \quad (2.3)$$

Here repeated indices are summed over, $k_\mathrm{B}$ is the Boltzmann's constant and $T$ is a reference temperature. The explicit microscopic terms of (2.3) are defined in (1.23)

$$\begin{aligned}
\hat{F}(\mathbf{c}) &= k_\mathrm{B}T \ln P^\mathrm{eq}(\mathbf{c})\,,\\
P^\mathrm{eq}(\mathbf{c}) &= \int d\mathbf{z}\,\rho^\mathrm{eq}(\mathbf{z})\delta(\hat{\mathbf{c}}(\mathbf{z}) - \mathbf{c})\,,\\
\hat{D}_{\mu\nu}(\mathbf{c}) &= \frac{1}{k_\mathrm{B}T}\int_0^\infty dt'\,\left\langle (i\mathcal{L}c_\nu - v_\nu)\exp\left\{\mathcal{Q}i\mathcal{L}t'\right\}(i\mathcal{L}c_\mu - v_\mu)\right\rangle^{\mathbf{c}}\,,\\
\hat{v}_\mu(\mathbf{c}) &= \left\langle i\mathcal{L}\hat{c}_\mu(\mathbf{z})\right\rangle^{\mathbf{c}}\,,\\
\langle\cdots\rangle^{\mathbf{c}} &= \frac{1}{P^\mathrm{eq}(\mathbf{c})}\int d\mathbf{z}\,\rho^\mathrm{eq}(\mathbf{z})\delta(\hat{\mathbf{c}}(\mathbf{z}) - \mathbf{c})\cdots\,.
\end{aligned} \quad (2.4)$$

Let us discuss in detail the structure of the above objects. The the drift term $\hat{v}_\mu(\mathbf{c})$ and the dissipative matrix $\hat{\mathbf{D}}(\mathbf{c})$ require the time derivative of the discrete concentration $\hat{c}_\mu(\mathbf{z})$, given by $i\mathcal{L}\hat{c}_\mu(\mathbf{z})$. With the definition of the dis-

crete concentration (2.1) we have[i]

$$i\mathcal{L}\hat{c}_\mu(\mathbf{z}) = i\mathcal{L}\sum_i \delta_\mu(\mathbf{r}_i) = \sum_i \mathbf{v}_i \nabla\delta_\mu(\mathbf{r}_i)\,, \tag{2.5}$$

where $\mathbf{v}_i = \dot{\mathbf{r}}_i$. Then, Eq. (2.5) can be written as

$$\begin{aligned} i\mathcal{L}\hat{c}_\mu(\mathbf{z}) &= \int d\mathbf{r} \sum_i \delta(\mathbf{r}-\mathbf{r}_i)\mathbf{v}_i\nabla\delta_\mu(\mathbf{r}) \\ &= \int d\mathbf{r}\, \hat{J}_\mathbf{r}(\mathbf{z})\nabla\delta_\mu(\mathbf{r})\,, \end{aligned} \tag{2.6}$$

where we defined the current

$$\hat{J}_\mathbf{r}(\mathbf{z}) \triangleq \sum_i \delta(\mathbf{r}-\mathbf{r}_i)\mathbf{v}_i\,. \tag{2.7}$$

### 2.2.1. The drift term, $\hat{v}_\mu(\mathbf{c})$

The drift term $\hat{v}_\mu(\mathbf{c})$ is

$$\begin{aligned} \hat{v}_\mu(\mathbf{c}) &= \left\langle i\mathcal{L}\hat{c}_\mu(\mathbf{z})\right\rangle^\mathbf{c} \\ &= \frac{1}{P^\mathrm{eq}(\mathbf{c})}\int d\mathbf{z}\,\rho^\mathrm{eq}(\mathbf{z})\prod_\sigma \delta(\hat{c}_\sigma(\mathbf{z})-c_\sigma) i\mathcal{L}\hat{c}_\mu(\mathbf{z})\,. \end{aligned}$$

Note that, for a canonical probability distribution, we have

$$\rho^\mathrm{eq}(\mathbf{z}) \propto \exp\left\{-\beta H(\mathbf{z})\right\}\,,$$

with $\beta \triangleq (k_\mathrm{B}T)^{-1}$ and the Hamiltonian $H(\mathbf{z})$ quadratic on $\mathbf{p}_i$. The time derivative of $\hat{c}_\mu(\mathbf{z})$ is proportional to $\mathbf{p}_i = \mathbf{v}_i/m_i$ (as indicated in (2.5)). Therefore, the integral over $d\mathbf{p}_i$ vanishes, and

$$\hat{v}_\mu(\mathbf{c}) = 0\,.$$

We conclude that, in this level of description, the drift term is zero.

[i] In the following, for notational convenience, we will rename $\mathbf{R}_j \to \mathbf{r}_i$ and $\mathbf{P}_j \to \mathbf{p}_i$ the position and momentum of the $i$-th colloidal particle.

### 2.2.2. The free energy, $\hat{F}(\mathbf{c})$

Before considering the free energy, let us consider first the equilibrium probability distribution. It is a matter of simple substitution to check that any distribution function of the form

$$P^{\mathrm{eq}}(\mathbf{c}) = \frac{1}{\mathcal{Z}}\phi\left(\sum_{\mu} V_\mu c_\mu\right) e^{-\beta\hat{F}(\mathbf{c})}\,, \tag{2.8}$$

with $\mathcal{Z}$ the suitable normalization, is a stationary solution of the FPE (2.3). In principle, $\phi(\cdots)$ is an *arbitrary* function. Its meaning, though, is obtained by looking at the probability that the system has exactly $N$ Brownian particles, that is

$$\begin{aligned} P^{\mathrm{eq}}(N) &= \int d\mathbf{c}\,\delta\left(N - \sum_{\mu} V_\mu c_\mu\right) P^{\mathrm{eq}}(\mathbf{c}) \\ &= \phi(N)\frac{1}{\mathcal{Z}}\int d\mathbf{c}\,\delta\left(N - \sum_{\mu} V_\mu c_\mu\right) e^{-\beta\hat{F}(\mathbf{c})}\,, \end{aligned}$$

so that

$$\phi(N) = \frac{\mathcal{Z}P^{\mathrm{eq}}(N)}{\int d\mathbf{c}\,\delta\left(N - \sum_{\mu} V_\mu c_\mu\right) e^{-\beta\hat{F}(\mathbf{c})}}\,.$$

If we know that we have exactly $N_0$ particles, then $P^{\mathrm{eq}}(N) = \delta(N - N_0)$. By substituting in (2.8) we obtain

$$\begin{aligned} P^{\mathrm{eq}}(\mathbf{c}) &= \frac{P^{\mathrm{eq}}(N)}{\int d\mathbf{c}\,\delta\left(N - \sum_{\mu} V_\mu c_\mu\right) e^{-\beta\hat{F}(\mathbf{c})}} e^{-\beta\hat{F}(\mathbf{c})} \\ &= \frac{\delta(N - N_0)}{\int d\mathbf{c}\,\delta\left(N - \sum_{\mu} V_\mu c_\mu\right) e^{-\beta\hat{F}(\mathbf{c})}} e^{-\beta F(\mathbf{c})} \\ &= \frac{1}{\mathcal{Z}}\delta\left(\sum_{\mu} V_\mu c_\mu - N_0\right) e^{-\beta\hat{F}(\mathbf{c})}\,. \end{aligned}$$

The presence of the Dirac delta function reflects the fact that the probability is different from zero only for those discrete fields that give precisely $N$ particles in the system. The free energy $\hat{F}(\mathbf{c})$, defined up to arbitrary functions of the total number of particles, is obtained directly as

$$\hat{F}(\mathbf{c}) = k_{\mathrm{B}}T \ln P^{\mathrm{eq}}(\mathbf{c}) \, .$$

In principle, the equilibrium distribution function could be computed from the microscopic expression (2.4) as

$$P^{\mathrm{eq}}(\mathbf{c}) = \frac{1}{\mathcal{Z}} \int d\mathbf{z} \, \rho^{\mathrm{eq}}(\mathbf{z}) \prod_{\mu=1}^{M} \delta\left(\hat{c}_\mu(\mathbf{z}) - c_\mu\right) \, , \tag{2.9}$$

where $\rho^{\mathrm{eq}}(\mathbf{z})$ is the equilibrium distribution of the Brownian particles. For an infinitely diluted suspension, i.e., non interacting Brownian particles, in a periodic box of volume $V_T$ in the absence of external fields, the equilibrium probability distribution is homogeneous in space, and by normalization it is given by

$$\rho^{\mathrm{eq}}(\mathbf{z}) = \frac{1}{V_T^N} \, .$$

Therefore,

$$P^{\mathrm{eq}}(\mathbf{c}) = \frac{1}{\mathcal{Z}} \int d\mathbf{z} \, \frac{1}{V_T^N} \prod_{\mu} \delta\left(\hat{c}_\mu(\mathbf{z}) - c_\mu\right) \, . \tag{2.10}$$

In this expressions, the solvent degrees of freedom are integrated out. Note that the calculation of the integral (2.10), which is a purely geometrical object, is extremely involved.

### 2.2.3. The dissipative matrix, $\hat{\mathbf{D}}(\mathbf{c})$

Let us consider now the dissipative matrix

$$\begin{aligned}\hat{D}_{\mu\nu}(\mathbf{c}) &= \frac{1}{k_{\mathrm{B}}T}\int_0^\infty dt\,\frac{1}{P^{\mathrm{eq}}(\mathbf{c})} \\ &\qquad\times\int d\mathbf{z}\,\rho^{\mathrm{eq}}(\mathbf{z})\prod_\sigma \delta(\hat{c}_\sigma(\mathbf{z})-c_\sigma) i\mathcal{L}\hat{c}_\nu(\mathbf{z}) e^{\mathcal{Q}i\mathcal{L}t} i\mathcal{L}\hat{c}_\mu(\mathbf{z}) \\ &= \frac{1}{k_{\mathrm{B}}T}\int_0^\infty dt\,\frac{1}{P^{\mathrm{eq}}(\mathbf{c})} \\ &\qquad\times\int d\mathbf{z}\,\rho^{\mathrm{eq}}(\mathbf{z})\prod_\sigma \delta(\hat{c}_\sigma(\mathbf{z})-c_\sigma) i\mathcal{L}\hat{c}_\nu(\mathbf{z}) i\mathcal{L}\hat{c}_\mu(\mathcal{T}_t\mathbf{z})\,.\end{aligned}$$

We use the definition (2.6) so that

$$\begin{aligned}\hat{D}_{\mu\nu}(\mathbf{c}) &= \frac{1}{k_{\mathrm{B}}T}\int_0^\infty dt\,\frac{1}{P^{\mathrm{eq}}(\mathbf{c})}\int d\mathbf{z}\,\rho^{\mathrm{eq}}(\mathbf{z})\prod_\sigma \delta(\hat{c}_\sigma(\mathbf{z})-c_\sigma) \\ &\qquad\times\int d\mathbf{r}\,J_{\mathbf{r}}(\mathbf{z})\nabla\delta_\nu(\mathbf{r})\int d\mathbf{r}'\,J_{\mathbf{r}'}(\mathcal{T}_t\mathbf{z})\nabla\delta_\mu(\mathbf{r}') \\ &= \frac{1}{k_{\mathrm{B}}T}\int d\mathbf{r}\int d\mathbf{r}'\,\nabla\delta_\nu(\mathbf{r})\nabla\delta_\mu(\mathbf{r}') \\ &\quad\times\int_0^\infty dt\,\frac{1}{P^{\mathrm{eq}}(\mathbf{c})}\int d\mathbf{z}\,\rho^{\mathrm{eq}}(\mathbf{z})\prod_\sigma \delta(\hat{c}_\sigma(\mathbf{z})-c_\sigma) J_{\mathbf{r}}(\mathbf{z})J_{\mathbf{r}'}(\mathcal{T}_t\mathbf{z}) \\ &= \frac{1}{k_{\mathrm{B}}T}\int d\mathbf{r}\int d\mathbf{r}'\,\nabla\delta_\nu(\mathbf{r})\nabla\delta_\mu(\mathbf{r}')\int_0^\infty dt\,\left\langle J_{\mathbf{r}}(\mathbf{z})J_{\mathbf{r}'}(\mathcal{T}_t\mathbf{z})\right\rangle^{\mathbf{c}}\,.\end{aligned} \tag{2.11}$$

The calculation of the dissipative matrix boils down to the calculation of the time integral of the conditional average of the current (2.7). This conditional average is difficult to compute in general, and we will need to take some approximations. We will assume that the positions of the Brownian particles evolve in a much slower scale than the velocities, so that during the time in which the correlation of the currents is different from zero, we may approxi-

mate the current (2.7) as

$$J_{\mathbf{r}}(t) = \sum_i \mathbf{v}_i(t)\delta(\mathbf{r} - \mathbf{r}_i(t)) \simeq \sum_i \mathbf{v}_i(t)\delta(\mathbf{r} - \mathbf{r}_i)\,.$$

For the times $t$ for which the correlation is different from zero the conditional average becomes

$$\begin{aligned}\langle J_{\mathbf{r}}(\mathbf{z}) J_{\mathbf{r}'}(\mathcal{T}_t\mathbf{z})\rangle^{\mathbf{c}} &= \left\langle \left(\sum_i \mathbf{v}_i\delta(\mathbf{r} - \mathbf{r}_i)\right)\left(\sum_j \mathbf{v}_j(t)\delta(\mathbf{r}' - \mathbf{r}_j)\right)\right\rangle^{\mathbf{c}} \\ &= \sum_i \langle \mathbf{v}_i\delta(\mathbf{r} - \mathbf{r}_i)\mathbf{v}_i(t)\delta(\mathbf{r}' - \mathbf{r}_i)\rangle^{\mathbf{c}} \\ &\qquad + \sum_{i\neq j} \langle \mathbf{v}_i\delta(\mathbf{r} - \mathbf{r}_i)\mathbf{v}_j(t)\delta(\mathbf{r}' - \mathbf{r}_j)\rangle^{\mathbf{c}}\,. \quad (2.12)\end{aligned}$$

In (2.12), the last term on the right hand side is the correlation between the velocity of the $i$-th particle in $\mathbf{r}$ with the velocity of the $j$-th particle in $\mathbf{r}'$. For a dilute solution, these particles are at large distances and this term can be neglected as compared with the first term on the right hand side of (2.12). Under this approximation we have

$$\langle J_{\mathbf{r}}(\mathbf{z}) J_{\mathbf{r}'}(\mathcal{T}_t\mathbf{z})\rangle^{\mathbf{c}} \simeq \sum_i \langle \mathbf{v}_i\mathbf{v}_i(t)\delta(\mathbf{r} - \mathbf{r}_i)\rangle^{\mathbf{c}}\,\delta(\mathbf{r} - \mathbf{r}')\,.$$

A second approximation, closely related to the assumed separation of time scales of positions and velocities, is the following decoupling approximation between positions and velocities

$$\langle J_{\mathbf{r}}(\mathbf{z}) J_{\mathbf{r}'}(\mathcal{T}_t\mathbf{z})\rangle^{\mathbf{c}} \simeq \sum_i \langle \mathbf{v}_i\mathbf{v}_i(t)\rangle^{\mathbf{c}}\,\langle\delta(\mathbf{r} - \mathbf{r}_i)\rangle^{\mathbf{c}}\,\delta(\mathbf{r} - \mathbf{r}')\,. \quad (2.13)$$

By inserting (2.13) in (2.11) we finally have

$$\hat{D}_{\mu\nu}(\mathbf{c}) \simeq \frac{1}{k_{\mathrm{B}}T} \int d\mathbf{r} \int d\mathbf{r}' \, \nabla\delta_\nu(\mathbf{r}) \nabla\delta_\mu(\mathbf{r}') \delta(\mathbf{r}-\mathbf{r}') \left\langle \sum_i \delta(\mathbf{r}-\mathbf{r}_i) \right\rangle^{\mathbf{c}} \times \int_0^\infty dt \, \langle \mathbf{v}_i \mathbf{v}_i(t) \rangle^{\mathbf{c}}$$

$$= \frac{D}{k_{\mathrm{B}}T} \int d\mathbf{r} \, \nabla\delta_\nu(\mathbf{r}) \nabla\delta_\mu(\mathbf{r}) \, \langle \hat{c}_{\mathbf{r}} \rangle^{\mathbf{c}} \, , \tag{2.14}$$

where we defined the diffusion coeffient in terms of a Green-Kubo expression

$$D \triangleq \int_0^\infty dt \, \langle \mathbf{v}_i \mathbf{v}_i(t) \rangle^{\mathbf{c}} \, ,$$

and the conditional expectation of the concentration field is

$$\langle \hat{c}_{\mathbf{r}} \rangle^{\mathbf{c}} \triangleq \left\langle \sum_i \delta(\mathbf{r}-\mathbf{r}_i) \right\rangle^{\mathbf{c}} \, .$$

The conditional expectation of the concentration field, $\langle \hat{c}_{\mathbf{r}} \rangle^{\mathbf{c}}$, is given in terms of an integral over the phase space and it is difficult to compute explicitly. In the following, we will suppose the diffusion coefficient $D$ as a constant.

## 2.3. The stochastic differential equation

The connection between the FPE and its equivalent SDE was already obtained in Chapter 1. For the present case of the FPE given in Eq. (2.3) the corresponding SDE is

$$dc_\mu(t) = -\hat{D}_{\mu\nu}(\mathbf{c}) \frac{\partial \hat{F}}{\partial c_\nu}(\mathbf{c}) dt + k_{\mathrm{B}}T \frac{\partial \hat{D}_{\mu\nu}}{\partial c_\nu}(\mathbf{c}) dt + d\tilde{c}_\mu(t) \, , \tag{2.15}$$

where $d\tilde{c}_\mu(t) \triangleq B_{\mu\sigma}(\mathbf{c}) dW_\sigma(t)$ is a linear combination of independent increments of the Wiener process, that fulfills the Fluctuation-Dissipation Theorem (FDT)

$$B_{\mu\sigma}(\mathbf{c}) B_{\nu\sigma}(\mathbf{c}) = 2k_{\mathrm{B}}T \hat{D}_{\mu\nu}(\mathbf{c}) \, ,$$

or, in a more informal way,

$$\frac{d\tilde{c}_\mu d\tilde{c}_\nu}{2k_{\mathrm{B}}Tdt} = \hat{D}_{\mu\nu}(\mathbf{c})\,. \tag{2.16}$$

The resulting Eq. (2.15) can be solved numerically if we know exactly how to compute the free energy $\hat{F}(\mathbf{c})$ and the dissipative matrix $\hat{D}(\mathbf{c})$. Note that the noise term $d\tilde{\mathbf{c}}$ can be determined directly through the dissipative matrix.

## 2.4. Summary

In this chapter we have obtained the SDE governing the discrete concentration variables $\hat{c}_\mu(\mathbf{z})$ defined in (2.1). The coarse grained variables are written with a general discretization basis $\delta_\mu(\mathbf{r})$. The basis function will be left unspecified until next chapters. Here, we just considered the basis function $\delta_\mu(\mathbf{r})$ as a function localized around $\mathbf{r}_\mu$, that counts how many Brownian particles are per unit volume in a region around $\mathbf{r}_\mu$. The resulting SDE (2.15) is completely general. The two elements that enter into the SDE (2.15) are the free energy $\hat{F}(\mathbf{c})$ (given by (2.10)), and the dissipative matrix $\hat{\mathbf{D}}(\mathbf{c})$ (given by (2.14)). The definitions of those blocks are general and valid for *any* basis function $\delta_\mu(\mathbf{r})$.

The assumptions under which the SDE is valid are the following. First, we have assumed that there is a separation of time scales in the dynamics of the solvent particles and in the dynamics of concentration variables. We expect that the number of particles in a region changes only due to the fact that particles enter or leave the region through its boundary. Therefore, the larger the region the slower will be the dynamics of the concentration variable. The second assumption considers an infinitely diluted colloidal suspension. In this case, there is no correlation between the velocities of different Brownian particles. Furthermore, the equilibrium probability distribution is just a homogeneous distribution where the positions for all the Brownian particles are equally probable. The third and last assumption is the separation of scales between the velocity of a Brownian particle and its position. This is expected to be true if the Brownian particle is sufficiently large in such a way that the time in which it diffuses its own radius is much larger than the time in which the velocity decays due to the collisions with the solvent.

# 3

# The Bottom-Up Approach for Discrete Diffusion with Finite Elements. Theory

Where we specify the basis functions $\delta_\mu(\mathbf{r})$ to be finite elements defined on the Delaunay triangulation.

## 3.1. Introduction

The SDE (2.15) is a discrete equation for the evolution of the discrete concentration variables $\hat{c}_\mu(\mathbf{z})$ defined in (2.1). The concentration variables depend on the specific form for the basis function $\delta_\mu(\mathbf{r})$. Also, the discrete free energy (defined through the equilibrium probability distribution (2.10)) and the dissipative matrix (2.14) depend on the particular functional form of the basis function.

The basis function $\delta_\mu(\mathbf{r})$ tell us how the Brownian particle $i$ contributes to the concentration in node $\mu$. There are of course many different possibilities to assign particles to nodes. For example, we might consider that a particle contributes only to the concentration of the node nearest to the position of that particle. In that way, a particle contributes *only* to no more than one node. This assignment corresponds to the so called *Voronoi construction*. The Voronoi construction is defined as follows. Given a domain $x \in \mathbb{R}^N$, and a set of points $\mathbf{r}_\mu \subset x$, a Voronoi cell $e_\nu$ (whose center is located at $\mathbf{r}_\nu$) is the set of all the points in $x$ that are closer to $\mathbf{r}_\nu$ than to any other point $\mathbf{r}_{\nu' \neq \nu}$. Fig. 3.1 shows, for a regular $2D$ lattice, a Voronoi cell (orange) surrounded by its six neighbors cells (green). Note that there is no overlapping between neighbor cells. That is, a point in the space (and, therefore, a Brownian particle locate at that point) belongs to one cell or another, but never contributes to more than one cell.

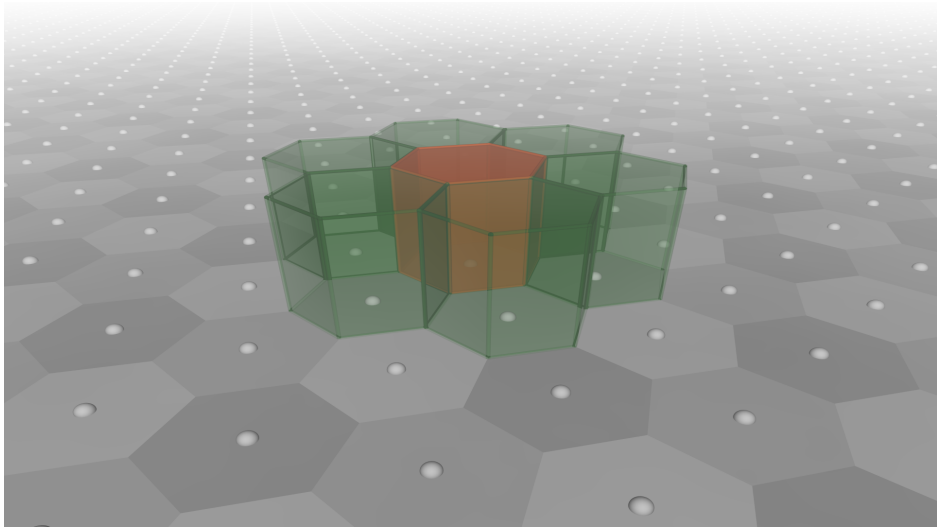

**Figure 3.1:** Voronoi tessellation in $2D$ for a regular grid. For a given node $\mu$, it is depicted the Voronoi cell associated to that node (orange), as well as the neighbor cells (green). Note that the cells do not overlap themselves.

Mathematically, we define a Voronoi cell as the region in which the function

$$\phi_\mu(\mathbf{r}) \triangleq \theta_{e_\mu}(\mathbf{r}) \,,$$

takes value 1. Here, $\theta_{e_\mu}$ is the characteristic function of the Voronoi cell (element) $e_\mu$. It takes the value 1 if $\mathbf{r}$ is inside the Voronoi cell and 0 otherwise. Note that there is a first kind discontinuity at the border of the cell, so that $\phi_\mu(\mathbf{r}) \notin \mathcal{C}^1$ and, therefore, its gradient is singular at the boundaries of the cell. Also note that the dissipative matrix obtained in (2.14) contains the gradient of the basis function $\delta_\mu(\mathbf{r})$. Therefore, it is clear that if we choose $\delta_\mu(\mathbf{r}) = \phi_\mu(\mathbf{r})$, the dissipative matrix will be ill-defined. We conclude that the Voronoi construction is not really useful for defining the concentration variable to be used for coarse-graining, in spite of its rather natural formulation. [35]

As suggested in Ref. [35], one way to avoid the above singularity is by using for $\delta_\mu(\mathbf{r})$ a usual finite element basis function based on the Delaunay triangulation. The Delaunay triangulation is the dual graph of the Voronoi tessellation. This is, if two nodes have Voronoi cells that are neighbours, then a link of the triangulation exists between these nodes. The finite element basis function $\psi_\mu(\mathbf{r})$ is defined as a pyramid made of triangular faces that takes the value 1 at node $\mu$ and zero at the neighbour nodes. To fix ideas, consider the Fig. 3.2, where a $2D$ Delaunay triangulation is shown for a regular mesh. An arbitrary cell (in orange) is composed by six sub-elements, or triangles. Note that there are six neighbor cells (in green) that overlap with the orange cell itself. The explicit form of the finite element basis function of node $\mu$ is

$$\psi_\mu(\mathbf{r}) \triangleq \sum_{e \in \mu} t_{e_\mu}(\mathbf{r}) \theta_{e_\mu}(\mathbf{r}) \,, \tag{3.1}$$

where $\theta_{e_\mu}(\mathbf{r})$ is the characteristic function of the element $e_\mu$ that belongs to the node $\mu$. The characteristic function takes value 1 if a point $\mathbf{r}$ is inside the element $e_\mu$, and 0 otherwise. The function $t_{e_\mu}(\mathbf{r})$ is a linear piecewise function which takes the value 1 at $\mathbf{r} = \mathbf{r}_\mu$ and decrease to 0 at the border of the element. It has the form

$$t_{e_\mu}(\mathbf{r}) = a + \mathbf{b}_{e \to \mu} \cdot \mathbf{r} \,, \tag{3.2}$$

where the notation $\mathbf{b}_{e\to\mu}$ means that the vector $\mathbf{b}$ that belongs to the element $e$ points toward the node $\mu$. The sum over $e_\mu$ in (3.1) indicates that the cell associated to the node $\mu$ is composed by many elements.

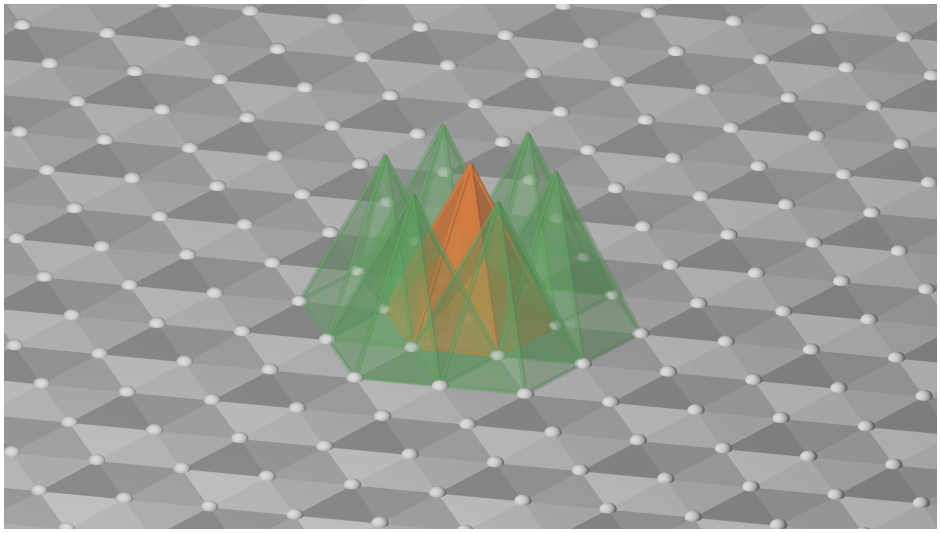

**Figure 3.2:** Delaunay tessellation in $2D$ for a triangular lattice. For a given node $\mu$ it is depicted the Delaunay cell associated to that node (orange), as well as the neighbor cells (green). Note that the cells do overlap themselves, as every neighbor cell partially penetrates into cell $\mu$.

The finite element $\psi_\mu(\mathbf{r})$ based on the Delaunay triangulation has the main advantage over the Voronoi construction of being a continuous function of $\mathbb{R}^N$, i.e., $\psi_\mu(\mathbf{r}) \in \mathcal{C}^1$. Therefore, it seems a good candidate to define the basis $\delta_\mu(\mathbf{r})$ function. By using the finite element $\psi_\mu(\mathbf{r})$ as the basis function in (3.1), the dissipative matrix (2.14) will not show any divergence, as opposed to the Voronoi characteristic function.

## 3.2. Finite element discretization basis

Motivated by the previous discussion, in this chapter we take as the discrete delta function

$$\delta_\mu(\mathbf{r}) \to \frac{\psi_\mu(\mathbf{r})}{V_\mu}\,, \tag{3.3}$$

where $V_\mu \triangleq \int d\mathbf{r}\, \psi_\mu(\mathbf{r})$ is the volume of the cell $\mu$ and $\psi_\mu(\mathbf{r})$ is the linear finite element with support on the Delaunay cell $\mu$. Therefore, the discrete concentration field $\hat{\mathbf{c}}(\mathbf{z})$ (2.1) at node $\mu$ is given by

$$\hat{c}_\mu(\mathbf{z}) = \sum_i \frac{\psi_\mu(\mathbf{r}_i)}{V_\mu}\,. \tag{3.4}$$

As indicated by (3.1) and (3.2), the finite element $\psi_\mu(\mathbf{r})$ is of the form

$$\begin{aligned}\psi_\mu(\mathbf{r}) &= \sum_{e\in\mu} t_{e_\mu}(\mathbf{r})\theta_{e_\mu}(\mathbf{r}) \\ &= \sum_{e\in\mu} \left(a_{e_\mu} + \mathbf{b}_{e\to\mu}\cdot\mathbf{r}\right)\theta_{e_\mu}\,.\end{aligned} \tag{3.5}$$

The function $\psi_\mu(\mathbf{r})$ has the nice property of preserving the partition of unity

$$\sum_\mu \psi_\mu(\mathbf{r}) = 1\,. \tag{3.6}$$

This property ensures that no matter the microscopic state $\mathbf{z}$, the sum of the discrete concentration variables gives the correct number of particles in the system. Indeed, by using the definition of the discrete concentration field (2.1) and the discrete delta function (3.3) we have

$$\sum_\mu V_\mu \hat{c}_\mu(\mathbf{z}) = \sum_i \sum_\mu \psi_\mu(\mathbf{r}_i) = \sum_i 1 = N\,,$$

irrespective of $\mathbf{z}$, as desired.

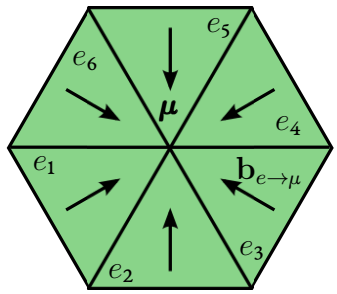


**Figure 3.3:** In $2D$, the Delaunay cell of node $\mu$ is surrounded by the triangular elements $e$. For each point of the triangular element $e$, there is a constant vector $\mathbf{b}_{e\to\mu}$ that points towards the node $\mu$ and that gives the derivative of the linear function $\psi_\mu(\mathbf{r})$ at that point.

The gradient of the finite element $\psi_\mu(\mathbf{r})$ is

$$\nabla\psi_\mu(\mathbf{r}) = \sum_{e\in\mu} \mathbf{b}_{e\to\mu}\theta_{e_\mu}(\mathbf{r})\,, \tag{3.7}$$

which is a discontinuous vector field that takes the constant vector value $\mathbf{b}_{e\to\mu}$ within each element $e_\mu$, and zero outside the Delaunay cell. This vector $\mathbf{b}_{e\to\mu}$ is directed towards the node $\mu$ (See Fig. 3.3, where there are depicted the six elements that compound a cell $\mu$ in a regular grid). In $1D$, for example, as we show in Fig. 3.4, each node $\mu$ has two elements, one on the left, $e^l_\mu$, and one on the right, $e^r_\mu$. The basis function has the explicit expression

$$\psi_\mu(x) = \frac{x - x_{\mu-1}}{x_\mu - x_{\mu-1}}\theta(x - x_{\mu-1})\theta(x_\mu - x) + \frac{x_{\mu+1} - x}{x_{\mu+1} - x_\mu}\theta(x - x_\mu)\theta(x_{\mu+1} - x)\,,$$

where $\theta(x)$ is the Heaviside step function. In this $1D$ example, the scalars $b_{e\to\mu}$ in (3.2) take the values

$$b_{e^l_\mu\to\mu} = \frac{1}{x_\mu - x_{\mu-1}} = \frac{1}{V^l_\mu}\,,$$
$$b_{e^r_\mu\to\mu} = -\frac{1}{x_{\mu+1} - x_\mu} = -\frac{1}{V^r_\mu}\,,$$

where $V^l_\mu$ and $V^r_\mu$ are defined precisely as the volume of each sub-element of node $\mu$.

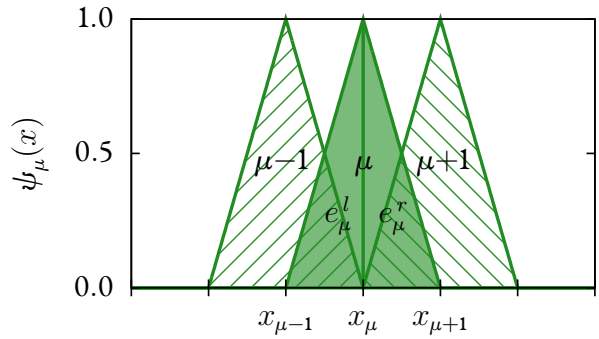


**Figure 3.4:** Delaunay triangulation in $1D$ for a regular grid. In solid green, the function $\psi_\mu(x)$ corresponding to an arbitrary node $\mu$. With patterns, the neighbor cells $\psi_{\mu-1}$ and $\psi_{\mu+1}$, showing an overlapping between them and the original $\psi_\mu$. The two shared elements are depicted as $e_\mu^l$ and $e_\mu^r$.

## 3.3. The Stochastic Differential Equation

Let us display again the stochastic differential equation for the discrete concentration field given by (2.15)

$$dc_\mu(t) = -\hat{D}_{\mu\nu}(\mathbf{c})\frac{\partial \hat{F}}{\partial c_\nu}(\mathbf{c})dt + k_\mathrm{B}T\frac{\partial \hat{D}_{\mu\nu}}{\partial c_\nu}(\mathbf{c})dt + d\tilde{c}_\mu(t)\,. \tag{3.8}$$

In Chapter 2 we have left the free energy function $\hat{F}(\mathbf{c})$, the dissipative matrix $\hat{\mathbf{D}}(\mathbf{c})$, and the thermal fluctuations $d\tilde{\mathbf{c}}$ unspecified. They have been written as functions of the basis functions $\delta_\mu(\mathbf{r})$. Now that we have the explicit form for $\delta_\mu(\mathbf{r})$ in (3.3), we may obtain explicit expressions for the three elements that enter into the SDE (3.8).

### 3.3.1. The free energy

As we pointed out in Chapter 2, the free energy function $\hat{F}(\mathbf{c})$ can be obtained from the microscopic equilibrium distribution function (2.9) as

$$P^\mathrm{eq}(\mathbf{c}) = \frac{1}{\mathcal{Z}}\int d\mathbf{z}\,\rho^\mathrm{eq}(\mathbf{z})\prod_\mu \delta\left(\hat{c}_\mu(\mathbf{z}) - c_\mu\right)\,. \tag{3.9}$$

Because the calculation of this multidimensional integral is unfeasible, we need to model the probability distribution $P^{\text{eq}}(\mathbf{c})$. For infinitely diluted suspensions (i.e., non interacting Brownian particles) we expect that under the assumption that the number of particles per node is sufficiently large, the probability $P^{\text{eq}}(\mathbf{c})$ should become a Gaussian, and the free energy should be a quadratic function of the concentration. In this approximation, by computing the first two moments of the probability distribution, the explicit expression for the free energy function can be obtained. This will be presented later on.

### 3.3.2. The dissipative matrix

We consider now the dissipative matrix defined in (2.14)

$$\hat{D}_{\mu\nu}(\mathbf{c}) = \frac{D}{k_{\text{B}}T} \int d\mathbf{r}\, \nabla\delta_\mu(\mathbf{r}) \nabla\delta_\nu(\mathbf{r}) \left\langle \hat{c}_{\mathbf{r}} \right\rangle^{\mathbf{c}} , \tag{3.10}$$

with the conditional average $\left\langle \hat{c}_{\mathbf{r}} \right\rangle^{\mathbf{c}}$ given by

$$\left\langle \hat{c}_{\mathbf{r}} \right\rangle^{\mathbf{c}} = \left\langle \sum_i^N \delta(\mathbf{r} - \mathbf{r}_i) \right\rangle^{\mathbf{c}} .$$

From the definition of the discrete delta function (3.3), the dissipative matrix (3.10) turns into

$$\hat{D}_{\mu\nu}(\mathbf{c}) = \frac{D}{k_{\text{B}}T} \int d\mathbf{r}\, \frac{\nabla\psi_\mu(\mathbf{r})}{V_\nu} \frac{\nabla\psi_\nu(\mathbf{r})}{V_\mu} \left\langle \hat{c}_{\mathbf{r}} \right\rangle^{\mathbf{c}} .$$

With the explicit form of the gradient of the finite element $\psi_\mu(\mathbf{r})$ given by (3.7), Eq. (3.10) becomes

$$\hat{D}_{\mu\nu}(\mathbf{c}) = \frac{D}{k_{\text{B}}T} \frac{1}{V_\mu V_\nu} \sum_{\substack{e\in\mu \\ e\in\nu}} \mathbf{b}_{e\to\mu} \cdot \mathbf{b}_{e\to\nu} \left\langle \sum_i^N \theta_{e_\mu}(\mathbf{r}_i)\theta_{e_\nu}(\mathbf{r}_i) \right\rangle^{\mathbf{c}} . \tag{3.11}$$

Because the sub-elements $e_\mu$ and $e_\nu$ do not overlap, the only surviving terms in the sum over particles in (3.11) are those with $e_\mu = e_\nu$. This results in

$$\begin{aligned}\hat{D}_{\mu\nu}(\mathbf{c}) &= \frac{D}{k_{\mathrm{B}}T}\sum_{e\in\mu\nu}\mathbf{b}_{e\to\mu}\cdot\mathbf{b}_{e\to\nu}\frac{V_e}{V_\mu V_\nu}c_e(\mathbf{c}) \\ &= \sum_{e\in\mu\nu}\mathbf{b}_{e\to\mu}\cdot\mathbf{b}_{e\to\nu}\frac{V_e}{V_\mu V_\nu}\Gamma_e(\mathbf{c})\,, \end{aligned} \tag{3.12}$$

where we introduced for notational convenience $\Gamma_e(\mathbf{c}) = Dc_e(\mathbf{c})/k_{\mathrm{B}}T$. Here, $e \in \mu\nu$ is any of the common elements of the neighbor nodes $\mu$ and $\nu$, $\mathbf{b}_{e\to\mu}$ is the vector of the element $e$, directed towards the node $\mu$, $\mathbf{b}_{e\to\nu}$ is the vector of the element $e$, directed towards the node $\nu$, and the concentration $c_e$ of the sub-element $e$ is defined as

$$c_e(\mathbf{c}) \triangleq \frac{1}{V_e}\left\langle\sum_i^N \theta_e(\mathbf{r}_i)\right\rangle^{\mathbf{c}}, \tag{3.13}$$

where $V_e$ is the volume of the sub-element $e$. In principle, the concentration of the element $e$ may depend on the value $\mathbf{c}$ of the concentration in all the nodes, that is, $c_e = c_e(\mathbf{c})$. However, we expect that for smooth distributions of particles, $c_e$ will only depend on the values of the nodal points of the element $e$.

For future references, we compute the gradient of the dissipative matrix (3.12). It is given by

$$\frac{\partial\hat{D}_{\mu\nu}(\mathbf{c})}{\partial c_\nu} = \frac{D}{k_{\mathrm{B}}T}\sum_{e\in\mu\nu}\mathbf{b}_{e\to\mu}\cdot\mathbf{b}_{e\to\nu}\frac{V_e}{V_\mu V_\nu}\frac{\partial c_e(\mathbf{c})}{\partial c_\nu}\,. \tag{3.14}$$

### 3.3.3. Thermal fluctuations

Motivated by the discussion in Section 2.3, the Fluctuation-Dissipation Theorem in (2.16), and the structure of the dissipative matrix in (3.12), a particular convenient possibility for the noise term is the following one

$$d\tilde{c}_\mu = \sum_{e\in\mu}\frac{1}{V_\mu}\mathbf{b}_{e\to\mu}\cdot d\tilde{\mathbf{J}}_{e_\mu}\,. \tag{3.15}$$

Here, $d\tilde{\mathbf{J}}_e = \left\{ d\tilde{J}_e^\alpha ; \alpha = 1, \ldots, M \right\}$ is a vector whose components are proportional to an independent Wiener process. Note that for each sub-element of the Delaunay triangulation we have a random vector $d\tilde{\mathbf{J}}_e$. As suggested in Ref. [67], a convenient form for the stochastic mass flux $d\tilde{\mathbf{J}}_e$ is

$$d\tilde{J}_e^\alpha \triangleq \sqrt{2Dc_eV_e}d\mathcal{W}_e^\alpha \,. \tag{3.16}$$

The independent increments of the Wiener process $d\mathcal{W}_e^\alpha$ satisfy the mnemotechnical Ito rule

$$d\mathcal{W}_e^\alpha d\mathcal{W}_{e'}^\beta = \delta_{ee'}\delta^{\alpha\beta}dt \,.$$

Therefore, we have the following variances of the stochastic mass flux defined in Eq. (3.16)

$$d\tilde{J}_e^\alpha d\tilde{J}_{e'}^\beta = \delta_{ee'}\delta^{\alpha\beta}2Dc_eV_edt \,, \tag{3.17}$$

and the proposed noise in Eq. (3.15) obeys

$$d\tilde{c}_\mu d\tilde{c}_\nu = \left[ \sum_{\substack{e\in\mu \\ e'\in\nu}} \sum_{\substack{\alpha \\ \beta}} \frac{1}{V_\mu V_\nu} b_{e\to\mu} b_{e'\to\nu} d\tilde{J}_e^\alpha d\tilde{J}_{e'}^\beta \right] \,. \tag{3.18}$$

By introducing (3.17) into (3.18) we have

$$\begin{aligned} d\tilde{c}_\mu d\tilde{c}_\nu &= 2D \sum_{e\in\mu\nu} \frac{1}{V_\mu V_\nu} \mathbf{b}_{e\to\mu} \cdot \mathbf{b}_{e\to\nu} V_e c_e dt \\ &= 2k_\mathrm{B}T\hat{D}_{\mu\nu}dt \,. \end{aligned}$$

Therefore, our proposal for $d\tilde{c}_\mu$ in (3.15) fulfills the Fluctuation-Dissipation Theorem (2.16), as desired.

### 3.3.4. The Stochastic Differential Equation

Now that we have obtained expressions for the dissipative matrix (3.12) and the thermal fluctuations (3.15)-(3.16), the SDE (3.8) becomes

$$\begin{aligned} dc_\mu(t) &= -\hat{D}_{\mu\nu}(\mathbf{c})\frac{\partial \hat{F}}{\partial c_\nu}(\mathbf{c})dt + k_{\mathrm{B}}T\frac{\partial \hat{D}_{\mu\nu}}{\partial c_\nu}(\mathbf{c})dt + d\tilde{c}_\mu(t) \\ &= -\frac{D}{k_{\mathrm{B}}T}\sum_\nu \sum_{e\in\mu\nu} \mathbf{b}_{e\to\mu}\cdot\mathbf{b}_{e\to\nu}\frac{V_e}{V_\mu V_\nu}c_e\frac{\partial \hat{F}}{\partial c_\nu}dt \\ &\qquad + D\sum_\nu \sum_{e\in\mu\nu} \mathbf{b}_{e\to\mu}\cdot\mathbf{b}_{e\to\nu}\frac{V_e}{V_\mu V_\nu}\frac{\partial c_e}{\partial c_\nu}dt \\ &\qquad + \sum_{e\in\mu}\sqrt{2Dc_eV_e}\frac{1}{V_\mu}\mathbf{b}_{e\to\mu}\cdot d\boldsymbol{\mathcal{W}}_e\,. \end{aligned} \tag{3.19}$$

The SDE (3.19) is to be interpreted in Ito sense. One essential property of Eq. (3.19) is that the total number of colloidal particles is conserved, that is, $\sum_\mu V_\mu c_\mu(t) = N$. This is a direct consequence of the definition of the concentration field in terms of the Delaunay cell and the fact that the finite element functions $\psi_\mu(\mathbf{r})$ satisfy the partition of unity property (3.6).

Note that the noise term $d\tilde{c}_\mu$ defined in (3.15)-(3.16) scales as the inverse of the square root of the volume of the cells, while the gradient of the dissipative matrix (3.14) scales as the inverse of the volume. The term that involves the derivatives of the free energy in (3.19) does not depend on the volume of the cell, because $\hat{F}(\mathbf{c})$ is an extensive quantity that scales with the volume of the cell. This means that by increasing the size of the cells and keeping the average concentration fixed, the effect of the noise terms and the gradient of the dissipative matrix diminish. In accordance with the usual view of equilibrium statistical mechanics, thermal fluctuations depend on the size of the system (in the present case, the size of the cell, determined by the resolution of the grid). That is consistent with the fact that the probability distribution $P(\mathbf{c})$ becomes more and more peaked as the cell size increases. In the limit of large cells, we may neglect both thermal fluctuations and the gradient of the dissipative matrix in Eq. (3.19). In this limit the SDE (3.19) becomes a deterministic ODE for

the concentration given by

$$\frac{dc_\mu(t)}{dt} = -\frac{D}{k_\mathrm{B}T}\sum_\nu \sum_{e\in\mu\nu} \mathbf{b}_{e\to\mu}\cdot\mathbf{b}_{e\to\nu}\frac{V_e}{V_\mu V_\nu}c_e\frac{\partial\hat{F}}{\partial c_\nu}$$
$$= -\sum_\nu \hat{D}_{\mu\nu}\frac{\partial\hat{F}}{\partial c_\nu}\,. \tag{3.20}$$

## 3.4. Connection with a continuum differential equation

The deterministic evolution equation (3.20) has been obtained by following a coarse-graining procedure. Remarkably, it can also be understood as a particular discrete representation of the diffusion equation (0.3) written in the Introduction

$$\frac{\partial c}{\partial t}(\mathbf{r},t) = -\boldsymbol{\nabla}\cdot\left[\Gamma(c(\mathbf{r},t))\boldsymbol{\nabla}\frac{\delta\mathcal{F}}{\delta c(\mathbf{r},t)}[c(\mathbf{r},t)]\right]\,, \tag{3.21}$$

where the mobility $\Gamma(c(\mathbf{r},t))$ has the form

$$\Gamma(c(\mathbf{r},t)) = \frac{D}{k_\mathrm{B}T}c(\mathbf{r},t)\,,$$

and it is a function of the concentration field in general, and the free energy functional $\mathcal{F}[c(\mathbf{r},t)]$ also depends on the concentration field. To fix ideas, consider a dilute solution. In this case we have an ideal gas form for the free energy functional

$$\mathcal{F}[c(\mathbf{r},t)] = k_\mathrm{B}T\int d\mathbf{r}\, c(\mathbf{r},t)\ln\left(\frac{c(\mathbf{r},t)}{c_0}-1\right)\,.$$

By taking the functional derivative and inserting the result into (3.21) we obtain Fick's diffusion equation

$$\frac{\partial c}{\partial t}(\mathbf{r},t) = D\nabla^2 c(\mathbf{r},t)\,.$$

Let us discretize Eq. (3.21). The discretization begins with the definition of the average discrete concentration field

$$c_\mu(t) \triangleq \int d\mathbf{r}\, \delta_\mu(\mathbf{r}) c(\mathbf{r}, t)\,. \tag{3.22}$$

If we multiply Eq. (3.21) by $\delta_\mu(\mathbf{r})$ and we integrate over all space we obtain an equation for the discrete concentration field $\overline{c}_\mu(t)$,

$$\frac{\partial c_\mu}{\partial t}(t) = -\int d\mathbf{r}\, \boldsymbol{\nabla}\delta_\mu(\mathbf{r}) \cdot \left[\Gamma(c(\mathbf{r}, t))\boldsymbol{\nabla}\frac{\delta\mathcal{F}}{\delta c(\mathbf{r}, t)}[c(\mathbf{r}, t)]\right]\,, \tag{3.23}$$

where an integration by parts has been done. Equation (3.23) is not a closed equation for the discrete values $c_\mu$. To close the equation we introduce a free energy *function* as

$$F(\mathbf{c}) = \mathcal{F}[\boldsymbol{\psi}\cdot\mathbf{c}]\,,$$

where $\boldsymbol{\psi}\cdot\mathbf{c} = \sum_\mu \psi_\mu(\mathbf{r})c_\mu$ is the interpolated field. The derivative of the free energy becomes

$$\frac{\partial F}{\partial c_\mu}(\mathbf{c}) = \int d\mathbf{r}'\, \frac{\delta\mathcal{F}}{\delta c(\mathbf{r}')}[\boldsymbol{\psi}\cdot\mathbf{c}]\psi_\mu(\mathbf{r}')\,.$$

By multiplying the above equation with $\delta_\mu(\mathbf{r})$ and summing over $\mu$ we have

$$\sum_\mu \delta_\mu(\mathbf{r})\frac{\partial F}{\partial c_\mu}(\mathbf{c}) = \int d\mathbf{r}'\, \frac{\delta\mathcal{F}}{\delta c(\mathbf{r}')}[\boldsymbol{\psi}\cdot\mathbf{c}]\sum_\mu \psi_\mu(\mathbf{r}')\delta_\mu(\mathbf{r})\,.$$

The function $\sum_\mu \psi_\mu(\mathbf{r}')\delta_\mu(\mathbf{r})$ is zero if the points $\mathbf{r}, \mathbf{r}'$ are separated by a distance larger than the typical size of the triangulation mesh. Under the assumption that the field $c(\mathbf{r})$ changes little in this length scale we may approximate

$$\sum_\mu \delta_\mu(\mathbf{r})\frac{\partial F}{\partial c_\mu}(\mathbf{c}) \approx \frac{\delta\mathcal{F}}{\delta c(\mathbf{r})}[\boldsymbol{\psi}\cdot\mathbf{c}]\,. \tag{3.24}$$

By inserting Eq. (3.24) into (3.23) we obtain

$$\frac{\partial \overline{c}_\mu}{\partial t}(t) = -\sum_\nu \int d\mathbf{r}\, \boldsymbol{\nabla}\delta_\mu(\mathbf{r}) \cdot \Gamma(c(\mathbf{r},t))\boldsymbol{\nabla}\delta_\nu(\mathbf{r})\frac{\partial F}{\partial c_\nu}(\mathbf{c})\,,$$

which, by using the definition of $\delta_\mu(\mathbf{r})$ in (3.3) and its gradient in (3.7), turns into

$$\frac{\partial \overline{c}_\mu}{\partial t}(t) = -\sum_\nu \frac{1}{V_\mu V_\nu} \sum_{\substack{e\in\mu \\ e\in\nu}} \mathbf{b}_{e\to\mu}\cdot\mathbf{b}_{e\to\nu} \int d\mathbf{r}\, \theta_{e_\mu}(\mathbf{r})\Gamma(c(\mathbf{r},t))\theta_{e_\nu}(\mathbf{r})\frac{\partial F}{\partial c_\nu}(\mathbf{c})\,. \tag{3.25}$$

Here, $e$ is any of the common elements of the neighbor nodes $\mu$ and $\nu$, $\mathbf{b}_{e\to\mu}$ is the vector of the element $e$, directed towards the node $\mu$, $\mathbf{b}_{e\to\nu}$ is the vector of the element $e$, directed towards the node $\nu$. This expression is not yet explicit due to the dependence on $\Gamma(c(\mathbf{r},t))$ of the field. We approximate the mobility $\Gamma(c(\mathbf{r},t))$ with the piece-wise linear function again

$$\Gamma(c(\mathbf{r},t)) \approx \overline{\Gamma}(\mathbf{r}) \triangleq \sum_\sigma \psi_\sigma(\mathbf{r})\Gamma(\overline{c}_\sigma)\,. \tag{3.26}$$

By inserting (3.26) into the integral in Eq. (3.25) we obtain

$$\int d\mathbf{r}\, \theta_{e_\mu}(\mathbf{r})\Gamma(c(\mathbf{r},t))\theta_{e_\nu}(\mathbf{r}) \approx \sum_\sigma \Gamma(\overline{c}_\sigma) \int d\mathbf{r}\, \theta_{e_\mu}(\mathbf{r})\theta_{e_\nu}(\mathbf{r})\psi_\sigma(\mathbf{r})\,. \tag{3.27}$$

By inserting (3.27) into (3.25) we get finally an explicit ODE for the discrete variables. The integral (3.27) vanishes unless $\mu$ and $\nu$ are neighboring nodes. In $2D$, for example, we have two sub-elements which are common to the nodes $\mu$ and $\nu$ that give a non-zero contribution (see Fig. 3.5). For each of these sub-elements, $\sigma$ may be any of the three nodes of the sub-element. For other values of $\sigma$ the integral in Eq. (3.27) vanishes. For $\sigma$ equal to any of the nodes of the element, the integral takes the same value, equal to $V_e/D$, where $V_e$ is the volume of the sub-element and $D$ is the space dimension. Therefore, Eq. (3.25)

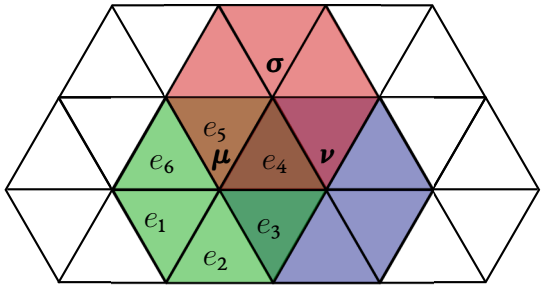


**Figure 3.5:** In a $2D$ regular grid, two neighbor nodes share two elements. For example, a node $\mu$ (green) and a node $\nu$ (blue) have in common the elements $e_3$ and $e_4$. The element $e_4$ is shared between the nodes $\mu, \nu$ and $\sigma$. Therefore, a particle located in $e_4$ will contribute to the concentration of the three nodes, $c_\mu$, $c_\nu$ and $c_\sigma$.

becomes

$$\begin{aligned}\frac{\partial \overline{c}_\mu}{\partial t}(t) &= -\sum_\nu \sum_{e\in\mu\nu} \mathbf{b}_{e\to\mu}\cdot\mathbf{b}_{e\to\nu}\frac{V_e}{V_\mu V_\nu}\Gamma_e\frac{\partial F}{\partial c_\nu}(\mathbf{c}) \\ &= -\sum_\nu \sum_{e\in\mu\nu} \mathbf{b}_{e\to\mu}\cdot\mathbf{b}_{e\to\nu}\frac{V_e}{V_\mu V_\nu}\frac{Dc_e}{k_{\mathrm{B}}T}\frac{\partial F}{\partial c_\nu}(\mathbf{c}) \\ &= -\sum_\nu D_{\mu\nu}\frac{\partial F}{\partial c_\nu}(\mathbf{c})\,, \end{aligned} \tag{3.28}$$

where

$$D_{\mu\nu} = \frac{D}{k_{\mathrm{B}}T}\sum_{e\in\mu\nu}\mathbf{b}_{e\to\mu}\cdot\mathbf{b}_{e\to\nu}\frac{V_e}{V_\mu V_\nu}c_e\,,$$

to be compared with (3.12). Eq. (3.28) is the final discretized version of the continuum diffusion equation (3.21). *This discretized diffusion equation coincides with the dynamic equation obtained microscopically in Eq.* (3.20).

## 3.5. Summary

In Chapter 2 we have obtained a discrete diffusion equation for the coarse grained variable $c_\mu(t)$. The definition of the discrete concentration field $\mathbf{c}$ has been given in terms of a general basis function $\delta_\mu(\mathbf{r})$. In this chapter we have proposed a specific form for the basis function: the finite element $\psi_\mu(\mathbf{r})$ with support on the Delaunay triangulation defined in (3.5). This basis function preserves the partition of unity so that the sum of the discrete concentrations gives exactly the correct number of particles in the system.

With the particular selection of the finite element $\psi_\mu(\mathbf{r})$ for the basis functions, we have obtained the explicit form (3.12) for the dissipative matrix $\hat{\mathbf{D}}(\mathbf{c})$. In principle, $\hat{\mathbf{D}}(\mathbf{c})$ depends on the concentration of the elements of the nodes through $c_e$, which is defined in (3.13) as a conditional expectation that depends on the concentration of all the nodes. In order to simplify the computation of $c_e$, we will assume in future chapters smooth concentration profiles. With this assumption the concentration of an element $e \in \mu$ should depend only on the concentration of nodes neighboring $\mu$. The computation of the free energy function (through the equilibrium probability distribution) is also complicated. We will assume in the next chapter a large number of particles per node, so that the probability becomes Gaussian. Therefore, the free energy should become a quadratic function of the concentration.

The SDE (3.19) can be understood, in the limit of large cells when thermal fluctuations are negligible, as a discretization of the deterministic continuum diffusion equation (3.21). Note that the two identical equations (3.20) and (3.28) are derived very differently. On one hand, the deterministic ODE (3.20) has been obtained from microscopic principles. We have defined the discrete concentration field by counting the number of particles inside a region with the help of the finite element $\psi_\mu(\mathbf{r})$. On the other hand, the ODE (3.28) has been obtained by defining an discretized version of the concentration field through (3.22). The fact that both procedures lead to the same ODE indicates a close relationship between the microscopically derived elements $\hat{D}_{\mu\nu}(\mathbf{c})$, $\hat{F}(\mathbf{c})$, and $D_{\mu\nu}(\mathbf{c})$, $\mathcal{F}[c]$. In the limit of large cells, we have shown that both expression for the dissipative matrix coincide. In addition to this, we have obtained the discrete free energy *function* by evaluating the free free energy *functional*

at the interpolated field $\overline{\mathbf{c}}$. This procedure allows one to obtain discrete free energy expressions from physically motivated free energy functionals, like the ones corresponding to the ideal gas or the van der Waals gas. This method for obtaining free energy functions avoids the computation of microscopic integrals like (3.9), and will be explored in next chapters.

# 4

# The Bottom-Up Approach for Discrete Diffusion with Finite Elements. Models and Numerical Results

Where we propose specific models for the free energy and the dissipative matrix and we perform numerical simulations of the resulting SDE.

## 4.1. Introduction

In previous chapters we have obtained the SDE (3.19) for discrete diffusion starting from the general evolution equation for coarse grained variables. The definition of the discrete concentration variables $\hat{c}_\mu(\mathbf{z})$ given by (2.1) is writ-

ten in terms of a generic discretization basis function $\delta_\mu(\mathbf{r})$ that we specified in CHAPTER 3 to be the finite element with support on the Delaunay triangulation, $\psi_\mu(\mathbf{r})/V_\mu$. The discrete free energy $\hat{F}(\mathbf{c})$ and the dissipative matrix $\hat{\mathbf{D}}(\mathbf{c})$ appearing in (3.19) have been obtained in CHAPTER 3. On one hand, the free energy (3.9) is obtained from the probability distribution

$$P^{\text{eq}}(\mathbf{c}) = \frac{1}{\mathcal{Z}} \int d\mathbf{z}\, \rho^{\text{eq}}(\mathbf{z}) \prod_{\mu=1}^{M} \delta\left(\hat{c}_\mu(\mathbf{z}) - c_\mu\right) , \tag{4.1}$$

On the other hand, the dissipative matrix (3.12) is

$$\hat{D}_{\mu\nu}(\mathbf{c}) = \frac{D}{k_{\text{B}}T} \sum_{e \in \mu\nu} \mathbf{b}_{e\to\mu} \cdot \mathbf{b}_{e\to\nu} \frac{V_e}{V_\mu V_\nu} c_e(\mathbf{c}) , \tag{4.2}$$

which depends on the concentration of the sub-element of node $\mu$ defined as

$$c_e(\mathbf{c}) \triangleq \frac{1}{V_e} \left\langle \sum_i^N \theta_e(\mathbf{r}_i) \right\rangle^{\mathbf{c}} .$$

Because the explicit evaluation of these quantities is impossible, we need to model the equilibrium probability (4.1) and the dissipative matrix (4.2). In this chapter we assume particular models for both quantities that give the explicit functional form of $\hat{F}(\mathbf{c})$ and $\hat{\mathbf{D}}(\mathbf{c})$. We will assume two approximations: the number of Brownian particles per node is large enough such that the probability distribution is a Gaussian. Also the concentration field is sufficiently smooth so that the concentration of a sub-element can be obtained from the concentration of its neighbor nodes. With these two approximation we end up with simple models that allow for the numerical simulation of the SDE.

## 4.2. FREE ENERGY MODELS

Under the assumption that the probability is Gaussian, the free energy becomes a quadratic function. The parameters of these quadratic function are obtained from the first two moments of the probability distribution (2.10). In

Appendix B we obtain these moments explicitly for non-interacting Brownian particles from microscopic principles. The resulting equilibrium probability distribution is

$$P^{\mathrm{eq}}(\mathbf{c}) = \frac{1}{\mathcal{Z}} \exp\left\{ -\sum_{\mu\nu} (c_\mu - c_0) V_\mu \frac{\left(M^\psi\right)^{-1}_{\mu\nu}}{2c_0} V_\nu (c_\nu - c_0) \right\}, \qquad (4.3)$$

so that the free energy is of the form

$$\hat{F}^{(\mathrm{GA})}(\mathbf{c}) = k_{\mathrm{B}} T \sum_{\mu\nu} (c_\mu - c_0) V_\mu \frac{\left(M^\psi\right)^{-1}_{\mu\nu}}{2c_0} V_\nu (c_\nu - c_0)\,. \qquad (4.4)$$

Here, $c_0 = N/V_T$ is the average concentration, $\delta\mathbf{c}$ is a vector whose $\mu$-th component is $\delta c_\mu = c_\mu - c_0$, and $\left[\mathbf{M}^\psi\right]^{-1}$ is the inverse of the *mass matrix* $\mathbf{M}^\psi$ defined as

$$M^\psi_{\mu\nu} \triangleq \int d\mathbf{r}\, \psi_\mu(\mathbf{r}) \psi_\nu(\mathbf{r})\,.$$

The matrix of correlations is directly related to $\mathbf{M}^\psi$ through (see (B.10))

$$\langle (c_\mu - c_0)(c_\nu - c_0) \rangle^{\mathrm{eq}} = \frac{c_0}{V_\mu V_\nu} M^\psi_{\mu\nu}\,,$$

In $1D$, the mass matrix is given by

$$\mathbf{M}^\psi = \frac{1}{6} \begin{pmatrix} 2\left(V_1^l + V_1^r\right) & V_1^r & 0 & \dots & V_1^l \\ V_2^l & 2\left(V_2^l + V_2^r\right) & V_2^r & \dots & 0 \\ 0 & V_3^l & 2\left(V_3^l + V_3^r\right) & \dots & 0 \\ \vdots & \vdots & \vdots & \ddots & \vdots \\ V_M^r & 0 & 0 & \dots & 2\left(V_M^l + V_M^r\right) \end{pmatrix}.$$

Note that the Gaussian form for the probability $P(\mathbf{c})$ given in (4.3) does not factorize into products of independent probabilities of each node. With the finite element basis function on the Delaunay triangulation, a Brownian particle

contributes to the concentration of all the nodes of the element in which the particle resides. In $1D$, for example, a particle in a given segment contributes to the nodes at the end of this segment. We conclude that there is a non-vanishing correlation of the concentration of neighbor nodes even for statistically independent particles. As a consequence, $P(\mathbf{c})$ cannot be factorized into products of the probability of the concentration of a single node and, therefore, *the free energy function is not an additive function in general*. Nevertheless, for the sake of comparison, we will consider also the local equilibrium approximation

$$P^{\mathrm{eq}}(\mathbf{c}) \approx \prod_{\mu} P(c_\mu)\,,$$

where $P(c_\mu)$ is the exact probability of finding $c_\mu$ particles per unit volume in the node $\mu$. This factorization approximation implies that the free energy is of the form $\hat{F}(\mathbf{c}) \approx \hat{F}^{(\mathrm{LE})}(\mathbf{c})$ where

$$\hat{F}^{(\mathrm{LE})}(\mathbf{c}) \triangleq \sum_{\mu} V_\mu f(c_\mu) \tag{4.5}$$

and the total free energy is the sum of the contribution of each cell, defined as $f(c_\mu)$.

The fact that "free energy is additive" as in (4.5) is one aspect of the *local equilibrium assumption*. The form of the free energy density $f(c_\mu)$ is determined by the form of the single node probability $P(c_\mu)$. We compute explicitly in Appendix B this probability. The result is given in (B.21), and it allows us to write the local free energy as

$$f(c_\mu) \triangleq k_{\mathrm{B}}T \frac{V_\mu^2}{M^{\psi}_{\mu\mu}} \frac{(c_\mu - c_0)^2}{4c_0}\,. \tag{4.6}$$

For future references, let us compute the gradients of the free energy functions (4.4) and (4.5)-(4.6)

$$\frac{\partial \hat{F}^{(\mathrm{GA})}}{\partial c_\mu}(\mathbf{c}) = k_{\mathrm{B}}T V_\mu \sum_{\nu} \left(M^{\psi}\right)^{-1}_{\mu\nu} V_\nu \frac{c_\nu - c_0}{c_0}\,, \tag{4.7}$$

$$\frac{\partial \hat{F}^{(\mathrm{LE})}}{\partial c_\mu}(\mathbf{c}) = k_{\mathrm{B}}T \frac{V_\mu^2}{M^{\psi}_{\mu\mu}} \frac{c_\mu - c_0}{2c_0}\,. \tag{4.8}$$

## 4.3. Dissipative matrix models

The dissipative matrix obtained in (3.12) requires the knowledge of the concentration of the sub-element $e$ defined in (3.13),

$$c_e(\mathbf{c}) \triangleq \frac{1}{V_e} \left\langle \sum_i^N \theta_e(\mathbf{r}_i) \right\rangle^{\mathbf{c}} . \tag{4.9}$$

The calculation of the conditional expectation of the number of particles in the sub-element $e$ appearing in (4.9) is difficult and we will need to make some approximate evaluation. To this end, we observe that when a node $\mu$ does not contain any Brownian particle and $c_\mu = 0$, all the sub-elements of this node should be also empty so that $c_e = 0$ for all the elements that belong to the node $\mu$. In order to satisfy this condition we might assume a geometric mean for the concentration of the element $c_e$. The geometrical mean has the advantage that it captures the physical property that when one of the nodes of the sub-element has zero concentration, meaning that the Delaunay cell has no Brownian particles within, the corresponding sub-element of the cell has no particles either. In a $D$ dimensional system the geometrical mean is defined as

$$c_e = \left( \prod_{\mu \in e} c_\mu \right)^{\frac{1}{D+1}} .$$

For example, in $1D$, each node $\mu$ has two elements, $e^l_\mu$ and $e^r_\mu$ (left and right), where the element $e^r_\mu$ coincides with the element $e^l_{\mu+1}$. The particles in each element contributes to the nodes $\mu$ and $\mu+1$, so that the concentration of that element will be, by using the geometrical mean,

$$c_e = \sqrt{c_\mu c_{\mu+1}} . \tag{4.10}$$

For smooth fields we may approximate $c_{\mu+1} \approx c_\mu + \Delta c$ and an expansion to first order in the small quantity $\Delta c$ gives the arithmetic mean

$$c_e = \frac{c_\mu + c_{\mu+1}}{2} . \tag{4.11}$$

Choosing between (4.10) and (4.11) is a sensible question. In spite of the simplicity of the arithmetic mean, the geometric mean approximation captures the physical property of empty elements for empty nodes (which is something that does not happen for the arithmetic mean). However, the derivative of the geometric mean is

$$\frac{\partial c_e}{\partial c_\mu} = \frac{1}{2}\sqrt{\frac{c_{\mu+1}}{c_\mu}}\,,$$

which diverges for $c_\mu = 0$. Because this derivative will appear in the stochastic differential equation (see (2.15)), it may lead to potential numerical problems. Moreover, due to random kicks performed by the fluctuating forces a node could reach a negative concentration, which gives non-sense in (4.10). In Appendix C we discuss, through the maximum entropy calculation of the conditional averages, that for smooth fields the arithmetic mean is recovered. Therefore, in this chapter we will approximate $c_e(\mathbf{c})$ by the arithmetic mean of the concentration of the $D+1$ nodal values of the sub-element $e$, that is,

$$c_e(\mathbf{c}) \approx \frac{1}{D+1}\sum_{\nu\in e} c_\nu\,. \tag{4.12}$$

For example, in a one dimensional case we recover (4.11), where $\mu$ and $\mu+1$ are the nodes corresponding to the sub-element $e$, in this case a line segment. The validity of this assumption is checked in Appendix D.

The dissipative matrix (3.12), with the arithmetic mean assumption (4.12), turns into a *state-dependent* matrix given by

$$\hat{D}_{\mu\nu}(\mathbf{c}) = \frac{D}{k_{\mathrm{B}}T}\sum_{e\in\mu\nu}\mathbf{b}_{e\to\mu}\cdot\mathbf{b}_{e\to\nu}\frac{V_e}{V_\mu V_\nu}\frac{1}{D+1}\sum_{\sigma\in e} c_\sigma\,. \tag{4.13}$$

Note that only those elements that belong to neighbor nodes contribute to the dissipative matrix. For example, in a $1D$ grid, the only surviving elements

related to a given node $\mu$ are

$$\hat{D}_{\mu\mu-1} = -\frac{D}{k_{\mathrm{B}}T}\frac{1}{V_\mu V_{\mu-1}}\frac{1}{V_\mu^l}\frac{c_{\mu-1}+c_\mu}{2}\,,$$
$$\hat{D}_{\mu\mu} = \frac{D}{k_{\mathrm{B}}T}\frac{1}{V_\mu^2}\left(\frac{1}{V_\mu^l}\frac{c_{\mu-1}+c_\mu}{2}+\frac{1}{V_\mu^r}\frac{c_{\mu+1}+c_\mu}{2}\right)\,,$$
$$\hat{D}_{\mu\mu+1} = -\frac{D}{k_{\mathrm{B}}T}\frac{1}{V_\mu V_{\mu+1}}\frac{1}{V_\mu^r}\frac{c_{\mu+1}+c_\mu}{2}\,,$$

which can be written in compact form as

$$\hat{D}_{\mu\nu} = \frac{D}{k_{\mathrm{B}}T}\frac{1}{V_\mu V_\nu}U_{\mu\nu}\,,$$

where

$$U_{\mu\nu} = \begin{cases} -\frac{1}{V_\mu^l}\frac{c_\mu+c_{\mu-1}}{2} & \text{iff } \nu=\mu-1\,,\\ \frac{1}{V_\mu^l}\frac{c_\mu+c_{\mu-1}}{2}+\frac{1}{V_\mu^r}\frac{c_\mu+c_{\mu+1}}{2} & \text{iff } \nu=\mu\,,\\ -\frac{1}{V_\mu^r}\frac{c_\mu+c_{\mu+1}}{2} & \text{iff } \nu=\mu+1\,,\\ 0 & \text{otherwise}\,. \end{cases}$$

Here, $V_\mu^l$ is defined as the volume of the sub-element $e_\mu^l$, while $V_\mu^r$ refers to the volume of the sub-element $e_\mu^r$.

Equation (4.13) is the explicit form of the dissipative matrix, in terms of geometric quantities and the coarse grained variables $\mathbf{c}$. We can also consider the dissipative matrix under the approximation that $\hat{D}_{\mu\nu}(\mathbf{c}) \approx \langle\hat{D}_{\mu\nu}\rangle^{\mathrm{eq}}$, as pointed in Ref. [68]. In this case we have simply

$$c_e = c_0\,, \tag{4.14}$$

and then the dissipative matrix $\hat{\mathbf{D}}$ is *state independent*

$$\hat{D}_{\mu\nu} = \frac{Dc_0}{k_{\mathrm{B}}T}\sum_{e\in\mu\nu}\mathbf{b}_{e\to\mu}\cdot\mathbf{b}_{e\to\nu}\frac{V_e}{V_\mu V_\nu} = \text{independent of } \mathbf{c}\,. \tag{4.15}$$

In the case of a $1D$ grid, the dissipative matrix takes the form

$$\begin{aligned}\hat{D}_{\mu\mu-1} &= -\frac{Dc_0}{k_{\mathrm{B}}T}\frac{1}{V_\mu V_{\mu-1}}\frac{1}{V_\mu^l}\,,\\ \hat{D}_{\mu\mu} &= \frac{Dc_0}{k_{\mathrm{B}}T}\frac{1}{V_\mu^2}\left(\frac{1}{V_\mu^l}+\frac{1}{V_\mu^r}\right)\,,\\ \hat{D}_{\mu\mu+1} &= -\frac{Dc_0}{k_{\mathrm{B}}T}\frac{1}{V_\mu V_{\mu+1}}\frac{1}{V_\mu^r}\,,\end{aligned}$$

which can be written in compact form as

$$\hat{D}_{\mu\nu} = \frac{Dc_0}{k_{\mathrm{B}}T}\frac{1}{V_\mu V_\nu}L^{\psi}_{\mu\nu}\,. \tag{4.16}$$

Here, $\mathbf{L}^{\psi}$ is the so-called *stiffness matrix* given by

$$\mathbf{L}^{\psi} = \begin{pmatrix} \left(\frac{1}{V_1^l}+\frac{1}{V_1^r}\right) & -\frac{1}{V_1^r} & 0 & \dots & -\frac{1}{V_1^l} \\ -\frac{1}{V_2^l} & \left(\frac{1}{V_2^l}+\frac{1}{V_2^r}\right) & -\frac{1}{V_2^r} & \dots & 0 \\ 0 & -\frac{1}{V_3^l} & \left(\frac{1}{V_3^l}+\frac{1}{V_3^r}\right) & \dots & 0 \\ \vdots & \vdots & \vdots & \ddots & \vdots \\ -\frac{1}{V_M^r} & 0 & 0 & \dots & \left(\frac{1}{V_M^l}+\frac{1}{V_M^r}\right) \end{pmatrix}.$$

## 4.4. Numerical results

In this section, we present the results of $1D$ numerical simulations of the fluctuating discrete diffusion equation (3.19) for both the Gaussian model (GA) in which $\hat{F}(\mathbf{c}) = \hat{F}^{(\mathrm{GA})}(\mathbf{c})$ as given by (4.7), and the local equilibrium model (LE) $\hat{F}(\mathbf{c}) = \hat{F}^{(\mathrm{LE})}(\mathbf{c})$ as given by (4.8). The results presented in this section have been conducted with the state-dependent dissipative matrix given in Eq. (3.12) with (4.12).

The results of the numerical simulations of the discrete diffusion equation will be compared with the "microscopic" dynamics of the independent Brownian particles governed by

$$d\mathbf{r}_i = \sqrt{2D}d\boldsymbol{\mathcal{W}}_i\,. \tag{4.17}$$

From the microscopic configuration $\mathbf{z} = \{x_i; i = 1, \ldots, N\}$ generated by Eq. (4.17), we will compute the mesoscopic concentration field $\hat{c}_\mu(\mathbf{z})$. The statistical properties of these mesoscopically obtained concentration fields will be compared with the results of the discrete diffusion equation (3.19).

### 4.4.1. The SDE to be solved

We consider the nodes located in a regular lattice separated by a distance $a$, with periodic boundary conditions (i.e. node $M+1$ coincides with node 1 and node 0 coincides with node $M$). First, we need to particularize the discrete diffusion equation (3.19) to this situation. For the sake of simplicity in the notation, let us introduce the chemical potential of node $\nu$ as

$$\mu_\nu \triangleq \frac{1}{V_\nu}\frac{\partial \hat{F}}{\partial c_\nu}\,,$$

so that for each free energy model (4.7) and (4.8) we have the following chemical potentials

$$\mu_\mu^{(\mathrm{GA})}(\mathbf{c}) = k_\mathrm{B}T\sum_\nu \left(M^\psi\right)^{-1}_{\mu\nu} V_\nu \frac{c_\nu - c_0}{c_0}\,, \tag{4.18}$$

$$\mu_\mu^{(\mathrm{LE})}(\mathbf{c}) = k_\mathrm{B}T\frac{3}{2}\frac{c_\mu - c_0}{c_0}\,. \tag{4.19}$$

For a regular lattice the SDE (3.19) may be written in the form

$$\begin{aligned} dc_\mu(t) &= a_\mu dt + d\tilde{c}_\mu \\ &= a_\mu^{(1)}dt + a_\mu^{(2)}dt + b_\mu^l dW_\mu^l + b_\mu^r dW_\mu^r\,. \end{aligned} \tag{4.20}$$

Where, $a_\mu^{(1)}$ is defined as

$$\begin{aligned} a_\mu^{(1)} &\triangleq -\frac{D}{k_\mathrm{B}T}\sum_\nu\left(\sum_{e\in\mu\nu}\mathbf{b}_{e\to\mu}\cdot\mathbf{b}_{e\to\nu}\frac{V_e}{V_\mu}c_e\right)\mu_\nu \\ &= -\frac{D}{k_\mathrm{B}T}\left(\sum_{e\in\mu\mu-1}\mathbf{b}_{e\to\mu}\cdot\mathbf{b}_{e\to\mu-1}c_e\right)\mu_{\mu-1} \\ &\qquad -\frac{D}{k_\mathrm{B}T}\left(\sum_{e\in\mu\mu}\mathbf{b}_{e\to\mu}\cdot\mathbf{b}_{e\to\mu}c_e\right)\mu_\mu \\ &\qquad -\frac{D}{k_\mathrm{B}T}\left(\sum_{e\in\mu\mu+1}\mathbf{b}_{e\to\mu}\cdot\mathbf{b}_{e\to\mu+1}c_e\right)\mu_{\mu+1} \end{aligned}$$

In $1D$, the vectors $\mathbf{b}_{e\to\mu}$ are simply the numbers $\pm\frac{1}{a}$. There is only one sub-element that is shared by the nodes $\mu$ and $\mu-1$, or by the nodes $\mu$ and $\mu+1$. However, the node $\mu$ shares two sub-elements $l, r$ (for left and right) with the node $\mu$ itself. This leads to

$$\begin{aligned} a_\mu^{(1)} &= -\frac{1}{a^2}c_\mu^l\mu_{\mu-1}+\frac{1}{a^2}(c_\mu^l+c_\mu^r)\mu_\mu-\frac{1}{a^2}c_\mu^r\mu_{\mu+1} \\ &= \frac{1}{a^2}c_\mu^l(\mu_\mu-\mu_{\mu-1})+\frac{1}{a^2}c_\mu^r(\mu_\mu-\mu_{\mu+1}) \end{aligned} \tag{4.21}$$

where

$$\begin{aligned} c_\mu^l &\triangleq \frac{c_\mu+c_{\mu-1}}{2}\,, \\ c_\mu^r &\triangleq \frac{c_\mu+c_{\mu+1}}{2}\,. \end{aligned}$$

The term $a_\mu^2$ in Eq. (4.20) is given from Eq. (4.13) by

$$a_\mu^2=\sum_\nu\left(\sum_{e\in\mu\nu}\mathbf{b}_{e\to\mu}\cdot\mathbf{b}_{e\to\nu}\frac{V_e}{V_\mu V_\nu}\right)\frac{1}{D+1}\,. \tag{4.22}$$

Due to the symmetry of the finite element construction,

$$\begin{aligned}\mathbf{b}^l_{e\to\mu} &= -\mathbf{b}^r_{e\to\mu-1}\,,\\ -\mathbf{b}^r_{e\to\mu} &= \mathbf{b}^l_{e\to\mu+1}\,,\end{aligned}$$

the sum in (4.22) will be zero regardless of the regularity of the grid. This implies that

$$a^{(2)}_\mu = 0\,.$$

Note that this result is completely general provided that the concentration of the element, $c_e$ is a linear function of the concentration of the nodes, because in this case the derivative of the concentration will be a constant. Therefore, this result is valid with the arithmetic approximation (4.12) and with the constant concentration approximation (4.14).

Finally, let us consider the thermal fluctuations in Eq. (3.19) in a regular lattice. From the definitions of $d\tilde{c}_\mu(t)$ in Eqs. (3.15)-(3.16), we have

$$\begin{aligned}d\tilde{c}_\mu &= \frac{1}{V_\mu}\sum_{e\in\mu}\mathbf{b}_{e\to\mu}\cdot\sqrt{2Dc_eV_e}d\mathcal{W}_e\\ &= b^l_\mu d\mathcal{W}^l_\mu + b^r_\mu d\mathcal{W}^r_\mu\,,\end{aligned}\tag{4.23}$$

with

$$\begin{aligned}b^l_\mu &\triangleq \frac{\sqrt{2Da}}{a^2}\sqrt{\frac{c_\mu+c_{\mu-1}}{2}}\,,\\ b^r_\mu &\triangleq \frac{\sqrt{2Da}}{a^2}\sqrt{\frac{c_\mu+c_{\mu+1}}{2}}\,.\end{aligned}\tag{4.24}$$

We can now collect the results (4.21), (4.22), and (4.23) to write down the final SDE satisfied by the discrete concentration variables in a regular lattice

$$\begin{aligned}dc_\mu = &\frac{D}{k_\mathrm{B}T}\frac{1}{a^2}\frac{c_\mu+c_{\mu-1}}{2}(\mu_\mu-\mu_{\mu-1})dt + \frac{D}{k_\mathrm{B}T}\frac{1}{a^2}\frac{c_\mu+c_{\mu+1}}{2}(\mu_\mu-\mu_{\mu+1})dt\\ &+\frac{\sqrt{Da}}{a^2}\left((c_\mu+c_{\mu-1})^{1/2}d\mathcal{W}^l_\mu-(c_\mu+c_{\mu+1})^{1/2}d\mathcal{W}^r_\mu\right)\,.\end{aligned}\tag{4.25}$$

In $1D$, for periodic boundary conditions, there are as many sub-elements as there are nodes. The noises also satisfy $d\mathcal{W}_\mu^l = d\mathcal{W}_{\mu-1}^r$ and $d\mathcal{W}_\mu^r = d\mathcal{W}_{\mu+1}^l$. Therefore, we will rename $d\mathcal{W}_\mu^l$ to $d\mathcal{W}_\mu$ and $d\mathcal{W}_\mu^r$ to $d\mathcal{W}_{\mu+1}$, respectively. The final Eqs. (4.25), with the different models for the given chemical potential in Eqs. (4.18) and (4.19) are the equations that will be simulated.

The above equations do exactly satisfy the conservation of the number of particles $N = \sum_\mu c_\mu V_\mu$ but do not necessarily ensure that the concentration of the nodes is always positive. Indeed, when the free energy function is a quadratic function and the dissipative matrix is proportional to the arithmetic mean, Eqs. (4.25) may lead, from time to time, to negative values of $c_\mu$ due to the random kicks of the Wiener process. However, physically an empty cell cannot go emptier. If this happens, Eq. (4.25) will be ill defined and the method will fail. If a cell is empty, then the noise terms corresponding to the sub-elements of that cell would need to vanish, preventing any stochasticity to empty already empty cells.

In the simulations presented later we observe that emptying empty cells occurs very infrequently when the number of particles per node is sufficiently large. When the concentration of a node becomes negative we need to restart the simulation again.

### 4.4.2. Time discretization

Equations (4.25) are discrete in space and continuum in time. For the numerical solution we also need a time discretization. There are many integrators that may be used to solve Stochastic Differential Equations. [69, 70] In this chapter we use a predictor-corrector Euler method [71]. This method gives an order of strong convergence of 0.5. A scheme converges strongly with order $\nu > 0$ at a time $t$ if there exists a positive constant $c$, which does not depend on $\Delta t$, such that for sufficiently small $\Delta t$

$$\sqrt{\langle(\mathbf{x}(t) - \mathbf{y}(t))^2\rangle} \leq c(\Delta t)^\nu \,,$$

where $\mathbf{x}(t)$ corresponds to the real solution and $\mathbf{y}(t)$ corresponds to the numerical solution. Strong convergence allows one to recover real individual trajectories, because the difference between the numerical and the real solution

decreases with the time step.

In order to write the explicit integration scheme, let us write Eq. (4.20) in integral form

$$\mathbf{c}_\mu(t) = \mathbf{c}_\mu(0) + \int_0^t ds\, a_\mu(s, \mathbf{c}(s)) + \int_0^t d\mathcal{W}_\mu^l(s)\, b_\mu^l(s, \mathbf{c}(s)) + \int_0^t d\mathcal{W}_\mu^r(s)\, b_\mu^r(s, \mathbf{c}(s))\,.$$

And define the function $\overline{a}^{\,\eta}$ with $\mu$-th component

$$\overline{a}_\mu^\eta(t, \mathbf{c}) \triangleq a_\mu(t, \mathbf{c}) + \eta_\mu \sum_\nu (b_\nu^l(t, \mathbf{c}) + b_\nu^r(t, \mathbf{c})) \frac{\partial}{\partial c_\nu} \left(b_\mu^l(t, \mathbf{c}) + b_\mu^r(t, \mathbf{c})\right)\,. \tag{4.26}$$

Then, the proposed family of strong predictor-corrector Euler schemes is given by the predictor

$$\overline{c}_\mu(t_i + \Delta t) = c_\mu(t_i) + a_\mu(t_i, \mathbf{c}(t_i))\Delta t + b_\mu^l(t_i, \mathbf{c}(t_i))\Delta\mathcal{W}_\mu^l + b_\mu^r(t_i, \mathbf{c}(t_i))\Delta\mathcal{W}_\mu^r\,, \tag{4.27}$$

and the corrector

$$\begin{aligned} c_\mu(t_i + \Delta t) = c_\mu(t_i) &+ \left[\theta_\mu \overline{a}_\mu^\eta(t_i + \Delta t, \overline{\mathbf{c}}(t_i + \Delta t)) + (1 - \theta_\mu)\overline{a}_\mu^\eta(t_i, \mathbf{c}(t_i))\right] \Delta t \\ &+ \left[\eta_\mu b_\mu^l(t_i + \Delta t, \overline{\mathbf{c}}(t_i + \Delta t)) + (1 - \eta_\mu) b_\mu^l(t_i, \mathbf{c}(t_i))\right] \Delta\mathcal{W}_\mu^l(t_i) \\ &+ \left[\eta_\mu b_\mu^r(t_i + \Delta t, \overline{\mathbf{c}}(t_i + \Delta t)) + (1 - \eta_\mu) b_\mu^r(t_i, \mathbf{c}(t_i))\right] \Delta\mathcal{W}_\mu^r(t_i)\,. \end{aligned} \tag{4.28}$$

Here, $\theta_\mu$ and $\eta_\mu \in [0, 1]$ correspond to the degree of implicitness in the drift and the diffusion coefficients, respectively. The case $\eta = \theta = 0$ recovers the usual Euler-Maruyama scheme. The symmetric predictor-corrector takes $\eta = \theta = \frac{1}{2}$.

Note that for a constant dissipative matrix like the one in (4.15) the stochastic drift term in (4.26) vanishes. On the other hand, for the arithmetic mean approximation for the dissipative matrix (4.13) we have

$$\overline{a}^{\eta}_{\mu}(t,\mathbf{c}) = \frac{D}{k_{\mathrm{B}}T}\frac{1}{a^2}\left(\frac{c_\mu + c_{\mu-1}}{2}(\mu_\mu - \mu_{\mu-1}) + \frac{c_\mu + c_{\mu+1}}{2}(\mu_\mu - \mu_{\mu+1})\right) + \eta_\mu \frac{\sqrt{Da}}{2a^2}\left(-\sqrt{\frac{c_\mu + c_{\mu+1}}{c_\mu + c_{\mu-1}}} + \sqrt{\frac{c_{\mu-1} + c_{\mu-2}}{c_\mu + c_{\mu-1}}} - \sqrt{\frac{c_\mu + c_{\mu-1}}{c_\mu + c_{\mu+1}}} + \sqrt{\frac{c_{\mu+1} + c_{\mu+2}}{c_\mu + c_{\mu+1}}}\right). \tag{4.29}$$

In a $1D$ regular grid with lattice spacing $a$, we must predict with (4.27) with $a_\mu$ given by (4.21), $b^{l,r}_{\mu}$ given by (4.24) and $\Delta\mathcal{W}^{l,r}_{\mu}$ random Gaussian noises (multiplied by $\sqrt{\Delta t}$). The random noises will be obtained with a Mersenne-Twister MT19937 algorithm [72] as initializator and the Ziggurat method [73] as generator. The corrector step (4.28) takes $\eta = \theta = 0.5$ and $\overline{a}^{\eta}_{\mu}$ given by (4.29).

### 4.4.3. Static properties

We first present results concerning the *static* properties of the model. In Fig. 4.1 we plot the probability that a single node has a particular value of the concentration at equilibrium. Three models, microscopic Brownian Dynamic (BD), Gaussian (GA) and local equilibrium (LE) are plotted. The relative error between BD and GA is less than 1%, while GA and LE coincide by construction. Indeed, the explicit expression for LE was obtained from the probability of the Gaussian model.

While the probability of a single node is essentially the correct one for the two models (GA and LE coinciding with BD), the situation is very different for the joint probability of neighbor nodes. In Fig. 4.2 we show the joint probability $P(c_\mu, c_{\mu+1})$ for the Gaussian model. This joint probability has a structure along the diagonal, which is a reflection of the non-vanishing correlation between neighboring cells. We have compared this joint probability with the BD

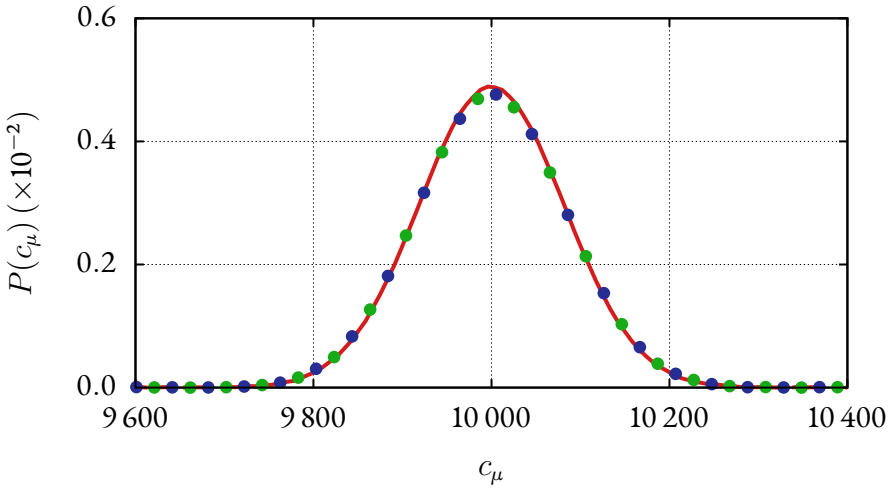


**Figure 4.1:** Probability of finding a particular value of the concentration, $c_\mu$, in a single node using three models. Red line shows a Brownian Dynamics simulation, green dots uses the Gaussian approximation (4.4) and blue dots uses the local equilibrium assumption (4.5) with (4.6). All three simulations were performed with $c_0 = 10000$ particles per node.

result, showing that in the region where the probability $P(c_\mu, c_{\mu+1})$ is greater than 0.01 %, the relative error is lower than 5%. The results show that very good agreement is obtained between the BD simulation and the GA model.

On the other hand, the LE model produces a perfectly isotropic distribution, as shown in Fig. 4.3. This isotropy is a reflection of the product structure of the joint probability in terms of the probability of a single node. Of course, the LE approximation neglects correlations between the concentration of neighboring cells, leading to large errors when compared with the true BD simulations or the essentially correct GA model in Fig. (4.2).

### 4.4.4. Dynamic properties

We have also considered the *dynamic* behavior of the different models by computing the correlation function $\langle c_\mu c_\nu(t)\rangle^{\text{eq}}$ of the concentration in different nodes. This correlation function has been computed analytically in Ref. [35],

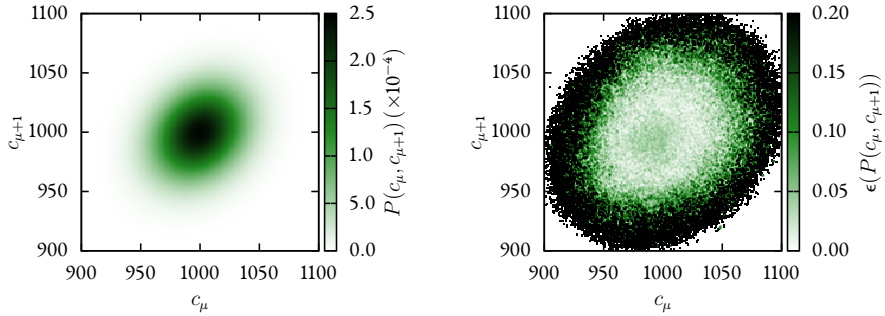


**Figure 4.2:** *Left panel.* Probability of finding a node with concentration $c_\mu$ and a neighbor node with concentration $c_{\mu+1}$, for the GA model. A structure along the diagonal can be appreciated, reflecting the correlation between neighbor nodes. *Right panel.* Relative error between the Gaussian model and the Brownian Dynamics. In the region where the probability $P(c_\mu, c_{\mu+1})$ is greater than 0.01 % the relative error is lower than 5 %.

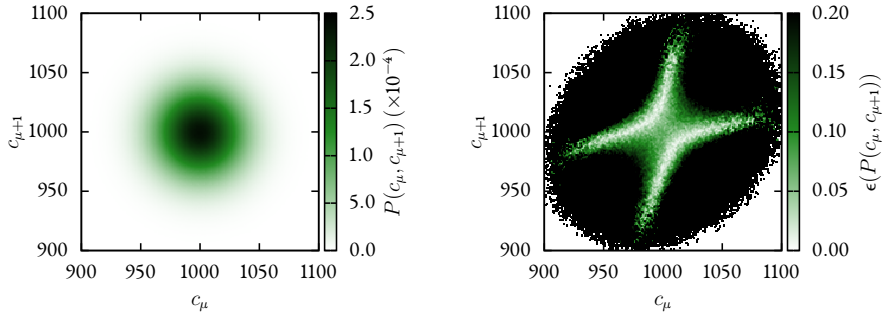


**Figure 4.3:** *Left panel.* Probability of finding a node with concentration $c_\mu$ and a neighbor node with concentration $c_{\mu+1}$, for the LE model. The structure is isotropic, because for the LE model two neighbor nodes are uncorrelated. The LE model does not reproduce correctly the joint probability of consecutive nodes. *Right panel.* Relative error between the Local Equilibrium model and the Brownian Dynamics, where errors as large as 20% are observed.

thanks to the simplicity of the Brownian dynamics of independent particles. In Fig. 4.4 we plot the analytical result (BD, red) together with the simulation results of the Gaussian (GA, green points) and Local Equilibrium (LE, blue points) models. Three groups of curves can be distinguished, corresponding to the autocorrelation $\mu = \nu$ and cross correlations with neighbors nodes. It is apparent that the GA model reproduces correctly the theoretical result in all cases, while the LE model fails to capture the correct behavior of the correlation function. Typically, the LE model produces a too quick decay towards zero, as compared with the actual behavior. This shows that not only static properties but also the dynamics is poorly captured by the local equilibrium model. This is a somewhat unexpected result and puts some caveats to the use of additive local equilibrium expressions for the free energy in finite element discretizations for stochastic theories of transport. What we observe is that, when "discretization effects" are taken into account, one should be cautious about directly using the concept of local equilibrium.

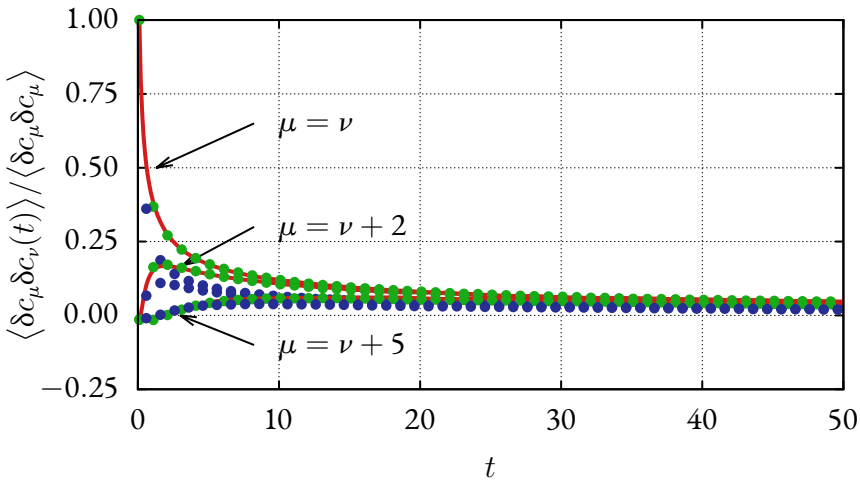


**Figure 4.4:** Correlation function for the different models. Red, correlation obtained analytically for the Brownian Dynamics. Green dots are the simulation results for the Gaussian model. Blue dots are the simulation results for the Local Equilibrium model. Three groups of correlations are plotted, corresponding to different distances between nodes (0, 2 and 5, respectively).

Is there any way to reconcile the failure of the local equilibrium in a discrete model with the expectation that it should prevail in a continuum theory? To answer this question, we have measured the root mean square error between the analytical result and the local equilibrium model for the correlation function of the concentration in different nodes. That is, we subtract both correlations, take its square, and average the result over time. Then we take the square root to get an error estimator of how much the LE model differs from the actual BD model. In Fig. 4.5 we plot this error as a function of the separation between the two nodes that are being correlated. There is a clear trend that suggest that for large separations, the LE model gives basically correct results. In conclusion, large scale dynamics is still correctly captured with the local equilibrium model, while small scale dynamics is not.

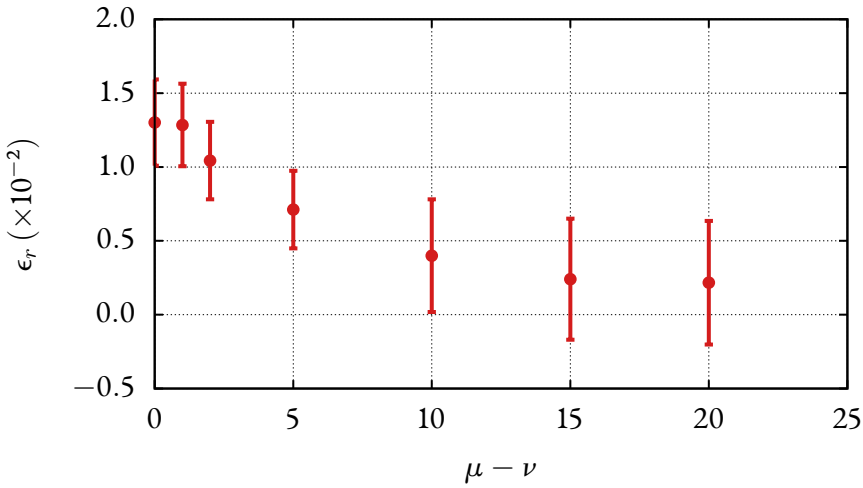


**Figure 4.5:** Root mean square error $\epsilon_r$ of the LE model with respect to the theoretical result, versus separation of the nodes. Error bars are estimated from the error bars of the simulation of the LE model.

## 4.5. Summary

In the first four chapters of this dissertation, we have studied the numerical behavior (Chapter 4) of a discrete model for diffusion based on the ToCG (Chapter 1) with a discretization basis (Chapter 2) constructed with the support of the Delaunay triangulation (Chapter 3) that has been proposed in Ref. [68]. The simplicity of the model describing non-interacting Brownian particles allows one to focus on the specific aspects of the Delaunay triangulation without having to bother about other issues that will necessarily arise when considering more complex systems like interacting colloidal particles and simple fluids. Discrete models based on the Delaunay triangulation for hydrodynamics are the natural outcome of a coarse-graining process that allows one to describe in a thermodynamically consistent way the introduction of thermal fluctuations in finite-element-like discretizations of Navier-Stokes equations. [68] This discrete hydrodynamic Delaunay model shows a great promise for the consistent coupling of atomically described fluids and hydrodynamic descriptions, where the coupling between regions of different detail is done with due account of thermal fluctuations. It is therefore, of utmost importance to understand the behavior of the models based on the Delaunay construction in simple cases before entering the more challenging and interesting situations. The discrete diffusion equation for non-interacting Brownian particles that we have considered here is one of these simplest cases.

Two building blocks, the free energy function and the dissipative matrix, appear in the discrete diffusion equation. Both are functions of the full state of the system, which is the set of concentrations in the $M$ nodes of the system. Although these building blocks are defined in terms of conditional averages, the calculation of this multidimensional functions is not an easy task in general. It is necessary to make modeling assumptions on the form of the free energy function. In the present chapter, we have considered two models, a Gaussian model, which works very well when the typical number of particles for node is large, and a Local Equilibrium model that captures correctly the statistical distribution of particles of a single node, but neglects correlations between neighboring nodes. The numerical results show that the LE model gives inaccurate results for both joint statistics of equilibrium fluctuations and

the dynamics of a single node. In other words, for the Delaunay triangulation, the overlapping of neighbor cells needs to be properly accounted for in the free energy function, which then becomes a non-additive function (it cannot be expressed as the sum of single free energies associated to each node). We find that a quadratic expression for the free energy reproduces very well both the static properties and also the dynamic properties of the underlying Brownian dynamics model. We have also shown that despite of the fact of providing poor results at small scales, the LE model is still appropriate for describing large scale results, in accordance with the idea that local discretization details should not affect large scale results.

Concerning the second building block, which is the dissipative matrix, we have proposed a state-dependent dissipative matrix based on a simple arithmetic mean ansatz. We have validated this ansatz from an explicit calculation of the conditional averages involved in the definition of the dissipative matrix. Nevertheless, it turns out that taking into account the state dependence of the dissipative matrix does not have a significant impact in the simulation results as compared with an even simpler ansatz for the dissipative matrix based on a state-independent assumption.

Both, the Gaussian approximation for the free energy and the state independent assumption for the dissipative matrix are expected to fail when the number of particles per node is very small. For the free energy, deviations from Gaussian behavior are expected already at the level of the single node equilibrium distribution function. On the other hand, the dissipative matrix must reflect the fact that the transport of particles out of an empty cell is forbidden, thus preventing any node from taking negative values of the concentration field. For the practical situations we have in mind (coupling of regions described at different detail but in near-equilibrium situations) such non-trivial behavior seems to be not necessary, but in highly non-equilibrium situations like shock and rarefaction situations, a proper modeling of the free energy function and the dissipative matrix may be necessary.

The present chapter considers a one dimensional CG model of non interacting Brownian particles but the main conclusion, which is the need of considering non-additive free energy models when using the Delaunay triangulation for the definition of the CG variables, is valid also for two and three dimen-

sions. In higher dimensions, the Delaunay cells also overlap as in $1D$, and the nodes are not statistical independent. Of course, the analytic calculation of the matrix of static covariances $\left(M^{\psi}\right)^{-1}_{\mu\nu}$ defining the Gaussian free-energy becomes much involved in high dimensions. In higher dimensions it seems much easier to evaluate the static covariances $\langle (c_\mu - c_0)(c_\nu - c_0)\rangle^{\mathrm{eq}}$ from a numerical simulation of the underlying microscopic system (BD for the case of colloidal particles, MD for the case of simple fluids).

In a similar way, the important message that even though a local equilibrium approximation gives correct large scale results it fails to capture the short scale physics remains valid at higher dimensions. This short scale physics is precisely what is needed in any hybrid scheme trying to match two different levels of description in two regions of the space connected with a boundary.

# Interlude

Where we propose a new basis function to discretize the diffusion equation.

Let us recall the procedure we have followed in Section 3.4 in order to discretize the continuum diffusion equation

$$\frac{\partial c}{\partial t}(\mathbf{r},t) = D\nabla^2 c(\mathbf{r},t)\,, \tag{4.30}$$

which is a particular example of the PDE (3.21) for a highly dilute solution. First, we stipulated how to discretize the continuum concentration field as

$$c_\mu(t) = \int d\mathbf{r}\,\delta_\mu(\mathbf{r})c(\mathbf{r},t)\,, \tag{4.31}$$

where the discrete delta function was given by (3.3)

$$\delta_\mu(\mathbf{r}) \to \frac{\psi_\mu(\mathbf{r})}{V_\mu}\,. \tag{4.32}$$

Here, $\psi_\mu(\mathbf{r})$ is the linear finite element with support on the Delaunay cell $\mu$. Second, we specified how to interpolate the discrete concentration field by introducing the interpolated field $\overline{c}(\mathbf{r},t)$ as

$$\overline{c}(\mathbf{r},t) = \sum_\mu \psi_\mu(\mathbf{r})c_\mu(t)\,. \tag{4.33}$$

By taking the time derivative of the discrete field (4.31) we obtain

$$\frac{\partial c_\mu}{\partial t}(t) = \int d\mathbf{r}\, \delta_\mu(\mathbf{r}) D \nabla^2 c(\mathbf{r}, t)\,, \tag{4.34}$$

which is not a closed equation for the discrete concentration field, because the obtained equation involves a discrete concentration field $c_\mu(t)$ *and* a continuous concentration field $c(\mathbf{r}, t)$. Then, in (4.34) we approximate the continuous field $c(\mathbf{r}, t)$ with the interpolated field $\overline{c}(\mathbf{r}, t)$ defined in (4.33), so that the discrete version of (4.30) becomes

$$\frac{\partial c_\mu}{\partial t}(t) = -D \frac{1}{V_\mu} \sum_\nu L^\psi_{\mu\nu} c_\nu\,,$$

where we did an integration by parts. Here, the stiffness matrix $\mathbf{L}^\psi$ is given by

$$L^\psi_{\mu\nu} = \int d\mathbf{r}\, \nabla\psi_\mu(\mathbf{r}) \nabla\psi_\nu(\mathbf{r})\,. \tag{4.35}$$

We may interpret the matrix

$$\Delta_{\mu\nu} = -\frac{1}{V_\mu} L^\psi_{\mu\nu} \tag{4.36}$$

as a discrete version of the Laplace operator $\boldsymbol{\nabla}^2$. Let us check how accurate is this discretization procedure by considering a $1D$ setting with periodic boundary conditions. In the continuum case, the action of the Laplace operator on the function

$$c(\mathbf{r}) = c_0 \cos\left(\frac{2\pi\mathbf{r}}{L}\right)$$

is

$$\begin{aligned}\nabla^2 c(\mathbf{r}) &= -c_0 \left(\frac{2\pi}{L}\right)^2 \cos\left(\frac{2\pi\mathbf{r}}{L}\right) \\ &= -\left(\frac{2\pi}{L}\right)^2 c(\mathbf{r})\,.\end{aligned}$$

Now, consider the following discrete solution of the concentration field for a node $\mu$ located at $\mathbf{r}_\mu$,

$$c_\mu = c_0 \cos\left(\frac{2\pi \mathbf{r}_\mu}{L}\right) . \tag{4.37}$$

If the action of the discrete Laplace operator (4.36) on this "discrete field" was

$$\sum_\nu \Delta_{\mu\nu} c_\nu = -\left(\frac{2\pi}{L}\right)^2 c_\mu ,$$

then we would have a perfect discrete representation of the Laplace operator. In summary, we would like to check the following identity

$$\left(\frac{2\pi}{L}\right)^2 c_\mu = \frac{1}{V_\mu} \sum_\nu L^\psi_{\mu\nu} c_\nu . \tag{4.38}$$

For a $1D$ regular grid of total length $L = 1$ with $M = 32$ nodes, we compare in Fig. 4.6 the left hand side (blue line) and the right hand side (red points) of (4.38) for the discrete cosine (4.37) with $c_0 = 1$. A perfect agreement is obtained. In fact, in CHAPTER 7 we will show that the vector $\mathbf{c}$ with component $c_\mu$ given by (4.37) is, in a regular grid, an eigenvector of $\mathbf{L}^\psi$ (see SECTION 7.4.1). Therefore, we conclude that the operator $\mathbf{L}^\psi$ is an exact representation of the Laplace operator acting on cosine functions, and the procedure followed in SECTION 3.4 to discretize a continuum equation is good.

The above argument is valid *for regular grids* only. For irregular lattices the discrete concentration vector $\mathbf{c}$ given by (4.37) is no longer an eigenvector of the operator $\mathbf{L}^\psi$. Therefore, $\mathbf{L}^\psi$ is just a *reasonable* approximation for the Laplace operator. In Fig. 4.7 we represent, in blue line, the left hand side of Eq. (4.38) in a 1D grid of length $L = 1$ with $M = 32$ nodes at completely random positions ($c_\mu$ is given by (4.37) with $c_0 = 1$). Red dots represent the right hand side of Eq. (4.38) for the same discrete profile. As compared with Fig. 4.6, it is obvious that for irregular lattices the discrete version of the Laplacian given by (4.35) is not as satisfactory as desired.

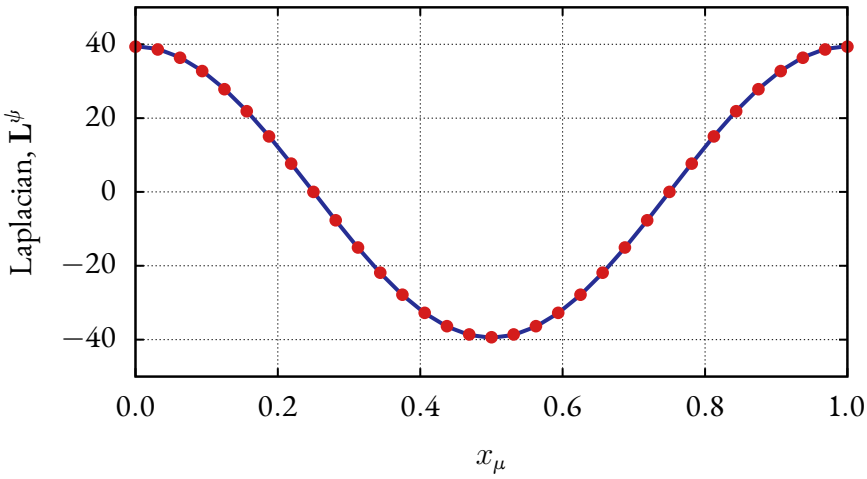


**Figure 4.6:** Discrete Laplacian $\mathbf{L}^{\psi}$ obtained from the basis function (4.32), applied to the cosine (4.37) in a 1D regular lattice.

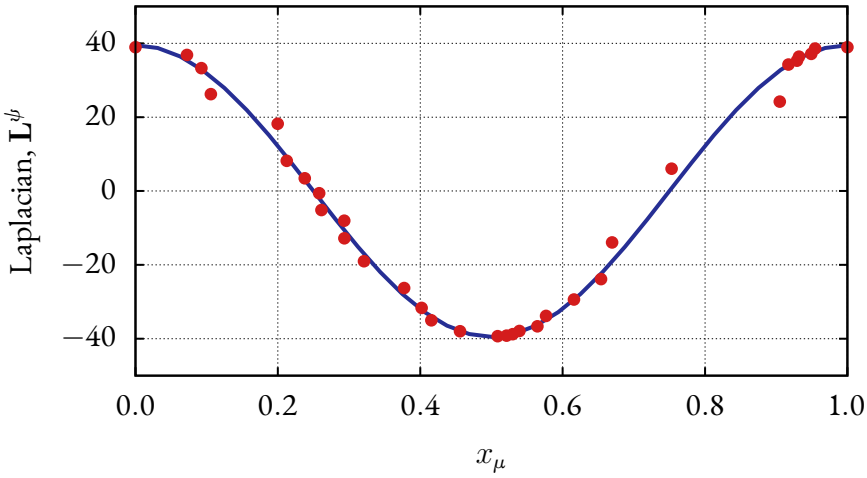


**Figure 4.7:** Discrete Laplacian $\mathbf{L}^{\psi}$ obtained from the basis function (4.32), applied to the cosine (4.37) in a 1D irregular lattice.

In order to find a better discrete Laplace operator for irregular grids, we make the following observation. Let us discretize a continuous field $c(\mathbf{r}, t)$ by using the discretization (4.31). If we replace the continuous field $c(\mathbf{r}, t)$ by the interpolated field $\overline{c}(\mathbf{r}, t)$ (4.33), we obtain

$$\begin{aligned} c_\mu(t) &= \int d\mathbf{r}\, \delta_\mu(\mathbf{r}) c(\mathbf{r}, t) \\ &= \frac{1}{V_\mu} \int d\mathbf{r}\, \psi_\mu(\mathbf{r}) c(\mathbf{r}, t) \\ &\approx \frac{1}{V_\mu} \int d\mathbf{r}\, \psi_\mu(\mathbf{r}) \overline{c}(\mathbf{r}, t) \\ &= \frac{1}{V_\mu} \sum_\nu \int d\mathbf{r}\, \psi_\mu(\mathbf{r}) \psi_\nu(\mathbf{r}) c_\nu(t) \\ &= \frac{1}{V_\mu} \sum_\nu M^\psi_{\mu\nu} c_\nu(t)\,, \end{aligned} \tag{4.39}$$

where the mass matrix $\mathbf{M}^\psi$ is given by

$$M^\psi_{\mu\nu} = \int d\mathbf{r}\, \psi_\mu(\mathbf{r}) \psi_\nu(\mathbf{r})\,.$$

In words, equation (4.39) expresses the fact that if we discretize an interpolated field constructed from a discrete field, we do not recover the original discrete field. Eq (4.39) is inconsistent unless the vector $\mathbf{c}$ with $\mu$-th component (4.37) is an eigenvector of the mass matrix $\mathbf{M}^\psi$. This is only true for regular lattices (see SECTION 7.4.1), Therefore, in irregular lattices (4.39) is inconsistent.

With this observation in mind, we will propose in CHAPTER 5 a basis function set *different* from (3.3). This new basis function is given by a linear combination of the finite element $\psi_\mu(\mathbf{r})$

$$\delta_\mu(\mathbf{r}) \to \sum_\nu M^\delta_{\mu\nu} \psi_\nu(\mathbf{r})\,, \tag{4.40}$$

where $\mathbf{M}^\delta$ is the inverse of the mass matrix $\mathbf{M}^\psi$. The basis function $\delta_\mu(\mathbf{r})$ defined in (4.40) will be called the *conjugate finite element basis function* or, simply, the *conjugate basis*.

Note that the basis (4.40) recovers the discrete field if we substitute the continuous field by the interpolated one

$$\begin{aligned} c_\mu(t) &= \int d\mathbf{r}\, \delta_\mu(\mathbf{r}) c(\mathbf{r},t) \\ &= \sum_\nu M^\delta_{\mu\nu} \int d\mathbf{r}\, \psi_\nu(\mathbf{r}) c(\mathbf{r},t) \\ &\approx \sum_\nu M^\delta_{\mu\nu} \int d\mathbf{r}\, \psi_\nu(\mathbf{r}) \bar{c}(\mathbf{r},t) \\ &= \sum_{\nu,\sigma} M^\delta_{\mu\nu} \int d\mathbf{r}\, \psi_\nu(\mathbf{r}) \psi_\sigma(\mathbf{r}) c_\sigma(t) \\ &= \sum_{\nu,\sigma} M^\delta_{\mu\nu} M^\psi_{\nu\sigma} c_\sigma(t) \\ &= \delta_{\mu\sigma} c_\sigma(t) \\ &= c_\mu(t)\,, \end{aligned}$$

irrespective of the regularity of the grid. In this way, if we interpolate a discrete field and then we discretize it, we get back the original discrete field.

We can now discretize the diffusion equation (4.30) with the new basis (4.40) to obtain

$$\frac{\partial c_\mu}{\partial t}(t) = -D \sum_{\nu,\sigma} M^\delta_{\mu\nu} L^\psi_{\nu\sigma} c_\sigma\,.$$

Instead of (4.38), in this case we obtain the condition

$$\left(\frac{2\pi}{L}\right)^2 c_\mu = \sum_{\nu,\sigma} M^\delta_{\mu\nu} L^\psi_{\nu\sigma} c_\sigma\,, \tag{4.41}$$

with the (conjugate) discrete Laplacian defined by the matrix multiplication $\mathbf{M}^\delta\mathbf{L}^\psi$. In Fig. 4.8 we plot, for the discrete cosine (4.37) with $L = 1$ and $c_0 = 1$, the left hand side (blue line) and the right hand side (green dots) of (4.41). We observe that, as compared with Fig. 4.7, this new prescription for the discrete Laplacian gives a much better agreement for irregular grids.

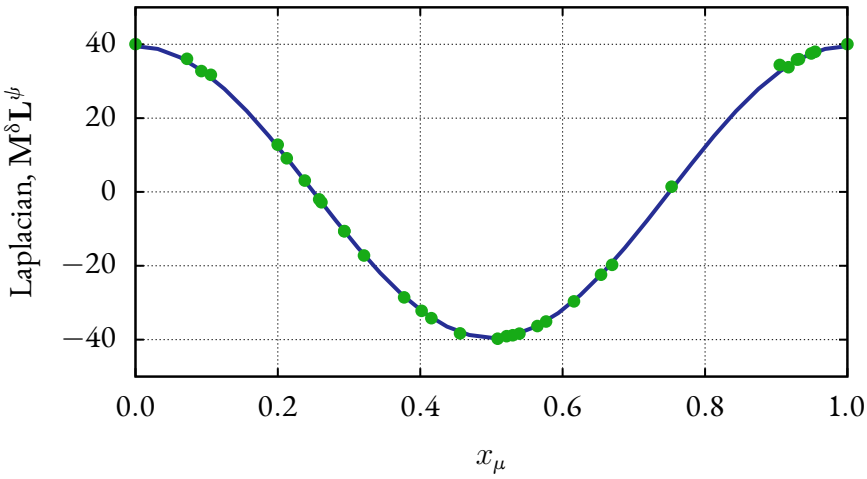


**Figure 4.8:** Conjugated discrete Laplacian $\mathbf{M}^\delta\mathbf{L}^\psi$ obtained from the basis function (4.40), applied to the cosine (4.37) in a 1D irregular lattice.

To obtain a quantitative measure of the improvement with the conjugate basis (4.40) with respect to the original basis (4.32), we look at the order of convergence of the two discrete Laplacian operators, $\mathbf{L}^\psi$ and the conjugate $\mathbf{M}^\delta\mathbf{L}^\psi$. For the discrete cosine (4.37) with $L = 1$ and $c_0 = 1$, we create 100 different $1D$ configurations with nodes at random positions and we compute, for each configuration, the following errors

$$\epsilon^\psi = \sqrt{\frac{1}{M}\sum_\mu \left(\sum_\nu L^\psi_{\mu\nu}c_\nu - \frac{4\pi^2}{L^2}c_\mu\right)^2},$$

$$\epsilon^\delta = \sqrt{\frac{1}{M}\sum_\mu \left(\sum_{\nu,\sigma} M^\delta_{\mu\nu}L^\psi_{\nu\sigma}c_\sigma - \frac{4\pi^2}{L^2}c_\mu\right)^2}.$$

These errors are plotted in Fig. 4.9. Red dots represent $\epsilon^\psi$, the error obtained for the discrete Laplacian $\mathbf{L}^\psi$. Green dots represent $\epsilon^\delta$, the error obtained for the conjugate discrete Laplacian $\mathbf{M}^\delta\mathbf{L}^\psi$. We also compute a least squares adjustment to $y = ax^b$, obtaining for $\mathbf{L}^\psi$ a coefficient $b^\psi \simeq -1$ (red line) and

for $\mathbf{M}^{\delta}\mathbf{L}^{\psi}$ a coefficient $b^{\delta} \simeq -2$ (green line). The conjugate discrete Laplacian operator $\mathbf{M}^{\delta}\mathbf{L}^{\psi}$ converges faster (with second order accuracy) than $\mathbf{L}^{\psi}$ (which is first order accurate) in irregular grids. Therefore, hereinafter we will use the conjugate basis function $\delta_{\mu}(\mathbf{r})$ defined in (4.40) to discretize any continuous field in a Top-down approach. The conjugate basis function $\delta_{\mu}(\mathbf{r})$ will be also used to define the discrete concentration variables $\hat{\mathbf{c}}_{\mu}(\mathbf{z})$ given by (2.1) in a Bottom-up approach.

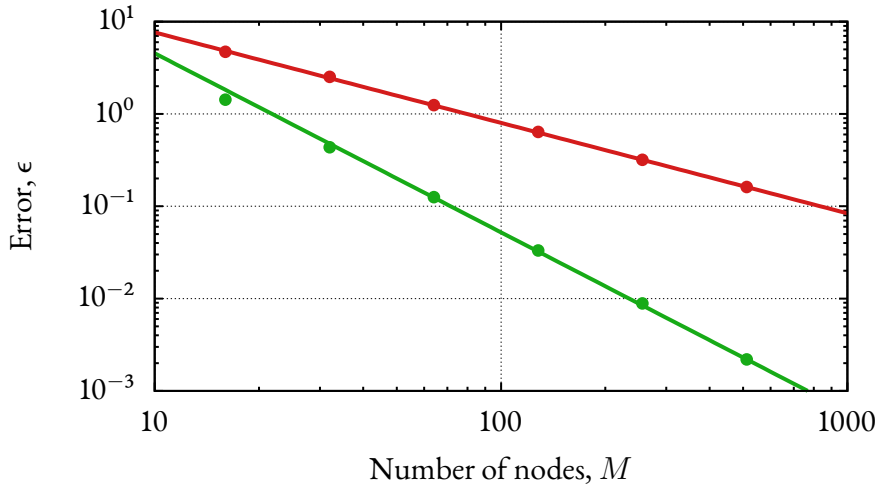


**Figure 4.9:** Error between the discrete Laplacian $\mathbf{L}^{\psi}$ (red) and $\mathbf{M}^{\delta}\mathbf{L}^{\psi}$ (green) for a discrete cosine (4.37). Dots represent the numerical error obtained with 100 configurations with nodes located at random positions. Lines represent a least squares adjustment.

# 5

# The Top-Down Approach for Discrete Diffusion

Where we discretize a continuum non-linear diffusion equation.

## 5.1. Introduction

In the previous chapters, by using the Theory of Coarse-Graining, we have obtained a discrete stochastic diffusion equation for the concentration field $\hat{c}_\mu(\mathbf{z})$. The discrete concentration field has been defined in terms of a discretization basis function $\psi_\mu(\mathbf{r})$, with support on the Delaunay triangulation. The SDE that describes the evolution of the coarse grained variables $\hat{c}_\mu(\mathbf{z})$ is given by (2.15). Two elements enter into that equation. A free energy functional $\hat{F}(\mathbf{c})$, and a dissipative matrix $\hat{\mathbf{D}}(\mathbf{c})$. We have obtained explicit expressions for them in terms of the basis function $\psi_\mu(\mathbf{r})$.

In SECTION 3.4 we have shown that the SDE (2.15) (which has been already displayed in (0.10)) can be understood as a discretization of the continuum PDE (0.3). We defined an space-averaged discrete concentration field $\overline{c}_\mu(t)$ based on the finite element $\psi_\mu(\mathbf{r})$. Then, we approximated continuum fields with interpolated fields constructed from the discrete concentration, by using the same finite element $\psi_\mu(\mathbf{r})$. In the INTERLUDE we have discussed the convenience of a new basis function $\delta_\mu(\mathbf{r})$, which is a linear combination of the finite element $\psi_\mu(\mathbf{r})$. The conjugate basis function $\delta_\mu(\mathbf{r})$ has the advantage of being a better discretization basis for irregular grids. We are interested in discretizations on *arbitrary* (not necessarily regular) grids because arbitrary grids can accommodate complex geometries and allow for adaptive spatial resolution.

The fact the SDE (0.10) and the PDE (0.3) lead to the same ODE under some assumptions indicates a possible connection between (0.10) and the *stochastic* PDE (0.4). Traditionally, the numerical solution of SPDEs of the kind (0.4) have resorted to finite difference schemes, [27, 74] that are easy to implement in regular lattices. However, as we pointed out in the INTRODUCTION, strictly speaking a finite difference scheme for an SPDE like (0.4) (without regularization) is meaningless in higher dimensions because taking the point-wise value of the field is not appropriate. Instead, one can use a finite volume method, in which the discrete variables are the fields integrated over the cell volume. [63] The resulting algorithm in regular grids looks like a finite difference method but the variables have very different meanings. While finite volumes may deal with adaptive resolutions and irregular grids [63], finite elements are often most natural when considering complicated boundary conditions. Finite element methods for the solution of SPDEs are just beginning to be explored [75–78]. In this chapter, we discuss in detail the general idea behind the definition of the conjugate basis function $\delta_\mu(\mathbf{r})$ defined in the INTERLUDE, and we construct a discretization method for the PDE (0.3). These are necessary steps prior to the obtention of a physically motivated SPDE in subsequent chapters.

## 5.2. Discretization and continuation operators

There are two basic operations in the process of discretizing a Partial Differential Equation. One is to discretize the fields and the other to interpolate discrete values of the fields. In this section we consider a general framework that leads to the definition of the conjugate basis functions.

Consider a continuous field $a(\mathbf{r})$ which is a differentiable function of space $\mathbf{r} \in \mathbb{R}^3$. We want to discretize this field in a set of points (or nodes) $R = \{\mathbf{r}_1, \ldots, \mathbf{r}_M\}$. This set of points $R$ is called a *configuration* and, if connectivity between points is defined, the points form a *mesh*. On every point $\mathbf{r}_\mu$ we associate a number $a_\mu$ that "represents" the field $a(\mathbf{r})$ at this point. The simplest option is to consider $a_\mu = a(\mathbf{r}_\mu)$, but there are of course many other possibilities. We call the collection $a_R$ of the pairs $(\mathbf{r}_\mu, a_\mu)$ a *discrete field*, while the original $(\mathbf{r}, a(\mathbf{r}))$ field is called the *continuous field*. It is obvious that a discrete field contains less information than a continuous field.

Let us generalize the procedure followed in Section 3.4 by introducing a *discretization operator* $\mathcal{D}_R$. It takes any continuous field and produces a discrete field, that is

$$\mathcal{D}_R\,[a(\mathbf{r})] = a_R\,.$$

The square brackets denote that $\mathcal{D}_R$ is a *functional* of $a(\mathbf{r})$ and the subindex $R$ denotes that the discretization depends on the configuration of the nodes $R$. Note that the discretization operator is surjective, that is, it converts many different continuous fields into the same discrete field. Loosely speaking, we say that the discretization operator *destroys*[i] information from the continuous field.

Reciprocally, we introduce a *continuation operator* $\mathcal{C}$ that takes a discrete field and transforms it into a continuous field, that is

$$\mathcal{C}(a_R) = a(\mathbf{r})\,.$$

The rounded parenthesis denote that $\mathcal{C}$ is a *function* of $a_R$. The continuation operator *creates*[ii] information in all points of space from the information $a_R$ given in a few points.

[i] For that reason, we will also call $\mathcal{D}$ the *destruction operator*.

[ii] By analogy with the destruction operator, we will also call $\mathcal{C}$ the *creation operator*.

### 5.2.1. Required properties for $\mathcal{D}_R$ and $\mathcal{C}$

A first property we would like to have for these operators is that if we continue a discrete field $a_R$ from a configuration $R$ and then we discretize it on the same configuration $R$, we should get the same original discrete field $a_R$. That is

$$\mathcal{D}_R\left[\mathcal{C}(a_R)\right] = a_R\,. \tag{5.1}$$

We call this the *projective property*. This seems a basic property to be satisfied by both $\mathcal{D}_R$ and $\mathcal{C}$.

The second property we would like to have is that the result of continuing a discrete field $a_R$ from a configuration $R$ and then discretizing at another configuration $R'$, that is, obtaining $a'_{R'}$, should be such that if we continue $a'_{R'}$ and discretize it at the configuration $R$, we get back $a_R$. Formally,

$$\begin{aligned} a'_{R'} &= \mathcal{D}_{R'}\left[\mathcal{C}(a_R)\right]\,, \\ a_R &= \mathcal{D}_R\left[\mathcal{C}(a'_{R'})\right]\,. \end{aligned} \tag{5.2}$$

We call this the *reversibility property*. This is a basic requirement that appears when considering the possibility of *remeshing* a field. Remeshing is the process by which a discrete field $a_R$, defined in a configuration $R$, is mapped onto a discrete field $a'_{R'}$ defined in another configuration $R'$. Therefore, the reversibility property states that the result of remeshing a discrete field into another configuration and remeshing again back to the original configuration should lead to the original discrete field. This property could be essential to reduce the "numerical diffusion" that appears in remeshing techniques. However, Eq. (5.2) implies

$$\mathcal{D}_R\left[\mathcal{C}(\mathcal{D}_{R'}\left[\mathcal{C}(a_R)\right])\right] = a_R\,. \tag{5.3}$$

Equation (5.1) shows that the operator $\mathcal{D}_R\mathcal{C}$ that takes discrete fields onto discrete fields is the identity operator, that is, $\mathcal{D}_R\mathcal{C} = \mathbf{1}$. This suggest that $\mathcal{D}_R$ and $\mathcal{C}$ may be inverse of each other. However, for a true inverse property, we would need to have also $\mathcal{C}\mathcal{D}_R = \mathbf{1}$. In general, the operator $\mathcal{C}\mathcal{D}_R$ transforms continuous fields into other continuous fields, for example,

$$\mathcal{C}(\mathcal{D}_{R'}\left[a(\mathbf{r})\right]) = \overline{a}(\mathbf{r})\,.$$

It is apparent that, in general, $\overline{a}(\mathbf{r}) \neq a(\mathbf{r})$ because many different continuous fields may discretize into the same discrete field. Note that Eq. (5.3) would be satisfied if and only if $\mathcal{C}\mathcal{D}_R$ would be the identity operator. However, necessarily the information contained in $\overline{a}(\mathbf{r})$ is smaller than the information contained in $a(\mathbf{r})$. We shall conclude that Eq. (5.3) cannot be generally valid. In fact, we have the following theorem. We define $f(\mathbf{r})$ as an *exactly continued field of* $\mathcal{C}$ if it satisfies

$$\mathcal{C}(f(\mathbf{r}_\mu)) = f(\mathbf{r})\,.$$

We may say that the operator $\mathcal{C}$ *exactly continues* these fields. Then, the projective property (5.1) implies that

$$\mathcal{D}_R\left[f(\mathbf{r})\right] = f(\mathbf{r}_\mu)\,.$$

And, as a consequence, for exactly continued fields, we have

$$\mathcal{C}\mathcal{D}_R\left[f(\mathbf{r})\right] = f(\mathbf{r})\,.$$

Therefore, given the projective property (5.1), the reversible property (5.2) is satisfied on all the continuous fields that are exactly continued by $\mathcal{C}$.

For example, assume that the exactly continued fields of $\mathcal{C}$ are quadratic functions. Then

$$\mathcal{C}(a + \mathbf{b}\cdot\mathbf{r}_\mu + \mathbf{c} : \mathbf{r}_\mu\mathbf{r}_\mu) = a + \mathbf{b}\cdot\mathbf{r} + \mathbf{c} : \mathbf{r}\mathbf{r}\,,$$

where $a$, $\mathbf{b}$ and $\mathbf{c}$ are constant. Then, by requiring that $\mathcal{D}_R\mathcal{C} = \mathbf{1}$ we obtain that the discretization operator $\mathcal{D}_R$ must satisfy

$$\begin{aligned}\mathcal{D}_R\left[1\right] &= 1\,,\\ \mathcal{D}_R\left[\mathbf{r}\right] &= \mathbf{r}_\mu\,,\\ \mathcal{D}_R\left[\mathbf{r}\mathbf{r}\right] &= \mathbf{r}_\mu\mathbf{r}_\mu\,.\end{aligned}$$

These properties, in turn, imply that,

$$\mathcal{C}\mathcal{D}_R\left[a + \mathbf{b}\cdot\mathbf{r} + \mathbf{c} : \mathbf{r}\mathbf{r}\right] = a + \mathbf{b}\cdot\mathbf{r} + \mathbf{c} : \mathbf{r}\mathbf{r}\,.$$

And, as a consequence, $\mathcal{C}\mathcal{D}_R = \mathbf{1}$ *if applied to quadratic functions.*

In conclusion, given the operators $\mathcal{D}_R$ and $\mathcal{C}$, it is very important to find out which are their exactly continued fields, because on these fields it is possible to have both the desired projective and reversibility properties.

### 5.2.2. Local operators

Up to now we have not specified the form of the operators $\mathcal{D}_R$ and $\mathcal{C}$. We introduce now a set of functions $\delta_\mu(\mathbf{r})$ and $\psi_\mu(\mathbf{r})$ associated to each point $\mathbf{r}_\mu$ that defines the position of a node $\mu$. We think about these functions as "localized" around each point, but this is not necessary for the moment. The discretization operator $\mathcal{D}_R$ is defined through the following action

$$\mathcal{D}_R\left[a(\mathbf{r})\right] \triangleq \int d\mathbf{r}\, \delta_\mu(\mathbf{r}) a(\mathbf{r}) = a_\mu\,,$$

that transforms an arbitrary field $a(\mathbf{r})$ into a set of discrete values $a_\mu$. The basis function $\delta_\mu(\mathbf{r})$ has dimensions of inverse of a volume. Reciprocally, the continuation operator $\mathcal{C}$ is defined as

$$\mathcal{C}(a_\mu) \triangleq \sum_\mu \psi_\mu(\mathbf{r}) a_\mu = a(\mathbf{r})\,.$$

The properties (5.1) and (5.3) now reflect onto properties for the functions $\delta_\mu(\mathbf{r})$ and $\psi_\mu(\mathbf{r})$. The first projection property in Eq. (5.1) becomes

$$\begin{aligned} a_\mu &= \mathcal{D}_\mu\left[\mathcal{C}(a_\mu)\right] \\ &= \mathcal{D}_\mu\left[\sum_\nu \psi_\nu(\mathbf{r}) a_\nu\right] \\ &= \sum_\nu \int d\mathbf{r}\, \delta_\mu(\mathbf{r}) \psi_\nu(\mathbf{r}) a_\nu\,. \end{aligned}$$

Because this must be true for all $a_\mu$, we obtain that the local versions of $\mathcal{D}_R$ and $\mathcal{C}$ will be projective if the basis functions satisfy the orthogonality condition

$$\int d\mathbf{r}\, \delta_\mu(\mathbf{r}) \psi_\nu(\mathbf{r}) = \delta_{\mu\nu}\,, \tag{5.4}$$

where $\delta_{\mu\nu}$ refers to the Kroenecker delta function, which takes the value 1 if and only if $\mu = \nu$ and 0 otherwise.

The reversibility property in Eq. (5.3) now becomes

$$\int d\mathbf{r}\, \delta_\nu(\mathbf{r}) \sum_{\mu'} \psi_{\mu'}(\mathbf{r}) \int d\mathbf{r}'\, \delta_{\mu'}(\mathbf{r}') \sum_{\mu} \psi_\mu(\mathbf{r}') a_\mu = a_\nu \,. \tag{5.5}$$

Note that here $\psi_{\mu'}(\mathbf{r})$ is the set of functions corresponding to the configuration $R'$, and it is different from $\psi_\mu(\mathbf{r})$ which is defined on the configuration $R$. Note that Eq. (5.5) implies, because $a_\mu$ is arbitrary, that

$$\int d\mathbf{r} \int d\mathbf{r}'\, \psi_\mu(\mathbf{r}) S(\mathbf{r},\mathbf{r}') \delta_\nu(\mathbf{r}') = \delta_{\mu\nu} \,, \tag{5.6}$$

where the *smoothing kernel* is defined as

$$S(\mathbf{r},\mathbf{r}') \triangleq \sum_{\sigma} \psi_\sigma(\mathbf{r}) \delta_\sigma(\mathbf{r}') \,. \tag{5.7}$$

The explicit form (5.6) of the reversibility condition is not very important because we already know that it is not possible to have Eq. (5.6) satisfied exactly in general. However, this identity will be satisfied automatically for the exactly continued fields.

### 5.2.3. The basis functions $\delta_\mu$ and $\psi_\mu$ are linearly related

We will assume now that the local discretization basis functions $\delta_\mu(\mathbf{r})$ can be expressed as linear combinations of the local continuation basis functions $\psi_\mu(\mathbf{r})$, that is

$$\delta_\mu(\mathbf{r}) \triangleq \sum_{\nu} M^{\delta}_{\mu\nu} \psi_\nu(\mathbf{r}) \,, \tag{5.8}$$

where $\mathbf{M}^\delta$ is the matrix of the linear combination. In this case, the projection property (5.1) turns into

$$\delta_{\mu\nu} = \int d\mathbf{r}\, \delta_\mu(\mathbf{r}) \psi_\nu(\mathbf{r}) = \sum_{\sigma} M^{\delta}_{\mu\sigma} M^{\psi}_{\sigma\nu} \,, \tag{5.9}$$

where the symmetric and positive definite *mass matrix* is defined as

$$M^{\psi}_{\mu\nu} \triangleq \int d\mathbf{r}\, \psi_{\mu}(\mathbf{r})\psi_{\nu}(\mathbf{r})\,. \tag{5.10}$$

If we assume that the basis functions $\psi_{\mu}(\mathbf{r})$ are dimensionless, the mass matrix $\mathbf{M}^{\psi}$ has dimensions of volume. According to the projective property (5.9), we have that the matrices $\mathbf{M}^{\delta}$ and $\mathbf{M}^{\psi}$ are inverse each other

$$\mathbf{M}^{\delta} = \left[\mathbf{M}^{\psi}\right]^{-1}\,.$$

It is easy to show that the matrix element $M^{\delta}_{\mu\nu}$ is given by

$$M^{\delta}_{\mu\nu} = \int d\mathbf{r}\, \delta_{\mu}(\mathbf{r})\delta_{\nu}(\mathbf{r})\,. \tag{5.11}$$

In summary, given a set of continuation weight functions $\psi_{\mu}(\mathbf{r})$ we can always construct a set of discretization weight functions $\delta_{\mu}(\mathbf{r})$ with

$$\delta_{\mu}(\mathbf{r}) = \sum_{\nu} \left(M^{\psi}\right)^{-1}_{\mu\nu} \psi_{\nu}(\mathbf{r})\,. \tag{5.12}$$

in such a way that the projective property (5.4) is satisfied.

In the following, we define the vectors

$$\boldsymbol{\delta}(\mathbf{r}) \triangleq \{\delta_1(\mathbf{r}), \ldots, \delta_M(\mathbf{r})\}\,,$$
$$\boldsymbol{\psi}(\mathbf{r}) \triangleq \{\psi_1(\mathbf{r}), \ldots, \psi_M(\mathbf{r})\}\,,$$

so that we may write (5.12) as

$$\boldsymbol{\delta}(\mathbf{r}) = \mathbf{M}^{\delta}\boldsymbol{\psi}(\mathbf{r})\,.$$

Then, the mass matrices $\mathbf{M}^{\delta}$ and $\mathbf{M}^{\psi}$ may be written as

$$\mathbf{M}^{\delta} = (\boldsymbol{\delta}^T, \boldsymbol{\delta})\,,$$
$$\mathbf{M}^{\psi} = (\boldsymbol{\psi}^T, \boldsymbol{\psi})\,,$$

with an obvious notation for the scalar product $(\cdot,\cdot)$ in functional space.

### 5.2.4. Linear consistency

We further assume that the functions $\psi_\mu(\mathbf{r})$ satisfy the partition of unity and linear consistency properties

$$\begin{aligned} \sum_\mu \psi_\mu(\mathbf{r}) &= 1\,, \\ \sum_\mu \mathbf{r}_\mu \psi_\mu(\mathbf{r}) &= \mathbf{r}\,. \end{aligned} \tag{5.13}$$

In this way, a linear discrete field of the form $a_\mu = a + \mathbf{b}\cdot\mathbf{r}_\mu$ is continued into a linear field, that is

$$\mathcal{C}(a + \mathbf{b}\cdot\mathbf{r}_\mu) = a + \mathbf{b}\cdot\mathbf{r}\,.$$

As a consequence of Eq. (5.4) and Eq. (5.13), we have that the functions $\delta_\mu(\mathbf{r})$ satisfy

$$\begin{aligned} \int d\mathbf{r}\, \delta_\mu(\mathbf{r}) &= 1\,, \\ \int d\mathbf{r}\, \mathbf{r}\delta_\mu(\mathbf{r}) &= \mathbf{r}_\mu\,. \end{aligned} \tag{5.14}$$

So, if the projective property (5.4) and the linear consistency property (5.13) are both satisfied, then the required reversibility property in (5.5) is fully ac-

complished for *linear discrete fields* of the form $a_\mu = a + \mathbf{b} \cdot \mathbf{r}_\mu$, that is,

$$\begin{aligned}
&\int d\mathbf{r}\, \delta_\nu(\mathbf{r}) \sum_{\mu'} \psi_{\mu'}(\mathbf{r}) \int d\mathbf{r}'\, \delta_{\mu'}(\mathbf{r}') \sum_{\mu} \psi_\mu(\mathbf{r}') a_\mu \\
&\qquad = \int d\mathbf{r}\, \delta_\nu(\mathbf{r}) \sum_{\mu'} \psi_{\mu'}(\mathbf{r}) \int d\mathbf{r}'\, \delta_{\mu'}(\mathbf{r}') \sum_{\mu} \psi_\mu(\mathbf{r}') \left[a + \mathbf{b} \cdot \mathbf{r}'_\mu\right] \\
&\qquad = \int d\mathbf{r}\, \delta_\nu(\mathbf{r}) \sum_{\mu'} \psi_{\mu'}(\mathbf{r}) \int d\mathbf{r}'\, \delta_{\mu'}(\mathbf{r}') \left[a + \mathbf{b} \cdot \mathbf{r}'\right] \\
&\qquad = \int d\mathbf{r}\, \delta_\nu(\mathbf{r}) \sum_{\mu'} \psi_{\mu'}(\mathbf{r}) \left[a + \mathbf{b} \cdot \mathbf{r}_{\mu'}\right] \\
&\qquad = \int d\mathbf{r}\, \delta_\nu(\mathbf{r}) \left[a + \mathbf{b} \cdot \mathbf{r}\right] \\
&\qquad = \left[a + \mathbf{b} \cdot \mathbf{r}_\nu\right] \\
&\qquad = a_\nu \,.
\end{aligned}$$

Let us investigate to what extent we may have properties similar to (5.13) for the discretization basis function $\delta_\mu(\mathbf{r})$. To this end, we first introduce the volume and center of mass of the cell corresponding to node $\mu$ through the definitions

$$\begin{aligned}
V_\mu &\triangleq \int d\mathbf{r}\, \psi_\mu(\mathbf{r}) \,, \\
\mathbf{r}_\mu^{\mathrm{cm}} &\triangleq \frac{1}{V_\mu} \int d\mathbf{r}\, \mathbf{r} \psi_\mu(\mathbf{r}) \,.
\end{aligned}$$

The linear consistency (5.13) has the following implications on the mass matrix defined in Eq. (5.10)

$$\begin{aligned}
\sum_\nu M^\psi_{\mu\nu} &= V_\mu \,, \\
\sum_\nu \mathbf{r}_\nu M^\psi_{\mu\nu} &= V_\mu \mathbf{r}_\mu^{\mathrm{cm}} \,.
\end{aligned}$$

These two equations can be thought as matrix equations that may be inverted, leading to

$$\sum_{\nu} V_{\nu} M^{\delta}_{\mu\nu} = 1 \,,$$
$$\sum_{\nu} V_{\nu} \mathbf{r}_{\nu} M^{\delta}_{\mu\nu} = \mathbf{r}^{\mathrm{cm}}_{\mu} \,.$$

By multiplying with $\psi_{\nu}(\mathbf{r})$ and summing over $\nu$, we have

$$\sum_{\nu} V_{\nu} \delta_{\nu}(\mathbf{r}) = 1 \,,$$
$$\sum_{\nu} V_{\nu} \mathbf{r}_{\nu} \delta_{\nu}(\mathbf{r}) = \sum_{\nu} \mathbf{r}^{\mathrm{cm}}_{\nu} \psi_{\nu}(\mathbf{r}) \,.$$

If the center of mass $\mathbf{r}^{\mathrm{cm}}_{\nu}$ of cell $\nu$ coincides with the node position $\mathbf{r}_{\nu}$, then we have a similar linear consistency relation for the discretization basis functions $\delta_{\mu}(\mathbf{r})$,

$$\sum_{\mu} V_{\mu} \delta_{\mu}(\mathbf{r}) = 1 \,,$$
$$\sum_{\mu} V_{\mu} \mathbf{r}_{\mu} \delta_{\mu}(\mathbf{r}) = \mathbf{r} \,. \tag{5.15}$$

In regular grids, with fixed lattice spacing, it always happens that the center of mass of a cell is just at the node of that cell. We may have grids with different cell size for which still the center of mass of the cell falls on top of the node. Such grids are called *centroidal*. Regular grids are a particular case of a centroidal grid. Therefore, *for centroidal grids* the destruction operators $\delta_{\mu}(\mathbf{r})$ are also linearly consistent.

Finally, for a linearly consistent scheme, we note the following identities re-

lated to the smoothing kernel $S(\mathbf{r}, \mathbf{r}')$

$$\begin{aligned}\int d\mathbf{r}\, S(\mathbf{r}, \mathbf{r}') &= \sum_{\nu} \int d\mathbf{r}\, \psi_{\nu}(\mathbf{r})\delta_{\nu}(\mathbf{r}') = \sum_{\mu\nu} \int d\mathbf{r}\, \psi_{\mu}(\mathbf{r})\psi_{\nu}(\mathbf{r})\delta_{\nu}(\mathbf{r}') \\ &= \sum_{\mu\nu} M^{\psi}_{\mu\nu}\delta_{\nu}(\mathbf{r}') = \sum_{\mu} \psi_{\mu}(\mathbf{r}') \\ &= 1\,,\end{aligned}$$

and

$$\begin{aligned}\int d\mathbf{r}\, \mathbf{r} S(\mathbf{r}, \mathbf{r}') &= \sum_{\nu} \int d\mathbf{r}\, \mathbf{r}\psi_{\nu}(\mathbf{r})\delta_{\nu}(\mathbf{r}') = \sum_{\mu\nu} \int d\mathbf{r}\, \mathbf{r}_{\mu}\psi_{\mu}(\mathbf{r})\psi_{\nu}(\mathbf{r})\delta_{\nu}(\mathbf{r}') \\ &= \sum_{\mu\nu} \mathbf{r}_{\mu} M^{\psi}_{\mu\nu}\delta_{\nu}(\mathbf{r}') = \sum_{\mu} \mathbf{r}_{\mu}\psi_{\mu}(\mathbf{r}') \\ &= \mathbf{r}'\,. \end{aligned} \tag{5.16}$$

In this sense, we may understand $S(\mathbf{r}, \mathbf{r}')$ as a "fat" Dirac delta that gives the same result as the Dirac delta for linear functions.

### 5.2.5. Spatial derivatives

Given the discrete version $a_R$ of a field, we now estimate spatial derivatives at the configuration $R$. One possibility is to continue $a_R$, compute the derivatives and then discretize back the derivative function at $R$. For the case of the gradient, for example, we may define

$$(\boldsymbol{\nabla} a)_R \triangleq \mathcal{D}_R \left[\boldsymbol{\nabla} \mathcal{C}(a_R)\right]\,.$$

For local operators we have the following estimate for the gradient

$$(\boldsymbol{\nabla} a)_{\mu} = \sum_{\nu} \Omega_{\mu\nu} a_{\nu}\,,$$

with

$$\Omega_{\mu\nu} \triangleq \int d\mathbf{r}\, \delta_{\mu}(\mathbf{r}) \boldsymbol{\nabla} \psi_{\nu}(\mathbf{r})\,.$$

Care should be taken if we consider the discretization of a field like $c(\mathbf{r}) = a(\mathbf{r})b(\mathbf{r})$. In principle, one can follow two different routes to obtain the derivatives of the discrete field. On one hand,

$$\begin{aligned}(\nabla c)_\mu = (\nabla ab)_\mu &= \sum_{\nu\nu'} \int d\mathbf{r}\, \delta_\mu(\mathbf{r}) \nabla \left(\psi_\nu(\mathbf{r})\psi_{\nu'}(\mathbf{r})\right) a_\nu b_{\nu'} \\ &= \sum_{\nu\nu'} \int d\mathbf{r}\, \delta_\mu(\mathbf{r}) \left(\psi_\nu(\mathbf{r}) a_\nu \nabla\psi_{\nu'} b_{\nu'} + \psi_{\nu'}(\mathbf{r}) b_{\nu'} \nabla\psi_\nu a_\nu\right) \\ &= (a\nabla b)_\mu + (b\nabla a)_\mu \,, \end{aligned} \tag{5.17}$$

which complies with Leibnitz's product rule.

On the other hand, one would also take the product $a(\mathbf{r})b(\mathbf{r})$ as a single block

$$\begin{aligned}(\nabla c)_\mu = (\nabla ab)_\mu &= \sum_{\nu} \int d\mathbf{r}\, \delta_\mu(\mathbf{r}) \nabla\psi_\nu(\mathbf{r}) a_\nu b_\nu \\ &\neq (a\nabla b)_\mu + (b\nabla a)_\mu \,. \end{aligned} \tag{5.18}$$

Note that the derivative (5.18) does not comply with the Leibnitz's product rule. In conclusion, we shall always prefer the form (5.17) over the form (5.18).

Let us move now to the definition of discrete second derivatives, obtained as

$$(\boldsymbol{\nabla}\boldsymbol{\nabla} a)_R \triangleq \mathcal{D}_R \left[\boldsymbol{\nabla}\boldsymbol{\nabla}\mathcal{C}(a_R)\right] \,, \tag{5.19}$$

which gives

$$(\boldsymbol{\nabla}\boldsymbol{\nabla} a)_\mu = -\sum_\nu \Delta_{\mu\nu} a_\nu$$

with

$$\begin{aligned}\Delta_{\mu\nu} &\triangleq -\int d\mathbf{r}\, \delta_\mu(\mathbf{r}) \boldsymbol{\nabla}\boldsymbol{\nabla}\psi_\nu(\mathbf{r}) \\ &= \int d\mathbf{r}\, \boldsymbol{\nabla}\delta_\mu(\mathbf{r}) \boldsymbol{\nabla}\psi_\nu(\mathbf{r}) \,. \end{aligned} \tag{5.20}$$

We may use the linear connection between the two sets of basis functions and write in compact matrix form the following identities

$$\Delta = \mathbf{M}^{\delta}\mathbf{L}^{\psi} = \mathbf{L}^{\delta}\mathbf{M}^{\psi}\,,$$

where we have introduced the *stiffness matrices* in each basis set as

$$\begin{aligned}\mathbf{L}^{\psi} &\triangleq \left(\boldsymbol{\nabla}\psi, \boldsymbol{\nabla}\psi^{T}\right)\,,\\ \mathbf{L}^{\delta} &\triangleq \left(\boldsymbol{\nabla}\delta, \boldsymbol{\nabla}\delta^{T}\right)\,.\end{aligned} \tag{5.21}$$

Note that $\mathbf{L}^{\psi}$ and $\mathbf{L}^{\delta}$ are related according to

$$\begin{aligned}\mathbf{L}^{\delta} &= \mathbf{M}^{\delta}\mathbf{L}^{\psi}\mathbf{M}^{\delta}\,,\\ \mathbf{L}^{\psi} &= \mathbf{M}^{\psi}\mathbf{L}^{\delta}\mathbf{M}^{\psi}\,.\end{aligned}$$

Also note that the matrix $\mathbf{L}^{\delta}$ satisfies, thanks to (5.13) and (5.15), the following identities

$$\begin{aligned}\sum_{\mu} L^{\psi}_{\mu\nu} &= 0\,,\\ \sum_{\mu} V_{\mu} L^{\delta}_{\mu\nu} &= 0\,,\end{aligned}$$

which shows that the vectors $(1, \cdots, 1)$ and $(V_1, \cdots, V_M)$ are eigenvectors in the null space of $\mathbf{L}^{\delta}$.

In principle, we may also define second derivatives in an alternative way as the result of two iterations of first derivatives. In particular, we could also define

$$\begin{aligned}(\boldsymbol{\nabla}\boldsymbol{\nabla}a)_R &= \mathcal{D}_R\left[\boldsymbol{\nabla}\mathcal{C}\left((\boldsymbol{\nabla}a)_R\right)\right]\\ &= \mathcal{D}_R\left[\boldsymbol{\nabla}\mathcal{C}\left(\mathcal{D}_R\left[\boldsymbol{\nabla}\mathcal{C}(a_R)\right]\right)\right]\,.\end{aligned} \tag{5.22}$$

Note the presence of the operator $\mathcal{C}\mathcal{D}_R$. As we discussed previously, this operator *is not* the identity in general. It acts as the identity only when we apply

it on exactly continued fields. Indeed, for exactly continued fields, we have $\mathcal{C}(\mathcal{D}_R[\boldsymbol{\nabla}\mathcal{C}(a_R)]) = \boldsymbol{\nabla}\mathcal{C}(a_R)$ and, therefore, (5.22) becomes again (5.19). In terms of the discrete operators $\Omega_{\mu\nu}$, the second derivative constructed iteratively is

$$(\boldsymbol{\nabla}\boldsymbol{\nabla}a)_\mu = \sum_{\nu\sigma} \Omega_{\mu\nu}\Omega_{\nu\sigma}a_\sigma$$

It is apparent that $\sum_\nu \Omega_{\mu\nu}\Omega_{\nu\sigma} \neq \Delta_{\mu\sigma}$ in general. However, when applied onto exactly continued fields, both discretizations of second order derivatives coincide.

## 5.3. Petrov-Galerkin Weighted Residuals method

Up to now we have just a language to discretize and interpolate functions and its derivatives, in a local form. We use now this language to discretize partial differential equations like the diffusion equation (0.3)

$$\frac{\partial c}{\partial t}(\mathbf{r},t) = \boldsymbol{\nabla}\cdot\left[\Gamma(c(\mathbf{r},t))\boldsymbol{\nabla}\frac{\delta\mathcal{F}}{\delta c(\mathbf{r},t)}[c(\mathbf{r},t)]\right] .$$

A general method for discretizing partial differential equations is the Weighted Residual method [79]. With the use of two different sets of basis functions, the method is known as the Petrov-Galerkin method. As we discuss in Appendix E, the order of convergence of the Petrov-Galerkin method with linearly consistent basis functions is of second order.

The idea of weighted residuals is to approximate the actual solution $c(\mathbf{r},t)$ of the PDE (0.3) with its interpolated version $\overline{c}(\mathbf{r},t)$, in such a way that

$$c(\mathbf{r},t) \approx \overline{c}(\mathbf{r},t) = \sum_\mu \psi_\mu(\mathbf{r})c_\mu(t) \tag{5.23}$$

where now

$$\begin{aligned} c_\mu(t) &= \int d\mathbf{r}\,\delta_\mu(\mathbf{r})c(\mathbf{r},t) \\ &= \sum_\nu M^\delta_{\mu\nu}\int d\mathbf{r}\,\psi_\nu(\mathbf{r})c(\mathbf{r},t)\,. \end{aligned} \tag{5.24}$$

becomes the unknown of the problem.

One defines the residual as the result obtained after substitution in the PDE (0.3) of the approximate field (5.23)

$$R(\mathbf{r}) \triangleq \frac{\partial \overline{c}}{\partial t}(\mathbf{r},t) - \boldsymbol{\nabla} \cdot \left[ \Gamma(\overline{c}(\mathbf{r},t)) \boldsymbol{\nabla} \frac{\delta \mathcal{F}}{\delta c(\mathbf{r})}[\overline{c}] \right] .$$

If $\overline{c}(\mathbf{r},t)$ was a solution of the diffusion equation (0.3), the residual would be zero. By weighting the residual with weights $\delta_\mu(\mathbf{r})$, and requiring the weighted residual to vanish we obtain

$$\begin{aligned} \frac{\partial \mathbf{c}}{\partial t}(t) &= \left( \delta, \boldsymbol{\nabla} \cdot \left[ \Gamma(\overline{c}(\mathbf{r},t)) \boldsymbol{\nabla} \frac{\delta \mathcal{F}}{\delta c}[\overline{c}(t)] \right] \right) \\ &= - \left( \boldsymbol{\nabla} \boldsymbol{\delta}, \Gamma(\overline{c}(\mathbf{r},t)) \boldsymbol{\nabla} \frac{\delta \mathcal{F}}{\delta c}[\overline{c}(t)] \right) , \end{aligned} \tag{5.25}$$

where we did an integration by parts. Formally, Eq. (5.25) is a set of $M$ ordinary differential equations for the $M$ unknowns $\mathbf{c}(t)$.

It is apparent that we cannot proceed until we have a way to compute the functional derivative $\frac{\delta \mathcal{F}}{\delta c}$. To this end we *define* the discrete free energy function $F(\mathbf{c})$ as

$$F(\mathbf{c}) \triangleq \mathcal{F}\left[ \boldsymbol{\psi} \cdot \mathbf{c} \right] , \tag{5.26}$$

that is, the free energy *function* of the discrete field $\mathbf{c}$ is obtained by evaluating the free energy *functional* at the interpolated field. What we need, though, is not a discrete approximation for the functional, but a discrete approximation for its functional derivative. By using the functional chain rule we may compute the derivative of the function (5.26)

$$\frac{\partial F}{\partial c_\mu}(\mathbf{c}) = \int d\mathbf{r}' \frac{\delta \mathcal{F}}{\delta c(\mathbf{r}')} \left[ \boldsymbol{\psi} \cdot \mathbf{c} \right] \psi_\mu(\mathbf{r}') . \tag{5.27}$$

Let us multiply Eq. (5.27) with the basis function $\delta(\mathbf{r})$

$$\delta(\mathbf{r}) \cdot \frac{\partial F}{\partial \mathbf{c}}(\mathbf{c}) = \int d\mathbf{r}' \frac{\delta \mathcal{F}}{\delta c(\mathbf{r}')} \left[ \psi \cdot \mathbf{c} \right] S(\mathbf{r},\mathbf{r}') , \tag{5.28}$$

where the smoothing kernel $S(\mathbf{r}, \mathbf{r}')$ is defined in (5.7). We will assume that the functional derivative does not change appreciably within the range of $S(\mathbf{r}, \mathbf{r}')$. In this case, we may simply write from Eq. (5.28)

$$\int d\mathbf{r}' \frac{\delta \mathcal{F}}{\delta c(\mathbf{r}')} \left[\boldsymbol{\psi} \cdot \mathbf{c}\right] S(\mathbf{r}, \mathbf{r}') \approx \frac{\delta \mathcal{F}}{\delta c(\mathbf{r})} \left[\boldsymbol{\psi} \cdot \mathbf{c}\right] \,,$$

and, therefore, we have an approximate expression for the functional derivative

$$\frac{\delta \mathcal{F}}{\delta c(\mathbf{r})}[\bar{c}] = \frac{\delta \mathcal{F}}{\delta c(\mathbf{r})} \left[\boldsymbol{\psi} \cdot \mathbf{c}\right] \approx \boldsymbol{\delta}(\mathbf{r}) \cdot \frac{\partial F}{\partial \mathbf{c}}(\mathbf{c}) \,. \tag{5.29}$$

We may introduce (5.29) into (5.25) and obtain

$$\frac{d\mathbf{c}}{dt}(t) = -\mathbf{D}(\mathbf{c}) \cdot \frac{\partial F}{\partial \mathbf{c}}(\mathbf{c}) \,, \tag{5.30}$$

where the dissipative matrix has the elements

$$D_{\mu\nu}(\mathbf{c}) = \int d\mathbf{r}\, \boldsymbol{\nabla} \delta_\mu(\mathbf{r}) \cdot \Gamma \left( \sum_\sigma \psi_\sigma(\mathbf{r}) c_\sigma \right) \boldsymbol{\nabla} \delta_\nu(\mathbf{r}) \,. \tag{5.31}$$

The form (5.31) for the dissipative matrix involves a space integral that needs to be computed explicitly in order to introduce it in a computer code. Note that the mobility depends on the position through its dependence on the concentration field and, therefore, such space integrals are not immediate. We will use the following approximation

$$\Gamma \left( \sum_\sigma \psi_\sigma(\mathbf{r}) c_\sigma \right) \approx \sum_\sigma \psi_\sigma(\mathbf{r}) \Gamma \left( c_\sigma \right) \,, \tag{5.32}$$

in such a way that the mobility function at the interpolated field is approximated by a linear interpolation of the mobility function at the nodes. The approximation is exact for the nodal points $\mathbf{r} = \mathbf{r}_\mu$. It is expected that this approximation is appropriate for smooth functions $\Gamma(c)$, provided that the mesh

size is sufficiently small. With the approximation in Eq. (5.32), the dissipative matrix (5.31) becomes

$$D_{\mu\nu}(\mathbf{c}) = \sum_{\sigma} \Gamma(c_\sigma) \int d\mathbf{r} \boldsymbol{\nabla}\delta_\mu(\mathbf{r}) \psi_\sigma(\mathbf{r}) \boldsymbol{\nabla}\delta_\nu(\mathbf{r}) \,, \tag{5.33}$$

This matrix is positive semi-definite because if we multiply both sides of the matrix with an arbitrary vector $a_\mu$ we have

$$\sum_{\mu\nu} a_\mu D_{\mu\nu}(\mathbf{c}) a_\nu = \sum_{\sigma} \Gamma(c_\sigma) \int d\mathbf{r} \left( \sum_{\mu} a_\mu \boldsymbol{\nabla}\delta_\mu(\mathbf{r}) \right)^2 \psi_\sigma(\mathbf{r}) \,,$$

which is clearly a positive quantity because $\Gamma > 0$ and the finite element $\psi_\mu(\mathbf{r}) \geq 0$. The semi character is due to the Eq. (5.15).

The integral in (5.33) is a geometric object readily computable as we show in what follows. For the linear finite elements $\psi_\mu(\mathbf{r})$, we may explicitly compute the gradient of the basis functions

$$\begin{aligned} \boldsymbol{\nabla}\delta_\mu(\mathbf{r}) &= \sum_{\mu'} M^{\delta}_{\mu\mu'} \boldsymbol{\nabla}\psi_{\mu'}(\mathbf{r}) \\ \boldsymbol{\nabla}\psi_{\mu'}(\mathbf{r}) &= \sum_{e\in\mu'} \mathbf{b}_{e\to\mu'} \theta_e(\mathbf{r}) \end{aligned} \tag{5.34}$$

where $\theta_e(\mathbf{r})$ is the characteristic function of the sub-element $e$. The gradient of the basis function $\psi_\mu(\mathbf{r})$ is a constant vector $\mathbf{b}_{e\to\mu}$ for those points $\mathbf{r}$ that are within the sub-element $e \in \mu$ of node $\mu$. [32] In Fig. 5.1 we show the sub-elements $e$ of the node $\mu$ and the corresponding vectors $\mathbf{b}_{e\to\mu}$ in 2D. By using (5.34) we have

$$\begin{aligned} D_{\mu\nu}(\mathbf{c}) &= \sum_{\mu'\nu'} M^{\delta}_{\mu\mu'} M^{\delta}_{\nu\nu'} \sum_{e\in\mu',\nu'} \mathbf{b}_{e\to\mu'} \mathbf{b}_{e\to\nu'} V_e \Gamma_e(\mathbf{c}) \\ &= \sum_{\mu'\nu'} M^{\delta}_{\mu\mu'} V_{\mu'} \hat{D}_{\mu'\nu'}(\mathbf{c}) V_{\nu'} M^{\delta}_{\nu'\nu} \,. \end{aligned} \tag{5.35}$$

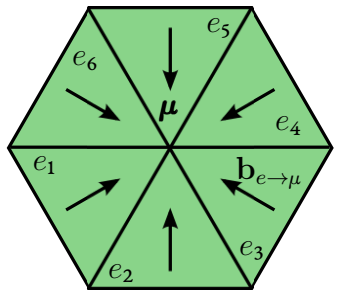


**Figure 5.1:** In $2D$, the Delaunay cell of node $\mu$ is surrounded by the triangular elements $e$. For each point of the triangular element $e$, there is a constant vector $\mathbf{b}_{e\to\mu}$ that points towards the node $\mu$ and that gives the derivative of the linear function $\psi_\mu(\mathbf{r})$ at that point.

Here, the dissipative matrix $\hat{D}_{\mu\nu}$ has been already defined in (3.12). Note that we also have introduced the mobility $\Gamma_e$ of the element $e$ as

$$\Gamma_e(\mathbf{c}) \triangleq \sum_{\sigma\in e} W_{\sigma e}\Gamma(c_\sigma)\,, \tag{5.36}$$

and represents a weighted average of the mobility associated to the nodes $\sigma$ that are the vertices of the element $e$. We have introduced the volume of element $e$ and the geometric ratio $W_{e\sigma}$ as

$$V_e \triangleq \int d\mathbf{r}\,\theta_e(\mathbf{r})\,,$$
$$W_{\sigma e} \triangleq \frac{\int d\mathbf{r}\,\theta_e(\mathbf{r})\psi_\sigma(\mathbf{r})}{\int d\mathbf{r}\,\theta_e(\mathbf{r})}\,.$$

## 5.4. Summary

In this chapter, we have used a Top-down approach to obtain a discrete diffusion equation for the concentration field. We have started from the continuum diffusion equation (0.3), and have used a Petrov-Galerkin Weighted Residual Method to write the discrete diffusion equation as in (5.30) that we write down again

$$\frac{\partial \mathbf{c}}{\partial t}(t) = -\mathbf{D}(\mathbf{c})\cdot\frac{\partial F}{\partial \mathbf{c}}(\mathbf{c})\,,$$

where the free energy function and the dissipative matrix take the explicit forms given by (5.26) and (5.35), respectively. The method uses the concept of mutually orthogonal sets of discretization basis functions $\delta_\mu(\mathbf{r})$ and continuation basis functions $\psi_\mu(\mathbf{r})$.

The total number of particles, defined as $N = \sum_\mu V_\mu \mathbf{c}_\mu(t)$ is a dynamical invariant of the equation (5.30). The time derivative of the discrete free energy $F(\mathbf{c}(t))$, which is given by

$$\frac{dF}{dt}(\mathbf{c}(t)) = -\frac{\partial F}{\partial \mathbf{c}}(\mathbf{c}) \cdot \mathbf{D}(\mathbf{c}) \cdot \frac{\partial F}{\partial \mathbf{c}}(\mathbf{c}) \leq 0\,,$$

is always negative or zero, because $\mathbf{D}(\mathbf{c})$ is semi-positive definite. Therefore, we have obtained in Eq. (5.30) a discrete version of the non-linear diffusion equation (0.3) that captures the two essential features about conservation of the number of particles and the Second Law (or H-theorem).

The Petrov-Galerkin method leads to a positive semi definite dissipative matrix. This property is crucial for representing at the discrete level the H-theorem satisfied by the original PDE (0.3). More importantly, the dissipative matrix needs to be positive definite if thermal fluctuations are to be introduced in the equation (as we will do in the next chapter) because, according to the Fluctuation-Dissipation Theorem, the positive-definite covariance matrix of the random terms is just the dissipative matrix.

The method presented for the discretization of the diffusion equation is general, valid for regular and irregular grids, and in any dimension. Given the linear consistency inherent in the scheme, we expect that the convergence of the equations will be of second order with respect to the lattice spacing.

This chapter generalizes the obtention of a discrete ODE for the diffusion starting from the continuum PDE (0.3). In SECTION 3.4 we obtained a similar ODE but using as basis function the finite element with support on the Delaunay triangulation. From the discussion in the INTERLUDE it is clear that, in order to work with arbitrary grids, the use of the conjugated finite element $\delta_\mu(\mathbf{r})$ defined in (5.12) is much better. With this idea, the proposed forms of the discrete free energy function (5.26) and the dissipative matrix (5.35) are expected to fit better to the continuum diffusion equation (0.3).

The only approximation that we have taken is that the functional derivative of the free energy functional hardly changes in the range of $S(\mathbf{r}, \mathbf{r}')$ defined in

Eq. (5.7). We plot this function in Fig. 5.2 and we observe that if the average lattice spacing is much smaller than the length scale of variation of the field, then the approximation (5.29) will be appropriate. Of course, this argument holds for the deterministic setting where the fields are smooth. In a stochastic setting as set forth in the next chapter, for which, in general, the fields are extremely irregular, the procedure should be understood not as an approximation but rather as a *definition* of the discrete model itself.

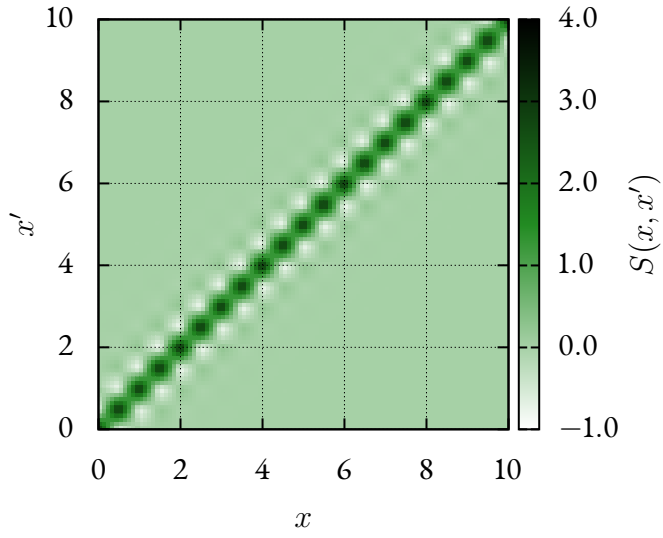


**Figure 5.2:** Plot of $S(x, x')$ in a $1D$ grid with length $L = 10$ and lattice spacing $a = 0.5$. The function $S(x, x')$ does not vanish only for points differing by a few (2 or 3) lattice spacings.

# 6

# The Bottom-Up Approach for Discrete Diffusion with Conjugate Finite Elements

Where the Bottom-up approach meets the Top-down approach.

## 6.1. Introduction

In the Introduction we mentioned that the non-linear diffusion equation (0.3)

$$\frac{\partial c}{\partial t}(\mathbf{r}, t) = \nabla \cdot \left[ \Gamma(c(\mathbf{r}, t)) \nabla \frac{\delta \mathcal{F}}{\delta c}[c(\mathbf{r}, t)] \right] \tag{6.1}$$

can be obtained from microscopic principles with the technique of projection operators. [49, 68] The basic idea of this technique is to obtain a closed dy-

namic equation for the ensemble average concentration field

$$c(\mathbf{r},t) = \int d\mathbf{z}\, \rho(\mathbf{z},t)\hat{c}_{\mathbf{r}}(\mathbf{z})\,,$$

where the microscopic concentration field is defined as

$$\hat{c}_{\mathbf{r}}(\mathbf{z}) = \sum_i \delta(\mathbf{r}-\mathbf{r}_i)\,. \tag{6.2}$$

Next, in CHAPTER 5 we discretized Eq. (6.1) with a Petrov-Galerkin Weighted Residual method [79] that produced a closed equation for the discrete concentration field defined as

$$c_\mu(t) = \int d\mathbf{r}\, \delta_\mu(\mathbf{r}) c(\mathbf{r},t)\,. \tag{6.3}$$

This variable can be obviously interpreted as the ensemble average

$$c_\mu(t) = \int d\mathbf{z}\, \rho(\mathbf{z},t)\hat{c}_\mu(\mathbf{z})\,,$$

where the coarse grained variable $\hat{c}_\mu(\mathbf{z})$ takes the form, by using the conjugate finite element $\delta_\mu(\mathbf{r})$ defined in (5.8)

$$\hat{c}_\mu(\mathbf{z}) = \sum_i \delta_\mu(\mathbf{r}_i) = \sum_\nu M^\delta_{\mu\nu} \sum_i \psi_\nu(\mathbf{r}_i)\,. \tag{6.4}$$

We could reproduce the steps leading to (6.1) made in the microscopic derivation in Ref. [68], that stars from (6.2), with (6.4) instead. The procedure (that we do not present here) results in a dynamic equation for the averages that has exactly the form of (5.30), with a dissipative matrix given by (2.14). However, we are interested in fluctuations and therefore we aim at the derivation of the FPE or the equivalent SDE when the discrete variables are given by (6.3), with the $\delta_\mu(\mathbf{r})$ basis functions given by (5.8),

$$\delta_\mu(\mathbf{r}) \to \sum_\nu M^\delta_{\mu\nu}\psi_\nu(\mathbf{r})\,. \tag{6.5}$$

Note that we already obtained in CHAPTER 3 the FPE for $\delta_\mu(\mathbf{r}) \to \psi_\mu(\mathbf{r})/V_\mu$, and therefore we only have to do small modifications.

## 6.2. Discrete diffusion with conjugate finite elements

In Chapter 2 we obtained the SDE for the discrete concentration field $\hat{c}_\mu(\mathbf{z})$, with the result[i]

$$dc_\mu(t) = -\hat{D}_{\mu\nu}(\mathbf{c})\frac{\partial \hat{F}}{\partial c_\nu}(\mathbf{c})dt + k_\mathrm{B}T\frac{\partial \hat{D}_{\mu\nu}}{\partial c_\nu}(\mathbf{c})dt + d\tilde{c}_\mu(t)\,.$$

This equation has the same structure no matter the actual shape of the basis function $\delta_\mu(\mathbf{r})$. Be it $\delta_\mu(\mathbf{r}) \to \psi_\mu(\mathbf{r})/V_\mu$ as we did in Chapter 3, or $\delta_\mu(\mathbf{r}) \to M^\delta_{\mu\nu}\psi_\nu(\mathbf{r})$ as we defined in Chapter 5. The only things that change are the functional form of the free energy and the dissipative matrix.

### 6.2.1. The free energy

The free energy can be obtained through the computation of the equilibrium probability distribution

$$\begin{aligned} P^\mathrm{eq}(\mathbf{c}) &= \delta\left(N - \sum_\mu V_\mu c_\mu\right)\exp\left\{-\beta\hat{F}(\mathbf{c})\right\} \\ &= \int d\mathbf{z}\prod_\mu \delta(\hat{c}_\mu(\mathbf{z}) - c_\mu)\rho^\mathrm{eq}(\mathbf{z})\,. \end{aligned} \tag{6.6}$$

Given the difficulty in computing the phase space integral and, therefore, the free energy, in Chapter 3 we made the assumption of a big number of particles per node, so that the probability become Gaussian. In the next chapter we will explore more general models. However, it is interesting to see what kind of Gaussian is obtained when the discrete concentration is given by (6.4). Because the first and second moments fix a Gaussian distribution, we need to

[i] Here, repeated indices are summed over.

compute these moments for $P^{\rm eq}(\mathbf{c})$. These moments are given by

$$\begin{aligned}\left\langle c_\mu \right\rangle &= \frac{1}{V_T^N}\int d\mathbf{z}\, c_\mu(\mathbf{z}) \\ &= \frac{1}{V_T^N}\int d\mathbf{z}\, \sum_i \delta_\mu(\mathbf{r}_i) \\ &= \frac{N}{V_T^N}\int d\mathbf{z}\, \delta_\mu(\mathbf{r}_i) \\ &= \frac{N}{V_T}\int d\mathbf{r}_i\, \delta_\mu(\mathbf{r}_i) \\ &= \frac{N}{V_T} = c_0\,,\end{aligned}$$

where we used the property (5.14). Concerning the second moment, we have

$$\begin{aligned}\left\langle c_\mu c_\nu \right\rangle &= \int d\mathbf{z}\, c_\mu(\mathbf{z}) c_\nu(\mathbf{z}) \\ &= \frac{1}{V_T^N}\int d\mathbf{z}\, \sum_i \delta_\mu(\mathbf{r}_i)\sum_j \delta_\mu(\mathbf{r}_j) \\ &= \frac{N}{V_T}\int d\mathbf{r}_i\, \delta_\mu(\mathbf{r}_i)\delta_\nu(\mathbf{r}_i) + \frac{N(N-1)}{V_T^2}\int d\mathbf{r}_i\, \delta_\mu(\mathbf{r}_i)\int d\mathbf{r}_j\, \delta_\nu(\mathbf{r}_j) \\ &= c_0 M^\delta_{\mu\nu} + c_0^2\left(1-\frac{1}{N}\right)\,,\end{aligned}$$

where we used the definition of $\mathbf{M}^\delta$ (5.11). In terms of central moments, for $N \gg 1$ we finally have

$$\left\langle \delta c_\mu \delta c_\nu \right\rangle \simeq c_0 M^\delta_{\mu\nu}\,.$$

Once the first and second moments of the probability distribution are obtained, we may write the Gaussian equilibrium probability in the form

$$P^{\rm eq}(\mathbf{c}) = \frac{1}{\mathcal{Z}}\exp\left\{-\delta\mathbf{c}^T\frac{\mathbf{M}^\psi}{2c_0}\delta\mathbf{c}\right\}\,,$$

so that the Gaussian free energy will be quadratic in the concentration, given by

$$F^{(\mathrm{GA})}(\mathbf{c}) = k_{\mathrm{B}}T\delta\mathbf{c}^T\frac{\mathbf{M}^{\psi}}{2c_0}\delta\mathbf{c}\,. \tag{6.7}$$

This free energy is different from the free energy obtained in (4.4). This is just a reflection of the fact that the second moments are different when the discrete concentration field is given either by the finite element $\psi_\mu(\mathbf{r})$ or by the conjugate finite element (6.5).

### 6.2.2. The dissipative matrix

The dissipative matrix is given by

$$\begin{aligned} D_{\mu\nu}(\mathbf{c}) &= \frac{D}{k_{\mathrm{B}}T}\int d\mathbf{r}\,\nabla\delta_\mu(\mathbf{r})\nabla\delta_\nu(\mathbf{r})\,\langle\hat{c}_{\mathbf{r}}\rangle^{\mathbf{c}} \\ &= \sum_{\mu'\nu'} M^{\delta}_{\mu\mu'}\frac{D}{k_{\mathrm{B}}T}\int d\mathbf{r}\,\nabla\psi_{\mu'}(\mathbf{r})\nabla\psi_{\nu'}(\mathbf{r})\,\langle\hat{c}_{\mathbf{r}}\rangle^{\mathbf{c}}\,M^{\delta}_{\nu'\nu} \\ &= \sum_{\mu'\nu'} M^{\delta}_{\mu\mu'}V_{\mu'}\hat{D}_{\mu'\nu'}V_{\nu'}M^{\delta}_{\nu'\nu}\,, \end{aligned} \tag{6.8}$$

where the matrix $\hat{\mathbf{D}}$ has been defined in (2.14). Note that this matrix, obtained by following the Bottom-up approach with the conjugate finite elements, coincides with the dissipative matrix obtained from the Top-down approach in Chapter 5 (5.35). We consider now the differences between the dissipative matrix (5.35) and the dissipative matrix obtained with the finite element based on the Delaunay triangulation (3.12). For example, for the state-independent dissipative matrix in (4.16)

$$\hat{D}_{\mu\nu} = \frac{Dc_0}{k_{\mathrm{B}}T}\frac{1}{V_\mu V_\nu}L^{\psi}_{\mu\nu}\,,$$

by using the conjugate basis function $\delta_\mu(\mathbf{r})$ in (6.5) we obtain

$$\begin{aligned}\mathbf{D} &= \frac{Dc_0}{k_B T}\mathbf{M}^\delta \mathbf{L}^\psi \mathbf{M}^\delta \\ &= \frac{Dc_0}{k_B T}\mathbf{L}^\delta \,. \end{aligned} \tag{6.9}$$

### 6.2.3. Thermal fluctuations

In Chapter 3 we obtained the thermal fluctuations for the discrete diffusion equation as specified in Eq. (3.15) as

$$d\tilde{c}_\mu = \sum_{e\in\mu} \frac{1}{V_\mu}\mathbf{b}_{e\to\mu}\cdot d\tilde{\mathbf{J}}_{e_\mu}\,.$$

By using the conjugate basis function (6.5), it is straightforward to obtain the explicit form for the thermal fluctuations as

$$d\tilde{c}_\mu = \sum_\nu M^\delta_{\mu\nu} \sum_{e\in\nu} \sqrt{2k_B T V_e \Gamma_e(\mathbf{c})}\mathbf{b}_{e\to\nu}\cdot d\boldsymbol{\mathcal{W}}_e(t)\,. \tag{6.10}$$

where $d\boldsymbol{\mathcal{W}}_e(t)$ is an independent increment of the Wiener process satisfying

$$\left\langle d\mathcal{W}^a_e(t) d\mathcal{W}^{a'}_{e'}(t')\right\rangle = \delta_{aa'}\delta_{ee'}dt\,.$$

Note that a similar result would be obtained following the discretization procedure explained in Chapter 5 for the stochastic partial differential equation (0.4). Recall that in the Weighted Residual procedure we multiplied the PDE (0.3) with $\delta_\mu(\mathbf{r})$ and integrated over space. If we do this for the stochastic term $\boldsymbol{\nabla}\cdot\tilde{\mathbf{J}}$ in Eq. (0.5) we obtain

$$\frac{d\tilde{c}_\mu}{dt} = -\int d\mathbf{r}\,\boldsymbol{\zeta}(\mathbf{r},t)\cdot\boldsymbol{\nabla}\delta_\mu(\mathbf{r})\sqrt{2k_B T\Gamma(\overline{c}(\mathbf{r},t))} \tag{6.11}$$

The correlations of the noises (6.11) are easily computed under the assumption that $\boldsymbol{\zeta}(\mathbf{r},t)$ is a white noise in space and time, satisfying

$$\langle\boldsymbol{\zeta}(\mathbf{r},t)\boldsymbol{\zeta}(\mathbf{r}',t')\rangle = \delta(\mathbf{r}-\mathbf{r}')\delta(t-t')\,,$$

and, therefore, (6.11) has the desired covariances

$$\left\langle \frac{d\tilde{\mathbf{c}}}{dt}(t)\frac{d\tilde{\mathbf{c}}}{dt}(t')\right\rangle = 2k_{\mathrm{B}}T\mathbf{D}(\mathbf{c})\delta(t-t')dt\,.$$

However (6.11) involves the white noise $\boldsymbol{\zeta}(\mathbf{r},t)$ and an integral over the whole space while what we are looking for is a linear combination of a finite number of independent Wiener processes. By using the gradient of the basis function given in (5.34) in (6.11), and taking the same approximation for the mobility that leads to (5.36), we obtain the following linear combination of white noises

$$\frac{d\tilde{c}_\mu}{dt} = \sum_\nu M^\delta_{\mu\nu}\sum_{e\in\nu}\sqrt{2k_{\mathrm{B}}TV_e\Gamma_e(\mathbf{c})}\mathbf{b}_{e\to\nu}\cdot d\boldsymbol{\mathcal{W}}_e(t)\,,$$

which is the same noise obtained in (6.10).

It is a matter of simple calculation to show that the Fluctuation-Dissipation Theorem is fulfilled under this assumption. Let us consider for example the state independent dissipative matrix (6.9), where $\Gamma_e(\mathbf{c}) = \Gamma_0$. The product $d\tilde{c}_\mu d\tilde{c}_\nu$ is

$$d\tilde{c}_\mu d\tilde{c}_\nu = \sum_{\mu'} M^\delta_{\mu\mu'}\sum_{e\in\mu'}\sqrt{2k_{\mathrm{B}}TV_e\Gamma_0}\mathbf{b}_{e\to\mu'}\cdot d\boldsymbol{\mathcal{W}}_e(t) \cdot\sum_{\nu'} M^\delta_{\nu\nu'}\sum_{e'\in\nu'}\sqrt{2k_{\mathrm{B}}TV_{e'}\Gamma_0}\mathbf{b}_{e'\to\nu'}\cdot d\boldsymbol{\mathcal{W}}_{e'}(t)\,,$$

where $\left\langle d\mathcal{W}_e^{\alpha}(t) d\mathcal{W}_{e'}^{\alpha'}(t) \right\rangle = \delta_{\alpha\alpha'}\delta_{ee'}dt$. So

$$\begin{aligned}
\left\langle d\tilde{c}_\mu d\tilde{c}_\nu \right\rangle &= \sum_{\mu'\nu'} M^{\delta}_{\mu\mu'} M^{\delta}_{\nu\nu'} \sum_{e\to\mu'} \sum_{e'\to\nu'} 2k_{\mathrm{B}}T\Gamma_0 \sqrt{V_e V_{e'}}\delta_{ee'}dt \\
&= \sum_{\mu'\nu'} M^{\delta}_{\mu\mu'} M^{\delta}_{\nu\nu'} 2k_{\mathrm{B}}T\Gamma_0 dt \sum_{e\in\mu'\nu'} V_e \mathbf{b}_{e\to\mu'} \cdot \mathbf{b}_{e\to\nu'} \\
&= \sum_{\mu'\nu'} M^{\delta}_{\mu\mu'}\, M^{\delta}_{\nu\nu'} 2k_{\mathrm{B}}T\Gamma_0 dt L^{\psi}_{\mu'\nu'} \\
&= 2k_{\mathrm{B}}T\Gamma_0 dt \sum_{\mu'\nu'} M^{\delta}_{\mu\mu'} L^{\psi}_{\mu'\nu'} M^{\delta}_{\nu'\nu} \\
&= 2k_{\mathrm{B}}T\Gamma_0 dt L^{\delta}_{\mu\nu} \\
&= 2k_{\mathrm{B}}T D_{\mu\nu} dt\,,
\end{aligned}$$

and the noise (6.10) satisfies the FDT, as desired.

For future references, let us compute the form of the noise in a 1D grid with constant mobility ($\Gamma_e(\mathbf{c}) = \Gamma_0$), which is

$$d\tilde{c}_\mu(t) = \sqrt{2Dc_0} \sum_\nu M^{\delta}_{\mu\nu} \left( \frac{dW^r_\nu(t)}{\sqrt{x_{\nu+1} - x_\nu}} - \frac{dW^l_\nu(t)}{\sqrt{x_\nu - x_{\nu-1}}} \right)\,,$$

where $l$ is referred to the *left* element of node $\nu$ and $r$ refers to the *right* element of node $\nu$.

## 6.3. Summary

In Chapter 3 we have obtained the SDE (0.10) by using finite elements with support on the Delaunay triangulation, $\psi_\mu(\mathbf{r})$. In the Interlude we have proposed a conjugate finite element to discretize not only regular but irregular meshes. We have found that on arbitrary grids the use of conjugate finite elements like (6.5) produces a discrete Laplacian which is more accurate than the use of the $\psi_\mu(\mathbf{r})$ finite elements. With this idea, following the same scheme that allows us to obtain a discrete diffusion equation in Chapter 3, we have started again from the general expressions for the free energy and the dissipative matrix in Chapter 2. By using the conjugate finite elements, we have

obtained different expression for the free energy (given for example by (6.7)) and the dissipative matrix (for example, (6.9)).

We have obtained an important message from the explicit expression of the dissipative matrix (6.8). This matrix is exactly the same that we have already obtained in CHAPTER 5 (see Eq. (3.12)). Again, this result allows one to connect the microscopically derived SDE for the discrete concentration field (Bottom-up approach, Eq. (0.10)), with the continuum equation (0.3) (Top-down approach). Therefore, the Top-down approach and the Bottom-up approach lead to the same deterministic equation, and the procedure explained in CHAPTER 5 to discretize a continuum equation like (0.3) is sounded. In this chapter we have followed both procedures and we conclude that they lead to the same expression for the noise terms.

We have obtained that the Bottom-up approach and the Top-down approach give the same discrete stochastic diffusion equation. This is one of the main result of this dissertation. The two levels of description (the continuum level and the microscopic level) are connected at a mesoscopic level of description. This mesoscopic level is characterized by the definition of the discrete concentration field as relevant variable, given by

$$\hat{c}_\mu(\mathbf{z}) = \sum_i \delta_\mu(\mathbf{r}_i) \, .$$

The discrete concentration field is written in terms of a (conjugate) finite element based on the Delaunay triangulation. The discretization procedure lead to a well behaved discrete evolution equation for the concentration field that fulfills the Fluctuation-Dissipation Theorem and the existence of a Second Law.

# 7

# Discrete Diffusion with Conjugate Finite Elements. Models and Numerical Results

Where we propose free energy models and a dissipative matrix model and we perform computer simulations.

## 7.1. Introduction

In Chapter 6 we have reproduced Chapter 3 with the conjugate finite element basis functions $\delta_\mu(\mathbf{r}) \rightarrow \sum_\nu M^\delta_{\mu\nu}\psi_\nu(\mathbf{r})$ instead of the finite element basis functions $\delta_\mu(\mathbf{r}) \rightarrow \frac{1}{V_\mu}\psi_\mu(\mathbf{r})$. The generic form of the blocks that enter into the SDE for the discrete diffusion have been already obtained in Chapter 2. We have obtained in Chapter 6 particular expressions for the free energy and the dissipative matrix. The dissipative matrix, for example, coin-

cides with the one obtained in the Top-down approach (Chapter 5). In this way, the Top-down formulation for the free energy function (through the free energy functional) and the dissipative matrix given in Chapter 5 is compatible with the Theory of Coarse-Graining. Therefore, the addition of thermal fluctuations to the deterministic PDE for diffusion (Eq. (0.3)) in order to obtain the SDE (0.4) is straightforward. In Chapter 6, in fact, we have obtained explicit expression for the noise term of the SDE.

In this chapter, we will propose particular models for both the free energy and the dissipative matrix appearing in the discrete diffusion equation (0.10). In Chapter 5 we have defined the free energy *function* as the evaluation of the free energy *functional* at the interpolated concentration field. In this chapter we propose several different free energy functionals and their corresponding free energy functions. These models go beyond the non-interacting Brownian system described by Gaussian statistics. We will also propose a model for the dissipative matrix. The noise term can be obtained directly with the Fluctuation-Dissipation Theorem from the specific model of the dissipative matrix.

The formulation of the discrete-in-space forms for the free energy and the dissipative matrix is a first step towards the simulation the SDE (0.10) in a computer. The numerical simulation also require a discretization-in-time. One objective of this chapter is to present a good time integration algorithm to compute efficiently the evolution of the discrete concentration field for a given free energy function and a dissipative matrix. Several "good" time discretization schemes for stochastic differential equations have been studied recently. [80, 81] Here, by "good" we understand integrators accurate enough *and* in agreement with the Fluctuation-Dissipation Theorem. Of course, such a good integrator should allow one to obtain both dynamic and static properties in a reasonable computational time, that is, with a sufficiently large time step. In Chapter 4 we have proposed an explicit strong Predictor Corrector Euler scheme [71] with a strong convergence order of 0.5. However, explicit algorithms are known to require small time steps in order to avoid instabilities in stiff equations. [82] In addition to this, by increasing the resolution on a discrete diffusion problem we need to use smaller time steps. For that reason, in this chapter we will propose a semi-implicit algorithm that allows one to

use larger time steps, ensuring the stability of the dynamics even for big time steps. [80] Fully implicit algorithms treats all the time integration implicitly, while semi-implicit algorithms split the integrator into two pieces: a first one treated implicitly for stability reasons and a second one that can be treated explicitly.

## 7.2. Free energy models

One of the basic objects appearing in the dynamic equation (5.30) is the free energy *function* $F(\mathbf{c})$. This function is obtained from the free energy functional through the definition in Eq. (5.26). In this section, we first consider physically motivated free energy *functionals* and their polynomial approximations and, afterwards, we present the corresponding free energy *functions*.

### 7.2.1. Physically motivated free energy functionals

Two physically motivated free energy functionals are given by the *ideal gas* and the *van der Waals* models. On one hand, the ideal gas free energy functional can be computed explicitly because there are no interactions between particles. The free energy functional of the ideal gas is

$$\mathcal{F}^{(\mathrm{ID})}[c(\mathbf{r})] = k_{\mathrm{B}}T \int d\mathbf{r}\, c(\mathbf{r}) \left[ \ln \frac{c(\mathbf{r})}{c_0} - 1 \right] ,$$

Here, $k_{\mathrm{B}}$ is the Boltzmann's constant, $T$ is the temperature, and $c_0$ is the equilibrium concentration.

The van der Waals free energy functional is useful to describe colloidal suspensions that may display a liquid-vapor phase separation with a liquid phase and a vapor phase.[83] It is usually derived for a fluid system interacting with a pair-wise potential that can be separated into a short range repulsive hard core and a long range attractive part $\phi(\mathbf{r}) < 0$, but the extension to interacting Brownian particles is trivial. The van der Waals free energy functional is

$$\mathcal{F}^{(\mathrm{vdW})}[c(\mathbf{r})] = \int d\mathbf{r} \left[ f_0(c(\mathbf{r}), \beta) + \frac{1}{2} \int d\mathbf{r}' c(\mathbf{r}) \phi(\mathbf{r} - \mathbf{r}') c(\mathbf{r}') \right] , \quad (7.1)$$

where the attractive part $\phi(\mathbf{r}-\mathbf{r}')$ of the potential of interaction between Brownian particles is treated in mean field and the short range part of the potential produces the local contribution $f_0(c(\mathbf{r}),\beta)$. Under the assumption that the density field hardly varies in the range of the attractive potential, we may expand $c(\mathbf{r}') = c(\mathbf{r}) + (\mathbf{r}'-\mathbf{r})\boldsymbol{\nabla} c(\mathbf{r}) + \ldots$ with the result

$$\frac{1}{2}\int d\mathbf{r}d\mathbf{r}'\, c(\mathbf{r})\,\phi(\mathbf{r}-\mathbf{r}')c(\mathbf{r}') = -a\int d\mathbf{r}\, c(\mathbf{r})^2 + \omega_2 \int d\mathbf{r}\,(\boldsymbol{\nabla} c(\mathbf{r}))^2\,,$$

where we have defined

$$\begin{aligned} a &\triangleq \frac{1}{2}\tilde{\phi}(0) = -\frac{1}{2}\int d\mathbf{r}\,\phi(r)\,,\\ \omega_2 &\triangleq \frac{1}{2}\tilde{\phi}''(0) = -\frac{1}{2}\int d\mathbf{r}\,\mathbf{r}^2\phi(r)\,. \end{aligned}$$

Note that $a > 0$ and $\omega_2 > 0$ for purely attractive potentials $\phi(\mathbf{r})$. With these definitions, the free energy functional (7.1) becomes

$$\mathcal{F}^{(\mathrm{vdW})}[c(\mathbf{r})] = \int d\mathbf{r}\,\left[f(c(\mathbf{r}),\beta) + \omega_2(\boldsymbol{\nabla} c(\mathbf{r}))^2\right]\,,$$

where $f(c(\mathbf{r}),\beta) = f_0(c(\mathbf{r}),\beta) - ac(\mathbf{r})^2$. For a van der Waals gas, the *free energy density* is given by

$$f(c,T) = k_{\mathrm{B}}Tc\left[\ln\left(\frac{c}{c_0(1-cb)}\right) - 1\right] - ac^2\,.$$

The constants $a, b$ are the attraction parameter and the excluded volume, respectively.

The van der Waals gas is characterized by two critical parameters, $T_c$ and $c_c$, obtained through the first and second derivatives of the pressure, which leads to

$$\begin{aligned} k_{\mathrm{B}}T_c &= \frac{8a}{27b}\,,\\ c_c &= \frac{1}{3b}\,. \end{aligned}$$

### 7.2.2. Polynomial free energy functionals

While we could use the above models directly, in the present chapter we are interested in the numerical aspects of the problem. For this reason, we prefer to work with free energy models that are *polynomials* of the concentration field. For this kind of models, the discrete free energy $F(\mathbf{c})$ defined in (5.26) can be computed exactly.

By expanding the ideal gas functional up to second order in the deviations $\delta c(\mathbf{r}) = c(\mathbf{r}) - c_0$ one obtains the Gaussian free energy functional

$$\begin{aligned}\mathcal{F}^{(\mathrm{GA})}[c(\mathbf{r})] &= \mathcal{F}[c_0] + \int d\mathbf{r}\, \frac{\delta \mathcal{F}}{\delta c(\mathbf{r})}\delta c(\mathbf{r}) \\ &\qquad + \frac{1}{2}\int d\mathbf{r} d\mathbf{r}'\, \frac{\delta^2 \mathcal{F}}{\delta c(\mathbf{r})\delta c(\mathbf{r}')}\delta c(\mathbf{r})\delta c(\mathbf{r}') \\ &= \mathcal{F}[c_0] + \frac{1}{2}\int d\mathbf{r} d\mathbf{r}'\, \frac{\delta^2 \mathcal{F}}{\delta c(\mathbf{r})\delta c(\mathbf{r}')}\delta c(\mathbf{r})\delta c(\mathbf{r}')\,.\end{aligned}$$

The derivatives of the free energy functional of the ideal gas are, respectively,

$$\begin{aligned}\frac{\delta \mathcal{F}}{\delta c(\mathbf{r})} &= k_{\mathrm{B}}T \ln \frac{c(\mathbf{r})}{c_0}\,, \\ \frac{\delta^2 \mathcal{F}}{\delta c(\mathbf{r})\delta c(\mathbf{r}')} &= k_{\mathrm{B}}T \frac{1}{c(\mathbf{r})}\delta(\mathbf{r}-\mathbf{r}')\,.\end{aligned}$$

Therefore, the resulting Gaussian free energy functional will be

$$\mathcal{F}^{(\mathrm{GA})}[c(\mathbf{r})] = \frac{k_{\mathrm{B}}T}{2c_0}\int d\mathbf{r}\, \delta c^2(\mathbf{r})\,, \tag{7.2}$$

where we omit the constant term $\mathcal{F}[c_0]$ without losing generality.

The van der Waals free energy can also be approximated by neglecting high order terms in an expansion around a constant concentration field, leading to the Ginzburg-Landau functional for the free energy. If we put $c(\mathbf{r}) = c_0 +$

$\delta c(\mathbf{r})$ we may expand to fourth order in $\delta c(\mathbf{r})$ as

$$\mathcal{F}^{(\mathrm{vdW})}[c(\mathbf{r})] = \int d\mathbf{r} \left\{ a_0 + b\delta c(\mathbf{r}) + \frac{1}{2}\left[ f_0''(c,\beta)|_{c_0} - 2a \right] \delta c(\mathbf{r})^2 \right.$$
$$+ \frac{1}{3!} f_0'''(c,\beta)|_{c_0} \, \delta c(\mathbf{r})^3$$
$$\left. + \frac{1}{4!} f_0''''(c,\beta)\Big|_{c_0} \delta c(\mathbf{r})^4 + \omega_2 (\boldsymbol{\nabla} \delta c(\mathbf{r}))^2 \right\} .$$

Any constant term is irrelevant in the free energy so that we can omit the term $a_0$. The linear term in $\delta c(\mathbf{r})$ disappears because of the normalization of the concentration field that ensures $\int d\mathbf{r}\, \delta c(\mathbf{r}) = 0$. *At the critical concentration* the derivatives of $f_0$ are

$$f_0' = k_\mathrm{B} T \left( \ln\left( \frac{b c_0}{2} \right) + \frac{1}{2} \right) ,$$
$$f_0'' = k_\mathrm{B} T \frac{27}{4} b ,$$
$$f_0''' = 0 ,$$
$$f_0'''' = k_\mathrm{B} T \frac{729}{8} b^3 ,$$

so the free energy functional is obtained as

$$\mathcal{F}^{(\mathrm{GL})}[\phi(\mathbf{r})] = k_\mathrm{B} T \int d\mathbf{r} \left\{ \frac{r_0}{2} \phi(\mathbf{r})^2 + \frac{K}{2} (\nabla \phi(\mathbf{r}))^2 + \frac{\lambda}{4} \phi(\mathbf{r})^4 \right\} , \quad (7.3)$$

where $\phi(\mathbf{r}) = \delta c(\mathbf{r})/c_0$ is the relative fluctuation on the concentration and we defined the following coefficients

$$r_0 \triangleq \frac{3}{4b} \left( 1 - \frac{T_c}{T} \right) ,$$
$$K \triangleq \frac{3}{4b} \sigma^2 \frac{T_c}{T} ,$$
$$\lambda \triangleq \frac{3}{16 b} ,$$
$$\sigma^2 \triangleq \frac{\omega_2}{a} . \quad (7.4)$$

These coefficients depend on the temperature but are assumed to be independent on the concentration field. Here, $b$ is the molecular volume of the van der Waals model, $T_c$ the critical temperature and $\sigma$ a length scale related to the range of the attractive part of the microscopic potential.

The approximation (7.3) to the van der Waals free energy functional is known as the Ginzburg-Landau free energy functional. In a similar way to the van der Waals model, the GL model shows phase separation when $T < T_c$ giving concentration fields that have two distinct values in different regions of space. In the present chapter, though, we will restrict ourselves to supercritical temperatures $T > T_c$ in such a way that there is no phase transition. Note that the statistics required in subcritical simulations needs to sample the diffusion of the phase separated droplets, which is usually very slow. [20] In addition, for supercritical temperatures translation invariance leads to simple forms for the structure factor, which will be the basic observable to be considered in CHAPTER 7.

We will also consider two analytically solvable models. The first one is a Gaussian model with surface tension (referred as $(\mathrm{GA}+\sigma)$) which is obtained by setting $\lambda = 0$ in the GL model (7.3):

$$\mathcal{F}^{(\mathrm{GA}+\sigma)}[c(\mathbf{r})] = k_{\mathrm{B}}T \int d\mathbf{r} \left\{ \frac{r_0}{2}\phi(\mathbf{r})^2 + \frac{K}{2}(\nabla\phi(\mathbf{r}))^2 \right\} . \tag{7.5}$$

The second model will be a purely Gaussian model derived from (7.3), with both $\lambda = 0$ and $K = 0$, i.e,

$$\mathcal{F}^{(\mathrm{GA})}[c(\mathbf{r})] = k_{\mathrm{B}}T \int d\mathbf{r} \left\{ \frac{r_0}{2}\phi(\mathbf{r})^2 \right\} . \tag{7.6}$$

Note that (7.6) has the ideal gas form (7.2), with $r_0 = c_0$.

It is obvious that the Ginzburg-Landau free energy functional is only a good approximation to the van der Waals free energy functional near the critical point for which the concentration profiles are close to the homogeneous profile. Nevertheless, the GL free energy already captures the essentials of a phase transition and non-Gaussian behavior, and we will restrict ourselves to this simpler polynomial model. Note that the van der Waals model does not allow

to have values of the concentration larger than $1/b$ (one molecule per molecular volume) nor smaller than zero. On the other hand, the GL model allows for unbounded values of $\phi(\mathbf{r})$. Also, if the temperature is much larger than the critical one, the GL model produces a Gaussian model like (7.2).

### 7.2.3. Free energy functions

In this subsection, we construct free energy *functions* corresponding to the free energy *functionals* $\mathcal{F}^{(\mathrm{GA})}[c(\mathbf{r})]$ in (7.6), $\mathcal{F}^{(\mathrm{GA}+\sigma)}[c(\mathbf{r})]$ in (7.5) and $\mathcal{F}^{(\mathrm{GL})}[c(\mathbf{r})]$ in (7.3). The prescription (5.26) tells us how to define the free energy function. We only need to substitute the field $\phi(\mathbf{r})$ by the interpolated field

$$\overline{\phi}(\mathbf{r}) = \sum_{\mu} \psi_{\mu}(\mathbf{r})\phi_{\mu}\,. \tag{7.7}$$

### 7.2.4. Gaussian free energy function

The Gaussian discrete free energy function $F^{(\mathrm{GA})}(\mathbf{c})$ is obtained from the definition (7.6) for $\lambda = K = 0$. By inserting (7.7) into the model (7.6) we obtain the corresponding free energy function

$$F^{(\mathrm{GA})}(\mathbf{c}) = k_{\mathrm{B}}T\frac{r_0}{2}\phi^T\mathbf{M}^{\psi}\phi\,. \tag{7.8}$$

This quadratic free energy produces an equilibrium probability which is Gaussian and for which the second moments can be explicitly computed (see Chapter 6), with the result

$$\begin{aligned}\left\langle \delta c_{\mu}\delta c_{\nu}\right\rangle &= c_0\left(M^{\delta}_{\mu\nu} - \frac{1}{V_T^D}\right)\\ &\approx c_0 M^{\delta}_{\mu\nu}\,,\end{aligned}$$

where we used that $r_0 = c_0$ and we have neglected a term that vanishes in the thermodynamic limit.

For future reference, let us compute the derivative of the free energy function (7.8)

$$\frac{\partial F^{(\mathrm{GA})}}{\partial \phi_\mu}(\mathbf{c}) = \sum_\nu k_\mathrm{B} T r_0 M^\psi_{\mu\nu} \phi_\nu \,.$$

where the repeated index summation convention has been adopted here and in what follows.

### 7.2.5. Gaussian with surface tension

Let us look at the result of evaluating the surface tension contribution at the interpolated field (7.7)

$$\begin{aligned}\int d\mathbf{r}\ (\nabla\phi(\mathbf{r}))^2 &= \int d\mathbf{r}\, \nabla\phi(\mathbf{r}) \cdot \nabla\phi(\mathbf{r}) \\ &= \int d\mathbf{r}\, \phi_\mu \nabla\psi_\mu(\mathbf{r}) \cdot \nabla\psi_\nu(\mathbf{r})\, \phi_\nu \\ &= \phi_\mu L^\psi_{\mu\nu} \phi_\nu \,,\end{aligned}$$

where $\mathbf{L}^\psi$ is the stiffness matrix given by Eq. (5.21).

The corresponding free energy function is then

$$F^{(\mathrm{GA}+\sigma)}(\phi) = k_\mathrm{B} T \left\{ \frac{r_0}{2} \phi^T \mathbf{M}^\psi \phi + \frac{K}{2} \phi^T \mathbf{L}^\psi \phi \right\} . \tag{7.9}$$

whose derivative is

$$\frac{\partial F^{(\mathrm{GA}+\sigma)}}{\partial \phi_\mu} = \sum_\nu k_\mathrm{B} T \left\{ r_0 M^\psi_{\mu\nu} \phi_\nu + K L^\psi_{\mu\nu} \phi_\nu \right\} .$$

### 7.2.6. Ginzburg-Landau

The Ginzburg-Landau free energy functional is given by Eq. (7.3) as

$$\mathcal{F}^{(\mathrm{GL})}[c(\mathbf{r})] = k_\mathrm{B} T \int d\mathbf{r} \left\{ \frac{r_0}{2} \phi(\mathbf{r})^2 + \frac{K}{2} (\nabla\phi(\mathbf{r}))^2 + \frac{\lambda}{4} \phi(\mathbf{r})^4 \right\} .$$

The quartic part leads to the following term in the free energy function

$$F^{(4)}(\phi) = \int d\mathbf{r}\, \phi(\mathbf{r})^4 = \phi_\mu \phi_{\mu'} \phi_\nu \phi_{\nu'} \int d\mathbf{r}\, \psi_\mu(\mathbf{r}) \psi_{\mu'}(\mathbf{r}) \psi_\nu(\mathbf{r}) \psi_{\nu'}(\mathbf{r})$$
$$= \phi_\mu \phi_{\mu'} \phi_\nu \phi_{\nu'} M^{\psi}_{\mu\mu'\nu\nu'} \, .$$

where the last equality defines the fourth point mass tensor. Therefore the discrete free energy will be given by

$$F^{(GL)}(\phi) = k_{\mathrm{B}} T \left\{ \frac{r_0}{2} \phi^T \mathbf{M}^{\psi} \phi + \frac{K}{2} \phi^T \mathbf{L}^{\psi} \phi + \frac{\lambda}{4} F^{(4)}(\phi) \right\} \, . \qquad (7.10)$$

Due to the form of $\psi_\mu(\mathbf{r})$ (see Fig. 5.1) only if nodes $\{\mu, \mu', \nu, \nu'\}$ are neighbors the integrand does not vanish. Otherwise, the integrand will be identically zero.

The form of the term $F^{(4)}(\phi)$ in 1D is as follows. For a given $\mu$ value, other indices should be either $\mu$, $\mu + 1$ or $\mu - 1$. That is, the sum over $\mu$, $\mu'$, $\nu$ and $\nu'$ will simplify to

$$\phi_\mu \phi_{\mu'} \phi_\nu \phi_{\nu'} M^{\psi}_{\mu\mu'\nu\nu'} = \sum_\mu \Big[ \phi_\mu^4 M^{\psi}_{\mu\mu\mu\mu}$$
$$+ 3\phi_\mu^3 \phi_{\mu-1} M^{\psi}_{\mu\mu\mu(\mu-1)} + 3\phi_\mu^2 \phi_{\mu-1}^2 M^{\psi}_{\mu\mu(\mu-1)(\mu-1)} + \phi_\mu \phi_{\mu-1}^3 M^{\psi}_{\mu(\mu-1)(\mu-1)(\mu-1)}$$
$$+ 3\phi_\mu^3 \phi_{\mu+1} M^{\psi}_{\mu\mu\mu(\mu+1)} + 3\phi_\mu^2 \phi_{\mu+1}^2 M^{\psi}_{\mu\mu(\mu+1)(\mu+1)} + \phi_\mu \phi_{\mu+1}^3 M^{\psi}_{\mu(\mu+1)(\mu+1)(\mu+1)} \Big] \, .$$

where the objects $M^{\psi}_{\mu\mu'\nu\nu'}$ can be computed explicitly. These objects are, re-

spectively,

$$
\begin{aligned}
M^{\psi}_{\mu\mu\mu\mu} &= \frac{1}{5}(x_{\mu+1} - x_{\mu-1})\,, \\
M^{\psi}_{\mu\mu\mu(\mu-1)} &= \frac{1}{20}(x_{\mu} - x_{\mu-1})\,, \\
M^{\psi}_{\mu\mu(\mu-1)(\mu-1)} &= \frac{1}{30}(x_{\mu} - x_{\mu-1})\,, \\
M^{\psi}_{\mu(\mu-1)(\mu-1)(\mu-1)} &= \frac{1}{20}(x_{\mu} - x_{\mu-1})\,, \\
M^{\psi}_{\mu\mu\mu(\mu+1)} &= \frac{1}{20}(x_{\mu+1} - x_{\mu})\,, \\
M^{\psi}_{\mu\mu(\mu+1)(\mu+1)} &= \frac{1}{30}(x_{\mu+1} - x_{\mu})\,, \\
M^{\psi}_{\mu(\mu+1)(\mu+1)(\mu+1)} &= \frac{1}{20}(x_{\mu+1} - x_{\mu})\,,
\end{aligned}
$$

so that

$$
\begin{aligned}
F^{(4)}_{\mu}(\phi) = \frac{1}{20}\left(4\phi^{4}_{\mu} + 3\phi^{3}_{\mu}\phi_{\mu+1} + 2\phi^{2}_{\mu}\phi^{2}_{\mu+1} + \phi_{\mu}\phi^{3}_{\mu+1}\right) V^{r}_{\mu} \\
+ \frac{1}{20}\left(4\phi^{4}_{\mu} + 3\phi^{3}_{\mu}\phi_{\mu-1} + 2\phi^{2}_{\mu}\phi^{2}_{\mu-1} + \phi_{\mu}\phi^{3}_{\mu-1}\right) V^{l}_{\mu}\,,
\end{aligned}
$$

where the volumes of the sub-elements are $V^{l}_{\mu} = x_{\mu} - x_{\mu-1}$ and $V^{r}_{\mu} = x_{\mu+1} - x_{\mu}$.

The derivative of this function with respect to $\phi_{\mu}$ will be

$$
\frac{\partial F^{(\mathrm{GL})}}{\partial \phi_{\mu}} = \sum_{\nu} k_{\mathrm{B}} T \left\{ r_0 M_{\mu\nu}\phi_{\nu} + K L_{\mu\nu}\phi\nu + \lambda F^{(3)}(\phi_{\mu}, \phi_{\mu\pm1}) \right\}\,,
$$

where

$$
\begin{aligned}
F^{(3)}(\phi_{\mu}, \phi_{\mu\pm1}) \triangleq \frac{1}{20}\left(4\phi^{3}_{\mu} + 3\phi^{2}_{\mu}\phi_{\mu+1} + 2\phi^{1}_{\mu}\phi^{2}_{\mu+1} + \phi^{3}_{\mu+1}\right) V^{r}_{\mu} \\
+ \frac{1}{20}\left(4\phi^{3}_{\mu} + 3\phi^{2}_{\mu}\phi_{\mu-1} + 2\phi^{1}_{\mu}\phi^{2}_{\mu-1} + \phi^{3}_{\mu-1}\right) V^{l}_{\mu}\,.
\end{aligned}
$$

## 7.3. Dissipative matrix model

In this chapter, we assume that the mobility $\Gamma(\mathbf{c}) = \frac{Dc_0}{k_B T}$ is a constant, where $D$ is a constant diffusion coefficient and $c_0$ is the equilibrium value of the concentration field. In this case, the dissipative matrix (5.33) is simply

$$D_{\mu\nu}(\mathbf{c}) = \frac{Dc_0}{k_B T} \int d\mathbf{r}\, \boldsymbol{\nabla}\delta_\mu(\mathbf{r}) \boldsymbol{\nabla}\delta_\nu(\mathbf{r}) = \frac{Dc_0}{k_B T} L^\delta_{\mu\nu}$$

where the stiffness matrix $L^\delta_{\mu\nu}$ is given by (5.21) as

$$L^\delta_{\mu\nu} = \int d\mathbf{r}\, \boldsymbol{\nabla}\delta_\mu(\mathbf{r}) \boldsymbol{\nabla}\delta_\nu(\mathbf{r}).$$

## 7.4. Time discretization

Inspired by the discussion in the introduction of this chapter, we propose here a second-order weakly accurate implicit trapezoidal predictor corrector scheme [80]. For its derivation, let us first consider the following SDE

$$\begin{aligned} \frac{d\mathbf{x}}{dt} &= \mathbf{a}(\mathbf{x}) + \mathbf{K}\boldsymbol{\mathcal{W}}(t) \\ &= \mathbf{L}(\mathbf{x})\mathbf{x} + \mathbf{g}(\mathbf{x}) + \mathbf{K}\boldsymbol{\mathcal{W}}(t)\,, \end{aligned} \tag{7.11}$$

where we split the drift term $\mathbf{a}(\mathbf{x})$ into a what we call a diffusive term $\mathbf{L}(\mathbf{x})\mathbf{x}$ (linear in $\mathbf{x}$), and an advective term $\mathbf{g}(\mathbf{x})$. Eq. (7.11) is a prototypical example of the fluctuating Navier-Stokes equation, where $\mathbf{L}$ is proportional to the Laplacian and $\mathbf{K}$ proportional to the divergence. Here, $\boldsymbol{\mathcal{W}}(t)$ is a collection of independent Wiener processes. The semi-implicit trapezoidal predictor-corrector scheme used in Ref. [84] treats the diffusive part implicitly and the advective part explicitly. Formally, the updated step of $\mathbf{x}$ from $t_i$ (referred as $\mathbf{x}^n = \mathbf{x}(t_i) = \mathbf{x}(n\Delta t)$) to $t_i + \Delta t$ (referred as $\mathbf{x}^{n+1} = \mathbf{x}((n+1)\Delta t)$) is given by a predictor step

$$\overline{\mathbf{x}}^{n+1} = \mathbf{x}^n + \frac{\Delta t}{2}\mathbf{L}^n\left(\mathbf{x}^n + \overline{\mathbf{x}}^{n+1}\right) + \Delta t \mathbf{g}^n + \sqrt{\Delta t}\mathbf{K}\boldsymbol{\mathcal{W}}^n\,,$$

and a corrector step

$$\mathbf{x}^{n+1} = \mathbf{x}^n + \frac{\Delta t}{2}\mathbf{L}^n\left(\mathbf{x}^n + \mathbf{x}^{n+1}\right) + \frac{\Delta t}{2}\left(\overline{\mathbf{L}}^{n+1} - \mathbf{L}^n\right)\overline{\mathbf{x}}^{n+1} + \frac{\Delta t}{2}\left(\overline{\mathbf{g}}^{n+1} - \mathbf{g}^n\right) + \sqrt{\Delta t}\mathbf{K}\boldsymbol{\mathcal{W}}^n\,,$$

where $\boldsymbol{\mathcal{W}}^n = \boldsymbol{\mathcal{W}}(n\Delta t)$ and we use the following notation

$$\mathbf{L}^n \equiv \mathbf{L}(\mathbf{x}^n)\,, \qquad \mathbf{g}^n \equiv \mathbf{g}(\mathbf{x}^n)\,,$$
$$\overline{\mathbf{L}}^{n+1} \equiv \mathbf{L}(\overline{\mathbf{x}}^{n+1})\,, \qquad \overline{\mathbf{g}}^{n+1} \equiv \mathbf{g}(\overline{\mathbf{x}}^{n+1})\,.$$

This scheme has the nice property of being unconditionally stable for any time step for lineal equations, giving the same static covariance independent of the time step size. [80] Therefore temporal integration errors in static covariances are eliminated by this scheme. However, it should be kept in mind that the dynamics of the fluctuations is not correctly reproduced for large time step sizes. In addition to this, if the advective term is not zero, some temporal discretization error will be observed both in static and dynamic properties. [80]

For the sake of simplicity, let us rearrange the scheme into the following form

$$\left(\mathbf{1} - \frac{\Delta t}{2}\mathbf{L}^n\right)\overline{\mathbf{x}}^{n+1} = \left(\mathbf{1} + \frac{\Delta t}{2}\mathbf{L}^n\right)\mathbf{x}^n + \Delta t\mathbf{g}^n + \sqrt{\Delta t}\mathbf{K}\boldsymbol{\mathcal{W}}^n\,,$$
$$\left(\mathbf{1} - \frac{\Delta t}{2}\mathbf{L}^n\right)\mathbf{x}^{n+1} = \left(\mathbf{1} + \frac{\Delta t}{2}\mathbf{L}^n\right)\mathbf{x}^n + \frac{\Delta t}{2}\left(\overline{\mathbf{L}}^{n+1} - \mathbf{L}^n\right)\overline{\mathbf{x}}^{n+1} + \frac{\Delta t}{2}\left(\overline{\mathbf{g}}^{n+1} + \mathbf{g}^n\right) + \sqrt{\Delta t}\mathbf{K}\boldsymbol{\mathcal{W}}^n\,.$$

Now, we have to particularize this scheme to the specific SDE in Chapter 6. In the assumption of a constant mobility the dissipative matrix is written as

$$\mathbf{D} = \Gamma_0\mathbf{M}^\delta\mathbf{L}^\psi\mathbf{M}^\delta\,.$$

The noise term has the explicit form

$$\mathbf{K}\boldsymbol{\mathcal{W}}^n = \sqrt{2Dc_0}\mathbf{M}^\delta\mathbf{N}^\psi\boldsymbol{\mathcal{W}}^n\,,$$

where, for example in $1D$, the matrix $\mathbf{N}^{\psi}$ is written as

$$\mathbf{N}^{\psi} = \begin{pmatrix} 0 & (V_1^r)^{-1/2} & 0 & 0 & \dots & -(V_1^l)^{-1/2} \\ -(V_2^l)^{-1/2} & 0 & (V_2^r)^{-1/2} & 0 & \dots & 0 \\ 0 & -(V_3^l)^{-1/2} & 0 & (V_3^r)^{-1/2} & \dots & 0 \\ \vdots & \vdots & \vdots & \vdots & \ddots & \vdots \\ (V_M^r)^{-1/2} & 0 & 0 & 0 & \dots & 0 \end{pmatrix},$$

and the vector $\boldsymbol{\mathcal{W}}^n$ is a collection of $M$ independent white-noise processes. Note that for periodic systems in $1D$ the number of elements (which are segments between the nodes) coincides with the number of nodes. Therefore, the number of Wiener processes is the same as the number of nodes. This is no longer true in higher dimensions.

The explicit integrator to be used for each free energy model and its resolution will be obtained in the next subsections.

### 7.4.1. Analytically solvable models

The purely Gaussian model given by (7.8) and the Gaussian with surface tension term (7.9) allow for an analytically solution the discrete diffusion equation. Both models have as the resulting SDE

$$\begin{aligned} \frac{d\mathbf{c}}{dt} &= -\frac{D}{c_0}\left(r_0\mathbf{M}^{\delta}\mathbf{L}^{\psi} + K\mathbf{M}^{\delta}\mathbf{L}^{\psi}\mathbf{M}^{\delta}\mathbf{L}^{\psi}\right)\mathbf{c} + \sqrt{2Dc_0}\mathbf{M}^{\delta}\mathbf{N}^{\psi}\boldsymbol{\mathcal{W}} \\ &\equiv \mathbf{L}(\mathbf{c})\mathbf{c} + \mathbf{g}(\mathbf{c}) + \mathbf{K}\boldsymbol{\mathcal{W}}\,, \end{aligned}$$

with the only difference of being $K = 0$ for the purely Gaussian model (7.8). Here, we may identify the following terms

$$\begin{aligned} \mathbf{L}(\mathbf{c}) &= -\frac{D}{c_0}\left(r_0\mathbf{M}^{\delta}\mathbf{L}^{\psi} + K\mathbf{M}^{\delta}\mathbf{L}^{\psi}\mathbf{M}^{\delta}\mathbf{L}^{\psi}\right)\,, \\ \mathbf{g}(\mathbf{c}) &= 0\,, \end{aligned}$$

so that the advective term is equal to zero. In that sense, the scheme is fully implicit and the predictor step can be neglected. The final scheme is written as

$$\left(\mathbf{1}+\frac{D\Delta t}{2c_0}\left(r_0\mathbf{M}^{\delta}\mathbf{L}^{\psi}+K\mathbf{M}^{\delta}\mathbf{L}^{\psi}\mathbf{M}^{\delta}\mathbf{L}^{\psi}\right)\right)\mathbf{c}^{n+1}$$
$$=\left(\mathbf{1}-\frac{D\Delta t}{2c_0}\left(r_0\mathbf{M}^{\delta}\mathbf{L}^{\psi}+K\mathbf{M}^{\delta}\mathbf{L}^{\psi}\mathbf{M}^{\delta}\mathbf{L}^{\psi}\right)\right)\mathbf{c}^{n}+\sqrt{2Dc_0\Delta t}\mathbf{M}^{\delta}\mathbf{N}^{\psi}\boldsymbol{\mathcal{W}}^{n}\,.$$

If we multiply by $\mathbf{M}^{\psi}$ on both sides we have

$$\left(\mathbf{M}^{\psi}+\frac{D\Delta t}{2c_0}\left(r_0\mathbf{L}^{\psi}+K\mathbf{L}^{\psi}\mathbf{M}^{\delta}\mathbf{L}^{\psi}\right)\right)\mathbf{c}^{n+1}$$
$$=\left(\mathbf{M}^{\psi}-\frac{D\Delta t}{2c_0}\left(r_0\mathbf{L}^{\psi}+K\mathbf{L}^{\psi}\mathbf{M}^{\delta}\mathbf{L}^{\psi}\right)\right)\mathbf{c}^{n}+\sqrt{2Dc_0\Delta t}\mathbf{N}^{\psi}\boldsymbol{\mathcal{W}}^{n}\,,$$

which can be written in a compact form as

$$\mathbf{T}^{n+1}\mathbf{c}^{n+1}=\mathbf{T}^{n}\mathbf{c}^{n}+\mathbf{W}^{n}\boldsymbol{\mathcal{W}}^{n}\,, \tag{7.12}$$

where we define

$$\begin{aligned}\mathbf{T}^{n+1}&\triangleq\mathbf{M}^{\psi}+\frac{D\Delta t}{2c_0}\left(r_0\mathbf{L}^{\psi}+K\mathbf{L}^{\psi}\mathbf{M}^{\delta}\mathbf{L}^{\psi}\right)\,,\\ \mathbf{T}^{n}&\triangleq\mathbf{M}^{\psi}-\frac{D\Delta t}{2c_0}\left(r_0\mathbf{L}^{\psi}+K\mathbf{L}^{\psi}\mathbf{M}^{\delta}\mathbf{L}^{\psi}\right)\,,\\ \mathbf{W}^{n}&\triangleq\sqrt{2Dc_0\Delta t}\mathbf{N}^{\psi}\,.\end{aligned} \tag{7.13}$$

Note that if we set $K=0$ in (7.13) one recovers the pure Gaussian model. Two strategies can be followed to solve efficiently the scheme (7.12). The first one assumes a regular grid and uses a Fast Fourier Transform (FFT) to decouple Eqs. (7.12). The other one is valid for irregular grids, where we avoid the multiplication of dense matrix by backward substitutions.

In the first case, we seek for a transformation in the original matricial SODE to a diagonal system, leading to a set of uncoupled SODE trivial to solve for each $c_\mu$ value. Fortunately, the $M$ vectors $\mathbf{v}(m)=\{e^{i\frac{2\pi}{L}mx_\mu},\mu=0,\ldots,M-$

1} for $m = 0, \ldots, M-1$ diagonalize simultaneously the three matrices involved in a 1D regular lattice of spacing $a$.

Let us begin with a base function $\mathbf{u}^1(m)$ with $\nu$ component

$$u^1_\nu(m) = \cos\left(\frac{2\pi m x_\nu}{L}\right) ,$$

Note that

$$\begin{aligned}
&\sum_\nu M^\psi_{\mu\nu} \cos\left(\frac{2\pi m}{L} x_\nu\right) \\
&\qquad = \frac{a}{6}\left[\cos\left(\frac{2\pi m}{L}(x_{\mu-1})\right) + 4\cos\left(\frac{2\pi m}{L}x_\mu\right) + \cos\left(\frac{2\pi m}{L}(x_{\mu+1})\right)\right] \\
&\qquad = \frac{a}{6}\left[\cos\left(\frac{2\pi m}{L}(x_\mu - a)\right) + 4\cos\left(\frac{2\pi m}{L}x_\mu\right) + \cos\left(\frac{2\pi m}{L}(x_\mu + a)\right)\right] \\
&\qquad = \frac{a}{3}\left[2 + \cos\left(\frac{2\pi m a}{L}\right)\right]\cos\left(\frac{2\pi m}{L}x_\mu\right)
\end{aligned}$$

that shows that the bas function is indeed an eigenvector

$$\mathbf{M}^\psi \mathbf{u}^1(m) = \widehat{m}(m)\mathbf{u}^1(m)$$

with eigenvalues

$$\widehat{m}(m) = \frac{a}{3}\left[2 + \cos\left(\frac{2\pi m a}{L}\right)\right] .$$

Equally, we define a base function $\mathbf{u}^2(m)$ with $\nu$ component

$$u^2_\nu(m) = \sin\left(\frac{2\pi m x_\nu}{L}\right) ,$$

so that

$$\begin{aligned}
&\sum_\nu M^\psi_{\mu\nu} \sin\left(\frac{2\pi m}{L} x_\nu\right) \\
&\qquad = \frac{a}{6}\left[\sin\left(\frac{2\pi m}{L}(x_{\mu-1})\right) + 4\sin\left(\frac{2\pi m}{L}x_\mu\right) + \sin\left(\frac{2\pi m}{L}(x_{\mu+1})\right)\right] \\
&\qquad = \frac{a}{3}\left[2 + \cos\left(\frac{2\pi m a}{L}\right)\right]\sin\left(\frac{2\pi m}{L}x_\mu\right) ,
\end{aligned}$$

so

$$\mathbf{M}^{\psi}\mathbf{u}^2(m) = \widehat{m}(m)\mathbf{u}^2(m)\,.$$

Hence, the linear combination

$$\mathbf{u}(m) \triangleq \mathbf{u}^1(m) + i\mathbf{u}^2(m) = \exp\left\{i\frac{2\pi}{L}m\mathbf{x}\right\}$$

is an eigenvector of $\mathbf{M}^{\psi}$ with eigenvalue $\widehat{m}(m)$.

Note that both the stiffness matrix $\mathbf{L}^{\psi}$ and the noise matrix $\mathbf{N}^{\psi}$ are also diagonalized by the same eigenvector $\mathbf{u}(m)$ with the eigenvalues given by

$$\begin{aligned}\widehat{l}(m) &= \frac{2}{a}\left[1 - \cos\left(\frac{2\pi ma}{L}\right)\right]\,,\\ \widehat{n}(m) &= \frac{2}{\sqrt{a}}\sin\left(\frac{\pi ma}{L}\right) \equiv \sqrt{\widehat{l}}\,.\end{aligned}$$

These expressions allow us to define a set of equations analogous to (7.12)-(7.13) in Fourier space as

$$\begin{aligned}\widehat{T}^{n+1}(m) &= \widehat{m}(m) + \frac{D\Delta t}{2c_0}\left(r_0\widehat{l}(m) + K\frac{\widehat{l}(m)^2}{\widehat{m}(m)}\right)\,,\\ \widehat{T}^{n}(m) &= \widehat{m}(m) - \frac{D\Delta t}{2c_0}\left(r_0\widehat{l}(m) + K\frac{\widehat{l}(m)^2}{\widehat{m}(m)}\right)\,,\\ \widehat{W}^{n}(m) &= \sqrt{2Dc_0\Delta t}\widehat{n}(m)\,,\end{aligned}$$

so that the SDE (7.12) turns into

$$\hat{c}^{n+1}(m) = \frac{\widehat{T}^{n}(m)}{\widehat{T}^{n+1}(m)}\hat{c}^{n} + \frac{\widehat{W}^{n}(m)}{\widehat{T}^{n+1}(m)}\widehat{\mathcal{W}}^{n}\,. \tag{7.14}$$

Being written in this form, note that the obtained SDE will be stable only if it fulfills

$$\left|\frac{\widehat{T}^{n}(m)}{\widehat{T}^{n+1}(m)}\right| < 1\,.$$

That is, if

$$\left|\widehat{m}(m)+\frac{D\Delta t}{2c_0}\left(r_0\widehat{l}(m)+K\frac{\widehat{l}(m)^2}{\widehat{m}(m)}\right)\right| < \left|\widehat{m}(m)-\frac{D\Delta t}{2c_0}\left(r_0\widehat{l}(m)+K\frac{\widehat{l}(m)^2}{\widehat{m}(m)}\right)\right| .$$

This inequality implies, necessarily,

$$\widehat{m}(m)>0 \quad \text{and} \quad \frac{D\Delta t}{2c_0}\left(r_0\widehat{l}(m)+K\frac{\widehat{l}(m)^2}{\widehat{m}(m)}\right)>0\,,$$

or

$$\widehat{m}(m)<0 \quad \text{and} \quad \frac{D\Delta t}{2c_0}\left(r_0\widehat{l}(m)+K\frac{\widehat{l}(m)^2}{\widehat{m}(m)}\right)<0\,.$$

Both $\widehat{m}(m)$ and $\widehat{l}(m)$ are greater than zero for any $m$ value, so that we finally have

$$\frac{D\Delta t}{2c_0}\left(r_0\widehat{l}(m)+K\frac{\widehat{l}(m)^2}{\widehat{m}(m)}\right)>0\,,$$

ensuring the stability of the scheme for any $\Delta t > 0$, provided that $r_0$ and $K$ are positives. We shall conclude then that the scheme is unconditionally stable for regular grids.

The FFT procedure, obtained for regular grids that diagonalize the matrices $\mathbf{M}^{\psi}$, $\mathbf{L}^{\psi}$ and $\mathbf{N}^{\psi}$, cannot be used for irregular lattices. Both $\mathbf{T}_K^n$ and $\mathbf{T}_K^{n+1}$ are dense matrices due to the product $\mathbf{L}^{\psi}\mathbf{M}^{\delta}\mathbf{L}^{\psi}$, so that the system (7.12) becomes computationally expensive if the number of nodes is large. However, consider $\mathbf{T}^n$ on the right hand side of (7.12). Instead of performing the dense matrix multiplication $\mathbf{L}^{\psi}\mathbf{M}^{\delta}\mathbf{L}^{\psi}$, which implies operations of order $\mathcal{O}(M^2)$, we will prefer to solve tridiagonal systems as follows. Consider the initial matrix multiplication

$$\mathbf{L}^{\psi}\mathbf{M}^{\delta}\mathbf{L}^{\psi}\mathbf{c}^n=\mathbf{L}^{\psi}\mathbf{M}^{\delta}\mathbf{c}_1^n\,,$$

where we define $\mathbf{c}_1^n \triangleq \mathbf{L}^\psi \mathbf{c}^n$. Being $\mathbf{L}^\psi$ a tridiagonal matrix, the computation of $\mathbf{c}_1^n$ is fast. Then, instead of computing the product $\mathbf{c}_2^n = \mathbf{M}^\delta c_1^n$, we solve the equivalent system of equations $\mathbf{M}^\psi \mathbf{c}_2^n = \mathbf{c}_1^n$, with the advantage that $\mathbf{M}^\psi$ is tridiagonal. With a backward substitution the obtention of $\mathbf{c}_2^n$ is, again, fast. As a result, there are only $\mathcal{O}(M)$ operations, which is much faster than computing the multiplication with the dense matrix.

Unfortunately, on the left hand side of (7.12) we cannot proceed in the same way with $\mathbf{T}^{n+1}$, because $\mathbf{c}^{n+1}$ is the variable we want to obtain. However, because $\mathbf{T}_K^{n+1}$ is a Hermitian positive-definite matrix, it can be decomposed with a Cholesky factorization, which allow us to solve Eq. (7.12) efficiently.

The final SDE can be solved efficiently for both regular and irregular lattices. Being anallytically solvable, we use the Gaussian model and the Gaussian with surface tension term model as benchmarks to test the accuracy and convergence of the proposed integrator. We will obtain static and dynamic properties for both models, and we will move to the non-analytical model of Gizburg-Landau to extract interesenting observables.

### 7.4.2. The Ginzburg-Landau model

The Ginzburg-Landau model is defined by the free energy (7.10), which gives the following SDE

$$\begin{aligned}\frac{d\mathbf{c}}{dt} &= -\frac{D}{c_0}\left(r_0\mathbf{M}^\delta\mathbf{L}^\psi + K\mathbf{M}^\delta\mathbf{L}^\psi\mathbf{M}^\delta\mathbf{L}^\psi\right)\mathbf{c} - D\lambda\mathbf{M}^\delta\mathbf{L}^\psi\mathbf{M}^\delta\mathbf{c}' \\ &\qquad + \sqrt{2Dc_0}\mathbf{M}^\delta\mathbf{N}^\psi\boldsymbol{\mathcal{W}} \\ &\equiv \mathbf{L}(\mathbf{c})\mathbf{c} + \mathbf{g}(\mathbf{c}) + \mathbf{K}\boldsymbol{\mathcal{W}}\,,\end{aligned}$$

where we identify

$$\begin{aligned}\mathbf{L}(\mathbf{c}) &= -\frac{D}{c_0}\left(r_0\mathbf{M}^\delta\mathbf{L}^\psi + K\mathbf{M}^\delta\mathbf{L}^\psi\mathbf{M}^\delta\mathbf{L}^\psi\right)\,, \\ \mathbf{g}(\mathbf{c}) &= -D\lambda\mathbf{M}^\delta\mathbf{L}^\psi\mathbf{M}^\delta\mathbf{c}'\,, \\ c'_\mu &= \frac{1}{20}\left(4\phi_\mu^3 + 3\phi_\mu^2\phi_{\mu+1} + 2\phi_\mu^1\phi_{\mu+1}^2 + \phi_{\mu+1}^3\right)V_\mu^r \\ &\qquad + \frac{1}{20}\left(4\phi_\mu^3 + 3\phi_\mu^2\phi_{\mu-1} + 2\phi_\mu^1\phi_{\mu-1}^2 + \phi_{\mu-1}^3\right)V_\mu^l\,.\end{aligned}$$

Now $\mathbf{g}(\mathbf{c}) \neq 0$, and we will need both the predictor and the corrector step in the algorithm. The semi-implicit trapezoidal scheme is given by

$$\begin{aligned}
\mathbf{T}_K^{n+1}\overline{\mathbf{c}}^{n+1} &= \mathbf{T}_K^n\mathbf{c}^n - \Delta t D\lambda\mathbf{L}^\psi\mathbf{M}^\delta\mathbf{c}'^n + \sqrt{2Dc_0\Delta t}\mathbf{N}^\psi\boldsymbol{\mathcal{W}}^n\,,\\
\mathbf{T}_K^{n+1}\mathbf{c}^{n+1} &= \mathbf{T}_K^n\mathbf{c}^n - D\lambda\mathbf{L}^\psi\mathbf{M}^\delta\left(\frac{\mathbf{c}'^n + \overline{\mathbf{c}}'^{n+1}}{2}\right) + \sqrt{2Dc_0\Delta t}\mathbf{N}^\psi\boldsymbol{\mathcal{W}}^n\,.
\end{aligned} \tag{7.15}$$

As we did before, regular lattices can be solved via FFT efficiently, where we should consider the FFT of the explicit term $\widehat{\mathbf{c}'}$ also. For irregular lattices we cannot uncouple the SODE, but we may use the specialized backward substitution already explained.

To sum up, we obtain a SODE (coupled or uncoupled depending on the regularity of the grid) that can be solved efficiently.

## 7.5. Observables

In this section we discuss the selection of good observables to monitor the dynamics. Gaussian models are analytically solvable and we present in this section analytic results for the static and dynamic structure factors for the Gaussian models in both continuum and discrete settings. The main result is that the numerical algorithm closely matches not only the infinite resolution limit, as it should, but also the predictions of the continuum theory for the fluctuations in finite resolution discrete lattices. In this way, we may compare theoretical and simulation results in order to test the goodness of our algorithm. These observables will also be considered for irregular grids and the Ginzburg-Landau model.

### 7.5.1. Static structure factor from the continuum

The equilibrium correlation of the fluctuations of the concentration is translationally invariant, which implies

$$\langle \delta c(\mathbf{r}, 0)\delta c(\mathbf{r}', 0)\rangle = S(\mathbf{r} - \mathbf{r}')\,, \tag{7.16}$$

for some function $S(\mathbf{r})$. We may obtain the Fourier transform of $S(\mathbf{r})$ as follows. The right hand side of (7.16)

$$\begin{aligned}
&\frac{1}{\mathcal{V}}\int_{\mathcal{V}} d\mathbf{r}\,\frac{1}{\mathcal{V}'}\int_{\mathcal{V}'} d\mathbf{r}'\,e^{-i\mathbf{k}\cdot\mathbf{r}}e^{-i\mathbf{k}'\cdot\mathbf{r}'}S(\mathbf{r}-\mathbf{r}') \\
&\qquad = \frac{1}{\mathcal{V}}\int_{\mathcal{V}} d\mathbf{r}\,\frac{1}{\mathcal{V}'}\int_{\mathcal{V}'} d\mathbf{r}'\,e^{-i\mathbf{k}\cdot(\mathbf{r}-\mathbf{r}')}e^{-i(\mathbf{k}'+\mathbf{k})\cdot\mathbf{r}'}S(\mathbf{r}-\mathbf{r}') \\
&\qquad = \frac{1}{\mathcal{V}'}\int_{\mathcal{V}'} d\mathbf{r}'\,e^{-i(\mathbf{k}'+\mathbf{k})\cdot\mathbf{r}'}\frac{1}{\mathcal{V}}\int_{\mathcal{V}} d\mathbf{r}''\,e^{-i\mathbf{k}\cdot\mathbf{r}''}S(\mathbf{r}'') \\
&\qquad = \delta_{\mathbf{k},-\mathbf{k}'}S(\mathbf{k})\,.
\end{aligned}$$

Respectively, the left hand side of (7.16) in Fourier space is

$$\begin{aligned}
&\frac{1}{\mathcal{V}}\int_{\mathcal{V}} d\mathbf{r}\,\frac{1}{\mathcal{V}'}\int_{\mathcal{V}'} d\mathbf{r}'\,e^{-i\mathbf{k}\cdot\mathbf{r}}e^{-i\mathbf{k}'\cdot\mathbf{r}'}\,\langle\delta c(\mathbf{r},0)\delta c(\mathbf{r}',0)\rangle \\
&= \sum_{\mathbf{k}''\mathbf{k}'''}\frac{1}{\mathcal{V}}\int_{\mathcal{V}} d\mathbf{r}\,\frac{1}{\mathcal{V}'}\int_{\mathcal{V}'} d\mathbf{r}'\,e^{-i\mathbf{k}\cdot\mathbf{r}}e^{-i\mathbf{k}'\cdot\mathbf{r}'}e^{i\mathbf{k}''\cdot\mathbf{r}}e^{i\mathbf{k}'''\cdot\mathbf{r}'}\,\langle\delta c(\mathbf{k}'',0)\delta c(\mathbf{k}''',0)\rangle \\
&= \sum_{\mathbf{k}''\mathbf{k}'''}\delta_{\mathbf{k}''\mathbf{k}}\delta_{\mathbf{k}'''\mathbf{k}'}\,\langle\delta c(\mathbf{k}'',0)\delta c(\mathbf{k}''',0)\rangle \\
&= \langle\delta c(\mathbf{k},0)\delta c(\mathbf{k}',0)\rangle\ .
\end{aligned}$$

This results give an equivalent relation in the Fourier space from a translational invariant in the real space. The Fourier transform of $S(r)$

$$\begin{aligned}
S(\mathbf{k}) &\triangleq \int d\mathbf{r}\,S(\mathbf{r})e^{-i\mathbf{k}\cdot\mathbf{r}} \\
&= \langle\delta c(\mathbf{k},0)\delta c(-\mathbf{k},0)\rangle\ ,
\end{aligned}$$

is known as *structure factor*.

Note that $S(\mathbf{k}) = c_0^2 S_\phi(\mathbf{k})$, with $S_\phi(\mathbf{k}) = \langle\phi(\mathbf{k},0)\phi(-\mathbf{k},0)\rangle$, and $\phi(\mathbf{r})$ is the relative fluctuations of the concentration field. The static structure factor is the Fourier transform of the second moments of the functional probability $P[c] \sim \exp\{-\frac{1}{k_B T}\mathcal{F}[c]\}$. For a Gaussian probability we may compute

the second moments in a straightforward manner. The probability functional with the model $\mathcal{F}^{GA+\sigma}[c]$ given in (7.5) can be written in operator notation as

$$P^{\rm eq}[c] \propto \exp\left\{-\frac{1}{2}\int d\mathbf{r}\int d\mathbf{r}'\,\phi(\mathbf{r})\mathcal{L}(\mathbf{r},\mathbf{r}')\phi(\mathbf{r}')\right\}\,,$$

where we have introduced the kernel

$$\mathcal{L}(\mathbf{r},\mathbf{r}') = r_0\delta(\mathbf{r}-\mathbf{r}') - K\nabla^2\delta(\mathbf{r}-\mathbf{r}')\,.$$

The covariance of the Gaussian probability functional is given by

$$\langle\phi(\mathbf{r})\phi(\mathbf{r}')\rangle = \mathcal{L}^{-1}(\mathbf{r},\mathbf{r}')\,,$$

where $\mathcal{L}^{-1}(\mathbf{r},\mathbf{r}')$ is the inverse of the operator $\mathcal{L}(\mathbf{r},\mathbf{r}')$, satisfying

$$\int d\mathbf{r}'\,\mathcal{L}(\mathbf{r},\mathbf{r}')\mathcal{L}^{-1}(\mathbf{r}',\mathbf{r}'') = \delta(\mathbf{r}-\mathbf{r}'')\,.$$

By inserting the form of the operator $\mathcal{L}(\mathbf{r},\mathbf{r}')$ one recognizes that the inverse operator is just the Green's function $\mathcal{L}^{-1}(\mathbf{r},\mathbf{r}') = S_\phi(\mathbf{r}-\mathbf{r}')$, which satisfies

$$r_0 S_\phi(\mathbf{r}-\mathbf{r}') - K\nabla^2 S_\phi(\mathbf{r}-\mathbf{r}') = \delta(\mathbf{r}-\mathbf{r}')\,. \tag{7.17}$$

The solution of this equation is obtained by going to Fourier space. We introduce the Fourier transform

$$\hat{S}_\phi(\mathbf{k}) = \int d\mathbf{r}\,e^{-i\mathbf{k}\cdot\mathbf{r}}S_\phi(\mathbf{r})\,,$$
$$S_\phi(\mathbf{r}) = \int \frac{d\mathbf{k}}{(2\pi)^D}\,e^{i\mathbf{k}\cdot\mathbf{r}}\hat{S}_\phi(\mathbf{k})\,.$$

In Fourier space, (7.17) becomes

$$r_0\hat{S}_\phi(\mathbf{k}) + Kk^2\hat{S}_\phi(\mathbf{k}) = 1\,,$$

which gives

$$\hat{S}_\phi(\mathbf{k}) = \frac{1}{r_0}\frac{1}{1+k^2/k_0^2}\,, \tag{7.18}$$

where $k_0^2 = r_0/K$. Therefore, the Green function is

$$S_\phi(\mathbf{r}) = \int \frac{d^D\mathbf{k}}{(2\pi)^D} e^{i\mathbf{k}\cdot\mathbf{r}} \frac{1}{r_0} \frac{1}{1+k^2/k_0^2} \,,$$

and the covariance, or correlation function, is given by

$$\langle \phi(\mathbf{r})\phi(\mathbf{r}')\rangle = \int \frac{d^D\mathbf{k}}{(2\pi)^D} e^{i\mathbf{k}\cdot(\mathbf{r}-\mathbf{r}')} \frac{1}{r_0} \frac{1}{1+k^2/k_0^2} \,.$$

For $D = 1$ this correlation takes the form

$$\langle \phi(x)\phi(x')\rangle = \frac{k_0}{2r_0} e^{-k_0|x-x'|} \,.$$

For $D = 2$ the result is

$$\langle \phi(\mathbf{r})\phi(\mathbf{r}')\rangle = \frac{k_0^2}{4\pi r_0} K_0(k_0|\mathbf{r}-\mathbf{r}'|) \,.$$

where $K_0(x)$ is a Bessel function. Finally, in $3D$ the result is

$$\langle \phi(\mathbf{r})\phi(\mathbf{r}')\rangle = \frac{k_0^2}{4\pi r_0} \frac{e^{-k_0|\mathbf{r}-\mathbf{r}'|}}{|\mathbf{r}-\mathbf{r}'|} \,. \tag{7.19}$$

Note that the quantity $\langle \phi^2(\mathbf{r})\rangle$ that gives the normalized fluctuations of the concentration field at a given point of space does not diverge in $1D$ but it diverges in $2D$ and $3D$, a phenomenon known as the *ultraviolet catastrophe*. We shall conclude that the point-wise fluctuations are unbounded in dimensions higher than one. *Any particular realization of a Gaussian field in $D > 1$ is extremely rough.*

Nevertheless, physical observables like the number of particles in a finite region are well behaved. From a physical point of view this quantity should be independent of the resolution used to discretize the problem. The number of particles in a region $V$ is given by

$$N_V = \int_V d\mathbf{r}\, c(\mathbf{r}) \,,$$

and the relative fluctuations are given by

$$\phi_V \triangleq \frac{N_V - Vc_0}{Vc_0} = \frac{1}{V}\int_V d\mathbf{r}\,\phi(\mathbf{r})\,.$$

The variance of this fluctuation is

$$\langle \phi_V^2 \rangle = \frac{1}{V^2}\int_V d\mathbf{r} \int_V d\mathbf{r}'\,\langle \phi(\mathbf{r})\phi(\mathbf{r}')\rangle\,.$$

This quantity is finite for any finite volume but as the domain shrinks to a point it diverges in $2D$ logarithmically with the size of the domain, and in $3D$ inversely with the size of the domain, in agreement with (7.19).

### 7.5.2. Dynamic structure factor from the continuum

In this subsection we compute the dynamic structure factor for the Gaussian model. Assume a constant mobility $\Gamma = Dc_0/k_{\mathrm{B}}T$ in (0.4) with the model $\mathcal{F}^{GA+\sigma}[c]$ in Eq. (7.5). The resulting SPDE is

$$\partial_t \delta c(\mathbf{r},t) = D\frac{r_0}{c_0}\left(\nabla^2\delta c(\mathbf{r},t) - \frac{1}{k_0^2}\nabla^2\nabla^2\delta c\right) + \sqrt{2Dc_0}\boldsymbol{\nabla}\cdot\boldsymbol{\zeta}(\mathbf{r},t) \quad (7.20)$$

where we have introduced $k_0^2 = r_0/K$, $\boldsymbol{\zeta}(\mathbf{r},t)$ is a white noise in space and time, this is, $\langle\boldsymbol{\zeta}(\mathbf{r},t)\rangle = 0$, and $\langle\boldsymbol{\zeta}(\mathbf{r},t)\boldsymbol{\zeta}(\mathbf{r}',t')\rangle = \delta(\mathbf{r}-\mathbf{r}')\delta(t-t')$. Let us solve the SPDE (7.20) by Fourier transform

$$\partial_t \delta\hat{c}(\mathbf{k},t) = -\frac{1}{\tau_k}\delta\hat{c}(\mathbf{k},t) - i\mathbf{k}\sqrt{2Dc_0}\cdot\hat{\boldsymbol{\zeta}}(\mathbf{k},t)\,, \quad (7.21)$$

where we have introduced the relaxation time

$$\tau_k = \left(\frac{D}{c_0}r_0\left(1+\frac{k^2}{k_0^2}\right)k^2\right)^{-1}\,.$$

The Fourier transform of a white noise is also a white noise which obeys the properties, $\left\langle\hat{\boldsymbol{\zeta}}(\mathbf{k},t)\right\rangle = 0$ and $\left\langle\hat{\boldsymbol{\zeta}}(\mathbf{k},t)\hat{\boldsymbol{\zeta}}(\mathbf{k}',t')\right\rangle = \delta(\mathbf{k}+\mathbf{k}')\delta(t-t')$.

The linear equation (7.21) has the explicit solution

$$\delta\hat{c}(\mathbf{k},t) = \delta\hat{c}(\mathbf{k},0)\exp\left\{-\frac{t}{\tau_k}\right\} - i\mathbf{k}\sqrt{2Dc_0}\int_0^t dt'\, e^{\frac{t-t'}{\tau_k}}\cdot\hat{\boldsymbol{\zeta}}(t')\,.$$

By multiplying with respect to the initial condition $\delta\hat{c}(-\mathbf{k},0)$ and averaging with respect to all possible equilibrium realization of the initial condition we obtain

$$\langle\delta\hat{c}(\mathbf{k},t)\delta\hat{c}(-\mathbf{k},0)\rangle = S^c(\mathbf{k})\exp\left\{-\frac{t}{\tau_k}\right\}\,,$$

where the static structure factor is given in Eq. (7.18).

### 7.5.3. The discrete static structure factor

The (continuum) structure factor is defined as the Fourier transform of the static correlation function

$$\hat{S}(k) = \int_\infty^\infty dr\,\langle\delta c(0)\delta c(r)\rangle e^{-ikr}\,.$$

Eq. (7.18) shows that

$$\hat{S}(k) = c_0^2 S_\phi(k) = \frac{c_0^2}{r_0}\frac{1}{1+k^2/k_0^2}\,. \tag{7.22}$$

We introduce the Fourier series representation of the continuum concentration field

$$c(r,t) = \sum_k \hat{c}(k,t)e^{ik\cdot r}\,,$$

where the sum is over all those $k = \frac{2\pi}{L}\kappa$, with $\kappa \in \mathbb{Z}$, this is the sum is over $k = 0, \pm\frac{2\pi}{L}, \pm\frac{2\pi}{L}2, ..., \pm\infty$. The Fourier coefficients are given by

$$\hat{c}(k,t) = \frac{1}{L}\int_0^L c(r,t)e^{-ikr}dr\,.$$

Note that translation invariance $\langle \delta c(r)\delta c(r')\rangle = S(r-r')$ implies that

$$\begin{aligned}\langle \delta c(k)\delta c(k')\rangle &= \frac{1}{L}\int_0^L dr \frac{1}{L}\int_0^L dr' e^{-ikr}e^{-ik'r'}\langle \delta c(r)\delta c(r')\rangle \\ &= \frac{1}{L}\int_0^L dr \frac{1}{L}\int_0^L dr' e^{-ikr}e^{-ik'r'}S(r-r') \\ &= \frac{1}{L}\int_0^L dr'' \frac{1}{L}\int_0^L dr' e^{-ik(r''+r')}e^{-ik'r'}S(r'') \\ &= \delta_{k,-k'}S(k)\,,\end{aligned}$$

where we have assumed that $L$ is sufficiently large for the following approximation to hold

$$\int_0^L dr' e^{-ikr'} = \delta(k)\,,$$

and $S(k)$ are the Fourier coefficients of $S(r)$

$$S(k) = \frac{1}{L}\int_0^L dr e^{-ikr}S(r)\,,$$

and we are abusing notation and understand $\delta_{k,-k'}$ as the Kroenecker delta $\delta_{\kappa,-\kappa'}$ for the integers $\kappa, \kappa'$ corresponding to $k = \frac{2\pi}{L}\kappa$, $k' = \frac{2\pi}{L}\kappa'$. The Fourier coefficient $S(k)$ and the Fourier transform $\hat{S}(k)$ (the structure factor) are related according to

$$\begin{aligned}S(k) &= \frac{1}{L}\int_0^L dr e^{-ikr}S(r) = \frac{1}{L}\int_0^L dr e^{-ikr}\int \frac{dk'}{2\pi}e^{ik'r}\hat{S}(k') \\ &= \int dk' \hat{S}(k')\frac{1}{L}\int_0^L \frac{dr}{2\pi}e^{-i(k-k')r} \approx \frac{1}{L}\hat{S}(k)\,.\end{aligned}$$

We express the second moments of the probability $P^{\text{eq}}(\mathbf{c})$ in terms of the

continuum structure factor $S(k)$ obtained above

$$\begin{aligned}\left\langle \delta c_\mu \delta c_\nu \right\rangle &= \int dr \delta_\mu(r) \int dr' \delta_\nu(r') \left\langle \delta c(r,0) \delta c(r',0) \right\rangle \\ &= \int dr \delta_\mu(r) \int dr' \delta_\nu(r') \sum_{kk'} e^{ikr} e^{ik'r'} \left\langle \delta\hat{c}(k) \delta\hat{c}(k') \right\rangle \\ &= \sum_k S(k) \delta_\mu(-k) \delta_\nu(k) \\ &= \frac{1}{L} \sum_k \hat{S}(k) \delta_\mu(-k) \delta_\nu(k) \,, \end{aligned} \tag{7.23}$$

where we have defined the Fourier transform of the basis function

$$\delta_\nu(k) \triangleq \int dr \delta_\nu(r) e^{-ikr} \,.$$

Let us compute explicitly this function. From the linear relationship between basis functions $\delta_\mu(r) = \sum_\nu M^\delta_{\mu\nu} \psi_\nu(r)$ we have

$$\delta_\mu(k) = \sum_\nu M^\delta_{\mu\nu} \int dr \psi_\nu(r) e^{-ikr} \,.$$

The Fourier transform of the basis function $\psi_\nu(r)$ for a $1D$ regular grid of lattice spacing $a$ is

$$\psi_\nu(k) = \int dr \, \psi_\nu(r) e^{-ikr} = a \, \mathrm{sinc}^2 \left( \frac{ka}{2} \right) e^{-ikr_\nu} = \psi_0(k) e^{-ikr_\nu} \,.$$

Note that the plane wave is an eigenvector of $\mathbf{M}^\delta$. In fact, because $\mathbf{M}^\delta$ is the inverse of $\mathbf{M}^\psi$, and we have that

$$\sum_\mu M^\psi_{\mu\nu} e^{-ikr_\mu} = \widehat{m}(k) e^{-ikr_\nu} \qquad \forall k \,, \tag{7.24}$$

with eigenvalues

$$\widehat{m}(k) = \frac{a}{3} \left[ 2 + \cos(ka) \right] , \tag{7.25}$$

we may multiply the vector equation (7.24) with $\mathbf{M}^{\delta}$ to obtain

$$\sum_{\mu} M^{\delta}_{\mu\nu} e^{-ikr_\mu} = \frac{1}{\widehat{m}(k)} e^{-ikr_\nu} \,.$$

This gives the following explicit functional form for the Fourier transform of the basis function

$$\delta_\mu(k) = \frac{\psi_\mu(k)}{\widehat{m}(k)} = \frac{\psi_0(k)}{\widehat{m}(k)} e^{-ikr_\mu} \qquad \text{where} \qquad k = \frac{2\pi}{L}\kappa \,. \tag{7.26}$$

Note that for $k \to 0$, we have $\delta_\mu(0) = 1$, which, from (7.26) and (5.13) is what it should be.

Eq. (7.23) gives the covariance of the discrete field in real space, in terms of the structure factor, but we are interested in the covariances of the discrete Fourier transform of the discrete field. To this end, we introduce the discrete Fourier transform $\hat{c}_m$ with $m = 0, M-1$ of the discrete concentration field $c_\mu$ according to

$$\begin{aligned} \hat{c}_m &= \frac{1}{M} \sum_{\mu=0}^{M-1} e^{-i\frac{2\pi}{L} m r_\mu} c_\mu \,, \\ c_\mu &= \sum_{m=0}^{M-1} e^{i\frac{2\pi}{L} m r_\mu} \hat{c}_m \,. \end{aligned}$$

We define the discrete static structure factor $\hat{S}^c(k_m)$ as the covariance of the discrete Fourier components $\hat{c}_m$

$$\begin{aligned} \hat{S}^c(k_m) &\triangleq L \left\langle \delta\hat{c}_m \delta\hat{c}^*_m \right\rangle \\ &= \frac{L}{M^2} \sum_{\mu,\nu} e^{-i\frac{2\pi}{L} m r_\mu} e^{i\frac{2\pi}{L} m r_\nu} \left\langle \delta c_\mu \delta c_\nu \right\rangle \\ &= \frac{L}{M^2} \sum_{\mu,\nu} e^{-i\frac{2\pi}{L} m r_\mu} e^{i\frac{2\pi}{L} m r_\nu} \sum_{k} S(k) \delta_\mu(k) \delta_\nu(-k) \\ &= \sum_{k} \hat{S}(k) \overline{\delta}_m(k) \overline{\delta}_{-m}(-k) \,, \end{aligned}$$

where $k_m = \frac{2\pi}{L} m$ and we have introduced the doubly Fourier transformed basis function

$$\begin{aligned}\overline{\delta}_m(k) &\triangleq \frac{1}{M} \sum_{\mu} e^{-i\frac{2\pi}{L} m r_\mu} \delta_\mu(k) = \frac{\psi_0(k)}{\widehat{m}(k)} \frac{1}{M} \sum_{\mu} e^{-i\frac{2\pi}{L} m r_\mu} e^{ikr_\mu} \\ &= \frac{\psi_0(k)}{\widehat{m}(k)} \sum_{a\in\mathbb{Z}} \delta_{m,\kappa+aM} \,,\end{aligned}$$

where $k = \frac{2\pi}{L}\kappa$ and we have used the mathematical identity

$$\frac{1}{M} \sum_{\mu} e^{i\frac{2\pi}{L} m r_\mu} = \sum_{a\in\mathbb{Z}} \delta_{m,aM} \,.$$

In this way, we have

$$\hat{S}^c(k_m) = \sum_{k} \sum_{a\in\mathbb{Z}} \delta_{m,\kappa+aM} \sum_{a'\in\mathbb{Z}} \delta_{m,\kappa+a'M} \hat{S}(k) \left[\frac{\psi_0(k)}{\widehat{m}(k)}\right]^2 \,,$$

where $k = \frac{2\pi}{L} m$. Note that we have

$$\sum_{a'\in\mathbb{Z}} \delta_{m,\kappa+aM} \delta_{m,\kappa+a'M} = \sum_{a'\in\mathbb{Z}} \delta_{m,\kappa+aM} \underbrace{\delta_{\kappa+aM,\kappa+a'M}}_{\delta_{aa'}} = \delta_{m,\kappa+aM} \,,$$

and then

$$\hat{S}^c(k_m) = \sum_{a\in\mathbb{Z}} \hat{S}\left(\frac{2\pi(m-aM)}{L}\right) \left[\frac{\psi_0\left(\frac{2\pi(m-aM)}{L}\right)}{\widehat{m}\left(\frac{2\pi(m-aM)}{L}\right)}\right]^2 \,. \tag{7.27}$$

After inserting (7.22) into (7.27) we obtain the discrete structure factor for the GA+$\sigma$ model,

$$\hat{S}^c(k) = \frac{c_0^2}{r_0} \frac{9}{\left[2+\cos(ka)\right]^2} \sum_{a\in\mathbb{Z}} \frac{\operatorname{sinc}^4\left(\frac{ka}{2} - \pi a\right)}{1 + \left(\frac{k}{k_0} - \frac{2\pi a}{k_0 a}\right)^2} \,, \tag{7.28}$$

where $k = \frac{2\pi}{L}m$. Note that in the limit of high resolution $a = L/M \to 0$, the only term that contributes in the sum over $\alpha$ is $\alpha = 0$. In this limit, then, the discrete structure factor (7.28) converges towards the continuum limit (7.22). Eq. (7.28) gives the prediction of the continuum theory for the fluctuations of the discrete concentration variables.

In the limit $k_0 \to \infty$ corresponding to the GA model, (7.28) becomes

$$\hat{S}^c(k) = \frac{c_0^2}{r_0}\frac{9}{\left[2+\cos\left(\frac{2\pi m a}{L}\right)\right]^2}\sum_{\alpha\in\mathbb{Z}}\operatorname{sinc}^4\left(\frac{\pi(m-\alpha M)}{M}\right),$$

which, on account of the following identity

$$\sum_{\alpha\in\mathbb{Z}}\operatorname{sinc}^4\left(\frac{\pi m}{M}-\pi\alpha\right) = \frac{1}{3}\left[2+\cos\left(\frac{2\pi m}{M}\right)\right],$$

becomes

$$\hat{S}^c(k) = \frac{c_0^2}{r_0}\frac{3}{\left[2+\cos\left(ka\right)\right]}, \tag{7.29}$$

where $k = \frac{2\pi m}{L}$. This is indeed the correct result of the GA model as it can be shown by a more direct route. In the GA model, we know that the second moments of the probability functional are given by

$$\langle \delta c(r)\delta c(r')\rangle = \frac{c_0^2}{r_0}\delta(r-r') \qquad \to \qquad \langle \delta c_\mu \delta c_\nu\rangle = \frac{c_0^2}{r_0}M^\delta_{\mu\nu},$$

where (5.24) has been used. Next

$$\begin{aligned}
S^d(k) = L\left\langle \delta\hat{c}_m\delta\hat{c}_m^*\right\rangle &= \frac{L}{M^2}\sum_{\mu,\nu}e^{-i\frac{2\pi}{L}mr_\mu}e^{i\frac{2\pi}{L}mr_\nu}\left\langle \delta c_\mu\delta c_\nu\right\rangle \\
&= \frac{c_0^2}{r_0}\frac{L}{M^2}\sum_{\mu,\nu}e^{-i\frac{2\pi}{L}mr_\mu}e^{i\frac{2\pi}{L}mr_\nu}M^\delta_{\mu\nu} \\
&= \frac{c_0^2}{r_0}\frac{L}{M^2}\sum_{\mu}e^{-i\frac{2\pi}{L}mr_\mu}e^{i\frac{2\pi}{L}mr_\mu}\frac{1}{\widehat{m}(k_n)} \\
&= \frac{c_0^2}{r_0}\frac{1}{M}\frac{1}{\widehat{m}(k_n)} = \frac{c_0^2}{r_0}\frac{3}{\left[2+\cos\left(ka\right)\right]},
\end{aligned}$$

where we have used (7.25) and coincides with (7.29).

### 7.5.4. The discrete structure factor of the numerical scheme

The static structure function (7.22) has been computed from the second moments of the probability functional and can also be obtained from the following argument that involves the continuum dynamic equation (7.21). In the limit $\Delta t \to 0$, a simple Euler integrator scheme for Eq. (7.21) gives

$$\delta\hat{c}^{n+1} = \delta\hat{c}^n - \frac{\Delta t}{\tau_k}\delta\hat{c}^n - i\mathbf{k}\sqrt{2Dc_0\Delta t}\cdot\hat{\boldsymbol{\zeta}}^n . \tag{7.30}$$

If we multiply this equation by itself and average we obtain

$$\begin{aligned}\left\langle \delta\hat{c}^{n+1}\delta\hat{c}^{n+1}\right\rangle &= \left(1-\frac{\Delta t}{\tau_k}\right)^2 \left\langle \delta\hat{c}^n\delta\hat{c}^n\right\rangle + 2k^2Dc_0\Delta t \\ &\simeq \left(1-2\frac{\Delta t}{\tau_k}\right)\left\langle \delta\hat{c}^n\delta\hat{c}^n\right\rangle + 2k^2Dc_0\Delta t\,,\end{aligned}$$

where we have neglected terms of order $(\Delta t)^2$. At equilibrium $\left\langle \delta\hat{c}^{n+1}\delta\hat{c}^{n+1}\right\rangle = \left\langle \delta\hat{c}^n\delta\hat{c}^n\right\rangle = S^c(\mathbf{k})$, so that

$$\hat{S}^c(k) = k^2Dc_0\tau_k = \frac{c_0^2}{r_0}\frac{1}{1+k^2/k_0^2}\,, \tag{7.31}$$

which coincides with (7.22).

The same strategy may be used to compute the discrete structure factor, by using the discrete time stepping scheme, and thus including effects due to the finite time step.[63] In this way, one may obtain an exact prediction for the discrete structure factor $S^d(k)$ that is produced by the numerical code. If the code is meant to reproduce the structure factor predicted by the continuum theory, we should have $S^d(k) \approx S^c(k)$ for sufficiently small times. The only difference from the procedure used to derive Eq. (7.31) is that both $k^2$ and $\tau_k$ are to be replaced by their corresponding discrete counterparts.

Namely, $\tau_k$ can simply be read from the fact that in the discrete setting the integrator scheme is given, in the GA+$\sigma$ model, by Eq. (7.15) with no explicit part. In Fourier space, this equation should give us Eq. (7.30). If we equal

(7.30) with the equivalent (7.15) in Fourier space we obtain

$$\tau_k \mapsto \frac{c_0}{Dr_0}\frac{\widehat{m}}{\widehat{l}+\frac{1}{k_0^2}\frac{\widehat{l}^2}{\widehat{m}}} + \mathcal{O}(\Delta t)\,.$$

In the same way, the discrete $k^2$ term can be obtained from the covariance of the noise term that appears in (7.30), which should coincide with the noise term in (7.15), giving as a result $k^2 \mapsto \frac{\widehat{l}}{\widehat{m}^2}$, where we have neglected terms of order $\mathcal{O}(\Delta t)$. In this way, the equivalent of Eq. (7.31) for the discrete structure factor will be

$$\begin{aligned}\hat{S}^d(k) &= k^2 D c_0 \tau_k = \frac{c_0^2}{r_0}\frac{1}{\widehat{m}}\frac{1}{\widehat{l}+\frac{1}{k_0^2}\frac{\widehat{l}^2}{\widehat{m}}} \\ &= \frac{c_0^2}{r_0}\frac{3}{[2+\cos(ka)]}\frac{1}{1+\frac{k^2}{k_0^2}\left(\frac{3\mathrm{sinc}^2(ka/2)}{(2+\cos ka)}\right)}\,. \end{aligned} \tag{7.32}$$

Another possibility is to consider the integrator scheme in the Fourier space (7.14)

$$\hat{c}^{n+1}(m) = \frac{\widehat{T}^n(m)}{\widehat{T}^{n+1}(m)}\hat{c}^n + \frac{\widehat{W}^n(m)}{\widehat{T}^{n+1}(m)}\widehat{\mathcal{W}}^n\,.$$

If we multiply by itself and we average we obtain

$$\left\langle \hat{c}^{n+1}\hat{c}^{n+1}\right\rangle = \frac{\widehat{T}^n\widehat{T}^n}{\widehat{T}^{n+1}\widehat{T}^{n+1}}\left\langle \hat{c}^n\hat{c}^n\right\rangle + \frac{\widehat{W}^n\widehat{W}^n}{\widehat{T}^{n+1}\widehat{T}^{n+1}}\,.$$

At equilibrium $\left\langle \hat{c}^{n+1}\hat{c}^{n+1}\right\rangle = \left\langle \hat{c}^n\hat{c}^n\right\rangle$, so that,

$$\begin{aligned}\left\langle \hat{c}^n\hat{c}^n\right\rangle &= \frac{\widehat{W}^n\widehat{W}^n}{\widehat{T}^n\widehat{T}^n - \widehat{T}^{n+1}\widehat{T}^{n+1}} \\ &= \frac{c_0^2}{r_0}\frac{1}{\widehat{m}}\frac{1}{1+\frac{K}{r_0}\frac{\widehat{l}}{\widehat{m}}} \\ &= \frac{c_0^2}{r_0}\frac{3}{[2+\cos(ka)]}\frac{1}{1+\frac{k^2}{k_0^2}\left(\frac{3\mathrm{sinc}^2(ka/2)}{(2+\cos ka)}\right)}\,,\end{aligned}$$

which coincides (as it should be) with (7.32).

In summary, we have computed both the static and the dynamic structure factors for Gaussian models and have checked that their discrete counterparts converge towards the analytical predictions. In the next section we will compute numerically the discrete static structure factor in regular and irregular grids, and we will also compare the relaxation time $\tau_k$ for the dynamic structure factor. This should allow us to validate the numerical algorithm.

## 7.6. Simulation results

In this section, we consider a $1D$ periodic system governed by the free energy functionals (7.6), (7.5) and (7.3). In $1D$ these models are well behaved, and the continuum equations have a precise interpretation. We are concerned with the convergence of the numerical method to the solution of the continuum equations as the grid is refined.

### 7.6.1. Parameters

The set of parameters in the van der Waals model and in its approximate form, the Ginzburg-Landau model, is the following. The parameters corresponding to the particular fluid being studied are the excluded volume $b$ of a van der Waals molecule, the length scale $\sigma$ of the potential, and the critical temperature $T_c$ of the van der Waals fluid. The parameters corresponding to the thermodynamic state are the temperature $T$ and the global concentration $c_0 = N/L$ where $N$ is the total number of particles and $L$ is the size of the box. Because the dynamics conserves the total number of particles $N = \int d\mathbf{r}\, c_0(\mathbf{r})$, the total number of particles is a parameter of the simulation that enters through the initial conditions specified through the initial profile $c_0(\mathbf{r})$. The parameter corresponding to the dynamic equation is the mobility $\Gamma$ assumed to be constant and given in terms of the diffusion coefficient $D$ as $\Gamma = Dc_0/k_{\mathrm{B}}T$. Finally, we have a set of numerical parameters, like the time step size $\Delta t$ and the total number $M$ of nodes of the mesh. Each node has a volume $V_\mu$ with $\sum_\mu V_\mu = L$.

From this set of parameters, we choose $b$, $k_B T_c$ and $D$ as our units, thus fixing the basic units of length, time, and mass. This results in the following dimensionless numbers as our free parameters $L/b, \sigma/b, T/T_c, N, M$. We will consider a fluid characterized by a fixed value of $b$, $\sigma$ and $k_B T_c$. In this way, we will fix the ratio $b/\sigma = 10$. We also fix $N$ in order to have the total concentration $N/L$ equal to the critical concentration $1/3b$, this is, $N = L/3b$. In this way, the number of free parameters to explore is reduced to $L/b$, $M$, $T/T_c$. The limit $L/b \to \infty$ is the *thermodynamic limit* or infinite system size limit, whereas the limit $Mb/L \to \infty$ (so the volume of each cell approaches zero) is the *continuum limit*.

In the following sections, all the simulations are performed at a box of size $L = 10$ at a temperature $k_B T = 1.11$ in the selected units, with the corresponding parameters in Eq. (7.4) being $r_0 \simeq 0.07$ and $K \simeq 0.007$. All simulations start from an initial state in which $c_\mu(t = 0) = c_0$ for all $\mu$, and employ a sufficiently small time step to ensure numerical stability and convergence of results. We ensure that we sample equilibrium configurations by compiling statistics only after a time of the order $L^2/D$. The number of particles $N = \sum_\mu c_\mu V_\mu$ is exactly conserved by the algorithm.

### 7.6.2. Observables

The structure factor is an observable that is specially suited when there is translation invariance. The structure factor is the discrete Fourier transform of the matrix of covariances, this is, the matrix of second moments of the probability distribution $P^{\text{eq}}(\mathbf{c})$ in Eq. (6.6). The $k$-dependent structure factor allows to discuss correlations of the concentration at different length scales. As shown in Section 7.5,the structure factor can be analytically computed in the continuum limit for a GA+$\sigma$ model with the result

$$S^c(k) = \langle \delta c(k,0) \delta c(-k,0) \rangle = \frac{c_0^2}{r_0} \frac{1}{1 + \frac{k^2}{k_0^2}} \tag{7.33}$$

where

$$k_0 = \left( \frac{r_0}{K} \right)^{1/2} = \frac{1}{\sigma} \left( \frac{T}{T_c} - 1 \right)^{1/2}$$

The typical length scale below which fluctuations start to decorrelate is given by $\lambda = 2\pi/k_0$.

The *dynamic* structure factor is the Fourier transform of the time dependent correlation function and can also be explicitly computed for the Gaussian models leading to

$$S^c(k,t) = \langle \delta\hat{c}(k,t)\delta\hat{c}(-k,0)\rangle = S^c(k)\exp\left\{-\frac{t}{\tau_k}\right\} \tag{7.34}$$

with a typical relaxation time given by

$$\tau_k = \left[\frac{D}{c_0}r_0\left(1+\frac{k^2}{k_0^2}\right)k^2\right]^{-1} \tag{7.35}$$

The continuum results (7.33) and (7.35) serves also as the basis for computing the structure factors of the discrete variables, as we have seen in SECTION 7.5.

In addition to the structure factor, we will also consider as observable the probability that a region of finite size $l$ has a given number of particles in its interior. In $1D$, this observable should be independent of the resolution, given a sufficiently large resolution, and will allow us to detect whether the GL model behaves in a Gaussian or non-Gaussian way, depending on the temperature.

### 7.6.3. Regular lattice results

*Static structure factor for Gaussian models*

While the structure factor (7.33) has an explicit expression, what we compute in a simulation is the covariance $\langle \delta c_\mu \delta c_\nu\rangle$ of the discrete variables $c_\mu$ or, for regular lattices, its Fourier transform. We introduce the discrete Fourier transform $\hat{c}_m$ with $m = 0, M-1$ of the discrete concentration field $c_\mu$ according to

$$\hat{c}_m = \frac{1}{M}\sum_\mu e^{-i\frac{2\pi}{L}mr_\mu}c_\mu$$

and define the discrete structure factor as [63]

$$\hat{S}^c(k) \triangleq L\,\langle \delta\hat{c}_m \delta\hat{c}_m^*\rangle$$

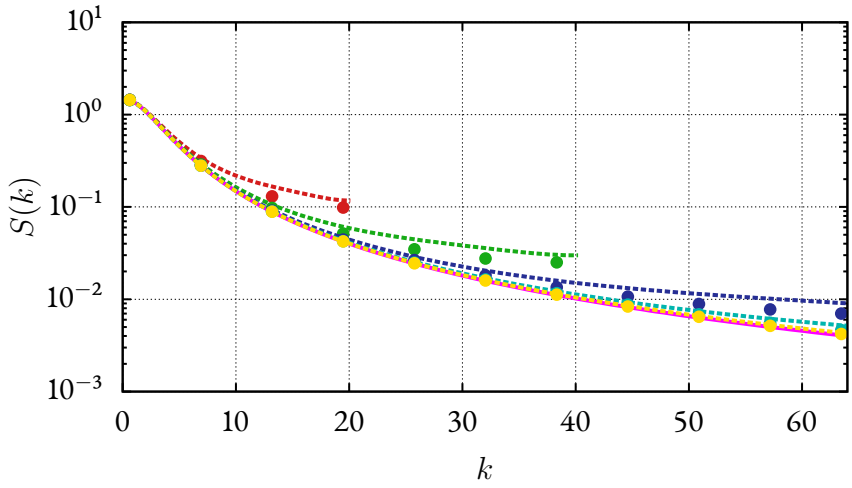


**Figure 7.1:** Comparison for the GA+$\sigma$ model of the static structure factors $S^c(k)$ (dashed lines) in Eq. (7.36), $S^d(k)$ (points) in Eq. (7.37), and $S(k)$ (solid pink line) in Eq. (7.33). From top to bottom: red, $M = 64$; green, $M = 128$, blue, $M = 256$; cyan, $M = 512$; yellow, $M = 1024$; pink, continuum structure factor. As the resolution increases, the range of $k$ for which there is no significant discrepancy between the discrete results and the continuum prediction $S(k)$ in Eq. (7.33) increases.

where $k = \frac{2\pi}{L}m$ for integer $m$. The modes $\hat{c}_m$ are related to $c_\mu$ which, in turn, are related to the continuum field through the basis delta function $\delta_\mu(\mathbf{r})$. For the GA+$\sigma$ model we know the correlations of the fluctuations of the continuum field and, therefore, we have an explicit expression for the discrete structure factor

$$\hat{S}^c(k) = \frac{c_0^2}{r_0}\frac{9}{\left[2+\cos\left(ka\right)\right]^2}\sum_{a\in\mathbb{Z}}\frac{\operatorname{sinc}^4\left(\frac{ka}{2}-\pi a\right)}{1+\left(\frac{k}{k_0}-\frac{2\pi a}{k_0 a}\right)^2} \tag{7.36}$$

The numerical integrator proposed in Refs. [38, 80] produces the same static structure factor regardless of the time step. As we show in SECTION 7.5.4, the actual discrete structure factor $\hat{S}^d(k)$ produced by our integrator for the

GA+$\sigma$ model is given by

$$\hat{S}^d(k) = \frac{c_0^2}{r_0}\frac{3}{[2+\cos(ka)]}\frac{1}{1+\frac{k^2}{k_0^2}\left(\frac{3\mathrm{sinc}^2(ka/2)}{(2+\cos ka)}\right)} \tag{7.37}$$

which is independent of the time step $\Delta t$. [38] This result (7.37) is useful as it allows to check for correct coding of the algorithm. We have indeed verified that the numerical results lead exactly to (7.37). Note that $\hat{S}^d(k)$ in (7.37) tends to the continuum limit $\hat{S}(k)$ in (7.33) for $k \ll \frac{\pi}{a}$. In the limit $k_0 \to \infty$, $\hat{S}^d(k) = \hat{S}^c(k)$ (see Eq. (7.29)). For finite $k_0$, $\hat{S}^d(k)$ is different from $\hat{S}^c(k)$, although both structure factors tend to the continuum value $\hat{S}(k)$ for sufficiently high resolutions. We compare in Fig. 7.1 $\hat{S}(k)$ in Eq. (7.33), $\hat{S}^c(k)$ in Eq. (7.36) and $\hat{S}^d(k)$ in Eq. (7.37) for increasing levels of resolution. The main observation is that $\hat{S}^d(k)$ and $\hat{S}^c(k)$ are very similar. In other words, not only the infinite limit resolution $\hat{S}(k)$ is well captured by the numerical method, but also the predictions of the continuum theory for a finite mesh are equally well reproduced.

The Gaussian model GA is obtained by setting $K = 0$ and suppressing the square gradient term. This implies $k_0 = \infty$ and results in that different points in space are completely uncorrelated. Figure 7.2 shows the *static* structure factor for different resolutions, from $M = 64$ to $M = 256$ as well as the continuum solution. [63] We also plot in Fig. 7.2 the theoretical discrete structure factor, given by Eq. (7.36), which takes into account the finite size of the cell. The simulation results are indistinguishable from the theoretical prediction at each resolution as they should, since in this case Eq. (7.36) is equal to (7.37). As we keep increasing the resolution, the range of wavenumber for which the structure factor coincides with the prediction $c_0^2/r_0$ of the continuum theory increases. However, there is always a discrepancy at large wave numbers corresponding to the inverse of the lattice spacing.

*Dynamic structure factor for Gaussian models*

The *dynamic* structure factor can also be obtained from Eq. (7.34) for a given $k$ value. Figure 7.3 shows the dynamic structure factor for $k = 5.02$ with

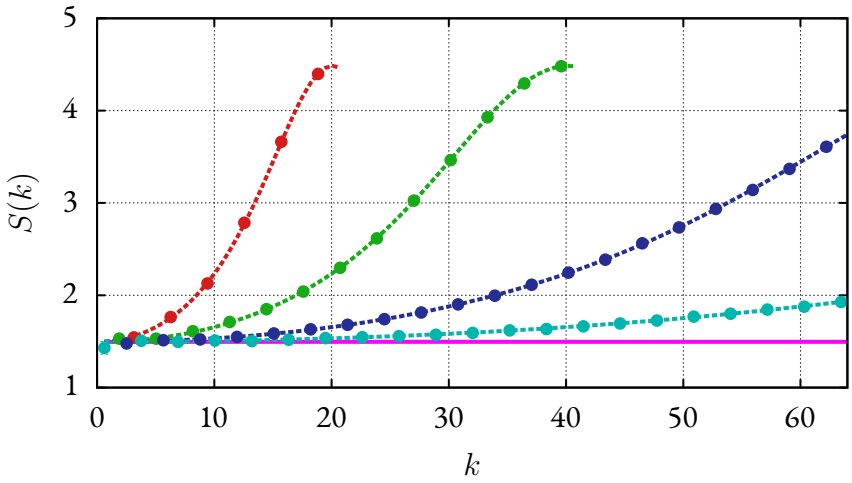


**Figure 7.2:** Static structure factor as a function of $k$ for the model GA. From left to right: red, $M = 64$ nodes ($\Delta t = 10^{-3}$); green, $M = 128$ ($\Delta t = \frac{1}{4}10^{-3}$); blue, $M = 256$ ($\Delta t = \frac{1}{16}10^{-3}$); cyan, $M = 512$ ($\Delta t = \frac{1}{32}10^{-3}$); pink solid line, continuum result $c_0^2/r_0$ given by Eq. (7.33) in the limit $k_0 \to \infty$. Dots correspond to the numerical structure factor obtained from simulations; dashed lines correspond to the theoretical prediction given by Eq. (7.36).

$M = 256$ (a sufficiently fine grid) for both the GA (circles) and the GA+$\sigma$ (squares) models, and compares numerical results with the theoretical prediction (pink solid line). In the GA case, the value $r_0 \simeq 0.07$ gives a relaxation time of $\tau_k = 0.2$. In the GA+$\sigma$ case, the parameter $r_0$ remains unchanged and $K \simeq 0.007$, with a time scale $\tau_k \simeq 0.05$. As can be seen, numerical simulations overlap with theoretical predictions. We also plot in Fig. 7.4 the relaxation time $\tau_k$ obtained through simulations for both the GA (circles) and GA+$\sigma$ (squares) models, and compares them with the theoretical result (7.35). Both results overlap the theoretical ones for time scales smaller than $10^{-4}$ in reduced units, which is comparable to the time step size $\Delta t = \frac{1}{16}10^{-3} = 6.25 \times 10^{-5}$. Note that this time step is much smaller than the relaxation time for the wavenumber plotted. We may still have good results for small wave numbers with much larger time steps, but we have decided to use a time step that would resolve also the smallest relaxation times, which is roughly $\tau_{\min} = \Delta x^2/D = L^2/(M^2 D) = 1.5 \times 10^{-3}$.

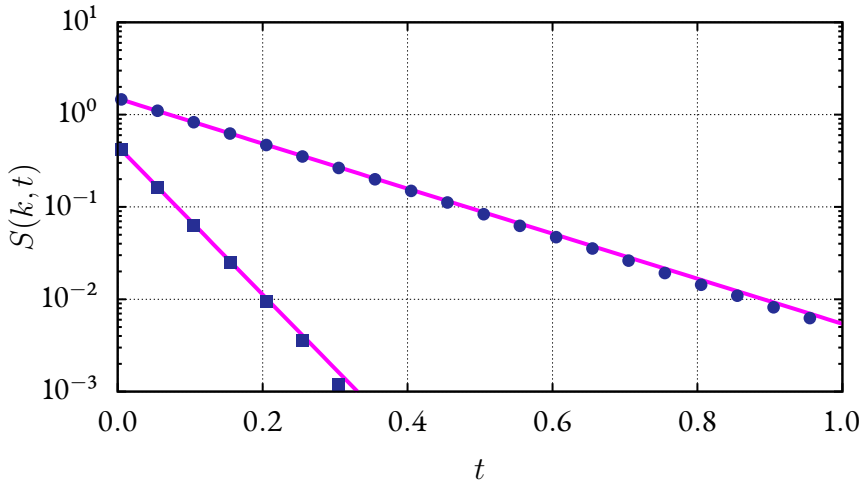


**Figure 7.3:** Dynamic structure factor for $k = 5.02$ as a function of time for the model GA (blue circles, top) and GA+$\sigma$ (blue squares, bottom). Averaged over 10 simulations at $M = 256$. Circles and squares correspond to the numerical result, solid pink line corresponds to the theoretical prediction (7.34). In the GA model, $\sigma^2 = 0$ gives a relaxation time $\tau_k = 0.2$. In the GA+$\sigma$ model, $\sigma^2 = 0.01$ ($K \simeq 0.007$) gives a relaxation time $\tau_k = 0.05$.

*Static structure factor for Ginzburg Landau model*

Once the code has been checked for the Gaussian models, we may move to the more interesting case of the Ginzburg-Landau model Eq. (7.3) with its discrete free energy function given in Eq. (7.10). This model shows phase separation at subcritical temperatures. For sufficiently high supercritical temperatures Gaussian behavior is recovered. In order to detect interesting non-linear effects, albeit in the single phase region, we will explore temperatures near (above) the critical temperature characterized by a single non Gaussian phase.

Figure 7.5 shows the probability distribution of finding a deviation from the mean of the number of particles, $\delta N$, inside a region of size $l = \frac{1}{16}L$. The simulation were done at $k_B T = 1.11$ ($r_0 \simeq 0.07$) and $\sigma^2 = 0.01$ ($K \simeq 0.007$) in the selected units. As we increase the resolution the probability distribution converges towards a unique limit. In a Gaussian model, one should expect a linear dependence between $(\delta N)^2$ and $P(\delta N)$. This is not observed in

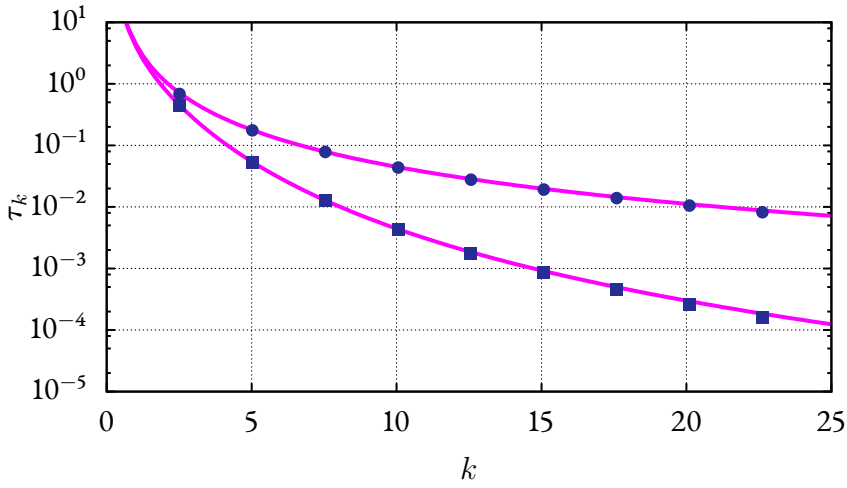


**Figure 7.4:** Relaxation time $\tau_k$ as a function of $k$ for $M = 256$ in both the GA model (blue circles, top) and the GA+$\sigma$ model (blue squares, bottom) averaging over 10 simulations with time step $\Delta t = \frac{1}{16}10^{-3}$. Dots correspond to the relaxation time obtained from a numerical fitting of the dynamic structure factor to an exponential function. Lines correspond to the theoretical prediction in Eq. (7.35).

the limit curve of Fig. 7.5, signaling non-Gaussian behavior for this thermodynamic point state.

Figure 7.6 shows the static structure factor for the Ginzburg-Landau model at different resolutions, $M = 64$ (red), $M = 128$ (green) and $M = 256$ (blue) and $M = 512$ (cyan). We observe that as we increase the resolution we converge towards a unique answer. The $L_2$-norm

$$L_2(M_1, M_2) = \sqrt{\sum_i (S^{M_1}(k_i) - S^{M_2}(k_i))^2}$$

is also shown in the inset of Fig.7.6, where we compare the structure factor obtained at resolution $M_1$ with the one obtained at a higher resolution $M_2 = M_1 + 32$. A pink line of slope $-2$ agrees well with the numerical results reflecting second order spatial convergence of the algorithm.

We also compare in Fig. 7.6 the static structure factor of the GL model with

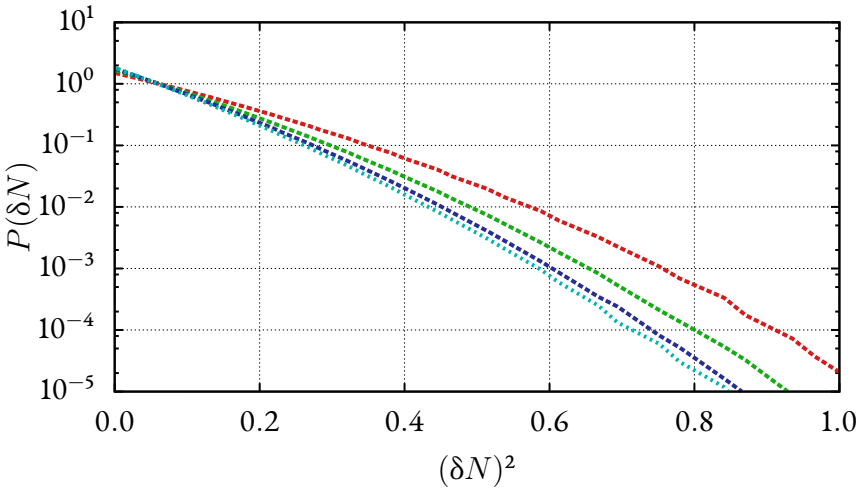


**Figure 7.5:** Probability distribution of finding a deviation from the mean of the number of particles inside a region of size $l = \frac{1}{16}L$ for the GL model. This is, $\delta N = c_0 l - \sum_{\mu \in l} c_\mu V_\mu$. From top to bottom, $M = 64$ nodes, $M = 128$, $M = 256$ and $M = 512$. We observe convergence of the probability distribution towards a non Gaussian distribution as the resolution is increased.

the continuum limit of the corresponding one in the GA+σ model. Two regions are clearly observed, separated by a value at around $k_c = 30$. On one hand, for $k < k_c$ (large length scales) there is a clear difference between the Gaussian and the GL model. For small wavenumbers, the contribution of the quartic term is important and suppresses the amplitude of the fluctuations relative to the GA+σ model. On the other hand, for $k > k_c$ there is no difference between both models in the limit of infinite resolution, and the quartic term has a minimal effect. The existence of two regions may be understood from the probability of finding a particular Fourier mode $\phi_k$ of the field, which will be given by the exponential of the free energy (7.3), expressed in Fourier space. The quadratic term in this free energy has a $k$-dependent prefactor $(r_0 + Kk^2)/2$. Near the critical point, we have $r_0 \sim 0$. Therefore, for $k \sim 0$, the free energy is entirely dominated by the quartic interaction (which in Fourier space is in the form of a convolution). At sufficiently large $k$, however, the quadratic term dominates over the quartic. The effect of the quartic

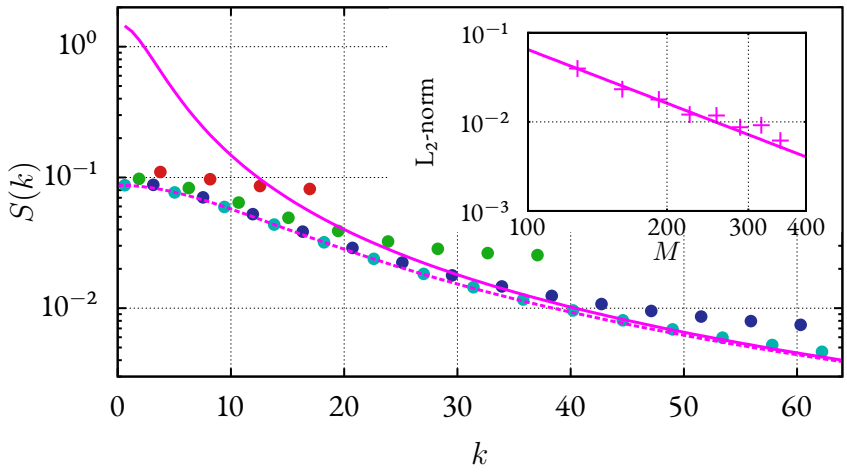


**Figure 7.6:** Static structure factor as a function of $k$ for the GL model. Red, $M = 64$ nodes ($\Delta t = 10^{-3}$); green, $M = 128$ ($\Delta t = \frac{1}{4}10^{-3}$); blue, $M = 256$ ($\Delta t = \frac{1}{16}10^{-3}$); cyan, $M = 512$ ($\Delta t = \frac{1}{32}10^{-3}$). Convergence of the numerical results is observed as the resolution increases. With solid pink line, the continuum structure factor of the GA+$\sigma$ model with the same parameters $r_0 \simeq 0.07$ $K \simeq 0.007$ as the GL model. Dashed pink line shows the continuum structure factor of a renormalized GA+$\sigma$ model which has the same variance as the GL model. The empirical fitting of the numerical data to the renormalized GA+$\sigma$ static structure factor gives $r_0 = 1.27$ and $K = 0.007$. *Inset*, $L_2$-norm indicating convergence.

term is to strongly suppress the amplitude of the long-wave fluctuations with respect to the Gaussian model with the same $r_0, K$ parameters.

*Dynamic structure factor for Ginzburg Landau model*

Figure 7.7 shows the dynamic structure factor of the GL model for $k = 5.02$ at different resolutions. We observe convergence as the resolution is increased in the region where the statistical errors are small ($S(k,t) \sim 10^{-3}$). The fact that the decay of the dynamic structure factor of the GL model is exponential suggests that its dynamics is very similar to that of a *renormalized* Gaussian model. In order to test this conjecture, we have considered the best GA+σ model that would reproduce the *static* structure factor of the GL model. The

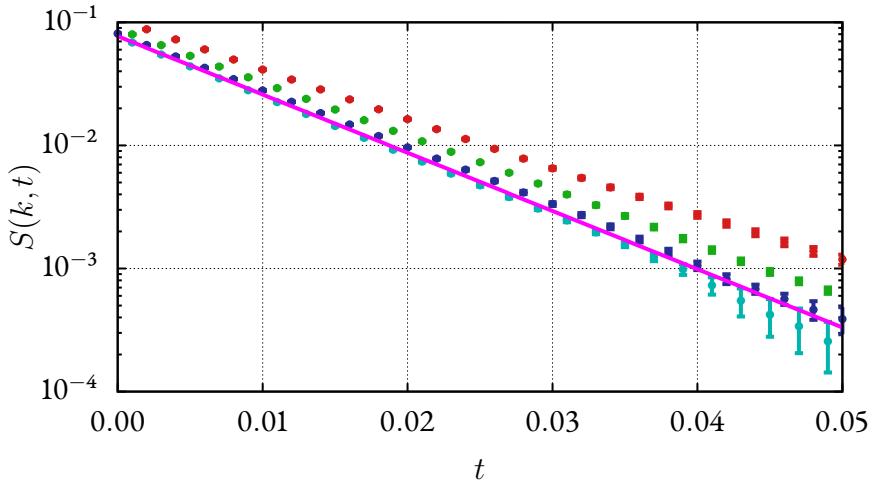


**Figure 7.7:** Dynamic structure factor as a function of $t$ for $k = 5.02$ for the GL model. With dots: red, $M = 64$ nodes ($\Delta t = 10^{-3}$); green, $M = 128$ ($\Delta t = \frac{1}{4}10^{-3}$); blue, $M = 256$ ($\Delta t = \frac{1}{16}10^{-3}$). With solid pink line, the dynamic structure factor of a renormalized GA+$\sigma$ model with parameters $r_0 = 1.27$ and $K = 0.007$.

best Gaussian model is the one that has the same structure factor as that of the GL model. The result of the fit is presented in Fig. 7.6 and gives the parameters $r_0 = 1.27$ and $K = 0.007$. Observe that in the renormalized GA+$\sigma$ model the surface tension coefficient $K$ is the same and only the value of the quadratic coefficient $r_0$ is renormalized, consistent with predictions of renormalization (perturbative) theories [30]. With these values of $r_0$, $K$ we compute independently the prediction for the relaxation time given by Eq. (7.35) for a GA+$\sigma$ model. The result is the solid line in 7.8. A very good agreement between the measured relaxation times of the GL model and the prediction of this renormalized Gaussian model is obtained. This suggests that, as far as the structure factor is concerned, the GL model behaves as a GA+$\sigma$ model with renormalized parameters.

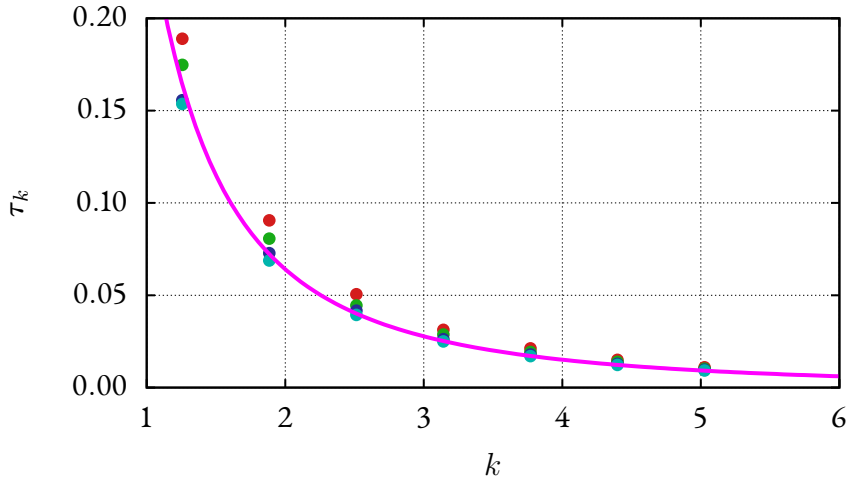


**Figure 7.8:** Relaxation time $\tau_k$ as a function of $k$ in the GL model at different resolutions $M = 64$ (red), $M = 128$ (green), $M = 256$ (blue) and $M = 512$ (cyan). All of them obtained averaging over 10 simulations. Dots correspond to the numerical relaxation time (obtained from a numerical fitting of the dynamic structure factor to an exponential function). Line corresponds to the theoretical prediction (7.35) of the renormalized GA+$\sigma$ model with $T = -1.4$ ($r_0 \simeq 1.27$) and $\sigma^2 = 0.01$ ($K \simeq 0.007$).

### 7.6.4. Irregular lattices

In this section, we present similar results as in the previous section but in this case for irregular lattices. Adaptive mesh resolution allow one to resolve interfaces appearing below critical conditions, and deal with complicated boundary conditions. In the present paper, while we still remain in the supercritical region of the GL model, where no interfaces are formed, we test the performance of the algorithm presented for irregular lattices. We consider irregular lattices constructed by displacing randomly the nodes of a regular lattice, allowing for a maximum fluctuation of $\pm$ 40% with respect to the regular lattice configuration. These random lattices are a worst case scenario and other lattices with slowly varying density of nodes behave much better in terms of numerical convergence. We compare regular and irregular lattice simulation results by using the same set of parameters in both cases. Typically, what we

observe is that higher resolutions are required in irregular lattices in order to achieve comparable accuracy as those in regular lattices. The time step in an irregular lattice is dictated by the shortest lattice distance $\Delta x_{\min}$ encountered according to $\Delta t \sim \Delta x_{\min}^2/D$.

From a numerical point of view, obtaining the static structure factor for regular grids can be efficiently done with Fast Fourier Transforms (FFT): we just need to perform a FFT of the concentration field and multiply it by its complex conjugate. However, irregular grids complicate the use of the FFT and we need to follow a different route to obtain the static structure factor. The idea is to interpolate the discrete field on the irregular coarse grid onto a very fine regular grid on which the FFT can be used. Of course, the interpolation procedure modifies the structure factor because we are creating information at the interpolated points.

At the same time, when we consider irregular grids, we do not have simple analytical results to compare, even for the Gaussian models. In this case, our strategy is to produce synthetic Gaussian fields generated in a very fine grid ensuring that they are distributed in such a way that have a structure factor given by (7.33). This is achieved by generating random Gaussian numbers in Fourier space with the correct mean and covariance for each wavenumber $k$ so that the theoretical $S(k)$ is recovered. These synthetic Gaussian fields are taken as the "truth" to compare with. From the synthetic Gaussian field, we compute a coarse-grained field on an irregular coarse grid by applying the coarsening operator $\delta_\mu(\mathbf{r})$ as in the first equation (5.24), where the integral is approximated as a sum over the very fine grid. This gives us realizations of a Gaussian field in a coarse irregular grid. We may now apply the methodology used for computing the structure factor in regular grids, by interpolating on a very fine regular grid and using the FFT.

Figures 7.9 and 7.10 show, for both a GA and a GA+$\sigma$ model, the agreement between simulations (in dots) and the synthetic procedure (dashed lines). We also show the predictions obtained from (7.33), demonstrating that we correctly discretized Eq. (3.21) on the irregular grid.

We move now to the GL model. We consider the probability distribution of a fluctuation of the number of particles in a fixed region of space for the GL model. The region of space is delimited by two nodes that are always at

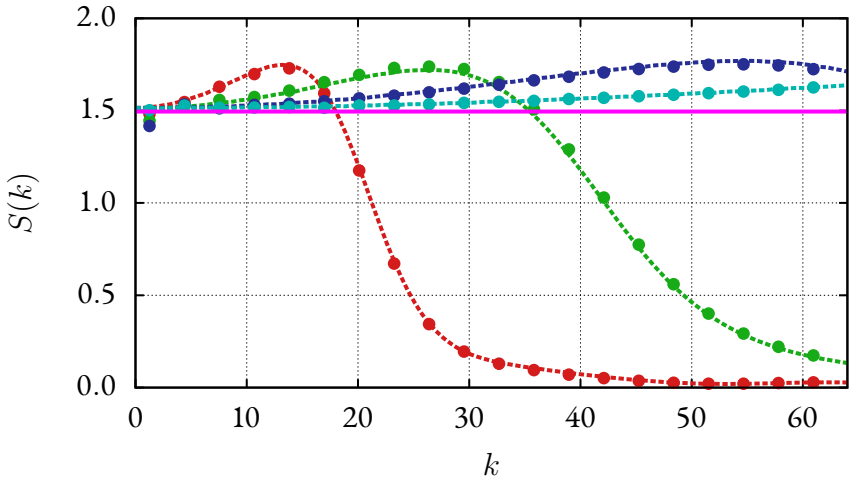


**Figure 7.9:** Static structure factor as a function of $k$ for the model GA in irregular lattices. From left to right, $M = 64$ nodes ($\Delta t = 10^{-3}$), $M = 128$ ($\Delta t = \frac{1}{4}10^{-3}$), $M = 256$ ($\Delta t = \frac{1}{16}10^{-3}$), $M = 512$ ($\Delta t = \frac{1}{32}10^{-3}$) and continuum limit of the GA model (solid pink line, Eq. 7.33). Dots correspond to the simulations of the diffusion equation, while dashed lines correspond to the synthetic Gaussian fields. The striking difference with Fig. 7.2 is due to the interpolation procedure used to compute the static structure factor in the irregular grid.

the same distance $l = L/16$. In a first simulation, we consider an arbitrary grid of nodes set at random in the whole domain, except for the two points delimiting the region of interest that are always fixed. In Fig. 7.11 we plot the result of increasing the number of nodes in the simulation.

In a second simulation, we divide the box in 16 equally spaced regions delimited by nodes of the grid. Then, in half of the boxes we have a coarse resolution and in the other half we have a finer resolution. The probability in any of the regions is essentially the same, as shown in Fig. 7.12, further validating the method for irregular grids.

Finally, we show in Fig. 7.13 the static structure factor for the GL model in an irregular random grid, where the simulations are performed with the same parameters as those in Figs. 7.9 and 7.10. We observe that by increasing the resolution the structure factor converges towards a continuum result, consistent with the results based on the regular grid. We conclude that the algorithm

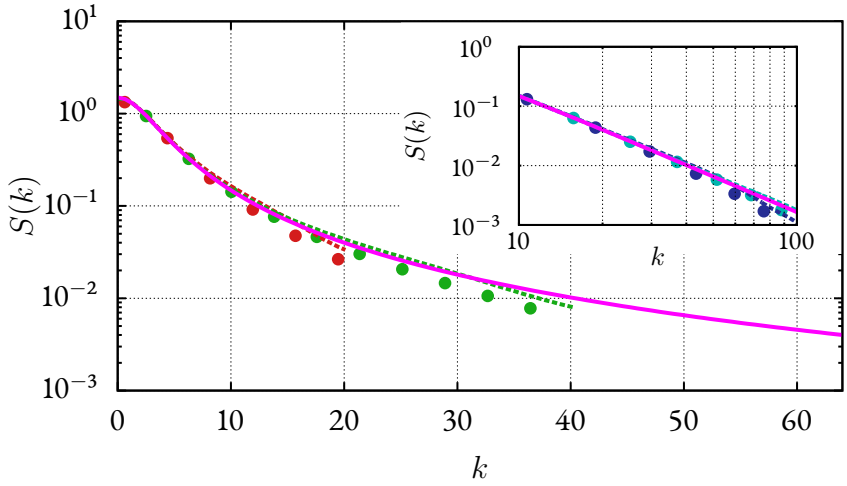


**Figure 7.10:** Structure factor in the GA+$\sigma$ model for an irregular lattice. In the main panel, $M = 64$ nodes (red, $\Delta t = 10^{-3}$) and $M = 128$ (green, $\Delta t = \frac{1}{4}10^{-3}$). In the inset we plot in log-log scale results for $M = 256$ nodes (blue, $\Delta t = \frac{1}{16}10^{-3}$) and $M = 512$ nodes (cyan, $\Delta t = \frac{1}{32}10^{-3}$). Dots correspond to the simulations of the diffusion equation. Dashed lines correspond to the synthetic Gaussian (with surface tension term) field. The theoretical prediction in Eq. (7.33) is also plotted in solid pink line.

presented displays convergence of the GL model for both regular and irregular grids.

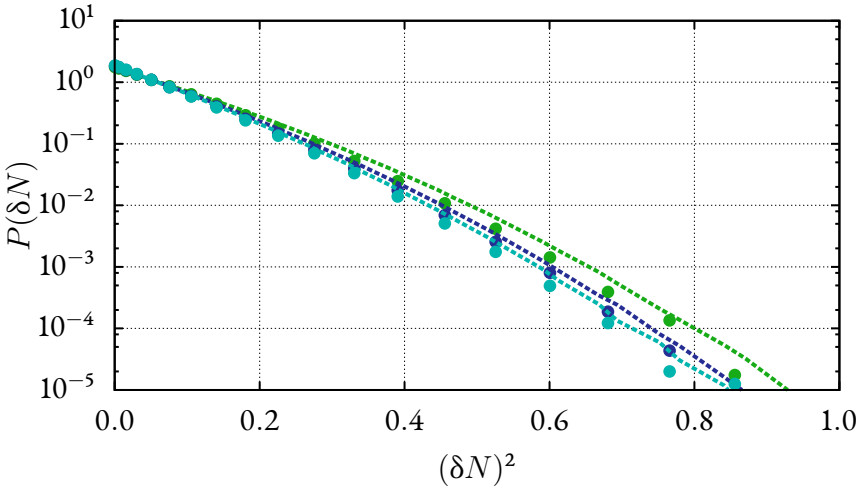


**Figure 7.11:** Probability of $\delta N$ in a given region of space $l = \frac{1}{16}L$ in a random grid. The points that limit the region are kept fixed as in the regular grid, inside the region the nodes are randomly distributed. Green, $M = 128$; blue, $M = 256$; cyan, $M = 512$. We compare the probability in a random grid (points) with the probability corresponding to a regular grid with the same resolution (dashed lines).

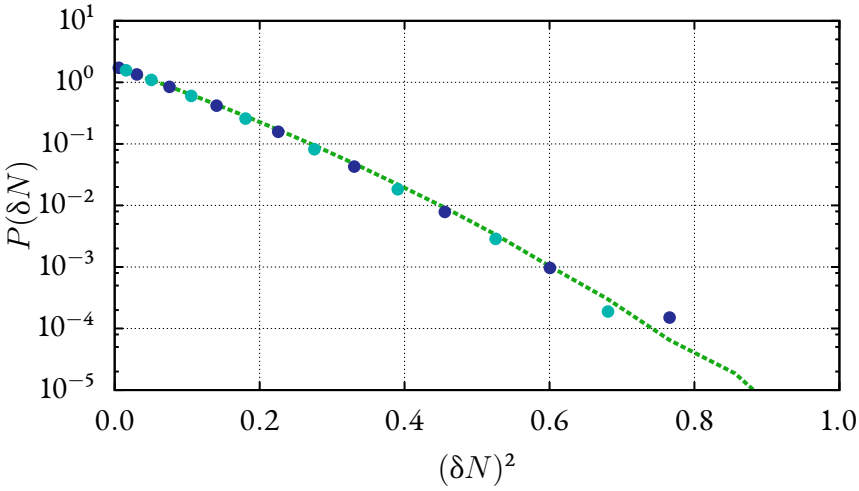


**Figure 7.12:** Probability of $\delta N$ in a given region of space $l = \frac{1}{16}L$. Green dashed line corresponds to a regular lattice with $M = 128$. Blue dots correspond to a grid with $M = 256$ and cyan dots correspond to a grid with $M = 512$. For the $M = 512$ grid, 64 nodes are uniformly distributed in half of the box while the remaining 448 nodes are distributed uniformly in the other half. In this way, we have a grid which is, in one region, seven times finer than the original one; in the other region, exactly the original one. The grid $M = 256$ is defined with 32 nodes in half of the box and 224 nodes in the other half.

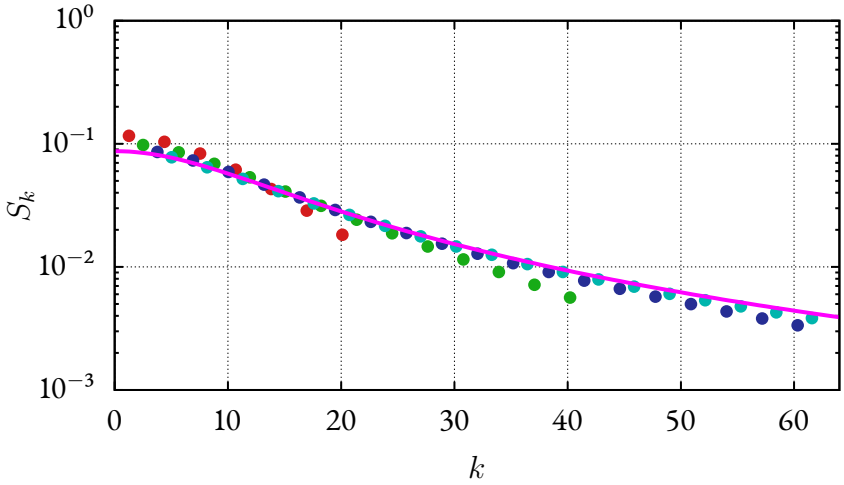


**Figure 7.13:** Static structure factor as a function of $k$ for the GL model in an irregular lattice. From bottom to top: red, $M = 64$ ($\Delta t = \frac{1}{16}10^{-3}$); green, $M = 128$ ($\Delta t = \frac{1}{32}10^{-3}$); blue, $M = 256$ ($\Delta t = \frac{1}{64}10^{-3}$) and cyan $M = 512$ ($\Delta t = \frac{1}{128}10^{-3}$). From $M = 64$ to $M = 256$, averaged over 10 simulations. Pink solid line shows the theoretical renormalized GA+$\sigma$ model (with $r_0 = 1.27$ and $K = 0.007$).

## 7.7. Summary

In this final chapter we have proposed particular models for the SDE (0.10). We have used the conjugate basis function (3.3) to build discrete models for the free energy and the dissipative matrix. The obtained equations for the evolution of the coarse-grained variables (the discrete concentration field) can be understood as a generalization of what has been done in Chapter 4, valid also for irregular grids. As we discussed in Chapter 6, the obtained SDE for the models of the free energy and the dissipative matrix can also be understood as discretizations of the continuum SPDE (0.4).

One of the main differences with respect to what it has been done in Chapter 4 is the use of an implicit algorithm for the time discretization. As we have discussed, implicit schemes allow one to use larger time steps in comparison with explicit algorithms. In that way, we may explore larger times and problems with bigger resolution at the same computational cost. The implicit method considered here is also unconditionally stable for any time step for the linear equations. Thus, static properties are correctly reproduced even for large time steps.

In this chapter, the observables selected are the static and dynamic structure factors (the second moments of the probability of the field) and the probability of having a number of particles in a fixed region of space. The fact that linear problems (like the Gaussian model) are analytically solvable allow one to check the accuracy of the proposed integration scheme. We have validated the scheme and have moved to the non-linear Ginzburg-Landau model. We have unambiguously observed that this model has, in $1D$, a well-defined continuum limit. As shown in Eq. (7.19), the structure factor for a Gaussian field presents a divergence for $D > 1$ in the limit $\mathbf{r} - \mathbf{r}' \to 0$. This so called ultraviolet catastrophe implies that products of four Gaussian fields are not really well defined and, therefore, the Ginzburg-Landau model is not really well defined in $D > 1$. Although we do not have conducted simulations in $2D$ or $3D$, we expect that a continuum limit will not be reached in these cases.

Finally, we point out that the finite element methodology presented in this dissertation may be extended to other SPDE like those appearing in the Landau-Lifshitz Navier-Stokes (LLNS) equations. For a compressible theory, the free

energy function plays essentially the same role as in the present theory. In LLNS one usually chooses a free energy which is Gaussian. We should expect similar ultraviolet catastrophic behavior as in the present simpler non-linear diffusion. However, the Gaussian theory should still give correct macroscopic observables like the amplitude of the fluctuations of the number of particles in a *finite* region of space. While the equilibrium properties in the Gaussian model do not have pathological behavior, the convective terms in the equations, involving non-linear terms, require a careful regularization. [31]

# 8 Conclusions

The general objective of this dissertation is a proper formulation, from both a mathematical and a physical perspective, of thermal fluctuations in partial differential equations. We have selected one of the simplest non-trivial transport equations, describing diffusion of colloidal particles in a quiescent fluid, in order to discuss such a formulation. This equation already captures two of the essential features that appear in more complex transport equations like those appearing in Fluctuating Hydrodynamics, namely, they are conservative and comply with an H-theorem.

In Fig. 8.1 we present a roadmap of the dissertation that will guide us in the following discussion. We have taken two very different approaches in order to obtain the coarse-grained dynamics of diffusing colloidal particles.

The first approach, termed Bottom-up, uses the Theory of Coarse-Graining in order to derive, from the underlying Hamiltonian dynamics (1.2) governing the motion of microscopic particles, the dynamics of phase functions that rep-

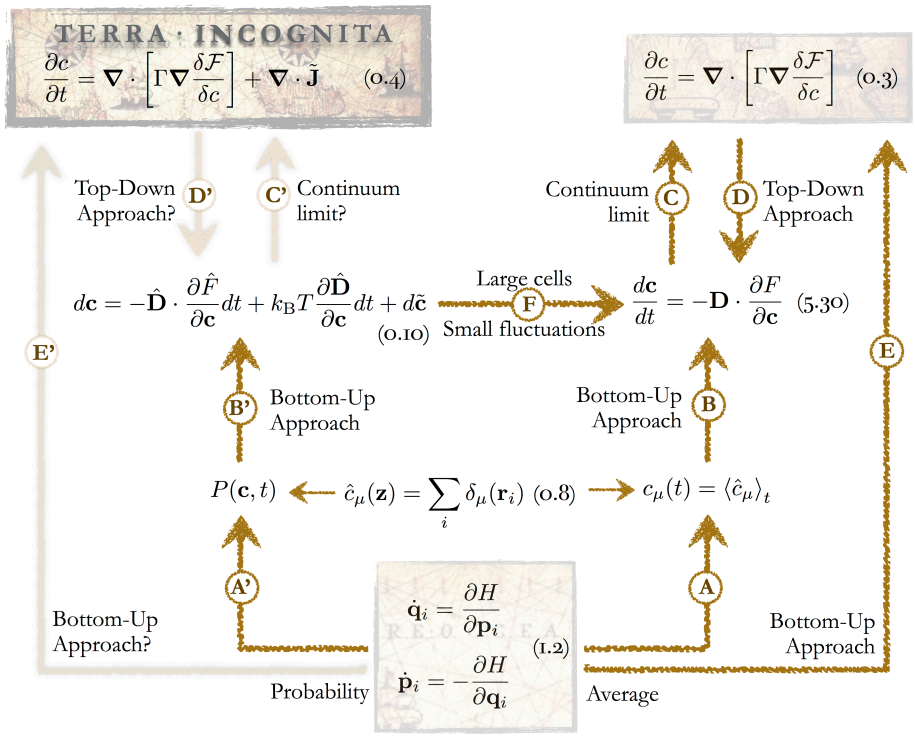


**Figure 8.1:** This dissertation studies the connection between a microscopic description given by Hamilton's equations (bottom) and a continuum description given by the diffusion equation (top right). This dissertation also explores *Terra Incognita* corresponding to the formulation of Stochastic Partial Differential Equations and its microscopic underpinning.

resent the system in a coarse-grained way. These variables are a set of discrete concentration variables (0.8) that give the number of particles per unit volume that are in a given region of space, or cell. Through road (A'), we consider the probability distribution $P(\mathbf{c}, t)$ of these concentration variables. The resulting dynamics is expressed either as a Fokker-Planck Equation or in terms of the mathematically equivalent Stochastic Differential Equation (0.10) for the dynamics of the concentration variables themselves. The Bottom-Up approach (B') in the road-map 8.1 is very powerful, as it gives the *structure* of the equations, but the two objects that appear in the FPE and SDE, which are the

free energy function $\hat{F}(\mathbf{c})$ and the dissipative matrix $\hat{D}(\mathbf{c})$, are given in microscopic terms through rather complicated expressions. In the limit where thermal fluctuations can be neglected, typically for sufficiently large cells, the SDE becomes deterministic, as depicted in (F) in Fig. 8.1.

Instead of looking at the full *probability*, we could have focused on obtaining dynamic equations for the *averages* of the concentration variables. This is depicted in (A) and (B) in the roadmap. We have not presented that route in the present dissertation, but we assure the reader that the derivation leads to (5.30). When the cells are sufficiently large, the fluctuations in the instantaneous value of the concentration variables become weaker, and the instantaneous values and averages behave in the same way. In a similar way, the Theory of Coarse-graining applied to the microscopic concentration field $\hat{c}_{\mathbf{r}}(\mathbf{z}) = \sum_i \delta(\mathbf{r}_i - \mathbf{r})$ leads, through route (E) to the non-linear diffusion equation (0.3) as shown in Ref. [68].

Of course, the following question readily emerges. Is it possible to derive the SPDE (0.4) directly from the Theory of Coarse-Graining, i.e. to follow route (E')? Unfortunately, the answer is no. It is rather clear that we cannot not use the microscopic field $\hat{c}_{\mathbf{r}}(\mathbf{z}) = \sum_i \delta(\mathbf{r}_i - \mathbf{r})$ as the coarse-grained variable, because we cannot give a physical meaning to the probability that these variables take particular values of a *continuum* field. They are too spiky objects. Therefore, the best we can do to arrive at *Terra Incognita* is to go through the road (B') until arriving at (0.10). The question then is whether the continuum limit of (0.10) exists as we increase the resolution of the mesh. We will return to this question below.

The second approach that we have considered is a numerical analysis approach in which we take for granted the validity of the continuum non-linear diffusion equation (0.3), and we discretize it with a Petrov-Galerkin method by using a set of basis functions. This approach, route (D) in the roadmap, is termed Top-down. Quite reassuringly, this route gives again (5.30). The argument can then be turned upside down and suggest that, because the Bottom-up discrete equation has the same form as the discretized Top-down equation, then a sequence of Bottom-up equations (5.30) with increasing resolution will converge towards a continuum limit (0.3).

Can we, then, use this argument for the SPDE (0.4), and take a Top-down

approach (D') in order to recover the microscopically derived (0.10)? This would solve all questions about the existence of a continuum limit, right? In fact, we have shown in SECTION 6.2.3 that, by treating (0.4) as if it was an ordinary PDE, the discretization procedure that we have followed produces a thermal noise $d\tilde{\mathbf{c}}$ out of the noise term $\boldsymbol{\nabla}\cdot\tilde{\mathbf{J}}$ that coincides with the one that is obtained from the Bottom-up approach.

The problem with this approach is that treating (0.4) as if it was a normal PDE is not mathematically correct in general. The signature of the problems show up when considering the Gaussian model, for which one can still give a sounded mathematical meaning to (0.4). We have seen that the realization of the continuum Gaussian field are extremely rough in $D > 1$. The point-wise variance of the field simply diverges in $D > 1$, a phenomenon known as the ultraviolet catastrophe. This implies that the fields $\phi(\mathbf{r})$ are extremely irregular and should be rather understood as *distributions* in $D > 1$. [22, 23, 29, 30] However, distributions cannot be multiplied and a quartic term in the free energy is ill-defined. This means that the Ginzburg-Landau model is ill defined in $D > 1$ because, without further amendments, does not have have a continuum limit in $D > 1$. If one naively discretizes the corresponding ill-posed nonlinear SPDE, pathological behavior will be observed in $D > 1$. For example, the number of particles in a given *finite* region of space have fluctuations that depend on the lattice spacing, which is obviously nonphysical.

There are two fundamentally different approaches to address this problem.

On one hand, in stochastic field theories as those appearing in Quantum Field Theory the governing SPDE is postulated from symmetry arguments without further connection to any other more microscopic description of the system. In this case, the SPDE is the fundamental equation for which the Ginzburg-Landau model is perhaps the simplest model. Because the GL model is not analytically resoluble, it requires perturbation theory for computing, for example, correlation functions. However a plague of infinities creep in perturbation theory, reflecting the ultraviolet catastrophe. These infinities are eliminated by Renormalization Group techniques, which in its more basic formulation says that the "correct" model is not the Ginzburg-Landau model, but one that contains an additional term (a *counterterm*) which depends on the lattice spacing. [24–28] By the way, these counterterms diverge in the contin-

uum limit, so one substracts infinities in the process, a somewhat awkward operation.

On the other hand, when a "more fundamental" theory exists, as is the case of colloidal suspension where the fundamental theory are Hamilton's equations we may take the point of view of the Coarse-Graining Physicist: *Forget about the continuum limit!* This point of view is substantiated as follows. We already know that the Gaussian model is just an approximate model that requires to have many particles per cell. In a similar way, we know that the Ginzburg-Landau model is an approximation to the van der Waals model when considering phase transitions. The van der Waals model is also an approximate model in which, in its construction, a basic assumption about the potential of interaction is made. This assumption says that the potential has two separate length scales, one short range $\sigma$ corresponding to the repulsive part of the potential, and one long ranged $\lambda$ corresponding to the attractive part of the potential. As was shown by van Kampen in his original derivation of the van der Waals model [39], only when the size $\Lambda$ of the cells comply with $\sigma \ll \Lambda \ll \lambda$, then the van der Waals form of the free energy emerges. The van der Waals model makes sense only for a given cell size (large enough to contain many particles, small enough for the attractive part of the potential to be treated in mean field) [39]. This means that *the cell size is fixed by physical conditions*. Indeed, if the cell size was to be taken too large, larger than droplet sizes, it would not be able to discriminate between liquid and vapor phases and the free energy functional to be used in that case would need to be different from the usual square gradient van der Waals free energy functional. In this state of affairs, it makes no sense to look at the mathematical continuum limit of the discrete SPDE, while the discrete version still has a physically sounded foundation.

The dissertation has two parts, separated by an Interlude. Each part corresponds to a particular definition of the concentration field and they correspond, chronologically, to our own process of understanding the problem. The first one is based on a standard finite element basis set, defined on Delaunay triangulation. This method for obtaining a discrete concentration field is valid for regular grids. The second possibility is given in terms of a linear combination of the standard finite element basis function. The main advantage of this second option is the fact that it is also valid for irregular meshes. In

addition, the convergence rate in irregular grids is superior for the definition in terms of conjugate basis functions.

We note that it is important to have discretization methods valid on irregular grids whenever phenomenology with separate length scales appear. Then, we may need a resolution in some regions of the space and a different resolution in other regions. For example, in phase transitions, we may need high resolution in the interface, but low resolution in other regions. The use of the conjugate finite elements is a clear advantage in comparison with the standard finite element choice.

Another sensible issue when solving efficiently a SDE is time discretization. In the first part of this dissertation we have tested *explicit* methods to discretize in time the diffusion equation. The explicit scheme that we have used gives a *strong* convergence order 0.5. Strong convergence schemes are useful to reproduce real trajectories of the mesoscopic variables along time. As a counterpart, the explicit scheme needs a small time step to be stable. Exploring the continuum limit requires tiny time steps. Solving the SDE becomes unpractical for such a fine resolution. For that reason, we have studied in the second part *implicit* methods to time discretize the SDE. The implicit method has the same strong convergence than the explicit method 0.5. But it is a second-order *weakly* accurate scheme. *Weak* convergence schemes are useful when there is an interest in reproducing correctly averages of the mesoscopic variables. The implicit method has the disadvantage of requiring the solution of a linear system of equations at every time step. But it has as main advantage the possibility of using a much larger time step. In balance, the implicit method has been proved to be more efficient that the explicit one. In addition to this, the specific scheme we have used in the last chapter is unconditionally stable for linear equations (as the Gaussian model), ensuring the obtention of stable static properties regardless of the time step used.

# 9
# Future Directions

In this dissertation we have presented a general methodology for the discretization of Stochastic Partial Differential Equations. We have seen how the Petrov-Galerkin method, with conjugate basis functions lead to *positive definite* dissipative matrices and, therefore, allow in a natural way for the formulation of stochastic differential equations, where the random forcing terms comply with the Fluctuation-Dissipation Theorem.

A natural extension and, admittedly, the original aim of the present dissertation is the finite element formulation of Fluctuating Hydrodynamics. Once we have understood the methodology, the writing of the discrete equations corresponding to the continuum Fluctuating Hydrodynamics is, in principle, straightforward. Of course, a complementary view in terms of the Theory of Coarse-Graining is recommended. In this view, one should derive the SDE governing the dynamics of mass, momentum, and energy density of nodes from first principles. While microscopic derivations of discrete hydrodynamic

exists [35], none have considered yet the conjugate finite element basis functions.

One issue that will be necessary to consider is the formulation of appropriate boundary conditions. In this dissertation we have used periodic boundary conditions in order to avoid the issue. Note that, from a microscopic point of view, boundary conditions arise from interactions with solid container walls. How these interactions are captured at a coarse-grained level is not trivial, and we may find some surprises when considering microscopically motivated boundary conditions for Fluctuating-Hydrodynamics.

The implementation in algorithmic terms of the method for the case of Fluctuating Hydrodynamics is also simple (in principle) in $1D$ and this is one of the next steps to take. Of course, in practical applications a formulation in $3D$ is required. Before going into this endeavor, we should probably formulate the diffusion problem in $3D$ first, which is much simpler because it involves only one transport equation. There are very good open source libraries for the calculation of Delaunay triangulations, but the task is, nevertheless, formidable.

In $3D$, as we have mentioned several times, we should expect interesting anomalous behavior with the continuum limit for Fluctuating Hydrodynamics. Both from a Coarse-Graining Physicist and from a Numerical Analysis Mathematician point of view, we would like to have a good understanding of what is going on in the continuum limit. Gaussian models, in which the free energy or entropy are quadratic functions, should be probably harmless, but other models allowing for the description of phase transitions, may not have a continuum limit. In those cases we would need to renormalize the transport coefficients, both free energy *and* mobilities, as a function of the grid spacing. These coefficients are not universal as are the macroscopic coefficients.

The problems arise because we stick to the Gaussian model for the free energy. Should we have general methods to *measure* the free energy function, i.e. to find the functional form of the free energy as a function of the discrete hydrodynamic variables, then we could address different resolutions in a physical reasonable way. Of course, this is very difficult in general.

Finally, another general open problem is the design of hybrid particle-continuum methods based on the conjugate finite element basis functions. Again,

there are many proposals in the literature about how to interface two such dissimilar algorithms (involving particles and meshes), but none has yet used the conjugate basis functions with its possibly improved performance.

# References


[1] M. Might. *The illustrated guide to a Ph.D.* Available at `http://matt.might.net/articles/phd-school-in-pictures/`.

[2] P. Kurtzweil. Skimming the milk label. *F.D.A. Consumer*, 32(1):22, 1998.

[3] R. Jost. Milk and dairy products. In *Ullmann's Encyclopedia of Industrial Chemistry*. Wiley-VCH Verlag GmbH & Co., 2005.

[4] R. Brown. A brief account of microscopical observations.... *The Edinburgh New Philosophical Journal*, 5:258–371, 1828.

[5] J. C. Maxwell. On the dynamical theory of gases. *Philosophical Transactions of the Royal Society of London*, 157:49–88, 1867.

[6] A. Einstein. Über die von der molekularkinetischen theorie der wärme geforderte bewegung von in ruhenden flüssigkeiten suspendierten teilchen. *Annalen der Physik*, 322(8):549–560, 1905.

[7] J. B. Perrin. Mouvement brownien et réalité moléculaire. *Annales de Chimie et de Physique (VIII)*, 18:5–114, 1909.

[8] Marquis de Laplace. *A Philosophical Essay on Probabilities (Dover Books on Mathematics)*. Dover Publications, 1996.

[9] S. Chandrasekhar. Stochastic problems in physics and astronomy. *Reviews of Modern Physics*, 15(1):1–89, 1943.

[10] P. Español. Statistical mechanics of coarse-graining. In M. Karttunen, A. Lukkarinen, and I. Vattulainen, editors, *Novel Methods in Soft Matter Simulations*, volume 640 of *Lecture Notes in Physics*, pages 69–115. Springer Berlin Heidelberg, 2004.

[11] T. J. Murphy and J. L. Aguirre. Brownian Motion of $N$ Interacting Particles. I. Extension of the Einstein Diffusion Relation to the $N$-Particle Case. *Journal of Chemical Physics*, 57(5):2098–2104, 1972.

[12] M. Von Smoluchowski. Drei vortrage uber diffusion. brownsche bewegung und koagulation von kolloidteilchen. *Physikalische Zeitschrift*, 17:557–585, 1916.

[13] A. Fick. Ueber diffusion. *Annalen der Physik*, 170(1):59–86, 1855.

[14] K. Kawasaki. Stochastic model of slow dynamics in supercooled liquids and dense colloidal suspensions. *Physica A*, 208(1):35–64, 1994.

[15] U. M. B. Marconi and P. Tarazona. *Journal of Physics: Condensed Matter*, (8A):A413.

[16] A. J. Archer and R. Evans. Dynamical density functional theory and its application to spinodal decomposition. *Journal of Chemical Physics*, 121(9):4246, 2004.

[17] T. Leonard, B. Lander, U. Seifert, and T. Speck. Stochastic thermodynamics of fluctuating density fields: Non-equilibrium free energy differences under coarse-graining. *Journal of Chemical Physics*, 139(20):204109, 2013.

[18] L. D. Landau and E. M. Lifshitz. *Fluid mechanics*. Pergamon Press Addison-Wesley Pub. Co, London Reading, Mass, 1959.

[19] A. J. Archer and M. Rauscher. Dynamical density functional theory for interacting Brownian particles: stochastic or deterministic? *Journal of Physics A: Mathematical and General*, 37(40):9325–9333, 2004.

[20] A. J. Bray. Theory of phase-ordering kinetics. *Advances in Physics*, 43(3):357–459, 1994.

[21] P. C. Hohenberg and B. I. Halperin. Theory of dynamic critical phenomena. *Reviews of Modern Physics*, 49(3):435–479, 1977.

[22] M. D. Ryser, N. Nigam, and P. F. Tupper. On the well-posedness of the stochastic Allen–Cahn equation in two dimensions. *Journal of Computational Physics*, 231(6):2537–2550, 2012.

[23] M. Hairer. A theory of regularity structures. *Inventiones mathematicae*, 198(2):269–504, 2014.

[24] R. Benzi, G. Jona-Lasinio, and A. Sutera. Stochastically perturbed Landau-Ginzburg equations. *Journal of Statistical Physics*, 55(3-4):505–522, 1989.

[25] L. Bettencourt, S. Habib, and G. Lythe. Controlling one-dimensional Langevin dynamics on the lattice. *Physical Review D*, 60(10):105039, 1999.

[26] C. J. Gagne and M. Gleiser. Lattice-independent approach to thermal phase mixing. *Physical Review E*, 61(4 Pt A):3483–9, 2000.

[27] G. Lythe and S. Habib. Stochastic PDEs: convergence to the continuum? *Computer Physics Communications*, 142(1-3):29–35, 2001.

[28] N. C. Cassol-Seewald, R. L. S. Farias, G. Krein, and R. S. Marques De Carvalho. Noise and Ultraviolet Divergences in Simulations of Ginzburg–Landau–Langevin Type of Equations. *International Journal of Modern Physics C*, 23(08):1240016, 2012.

[29] M. Hairer. Introduction to Regularity Structures. *e-prints arXiv:1401.3014 [math.AP]*, 2014.

[30] M. Hairer, M. Ryser, and H. Weber. Triviality of the $2D$ stochastic Allen-Cahn equation. *Electronic Journal of Probability*, 17(39):1–14, 2012.

[31] A. Donev, T. G. Fai, and E. Vanden-Eijnden. A reversible mesoscopic model of diffusion in liquids: from giant fluctuations to Fick's law. *Journal of Statistical Mechanics: Theory and Experiment*, 2014(4):P04004, 2014.

[32] P. Español, J. G. Anero, and I. Zúñiga. Microscopic derivation of discrete hydrodynamics. *Journal of Chemical Physics*, 131(24):244117, 2009.

[33] D. N. Zubarev and V. G. Morozov. Statistical mechanics of nonlinear hydrodynamic fluctuations. *Physica A*, 120(3):411 – 467, 1983.

[34] W. Van Saarloos, D. Bedeaux, and P. Mazur. Non-linear hydrodynamic fluctuations around equilibrium. *Physica A*, 110(1):147–170, 1982.

[35] P. Español and I. Zúñiga. On the definition of discrete hydrodynamic variables. *Journal of Chemical Physics*, 131(16):164106, 2009.

[36] J. A. de la Torre and P. Español. Coarse-graining Brownian motion: From particles to a discrete diffusion equation. *Journal of Chemical Physics*, 135(11):114103, 2011.

[37] J. A. de la Torre, P. Español, and A. Donev. Finite element discretization of non-linear diffusion equations with thermal fluctuations. *Journal of Chemical Physics*, 142(9):094115, 2015.

[38] A. Donev and E. Vanden-Eijnden. Dynamic density functional theory with hydrodynamic interactions and fluctuations. *Journal of Chemical Physics*, 140(23):234115, 2014.

[39] N. G. Van Kampen. Condensation of a classical gas with long-range attraction. *Physical Review*, 135(2A):A362, 1964.

[40] L. E. Reichl. *A modern course in statistical physics*. Univ. of Texas Press, Austin, 1980.

[41] P. Español. Thermohydrodynamics for a van der Waals fluid. *Journal of Chemical Physics*, 115(12):5392, 2001.

[42] J. W. Gibbs. *Elementary Principles in Statistical Mechanics*. Yale Univ. Press, 1902. Dover, New York, 1960.

[43] Lars Onsager. Reciprocal Relations in Irreversible Processes. I. *Physical Review*, 37(4):405–426, 1931.

[44] J. G. Kirkwood. The Statistical Mechanical Theory of Transport Processes. I. General Theory. *Journal of Chemical Physics*, 14(3):180–201, 1946.

[45] M. S. Green. Markoff random processes and the statistical mechanics of time-dependent phenomena. *Journal of Chemical Physics*, 20(8):1281–1295, 1952.

[46] M. S. Green. Markoff Random Processes and the Statistical Mechanics of Time-Dependent Phenomena. II. Irreversible Processes in Fluids. *Journal of Chemical Physics*, 22(3):398–413, 1954.

[47] R. Zwanzig. Memory effects in irreversible thermodynamics. *Physical Review*, 124(4):983–992, 1961.

[48] H. Mori. Transport, collective motion, and brownian motion. *Progress of Theoretical Physics*, 33(3):423–455, 1965.

[49] H. Grabert. *Projection operator techniques in nonequilibrium statistical mechanics*. Springer-Verlag, Berlin New York, 1982.

[50] C. W. Gardiner. *Handbook of Stochastic Methods for Physics, Chemistry and the Natural Sciences*. Springer Series in Synergetics. Springer-Verlag, Berlin, 1985.

[51] F. Gantmacher. *Lectures in Analytical Mechanics*. Mir, 1970.

[52] E. T. Jaynes. Information theory and statistical mechanics. *Physical Review*, 106(4):620–630, 1957.

[53] J. Español I Garrigós. Initial ensemble densities through the maximization of entropy. *Physics Letters A*, 146(1):21–24, 1990.

[54] R. Kubo. Statistical-Mechanical Theory of Irreversible Processes. I. General Theory and Simple Applications to Magnetic and Conduction Problems. *Journal of the Physical Society of Japan*, 12(6):570–586, 1957.

[55] R. Kubo. The fluctuation-dissipation theorem. *Reports on Progress in Physics*, 29(1):255–284, 1966.

[56] P. Español, J. A. de la Torre, M. Ferrario, and G. Ciccotti. Coarse-graining stiff bonds. *The European Physical Journal Special Topics*, 200(1):107–129, 2011.

[57] G. K. Batchelor. *An Introduction to Fluid Dynamics (Cambridge Mathematical Library)*. Cambridge University Press, 2000.

[58] C. Prévôt and M. Röckner. *A Concise Course on Stochastic Partial Differential Equations (Lecture Notes in Mathematics)*. Springer, 2007.

[59] J. Garcia-Ojalvo and J. Sancho. *Noise in Spatially Extended Systems (Institute for Nonlinear Science)*. Springer, 2012.

[60] J. B. Bell, A. L. Garcia, and S. A. Williams. Numerical methods for the stochastic Landau-Lifshitz Navier-Stokes equations. *Physical Review E*, 76(1):016708, 2007.

[61] S. Williams, J. Bell, and A. Garcia. Algorithm refinement for fluctuating hydrodynamics. *Multiscale Modeling & Simulation*, 6(4):1256–1280, 2008.

[62] B. Dünweg, U. D. Schiller, and A. J. C. Ladd. Statistical mechanics of the fluctuating lattice Boltzmann equation. *Physical Review E*, 76(3):036704, 2007.

[63] A. Donev, E. Vanden-Eijnden, A. Garcia, and J. Bell. On the accuracy of finite-volume schemes for fluctuating hydrodynamics. *Communications in Applied Mathematics and Computational Science*, 5(2):149–197, 2010.

[64] R. Delgado-Buscalioni, K. Kremer, and M. Praprotnik. Concurrent triple-scale simulation of molecular liquids. *Journal of Chemical Physics*, 128(11):114110, 2008.

[65] A. Donev, J. Bell, A. Garcia, and B. Alder. A hybrid particle-continuum method for hydrodynamics of complex fluids. *Multiscale Modeling & Simulation*, 8(3):871–911, 2010.

[66] K. M. Mohamed and A. A. Mohamad. A review of the development of hybrid atomistic–continuum methods for dense fluids. *Microfluidics and Nanofluidics*, 8(3):283–302, 2010.

[67] P. Español. Stochastic differential equations for non-linear hydrodynamics. *Physica A: Statistical Mechanics and its Applications*, 248(1):77–96, 1998.

[68] P. Español and H. Löwen. Derivation of dynamical density functional theory using the projection operator technique. *Journal of Chemical Physics*, 131(24):244101, 2009.

[69] C. W. Gardiner. *Stochastic Methods: A Handbook for the Natural and Social Sciences (Springer Series in Synergetics).* Springer, 2009.

[70] P. E. Kloeden and E. Platen. *Numerical solution of stochastic differential equations*, volume 23. Springer, 1992.

[71] N. Bruti-Liberati and E. Platen. Strong Predictor-Corrector Euler Methods for Stochastic Differential Equations. *Stochastics and Dynamics*, 8(3):561–581, 2008.

[72] M. Matsumoto and T. Nishimura. Mersenne twister: A 623-dimensionally equidistributed uniform pseudo-random number generator. *ACM Transactions on Modeling and Computer Simulation*, 8(1):3–30, 1998.

[73] G. Marsaglia and W. W. Tsang. The Ziggurat method for generating random variables. *Journal of Statistical Software*, 5(8):1–7, 2000.

[74] J. García-Ojalvo and J.M. Sancho. *Noise in Spatially Extended Systems*. Springer Verlag, Berlin, 1999.

[75] J. B. Walsh. Finite Element Methods for Parabolic Stochastic PDE's. *Potential Analysis*, 23(1):1–43, 2005.

[76] Y. Yan. Galerkin Finite Element Methods for Stochastic Parabolic Partial Differential Equations. *SIAM Journal on Numerical Analysis*, 43(4):1363–1384, 2005.

[77] G. Krein, J. M. Machado, and A. O. Pereira. Dynamics of the deconfinement transition of quarks and gluons in a finite volume. *Computer Physics Communications*, 180(4):564–573, 2009.

[78] P. Plunkett, J. Hu, C. Siefert, and P. J. Atzberger. Spatially adaptive stochastic methods for fluid–structure interactions subject to thermal fluctuations in domains with complex geometries. *Journal of Computational Physics*, 277:121–137, 2014.

[79] B. A. Finlayson and L. E. Scriven. The method of weighted residuals—a review. *Applied Mechanics Reviews*, 19(9):735–748, 1966.

[80] S. Delong, B. E. Griffith, E. Vanden-Eijnden, and A. Donev. Temporal integrators for fluctuating hydrodynamics. *Physical Review E*, 87(3):033302, 2013.

[81] S. Delong, Y. Sun, B.E. Griffith, E. Vanden-Eijnden, and A. Donev. Multiscale temporal integrators for fluctuating hydrodynamics. *Physical Review E*, 90(6):063312, 2014.

[82] W. Press. *Numerical recipes : the art of scientific computing*. Cambridge University Press, Cambridge, UK New York, 2007.

[83] B. V. R. Tata, M. Rajalakshmi, and A. K. Arora. Vapor-liquid condensation in charged colloidal suspensions. *Physical Review Letters*, 69(26):3778–3782, 1992.

[84] F. BalboaUsabiaga, J. Bell, R. Delgado-Buscalioni, A. Donev, T. Fai, B. Griffith, and C. Peskin. Staggered schemes for fluctuating hydrodynamics. *Multiscale Modeling & Simulation*, 10(4):1369–1408, 2012.

[85] J. A. de la Torre, P. Español, and A. Donev. Discretizing stochastic non-linear diffusion equations with finite elements, 2015. Poster presented at Molecular hydrodynamics meets fluctuating hydrodynamics, May 10–14, Universidad Autónoma de Madrid/CECAM, Miraflores de la Sierra, Spain.

[86] J. A. de la Torre, P. Español, and D. Duque. Free energy models in a non linear fluctuating diffusion equation, 2012. Poster presented at Fluid-Structure Interactions in Soft-matter Systems, November 26–30, Monash University, Prato, Italy.

[87] J. A. de la Torre, P. Español, and D. Duque. Discretization methods for fluctuating equations, 2012. Poster presented at XVIII Congreso Física Estadística, October 18–20, IFISC/Universitat de les Illes Balears, Palma de Mallorca, Spain.

[88] J. A. de la Torre, D. Duque, and P. Español. Discretization of a non-linear diffusion equation, 2012. Poster presented at IAS Winterschool 2012: Hierarchical Methods for Dynamics in Complex Molecular Systems, March 5–9, Jülich Supercomputing Center, Jülich, Germany.

[89] J. A. de la Torre and P. Español. A coarse grained discrete model for the diffusion equation, 2011. Poster presented at Multiscale Modeling of Simple and Complex Liquid Flow Using Particle-Continuum Hybrids, October 5–7, Zaragoza Scientific Center for Advanced Modeling, Zaragoza, Spain.

[90] J. A. de la Torre and P. Español. Coarse graining en dinámica browniana: modelos de difusión discreta (*Coarse graining in Brownian dynamics: models for discrete diffusion*), 2011. Poster presented at XVII Congreso Física Estadística, June 2–4, University of Barcelona, Barcelona, Spain.

[91] D. Cámpora, J. A. de la Torre, J. C. García, and F. Sancho-Caparrini. BML model on non-orientable surfaces. *Physica A*, 389(16):3290–3298, 2010.

[92] M. C. Lemos, A. Córdoba, and J. A. de la Torre. Effects of periodic perturbations on the oscillatory behavior in the $NO + H_2$ reaction on $Pt(100)$. *Physical Review E*, 81(3):036116, 2010.

[93] J. A. de la Torre, M. C. Lemos, and A. Córdoba. Control of cellular glycolisis by perturbation in the glucose influx. In F. Masulli, R. Tagliaferri, and G. M. Verkhivker, editors, *Computational Intelligence Methods for Bioinformatics and Biostatistics*, volume 5488 of *Lecture Notes in Computer Sciences*, pages 132–143. Springer Verlag, 2009.

[94] M. C. Lemos, A. Córdoba, and J. A. de la Torre. Efecto de las perturbaciones periódicas en el comportamiento oscilatorio de la reacción $NO + H_2$ sobre Pt(100), (*Effects on periodic perturbations in the oscillatory behavior of the reaction* $NO + H_2$ *over* $Pt(100)$), 2009. Poster presented at Bienal de la Real Sociedad Española de Física, September 7–11, Real Sociedad Española de Física, Ciudad Real, Spain.

[95] M. C. Lemos, A. Córdoba, and J. A. de la Torre. Modulación de la frecuencia perturbante en el comportamiento oscilatorio de la reacción $NO + H_2/Pt(100)$, (*Modulation of the perturbative frequency in the oscillatory behavior of the reaction* $NO + H_2/Pt(100)$), 2009. Poster presented at XVI Congreso Física Estadística, September 10–12, Universidad de Huelva, Huelva, Spain.

[96] M. A. El-Shehawey, Gh. A. El-Shreef, and A. Sh. Al-Henawy. Analytical inversion of general periodic tridiagonal matrices. *Journal of Mathematical Analysis and Applications*, 345(1):123–134, 2008.

# A
# Contributions

The following published articles and posters are related with this dissertation.

- [37] J. A. de la Torre, P. Español, and A. Donev. Finite element discretization of non-linear diffusion equations with thermal fluctuations. *Journal of Chemical Physics*, 142(9):094115, 2015.
- [36] J. A. de la Torre and P. Español. Coarse-graining Brownian motion: From particles to a discrete diffusion equation. *Journal of Chemical Physics*, 135(11):114103, 2011.
- [56] P. Español, J. A. de la Torre, M. Ferrario, and G. Ciccotti. Coarse-graining stiff bonds. *The European Physical Journal Special Topics*, 200(1):107–129, 2011.
- [85] J. A. de la Torre, P. Español, and A. Donev. Discretizing stochastic non-linear diffusion equations with finite elements, 2015. Poster presented at Molecular hydrodynamics meets fluctuating hydrodynamics,

May 10–14, Universidad Autónoma de Madrid/CECAM, Miraflores de la Sierra, Spain.

- [86] J. A. de la Torre, P. Español, and D. Duque. Free energy models in a non linear fluctuating diffusion equation, 2012. Poster presented at Fluid-Structure Interactions in Soft-matter Systems, November 26–30, Monash University, Prato, Italy.

- [87] J. A. de la Torre, P. Español, and D. Duque. Discretization methods for fluctuating equations, 2012. Poster presented at XVIII Congreso Física Estadística, October 18–20, IFISC/Universitat de les Illes Balears, Palma de Mallorca, Spain.

- [88] J. A. de la Torre, D. Duque, and P. Español. Discretization of a non-linear diffusion equation, 2012. Poster presented at IAS Winterschool 2012: Hierarchical Methods for Dynamics in Complex Molecular Systems, March 5–9, Jülich Supercomputing Center, Jülich, Germany.

- [89] J. A. de la Torre and P. Español. A coarse grained discrete model for the diffusion equation, 2011. Poster presented at Multiscale Modeling of Simple and Complex Liquid Flow Using Particle-Continuum Hybrids, October 5–7, Zaragoza Scientific Center for Advanced Modeling, Zaragoza, Spain.

- [90] J. A. de la Torre and P. Español. Coarse graining en dinámica browniana: modelos de difusión discreta (*Coarse graining in Brownian dynamics: models for discrete diffusion*), 2011. Poster presented at XVII Congreso Física Estadística, June 2–4, University of Barcelona, Barcelona, Spain.

Furthermore, there are some other works not directly related to this dissertation in which I also contributed.

- [91] D. Cámpora, J. A. de la Torre, J. C. García, and F. Sancho-Caparrini. BML model on non-orientable surfaces. *Physica A*, 389(16):3290–3298, 2010.

- [92] M. C. Lemos, A. Córdoba, and J. A. de la Torre. Effects of periodic perturbations on the oscillatory behavior in the $NO + H_2$ reaction on $Pt(100)$. *Physical Review E*, 81(3):036116, 2010.

- [93] J. A. de la Torre, M. C. Lemos, and A. Córdoba. Control of cellular glycolisis by perturbation in the glucose influx. In F. Masulli, R. Tagliaferri, and G. M. Verkhivker, editors, *Computational Intelligence Methods for Bioinformatics and Biostatistics*, volume 5488 of *Lecture Notes in Computer Sciences*, pages 132–143. Springer Verlag, 2009.

- [94] M. C. Lemos, A. Córdoba, and J. A. de la Torre. Efecto de las perturbaciones periódicas en el comportamiento oscilatorio de la reacción $NO + H_2$ sobre Pt(100), (*Effects on periodic perturbations in the oscillatory behavior of the reaction $NO + H_2$ over $Pt(100)$*), 2009. Poster presented at Bienal de la Real Sociedad Española de Física, September 7–11, Real Sociedad Española de Física, Ciudad Real, Spain.

- [95] M. C. Lemos, A. Córdoba, and J. A. de la Torre. Modulación de la frecuencia perturbante en el comportamiento oscilatorio de la reacción $NO + H_2/Pt(100)$, (*Modulation of the perturbative frequency in the oscillatory behavior of the reaction $NO + H_2/Pt(100)$*), 2009. Poster presented at XVI Congreso Física Estadística, September 10–12, Universidad de Huelva, Huelva, Spain.

# B

# Gaussian Probability Distribution in the Bottom-Up Approach

In this appendix we consider a Gaussian approximation for the discrete concentration field $\hat{c}_\mu(\mathbf{z})$, which is given in terms of the finite element with support on the Delaunay cell, (3.4). We start from the microscopic probability of non interacting Brownian particles to obtain the first two moments of the probability distribution. If the number of particles per node is large enough, it is expected that the probability distribution becomes a Gaussian, so that obtaining the first two moments we may fully characterize $P^{\text{eq}}(\mathbf{c})$.

Let us compute the probability distribution $P(\mathbf{c})$ that, at equilibrium, a discrete concentration field takes the value $\mathbf{c} = \{c_\mu; \mu = 1, \dots, M\}$. We consider a $D$ dimensional domain where $N$ Brownian particles move in a volume of length $V_T$. The configuration of the particles is denoted by the collection of positions $\mathbf{z} = \{\mathbf{r}_i; i = 1, \dots, N\}$, where $\mathbf{r}_i$ is the position of the $i$-th particle. We seed the volume $V_T$ in a uniform grid of $M$ nodes located at $\mathbf{r}_\mu$, and we assume periodic boundary conditions (i.e., we have $\mathbf{r}_M \equiv \mathbf{r}_1$). The average

concentration is defined as $c_0 \triangleq N/V_T$. The concentration variable $\hat{c}_\mu(\mathbf{z})$ in the node $\mu$ given in general by (3.4) is

$$\hat{c}_\mu(\mathbf{z}) = \frac{1}{V_\mu} \sum_i \psi_\mu(\mathbf{r}_i) \,. \tag{B.1}$$

The probability $P(\mathbf{c})$ introduced in (4.1), provided that $\rho^{\text{eq}}(\mathbf{z}) = 1/V_T^N$, now takes the form

$$P(\mathbf{c}) = \frac{1}{V_T^N} \int d\mathbf{z} \prod_\mu \delta\left(\hat{c}_\mu(\mathbf{z}) - c_\mu\right) \,. \tag{B.2}$$

Before computing approximately the probability from Eq. (B.2) it is instructive to compute exactly the first and second moments of the distribution (B.2). The first moments are

$$\begin{aligned}
\langle c_\mu \rangle &= \int dc_1 \cdots dc_M \, P(\mathbf{c}) c_\mu \\
&= \frac{1}{V_T^N} \int d\mathbf{z} \int dc_1 \, \delta(\hat{c}_1(\mathbf{z}) - c_1) \cdots \int dc_\mu \, \delta(\hat{c}_\mu(\mathbf{z}) - c_\mu) c_\mu \cdots \\
&= \frac{1}{V_T^N} \int d\mathbf{z} \, \hat{c}_\mu(\mathbf{z}) \\
&= \frac{1}{V_T^N} \frac{1}{V_\mu} \int d\mathbf{z} \sum_i \psi_\mu(\mathbf{r}_i) \\
&= \frac{1}{V_T^N} \frac{1}{V_\mu} N \int d\mathbf{z} \, \psi_\mu(\mathbf{r}) \\
&= \frac{1}{V_T} \frac{1}{V_\mu} N \int d\mathbf{r} \, \psi_\mu(\mathbf{r}) \\
&= \frac{N}{V_T} = c_0 \,.
\end{aligned} \tag{B.3}$$

Let us compute now the second moments

$$
\begin{aligned}
\langle c_\mu c_\nu \rangle &= \int dc_1 \cdots dc_M \, P(\mathbf{c}) c_\mu c_\nu \\
&= \frac{1}{V_T^N} \int d\mathbf{z} \, \hat{c}_\mu(\mathbf{z}) \hat{c}_\nu(\mathbf{z}) \\
&= \frac{1}{V_T^N} \frac{1}{V_\mu V_\nu} \int d\mathbf{z} \sum_i \psi_\mu(\mathbf{r}_i) \sum_j \psi_\nu(\mathbf{r}_j) \\
&= \frac{1}{V_T^N} \frac{1}{V_\mu V_\nu} \int d\mathbf{z} \sum_i \psi_\mu(\mathbf{r}_i) \psi_\nu(\mathbf{r}_i) \\
&\qquad\qquad + \frac{1}{V_T^N} \frac{1}{V_\mu V_\nu} \sum_{i \neq j} \int d\mathbf{z} \, \psi_\mu(\mathbf{r}_i) \psi_\nu(\mathbf{r}_j) \\
&= \frac{1}{V_T} \frac{1}{V_\mu V_\nu} N \int d\mathbf{r} \, \psi_\mu(\mathbf{r}) \psi_\nu(\mathbf{r}) \\
&\qquad\qquad + \frac{1}{V_T^2} \frac{1}{V_\mu V_\nu} N(N-1) \int d\mathbf{r} \, \psi_\mu(\mathbf{r}) \int d\mathbf{r}' \, \psi_\nu(\mathbf{r}') \\
&= \frac{c_0}{V_\mu V_\nu} \int d\mathbf{r} \, \psi_\mu(\mathbf{r}) \psi_\nu(\mathbf{r}) + \left(1 - \frac{1}{N}\right) c_0^2 \\
&= \frac{c_0}{V_\mu V_\nu} M_{\mu\nu}^{\psi} + \left(1 - \frac{1}{N}\right) c_0^2 \,, \qquad \text{(B.4)}
\end{aligned}
$$

where the *mass matrix* $\mathbf{M}^{\psi}$ is defined as

$$
M_{\mu\nu}^{\psi} \triangleq \int d\mathbf{r} \, \psi_\mu(\mathbf{r}) \psi_\nu(\mathbf{r}) \,. \qquad \text{(B.5)}
$$

Note that, due to the form of the finite element $\psi_\mu(\mathbf{r})$ (see, for example, Fig. 3.4), neighbor nodes do overlap. Therefore, for neighbor nodes the mass matrix $\mathbf{M}^{\psi}$ does not vanish, and there exist correlations between them. In fact, in terms of central moments we have

$$
\langle \delta c_\mu \delta c_\nu \rangle = \frac{c_0}{V_\mu V_\nu} M_{\mu\nu}^{\psi} - \frac{1}{N} c_0^2 \,, \qquad \text{(B.6)}
$$

with the obvious notation $\delta c_\mu = c_\mu - c_0$. In the limit of a number of particles large enough (i.e., $N \gg 1$) we may approximate central moments to

$$\langle \delta c_\mu \delta c_\nu \rangle \approx \frac{c_0}{V_\mu V_\nu} M^\psi_{\mu\nu} \,. \tag{B.7}$$

Once we know the first and second moments of $P(\mathbf{c})$ it is straightforward to calculate the probability under a Gaussian approximation that has precisely these moments. In general, we have for a multivariate system

$$P(\mathbf{c}) = \frac{1}{\mathcal{Z}} \exp\left\{ -(\mathbf{c} - \mathbf{c}_0) \frac{\mathbf{C}^{-1}}{2} (\mathbf{c} - \mathbf{c}_0) \right\} , \tag{B.8}$$

where $\mathcal{Z}$ is a normalization factor, $\mathbf{c}_0$ a vector with all its $\mu$-th component equals to $c_0$ and $\mathbf{C}^{-1}$ is related to the second moments through

$$C_{\mu\nu} = \left\langle \delta c_\mu \delta c_\nu \right\rangle \,. \tag{B.9}$$

From (B.7) it follows, then

$$C_{\mu\nu} = \frac{c_0}{V_\mu V_\nu} M^\psi_{\mu\nu} \,, \tag{B.10}$$

so that the explicit form of the probability becomes

$$P(\mathbf{c}) = \frac{1}{\mathcal{Z}} \exp\left\{ -\sum_{\mu\nu} \delta c_\mu V_\mu \frac{\left(M^\psi\right)^{-1}_{\mu\nu}}{2c_0} V_\nu \delta c_\nu \right\} , \tag{B.11}$$

where we introduced $\delta c_\mu = c_\mu - c_0$ and we used the usual notation of $\left(\mathbf{M}^\psi\right)^{-1}$ for the inverse of the mass matrix $\mathbf{M}^\psi$.

The free energy that arises in this Gaussian approximation can be obtained from its canonical definition

$$P(\mathbf{c}) = \frac{1}{\mathcal{Z}} \exp\left\{ \frac{-F(\mathbf{c})}{k_\mathrm{B} T} \right\} , \tag{B.12}$$

so that

$$
\begin{aligned}
F^{\mathrm{GA}}(\mathbf{c}) &= -k_{\mathrm{B}}T\left(\ln \mathcal{Z} + \ln P(\mathbf{c})\right) \\
&= k_{\mathrm{B}}T \sum_{\mu\nu} (c_\mu - c_0) V_\mu \frac{\left(M^{\psi}\right)^{-1}_{\mu\nu}}{2c_0} V_\nu (c_\nu - c_0)\,, \qquad \text{(B.13)}
\end{aligned}
$$

where we omit the constant term $k_{\mathrm{B}}T \ln \mathcal{Z}$ in the free energy without losing generality. Therefore, in order to have an explicit form for the free energy, we need to compute the inverse of the matrix $\mathbf{M}^{\psi}$. Fortunately, the inverse of the Toeplitz periodic matrix (B.5) is known analytically (see Eq. (4.6) of Ref. [96]), which is

$$
\left(M^{\psi}\right)^{-1}_{\mu\nu} = \frac{1}{4h_n + 2h_{n-1} + 2} \begin{cases} h_{n-\nu+1}h_\mu - h_{\mu-1}h_{n-\nu} + h_{\nu-\mu} & \text{for } \mu \leq \nu \\ h_{n-\mu+1}h_\nu - h_{\nu-1}h_{n-\mu} + h_{\mu-\nu} & \text{for } \nu \leq \mu \end{cases} \qquad \text{(B.14)}
$$

where

$$
\begin{aligned}
h_k &\equiv \frac{\lambda_1^k - \lambda_2^k}{\lambda_1 - \lambda_2} \\
\lambda_{1,2} &\equiv -2 \pm \sqrt{3}\,. \qquad \text{(B.15)}
\end{aligned}
$$

In order to obtain the probability of the concentration in a single node we may integrate the Gaussian joint probability in (B.11) over all except one variable:

$$
\begin{aligned}
P(\overline{c}_\mu) &= \int d\mathbf{c}\, \delta(\overline{c}_\mu - c_\mu) P(\mathbf{c}) \\
&= \frac{1}{\mathcal{Z}} \int d\mathbf{c}\, \delta(\overline{c}_\mu - c_\mu) \exp\left\{ -\sum_{\mu\nu} \delta c_\mu V_\mu \frac{\left(M^{\psi}\right)^{-1}_{\mu\nu}}{2c_0} V_\nu \delta c_\nu \right\}\,. \qquad \text{(B.16)}
\end{aligned}
$$

By using the definition of the Dirac's delta function in Fourier space

$$P(\overline{c}_\mu) = \frac{1}{\mathcal{Z}} \int_{-\infty}^{\infty} d\boldsymbol{\omega}_\mu \, \exp\left\{-i\boldsymbol{\omega}_\mu(\overline{c}_\mu - c_0)\right\} \times \int d\mathbf{y} \exp\left\{-\mathbf{y}^T \frac{\left[\mathbf{M}^\psi\right]^{-1}}{2c_0}\mathbf{y} + \mathbf{b}^T\mathbf{y}\right\}, \tag{B.17}$$

where we defined the vector $\mathbf{y}$ which $\mu$ component $y_\mu = V_\mu(c_\mu - c_0)$ and the auxiliary vector $\mathbf{b}$ is

$$\begin{aligned} b_\nu &= i\frac{\boldsymbol{\omega}_\mu}{V_\mu}, \qquad \text{iff } \nu = \mu, \\ b_\nu &= 0, \qquad \text{otherwise}. \end{aligned} \tag{B.18}$$

We know the analytical expression for the displaced Gaussian integral, which is

$$\int d\mathbf{y} \exp\left\{-\mathbf{y}^T \frac{\left[\mathbf{M}^\psi\right]^{-1}}{2}\mathbf{y} + \mathbf{b}^T\mathbf{y}\right\} = \frac{1}{\mathcal{Z}} \exp\left\{\mathbf{b}^T\mathbf{M}^\psi\mathbf{b}\right\}, \tag{B.19}$$

so that the one node probability turns into

$$\begin{aligned} P(\overline{c}_\mu) &= \frac{1}{\mathcal{Z}} \int_{-\infty}^{\infty} d\boldsymbol{\omega}_\mu \, \exp\left\{-i\boldsymbol{\omega}_\mu(\overline{c}_\mu - c_0)\right\} \frac{1}{\mathcal{Z}'} \exp\left\{c_0\mathbf{b}^T\frac{\mathbf{M}^\psi}{2}\mathbf{b}\right\} \\ &= \frac{1}{\mathcal{Z}''} \int_{-\infty}^{\infty} d\boldsymbol{\omega}_\mu \, \exp\left\{-\frac{c_0}{V_\mu^2}M^\psi_{\mu\mu}\boldsymbol{\omega}_\mu^2 - i(\overline{c}_\mu - c_0)\boldsymbol{\omega}_\mu\right\} \\ &= \frac{1}{\mathcal{Z}'''} \exp\left\{-\frac{(\overline{c}_\mu - c_0)^2}{4c_0}\frac{V_\mu^2}{M^\psi_{\mu\mu}}\right\}. \end{aligned} \tag{B.20}$$

The normalization constant $\mathcal{Z}'''$ can be obtained by integrating over the

whole domain, giving as a final result

$$P(\overline{c}_\mu) = \sqrt{\frac{V_\mu^2}{4\pi c_0 M_{\mu\mu}^{\psi}}} \exp\left\{ -\frac{(\overline{c}_\mu - c_0)^2}{4c_0} \frac{V_\mu^2}{M_{\mu\mu}^{\psi}} \right\} . \tag{B.21}$$

Once we have this result, it is straightforward to use it under the local equilibrium assumption in Eq. (4.6) so that to obtain the explicit expression for the LE model in (4.5).

# C

# Analytic Calculation of the Conditional Average

In this appendix we compute, by resorting to the maximum entropy principle the conditional average of a certain class of phase functions $F(\mathbf{z})$ that can be written as a functional of the one particle operator $c_{\mathbf{r}}(\mathbf{z}) = \sum_i \delta(\mathbf{r} - \mathbf{r}_i)$, this is

$$F(\mathbf{z}) = F[c_{\mathbf{r}}(\mathbf{z})]\,. \tag{C.1}$$

When computing conditional averages of this kind of functions, we will assume the following ansatz

$$\langle F[c_{\mathbf{r}}]\rangle^{\mathbf{c}} = F[c^*(\mathbf{r})]\,, \tag{C.2}$$

where $c^*(\mathbf{r})$ is the least biased one particle probability (i.e. density field) that is compatible with the values $\mathbf{c}$. Therefore, $c^*(\mathbf{r})$ has an implicit functional dependence on $\mathbf{c}$.

The least biased $c^*(\mathbf{r})$ can be obtained from the maximization of the entropy functional

$$S[c] = -\int d\mathbf{r}\, c(\mathbf{r}) \ln\left(\frac{c(\mathbf{r})}{c_0}\right) \tag{C.3}$$

subject to the constraints

$$\begin{aligned} \int d\mathbf{r}\, c(\mathbf{r}) &= c_0 V_T \\ \int d\mathbf{r}\, c(\mathbf{r}) \delta_\mu(\mathbf{r}) &= c_\mu \,. \end{aligned} \tag{C.4}$$

Here, $c_0$ is a (prior) homogeneous distribution function and $V_T$ is the volume of the system. The solution of the maximization problem is standard in terms of a dimensionless vector $\lambda$ of Lagrange multipliers $\lambda_\mu$

$$c^*(\mathbf{r}) = c_0 \frac{\exp\left\{-\sum_\mu V_\mu \lambda_\mu \delta_\mu(\mathbf{r})\right\}}{\frac{1}{V_T}\int d\mathbf{r}'\, \exp\left\{-\sum_\mu V_\mu \lambda_\mu \delta_\mu(\mathbf{r}')\right\}} \,. \tag{C.5}$$

The actual value of the Lagrange multipliers $\lambda$ is fixed by requiring that $c^*(\mathbf{r})$ satisfies the constraints in (C.4). In this way, $\lambda$ become a (one-to-one) function of the imposed constraining $\mathbf{c}$.

The calculations can be performed explicitly in $1D$ for a regular lattice. Let us consider the integral over $x$, by dividing the interval $[0, L]$ into sub-elements of size $a$, this is

$$\begin{aligned} \frac{1}{L}\int_0^L dx\, \exp\left\{-\sum_\mu a\lambda_\mu \delta_\mu(x)\right\} = \frac{1}{L}\left[\sum_\nu \int_{x_\nu}^{x_{\nu+1}} dx\right] \\ \times \exp\left\{-\sum_\mu a\lambda_\mu \delta_\mu(x)\right\} \,. \end{aligned} \tag{C.6}$$

Now, consider just the term

$$\frac{1}{L}\int_{x_\nu}^{x_{\nu+1}} dx\ \exp\left\{-\sum_\mu \lambda_\mu \delta_\mu(x)\right\}$$
$$= \frac{1}{L}\int_{x_\nu}^{x_{\nu+1}} dx\ \exp\left\{-\lambda_\nu\left(\frac{r_{\nu+1}-r}{a}\right) - \lambda_{\nu+1}\left(\frac{x-x_\nu}{a}\right)\right\}$$
$$= -\frac{a}{L}\frac{e^{-\lambda_{\nu+1}} - e^{-\lambda_\nu}}{\lambda_{\nu+1}-\lambda_\nu}\,. \tag{C.7}$$

Therefore, Eq. (C.6) becomes

$$G_M \triangleq \frac{1}{L}\int_0^L dx\ \exp\left\{-\sum_\mu a\lambda_\mu \delta_\mu(x)\right\} = -\frac{1}{M}\sum_\mu \frac{e^{-\lambda_{\mu+1}} - e^{-\lambda_\mu}}{\lambda_{\mu+1}-\lambda_\mu}\,. \tag{C.8}$$

We can also perform the integral

$$
\begin{aligned}
&\int dx\, \delta_\mu(x) \exp\left\{-\sum_\nu \lambda_\nu \delta_\nu(x)\right\} \\
&\quad = \int_{x_{\mu-1}}^{x_\mu} dx\, \frac{1}{a}\left(\frac{r - x_{\mu-1}}{a}\right) \exp\left\{-\sum_\nu \lambda_\nu \delta_\nu(x)\right\} \\
&\qquad\qquad + \int_{x_\mu}^{x_{\mu+1}} dx\, \frac{1}{a}\left(\frac{x_{\mu+1} - x}{a}\right) \exp\left\{-\sum_\nu \lambda_\nu \delta_\nu(x)\right\} \\
&\quad = \int_{x_{\mu-1}}^{x_\mu} dx\, \frac{1}{a}\left(\frac{x - x_{\mu-1}}{a}\right) \exp\left\{-\lambda_{\mu-1}\left(\frac{x_\mu - x}{a}\right) - \lambda_\mu\left(\frac{x - x_{\mu-1}}{a}\right)\right\} \\
&+ \int_{x_\mu}^{x_{\mu+1}} dx\, \frac{1}{a}\left(\frac{x_{\mu+1} - x}{a}\right) \exp\left\{-\lambda_\mu\left(\frac{x_{\mu+1} - x}{a}\right) - \lambda_{\mu+1}\left(\frac{x - x_\mu}{a}\right)\right\} \\
&\quad = \int_0^1 dx'\, x' \exp\left\{-\lambda_{\mu-1}(1 - x') - \lambda_\mu x'\right\} \\
&\qquad\qquad + \int_0^1 dx'\, (1 - x') \exp\left\{-\lambda_\mu(1 - x') - \lambda_{\mu+1} x'\right\} \\
&\quad = \frac{e^{-\lambda_{\mu-1}} - e^{-\lambda_\mu}}{(\lambda_\mu - \lambda_{\mu-1})^2} - \frac{e^{-\lambda_\mu}}{(\lambda_\mu - \lambda_{\mu-1})} + \frac{e^{-\lambda_{\mu+1}} - e^{-\lambda_\mu}}{(\lambda_\mu - \lambda_{\mu+1})^2} - \frac{e^{-\lambda_\mu}}{(\lambda_\mu - \lambda_{\mu+1})}\,.
\end{aligned}
\tag{C.9}
$$

We may now collect the results and find the result linking $\mathbf{c}$ with $\lambda$,

$$
c_\mu = G(\lambda_\mu, \lambda_{\mu+1}) + G(\lambda_\mu, \lambda_{\mu-1})\,, \tag{C.10}
$$

where we have introduced

$$
G(\lambda_\mu, \lambda_{\mu+1}) \triangleq \frac{c_0}{G_M}\left(\frac{e^{-\lambda_{\mu+1}} - e^{-\lambda_\mu}}{(\lambda_\mu - \lambda_{\mu+1})^2} - \frac{e^{-\lambda_\mu}}{(\lambda_\mu - \lambda_{\mu+1})}\right)\,. \tag{C.11}
$$

Note that the relationship between $\mathbf{c}$ and $\lambda$ is not one to one. In fact, note that if we make the substitution $\lambda_\mu \to \lambda_\mu + c$, $\mathbf{c}$ remains unchanged.

Now, we can compute the conditional average of the sub-element density

$c_e(\mathbf{c})$, which is of the form considered

$$c_e(\mathbf{c}) = \left\langle \sum_i^N \theta_e(\mathbf{r}_i) \right\rangle^{\mathbf{c}} = \int d\mathbf{r}\, \theta_e(\mathbf{r})\, \langle c_{\mathbf{r}} \rangle^{\mathbf{c}} \approx \int d\mathbf{r}\, \theta_e(\mathbf{r}) c^*(\mathbf{r})$$
$$= \frac{c_0}{G_M} \int d\mathbf{r}\, \theta_e(\mathbf{r}) \exp\left\{ -\sum_\mu V_\mu \lambda_\mu \delta_\mu(\mathbf{r}) \right\}, \tag{C.12}$$

where we have used Eq. (C.5). In 1D we obtain for the element $e \in (x_\mu, x_{\mu+1})$

$$c_e(\mathbf{c}) = \frac{c_0}{G_M} \int_{x_\mu}^{x_{\mu+1}} dx\, \exp\left\{ -\lambda_\mu \left( \frac{x_{\mu+1} - x}{a} \right) - \lambda_{\mu+1} \left( \frac{x - x_\mu}{a} \right) \right\}$$
$$= -\frac{c_0}{G_M} \int_0^1 dx' \exp\left\{ -\lambda_\mu (1 - x') - \lambda_{\mu+1} x' \right\}$$
$$= -\frac{c_0}{G_M} \frac{e^{-\lambda_{\mu+1}} - e^{-\lambda_\mu}}{\lambda_{\mu+1} - \lambda_\mu}. \tag{C.13}$$

This form satisfies $\sum_e V_e c_e = N$.

It is worth exploring the case when $\lambda_{\mu+1} = \lambda_\mu + \Delta\lambda_\mu$ with $\Delta\lambda_\mu$ comparatively small. Consider first the normalization $G_M$ introduced in Eq. (C.8)

$$G_M = -\frac{1}{M} \sum_\mu \frac{e^{-\lambda_{\mu+1}} - e^{-\lambda_\mu}}{\lambda_{\mu+1} - \lambda_\mu}$$
$$= \frac{1}{M} \sum_\mu e^{-\lambda_\mu} \left( 1 - \frac{\Delta\lambda_\mu}{2} \right) + \mathcal{O}(\Delta\lambda^2). \tag{C.14}$$

Next, consider the function $G(\lambda_{\mu+1}, \lambda_\mu)$ introduced in (C.11)

$$
\begin{aligned}
G(\lambda_{\mu+1},\lambda_\mu) &= c_0\left(\frac{e^{-\lambda_{\mu+1}}-e^{-\lambda_\mu}}{(\lambda_{\mu+1}-\lambda_\mu)^2}+\frac{e^{-\lambda_\mu}}{(\lambda_{\mu+1}-\lambda_\mu)}\right)\\
&= \frac{c_0}{G_M}e^{-\lambda_\mu}\left(\frac{1}{2}-\frac{\Delta\lambda_\mu}{6}\right)+\mathcal{O}(\Delta\lambda^2)\\
&= c_0\frac{e^{-\lambda_\mu}\left(\frac{1}{2}-\frac{\Delta\lambda_\mu}{6}\right)+\mathcal{O}(\Delta\lambda^2)}{\frac{1}{M}\sum_\nu e^{-\lambda_\nu}\left(1-\frac{\Delta\lambda_\nu}{2}\right)+\mathcal{O}(\Delta\lambda^2)}\\
&= c_0\frac{e^{-\lambda_\mu}\left(\frac{1}{2}-\frac{\Delta\lambda_\mu}{6}\right)}{\frac{1}{M}\sum_\nu e^{-\lambda_\nu}}\left(1+\frac{\sum_\nu e^{-\lambda_\nu}\Delta\lambda_\nu}{2\sum_\nu e^{-\lambda_\nu}}\right)+\mathcal{O}(\Delta\lambda^2)\\
&= c_0\frac{e^{-\lambda_\mu}}{\frac{1}{M}\sum_\nu e^{-\lambda_\nu}}\left(\frac{1}{2}-\frac{\Delta\lambda_\mu}{6}+\frac{\sum_\nu e^{-\lambda_\nu}\Delta\lambda_\nu}{4\sum_\nu e^{-\lambda_\nu}}\right)+\mathcal{O}(\Delta\lambda^2)\,.
\end{aligned}
\tag{C.15}
$$

Therefore, we have, to first order

$$
c_\mu = c_0\frac{e^{-\lambda_\mu}}{\frac{1}{M}\sum_\nu e^{-\lambda_\nu}}\left(1-\frac{\Delta\lambda_r+\Delta\lambda_l}{6}+\langle\Delta\lambda\rangle\right)\,, \tag{C.16}
$$

where $\Delta\lambda_r = \lambda_{\mu+1}-\lambda_\mu$ is the increment of the right sub-element of $\mu$ and $\Delta\lambda_l = \lambda_{\mu-1}-\lambda_\mu$ is the increment of the left sub-element of $\mu$. The term

$$
\langle\Delta\lambda\rangle \triangleq \frac{1}{6\sum_\nu e^{-\lambda_\nu}}\sum_\nu e^{-\lambda_\mu}\left(\Delta\lambda_r+\Delta\lambda_l\right) \tag{C.17}
$$

ensures that $c_\mu$ is normalized. To zero order we have simply

$$
c_\mu = c_0\frac{e^{-\lambda_\mu}}{\frac{1}{M}\sum_\nu e^{-\lambda_\nu}}\,. \tag{C.18}
$$

Note that if we assume that $\lambda_\mu$ varies "smoothly", then $c_\mu$ also varies in a smooth way.

In this level of approximation, the sub-element density (3.13) becomes

$$\begin{aligned} c_e(\mathbf{c}) &= -\frac{c_0}{G_M}\frac{e^{-\lambda_{\mu+1}} - e^{-\lambda_\mu}}{\lambda_{\mu+1} - \lambda_\mu} \\ &= c_0 \frac{e^{-\lambda_\mu}\left(1 - \frac{\Delta\lambda_\mu}{2}\right)}{\frac{1}{M}\sum_\nu e^{-\lambda_\nu}} \left(1 + \frac{\sum_\nu e^{-\lambda_\nu}\Delta\lambda_\nu}{2\sum_\nu e^{-\lambda_\nu}}\right) + \mathcal{O}(\Delta\lambda^2) \\ &= c_0 \frac{e^{-\lambda_\mu}}{\frac{1}{M}\sum_\nu e^{-\lambda_\nu}} \left(1 - \frac{\Delta\lambda_\mu}{2} + \frac{\sum_\nu e^{-\lambda_\nu}\Delta\lambda_\nu}{2\sum_\nu e^{-\lambda_\nu}}\right) + \mathcal{O}(\Delta\lambda^2)\,. \end{aligned} \tag{C.19}$$

Clearly, this is not symmetric with respect $\mu, \mu+1$. We can obtain a symmetrized result by noting that to first order we also have (by changing $\mu$ by $\mu+1$)

$$c_e(\mathbf{c}) = c_0 \frac{e^{-\lambda_{\mu+1}}}{\frac{1}{M}\sum_\nu e^{-\lambda_\nu}} \left(1 + \frac{\Delta\lambda_\mu}{2}\frac{\sum_\nu e^{-\lambda_\nu}\Delta\lambda_\nu}{2\sum_\nu e^{-\lambda_\nu}}\right) + \mathcal{O}(\Delta\lambda^2)\,. \tag{C.20}$$

Therefore, we have simply that

$$c_e = \frac{c_{\mu+1} + c_\mu}{2} + \mathcal{O}(\Delta\lambda^2)\,. \tag{C.21}$$

In summary, we have proved that for smooth fields, the maximum entropy calculation of the conditional averages provides the arithmetic mean for the sub-element density.

# D

# Computing the Condition Expectation

In order to validate the approximation (4.12) we may compute numerically the conditional expectation (3.13). This conditional expectation is defined as

$$\begin{aligned}\langle \cdots \rangle^{\mathbf{c}} &= \frac{1}{P^{\mathrm{eq}}(\mathbf{c})} \int d\mathbf{z}\, \rho^{\mathrm{eq}}(\mathbf{z}) \delta(\mathbf{c}(\mathbf{z}) - \mathbf{c}) \cdots \\ &= \frac{1}{P^{\mathrm{eq}}(\mathbf{c})} \int d\mathbf{z}\, \rho^{\mathrm{eq}}(\mathbf{z}) \prod_{\mu} \delta(\hat{c}_\mu(\mathbf{z}) - c_\mu) \cdots . \end{aligned} \tag{D.1}$$

For $N$ non-interacting Brownian particles $\rho^{\mathrm{eq}}(z) = 1/V_T^N$. This gives

$$\langle \cdots \rangle^{\mathbf{c}} = \frac{1}{V_T^N} \frac{1}{P^{\mathrm{eq}}(\mathbf{c})} \int d\mathbf{z} \prod_{\mu} \delta(\hat{c}_\mu(\mathbf{z}) - c_\mu) \cdots . \tag{D.2}$$

The evaluation of the average over the Dirac delta functions in hindered by the singular nature of these functions. We regularize this average by approximating the Dirac delta function with a Gaussian so that

$$\langle \cdots \rangle^{\mathbf{c}} = \frac{1}{V_T^N} \frac{1}{\mathcal{Z}} \int d\mathbf{z} \, \exp\left\{ -\frac{1}{2} \left( \frac{\hat{c}_\mu(\mathbf{z}) - c_\mu}{c_0} \right)^2 \right\} \cdots . \tag{D.3}$$

In the limit $c_0 \to 0$ this regularized conditional expectation coincides with (D.2).

The regularized average is computed by sampling the Gaussian distribution with a fictitious dynamics given by

$$d\mathbf{r}_i = -D \frac{\partial V}{\partial \mathbf{r}_i}(\mathbf{z}) dt + \sqrt{2D} d\boldsymbol{\mathcal{W}}_i \,, \tag{D.4}$$

with

$$V(\mathbf{z}) = \frac{1}{2} \sum_\mu \left( \frac{c_\mu(\mathbf{z}) - c_\mu}{c_0} \right)^2 . \tag{D.5}$$

Here, $V(\mathbf{z})$ is a dimensionless potential that depends on the microstate $\mathbf{z} \triangleq \{\mathbf{r}_i; i = 1, \ldots, N\}$ of the system and $d\boldsymbol{\mathcal{W}}_i$ are independent increments of the Wiener process. The Fokker-Planck Equation corresponding to (D.4) is

$$\frac{\partial P}{\partial t}(\mathbf{z}) = D \frac{\partial}{\partial \mathbf{r}_i} \left( \frac{\partial}{\partial \mathbf{r}_i} V(\mathbf{z}) \right) P(\mathbf{z}) + D \frac{\partial}{\partial \mathbf{r}_i} \frac{\partial}{\partial \mathbf{r}_i} P(\mathbf{z}) \,. \tag{D.6}$$

The equilibrium solution of the FPE (D.6) is

$$P^{\text{eq}}(\mathbf{z}) = \frac{1}{\mathcal{Z}} \exp\{-V(\mathbf{z})\} \,, \tag{D.7}$$

where $\mathcal{Z}$ is the normalization factor. The stationary solution (D.7) of the FPE

(D.6) is

$$P^{\mathrm{eq}}(\mathbf{z}) = \frac{1}{\mathcal{Z}} \exp\left\{ -\frac{1}{2} \sum_{\mu} \left( \frac{c_\mu(\mathbf{z}) - c_\mu}{c_0} \right)^2 \right\} .$$

In the limit $c_0 \to 0$ this goes to the distribution

$$P^{\mathrm{eq}}(\mathbf{z}) = \frac{1}{\mathcal{Z}} \prod_{\mu} \delta(c_\mu(\mathbf{z}) - c_\mu) . \tag{D.8}$$

Then, the SDE (D.4) becomes with the potential (D.5)

$$d\mathbf{r}_i = -\frac{D}{c_0^2} \sum_{\mu} (c_\mu(\mathbf{z}) - c_\mu) \nabla \delta_\mu(\mathbf{r}_i) dt + \sqrt{2D} d\boldsymbol{\mathcal{W}}_i . \tag{D.9}$$

Equation (D.9) samples, in the steady state and for sufficiently small $c_0$, the distribution (D.8). It is clear that in order to achieve small values of $c_0$ one needs to reduce correspondingly the time step in the numerical solution of (D.9).

For a one-dimensional situation with a regular grid of spacing $a$, every node has two sub-elements as shown in Fig. 3.4, where the vectors $\mathbf{b}_{e\to\mu}$ in (3.7) are simply the numbers $\pm\frac{1}{a}$. The term $\nabla\delta_\mu(\mathbf{r})$ is then (neglecting the discontinuities at the nodes)

$$\nabla \delta_\mu(x) = -\frac{1}{a^2} \theta(x - x_\mu) \theta(x_{\mu+1} - x) + \frac{1}{a^2} \theta(x - x_{\mu-1}) \theta(x_\mu - x) . \tag{D.10}$$

And the SDE (D.9) becomes

$$dx_i = \frac{D}{c_0^2 a^2} \sum_{\mu} (c_\mu(\mathbf{z}) - c_\mu)\theta(x_i - x_\mu)\theta(x_{\mu+1} - x_i)dt \\ - \frac{D}{c_0^2 a^2} \sum_{\mu} (c_\mu(\mathbf{z}) - c_\mu)\theta(x_i - x_{\mu-1})\theta(x_\mu - x_i)dt \\ + \sqrt{2D}d\mathcal{W}_i \,. \tag{D.11}$$

In order to see how this dynamics works, assume that the $i$-th particle is in the element $(x_3, x_4)$. Then,

$$dx_i = \frac{D}{c_0^2 a^2}(c_3(\mathbf{z}) - c_3)dt - \frac{D}{c_0^2 a^2}(c_4(\mathbf{z}) - c_4)dt + \sqrt{2D}d\mathcal{W}_i \,. \tag{D.12}$$

Assume further that $c_4(\mathbf{z}) = c_4$ and $c_3(\mathbf{z}) > c_3$. This means that there is an excess of particles near node 3. In that case, Eq. (D.12) tend to move the particle to the right, this is, reducing the concentration of node 3, as it should.

In Fig. D.1 we plot the approximation (4.12) with the numerically evaluated conditional expectation (3.13) for the case that the profile $\mathbf{c}$ is a sinusoidal shape $c_\mu = 10 + 3\sin(2\pi a\mu/L)$, with $L = 20$ and $a = 1$. The agreement is very good and shows indeed that the concentration $c_e$ of the sub-element $e$ is the arithmetic mean of the nodal concentrations, as assumed in Eq. (4.12).

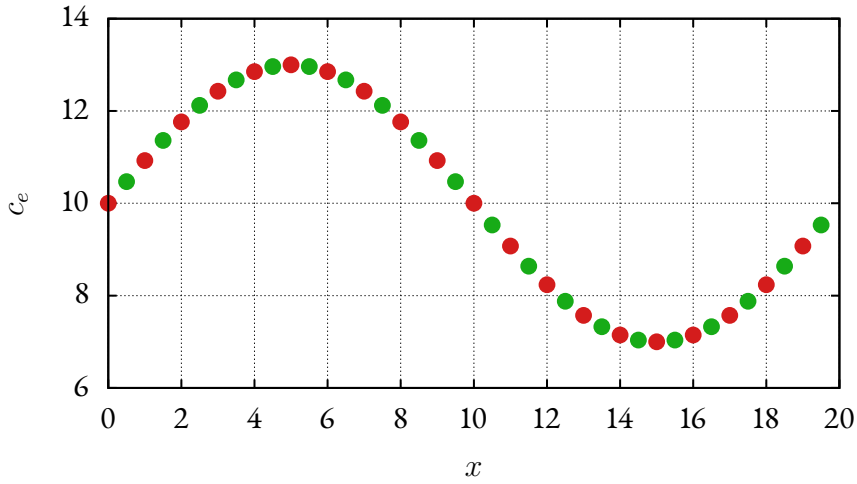


**Figure D.1:** The conditional average $c_e$ defined in Eq. (3.13) for a regular grid of length $L = 20$ and spacing $a = 1$. Red dots are the input value $\mathbf{c}$, which in this case is $c_\mu = 10 + 3\sin(2\pi a\mu/L)$. Green dots are the result of performing the conditional average average in Eq. (3.13) with the sampling method given in Eq. (D.11).

# E

# Error Estimates for Linearly Consistent Operators.

In Section 5.3 we only considered the formal aspects of the construction of discrete ordinary differential equations (ODE) like (5.30) from continuum partial differential equations (PDE) like (0.3). With the Petrov-Galerkin method we made an approximation in the process without worrying about the error committed. In this appendix, we pay attention to this issue by focusing on basis functions $\psi(\mathbf{r})$ that have as continued functions the linear functions.

Let us consider the PDE (0.3) for a highly dilute suspension. In this case, the general diffusion equation (0.3) turns into the Fick's diffusion equation

$$\frac{\partial c}{\partial t}(\mathbf{r}, t) = \nabla^2 c(\mathbf{r}, t)\,. \tag{E.1}$$

Let us start by using the discretization operator $\mathcal{D}_R$ on the diffusion equa-

tion (E.1). By applying the discretization operator on both sides

$$\mathcal{D}_R\left[\frac{\partial c}{\partial t}(\mathbf{r},t)\right] = \mathcal{D}_R[\nabla^2 c(\mathbf{r},t)]\,.$$

The effect of the discretization operator is achieved by multiplying (E.1) with respect to $\delta_\mu(\mathbf{r})$ and integrating over the whole space, which leads to

$$\frac{d}{dt}\mathbf{c}(t) = \int d\mathbf{r}\,\delta(\mathbf{r})\nabla^2 c(\mathbf{r},t)\,, \tag{E.2}$$

where

$$\mathbf{c}(t) \triangleq \int d\mathbf{r}\,\delta(\mathbf{r})c(\mathbf{r},t)\,.$$

The exact equation (E.2) is not a closed equation for $c_\mu(t)$ until we represent the continuous field $c(\mathbf{r},t)$ in terms of the discrete values $c_\mu(t)$. To this end, we write

$$c(\mathbf{r},t) = \psi^T(\mathbf{r})\mathbf{c}(t) + \epsilon(\mathbf{r},t)\,, \tag{E.3}$$

where the error field $\epsilon(\mathbf{r},t)$ is precisely defined as

$$\epsilon(\mathbf{r},t) \triangleq c(\mathbf{r},t) - \psi^T(\mathbf{r})\mathbf{c}(t)\,.$$

By inserting Eq. (E.3) into (E.2), we have

$$\frac{d}{dt}\mathbf{c}(t) = -\Delta\mathbf{c}(t) + \epsilon\,,$$

where the discrete Laplacian operator is defined in Eq. (5.20) and the error term is

$$\epsilon = \int d\mathbf{r}\delta\left(\mathbf{r}\right)\nabla^2\epsilon(\mathbf{r},t)\,. \tag{E.4}$$

We analyze now this error term by noting that the error field can be written as

$$\epsilon(\mathbf{r}) = c(\mathbf{r}) - \int d\mathbf{r}'\, S(\mathbf{r}, \mathbf{r}')c(\mathbf{r}')\,.$$

By Taylor expanding the field $c(\mathbf{r}')$ inside the integral around $\mathbf{r}$ we have

$$\epsilon(\mathbf{r}) = \sum_{n=1}^{\infty} \boldsymbol{\nabla}^n c(\mathbf{r}) m^n(\mathbf{r})\,,$$

where the moments $m^n(\mathbf{r})$ are given by

$$m^n(\mathbf{r}) \triangleq \int d\mathbf{r}'\, S(\mathbf{r}, \mathbf{r}')(\mathbf{r}' - \mathbf{r})^n\,.$$

Therefore, the error term (E.4) has the form

$$\epsilon = \int d\mathbf{r}\, \delta(\mathbf{r}) \nabla^2 \sum_{n=1}^{\infty} \boldsymbol{\nabla}^n c(\mathbf{r}) m^n(\mathbf{r})\,.$$

The discussion of the error in the discretization procedure requires the knowledge of the moments of the smoothing kernel $S(\mathbf{r}, \mathbf{r}')$. The conditions (5.16) show that for linearly consistent interpolations, the smoothing kernel $S(\mathbf{r}, \mathbf{r}')$ has the moments $m^0(\mathbf{r}) = 0$ and $m^1(\mathbf{r}) = 0$. Given the locality of $S(\mathbf{r}, \mathbf{r}')$ we expect that $m^n(\mathbf{r}) \propto h^n$ where $h$ is a typical value of the lattice spacing around the point $\mathbf{r}$. In conclusion, we expect that for a linearly consistent scheme, the error committed in solving the discrete equation instead of the continuum one will be of order $h^2$.

# F

# Dissipative Term in 1$D$

In this appendix we compute the dissipative term (5.33) in 1$D$ for regular lattices of spacing $a$. Due to the form of the Delaunay construction, the $\psi_\mu(x)$ functions are zero for all $x$ positions far away to the node $\mu$. Keeping this in mind, it is straightforward to compute the dissipative matrix explicitly.

## F.1. Obtention of the dissipative matrix in 1$D$

The dissipative matrix can be obtained ny evaluating the mobility coefficient $\Gamma(c)$ at the interpolated field $c(x) = \sum_\mu \psi_\mu(x) c_\mu$ so that

$$\begin{aligned} D_{\mu\nu} &= \int dx\, \nabla\delta_\mu(x) \nabla\delta_\nu(x) \Gamma(\boldsymbol{\psi}\cdot\mathbf{c}) \\ &= \frac{D}{k_{\mathrm{B}}T} \int dx\, \left[\nabla\delta_\mu(x)\right] \left[\nabla\delta_\nu(x)\right] \left[\sum_\sigma \psi_\sigma(x)\Gamma_\sigma\right] . \end{aligned} \tag{F.1}$$

The basis function $\delta_\mu(x)$ and its gradient are given by

$$\delta_\mu(x) = \sum_{\mu'} M^{\delta}_{\mu\mu'} \psi_{\mu'}(x)\,, \tag{F.2}$$

$$\begin{aligned}\nabla\delta_\mu(x) &= \frac{1}{a}\sum_{\mu'} M^{\delta}_{\mu\mu'}\left[\theta(x - x_{\mu'-1})\theta(x_{\mu'} - x) - \theta(x - x_{\mu'})\theta(x_{\mu'+1} - x)\right] \\ &= \frac{1}{a}\sum_{\mu'} M^{\delta}_{\mu\mu'}\left[\theta_{x^l_{\mu'}} - \theta_{x^r_{\mu'}}\right]\,,\end{aligned} \tag{F.3}$$

where $\theta(x)$ is the Heaviside step function. Therefore, the dissipative matrix will be

$$\begin{aligned}D_{\mu\nu} = \frac{D}{k_{\mathrm{B}}T}\frac{1}{a^3}\int dx\ &\left[\sum_{\mu'} M^{\delta}_{\mu\mu'}\left[\theta_{x^l_{\mu'}} - \theta_{x^r_{\mu'}}\right]\right]\left[\sum_{\nu'} M^{\delta}_{\nu\nu'}\left[\theta_{x^l_{\nu'}} - \theta_{x^r_{\nu'}}\right]\right] \\ &\times\left[\sum_{\sigma}\left[\theta_{x^l_\sigma}(x - x_{\sigma-1}) - \theta_{x^r_\sigma}(x_{\sigma+1} - x)\right]c_\sigma\right] \\ = \frac{D}{k_{\mathrm{B}}T}\frac{1}{a^3}\sum_{\mu'} M^{\delta}_{\mu\mu'}\Bigg\{&\int dx\,\theta_{x^l_{\mu'}}\left[\sum_{\nu'} M^{\delta}_{\nu\nu'}\left[\theta_{x^l_{\nu'}} - \theta_{x^r_{\nu'}}\right]\right] \\ &\times\left[\sum_{\sigma}\left[\theta_{x^l_\sigma}(x - x_{\sigma-1}) - \theta_{x^r_\sigma}(x_{\sigma+1} - x)\right]c_\sigma\right] \\ &- \int dx\,\theta_{x^r_{\mu'}}\left[\sum_{\nu'} M^{\delta}_{\nu\nu'}\left[\theta_{x^l_{\nu'}} - \theta_{x^r_{\nu'}}\right]\right] \\ &\times\left[\sum_{\sigma}\left[\theta_{x^l_\sigma}(x - x_{\sigma-1}) - \theta_{x^r_\sigma}(x_{\sigma+1} - x)\right]c_\sigma\right]\Bigg\}\,.\end{aligned} \tag{F.4}$$

Of the sum over all $\nu'$ nodes (and, respectively, all the $\sigma$ nodes) only those nodes whose elements left and right overlap with the $\mu'$-th node will be different from zero. The element $x^l_{\mu'}$, for example, overlaps only with nodes

$\nu' = \mu' - 1$ and $\nu' = \mu'$, so

$$
\begin{aligned}
D_{\mu\nu} = \frac{D}{k_{\mathrm{B}}T}\frac{1}{a^3}\sum_{\mu'} M^{\delta}_{\mu\mu'} & \\
& \times \left\{ \int_{x_{\mu'-1}}^{x_{\mu'}} dx \, \left[ -M^{\delta}_{\nu\mu'-1} + M^{\delta}_{\nu\mu'} \right] \left[ (x_{\mu'} - x)u_{\mu'-1} + (x - x_{\mu'-1})u_{\mu'} \right] \right. \\
& \left. - \int_{x_{\mu'}}^{x_{\mu'+1}} dx \, \left[ -M^{\delta}_{\nu\mu'} + M^{\delta}_{\nu\mu'+1} \right] \left[ (x_{\mu'+1} - x)u_{\mu'} + (x - x_{\mu'})u_{\mu'+1} \right] \right\} \\
= \frac{D}{k_{\mathrm{B}}T}\frac{1}{a^3}\sum_{\mu'} M^{\delta}_{\mu\mu'} & \\
& \times \left\{ \left[ M^{\delta}_{\nu\mu'} - M^{\delta}_{\nu\mu'-1} \right] \left[ c_{\mu'-1} \int_{x_{\mu'-1}}^{x_{\mu'}} dx \, (x_{\mu'} - x) + c_{\mu'} \int_{x_{\mu'-1}}^{x_{\mu'}} dx \, (x - x_{\mu'-1}) \right] \right. \\
& \left. + \left[ M^{\delta}_{\nu\mu'} - M^{\delta}_{\nu\mu'+1} \right] \left[ c_{\mu'+1} \int_{x_{\mu'}}^{x_{\mu'+1}} dx \, (x - x_{\mu'}) + c_{\mu'} \int_{x_{\mu'}}^{x_{\mu'+1}} dx \, (x_{\mu'+1} - x) \right] \right\} \\
= \frac{D}{k_{\mathrm{B}}T}\frac{1}{a}\sum_{\mu'} M^{\delta}_{\mu\mu'} & \\
& \times \left\{ \left[ M^{\delta}_{\nu\mu'} - M^{\delta}_{\nu\mu'-1} \right] \left[ \frac{c_{\mu'-1} + c_{\mu'}}{2} \right] + \left[ M^{\delta}_{\nu\mu'} - M^{\delta}_{\nu\mu'+1} \right] \left[ \frac{c_{\mu'} + c_{\mu'+1}}{2} \right] \right\} \\
= \frac{D}{k_{\mathrm{B}}T}\frac{1}{a}\sum_{\mu'} M^{\delta}_{\mu\mu'} & \left[ - \left( \frac{c_{\mu'-1} + c_{\mu'}}{2} \right) M^{\delta}_{\mu'-1\nu} \right. \\
& \left. + \left( \frac{c_{\mu'-1} + c_{\mu'}}{2} + \frac{c_{\mu'} + c_{\mu'+1}}{2} \right) M^{\delta}_{\mu'\nu} - \left( \frac{c_{\mu'-1} + c_{\mu'}}{2} \right) M^{\delta}_{\mu'+1\nu} \right] \\
= \frac{D}{k_{\mathrm{B}}T} M^{\delta}_{\mu\mu'} U_{\mu'\nu'} M^{\delta}_{\nu'\nu} , &
\end{aligned}
$$

where the matrix $\mathbf{U}$ is

$$
U_{\mu\nu} = \frac{1}{a} \begin{cases} -\frac{c_{\mu} + c_{\mu-1}}{2} & \text{iff } \nu = \mu - 1 , \\ \frac{c_{\mu} + c_{\mu-1}}{2} + \frac{c_{\mu} + c_{\mu+1}}{2} & \text{iff } \nu = \mu , \\ -\frac{c_{\mu} + c_{\mu+1}}{2} & \text{iff } \nu = \mu + 1 , \\ 0 & \text{otherwise} . \end{cases}
$$

## F.2. Gradient of the dissipative matrix

Once obtained the dissipative matrix, we may compute its derivative. Let us expand the sum over $\mu'$ around $\nu$ so that

$$\begin{aligned}
D_{\mu\nu} = \frac{D}{k_{\mathrm{B}}T}\frac{1}{a}\sum_{\mu'} M^{\delta}_{\mu\mu'} \Bigg[ & -\left(\frac{c_{\mu'-1}+c_{\mu'}}{2}\right) M^{\delta}_{\mu'-1\nu} \\
& + \left(\frac{c_{\mu'-1}+c_{\mu'}}{2} + \frac{c_{\mu'}+c_{\mu'+1}}{2}\right) M^{\delta}_{\mu'\nu} - \left(\frac{c_{\mu'-1}+c_{\mu'}}{2}\right) M^{\delta}_{\mu'+1\nu}\Bigg] \\
= \frac{D}{k_{\mathrm{B}}T}\frac{1}{a}\Bigg\{ & \cdots \\
& + M^{\delta}_{\mu\nu-1}\left[-\left(\frac{c_{\nu-2}+c_{\nu-1}}{2}\right) M^{\delta}_{\nu-2\nu} + \left(\frac{c_{\nu-2}+c_{\nu-1}}{2} + \frac{c_{\nu-1}+c_{\nu}}{2}\right) M^{\delta}_{\nu-1\nu}\right. \\
& \qquad \left. - \left(\frac{c_{\nu-2}+c_{\nu-1}}{2}\right) M^{\delta}_{\nu\nu}\right] \\
& + M^{\delta}_{\mu\nu}\left[-\left(\frac{c_{\nu-1}+c_{\nu}}{2}\right) M^{\delta}_{\nu-1\nu} + \left(\frac{c_{\nu-1}+c_{\nu}}{2} + \frac{c_{\nu}+c_{\nu+1}}{2}\right) M^{\delta}_{\nu\nu}\right. \\
& \qquad \left. - \left(\frac{c_{\nu-1}+c_{\nu}}{2}\right) M^{\delta}_{\nu+1\nu}\right] \\
& + M^{\delta}_{\mu\nu+1}\left[-\left(\frac{c_{\nu}+c_{\nu+1}}{2}\right) M^{\delta}_{\nu\nu} + \left(\frac{c_{\nu}+c_{\nu+1}}{2} + \frac{c_{\nu+1}+c_{\nu+2}}{2}\right) M^{\delta}_{\nu+1\nu}\right. \\
& \qquad \left. - \left(\frac{c_{\nu+1}+c_{\nu+2}}{2}\right) M^{\delta}_{\nu+2\nu}\right] \\
& + \cdots \Bigg\} .
\end{aligned} \tag{F.5}$$

The derivative with respect to $c_\nu$ will be, hence,

$$\begin{aligned}
\frac{\partial D_{\mu\nu}}{\partial c_\nu} = \frac{D}{k_{\mathrm{B}}T}\frac{1}{2a}\Big\{ & M^{\delta}_{\mu\nu-1}\left[M^{\delta}_{\nu-1\nu} - M^{\delta}_{\nu\nu}\right] \\
& + M^{\delta}_{\mu\nu}\left[-M^{\delta}_{\nu-1\nu} + 2M^{\delta}_{\nu\nu} - M^{\delta}_{\nu+1\nu}\right] + M^{\delta}_{\mu\nu+1}\left[-M^{\delta}_{\nu\nu} + M^{\delta}_{\nu+1\nu}\right]\Big\} .
\end{aligned} \tag{F.6}$$

So that the gradient, expanding around the node $\mu$, is

$$\begin{aligned}\sum_{\nu}\frac{\partial D_{\mu\nu}}{\partial c_{\nu}} = \frac{D}{k_{\mathrm{B}}T}\frac{1}{2a}\Big\{\cdots \\ &+ M^{\delta}_{\mu\mu-2}\left[M^{\delta}_{\mu-2\mu-1} - M^{\delta}_{\mu-1\mu-1}\right] \\ &+ M^{\delta}_{\mu\mu-1}\left[-M^{\delta}_{\mu-2\mu-1} + 2M^{\delta}_{\mu-1\mu-1} - M^{\delta}_{\mu\mu-1}\right] \\ &+ M^{\delta}_{\mu\mu}\left[-M^{\delta}_{\mu-1\mu-1} + M^{\delta}_{\mu\mu-1}\right] \\ &+ M^{\delta}_{\mu\mu-1}\left[M^{\delta}_{\mu-1\mu} - M^{\delta}_{\mu\mu}\right] \\ &+ M^{\delta}_{\mu\mu}\left[-M^{\delta}_{\mu-1\mu} + 2M^{\delta}_{\mu\mu} - M^{\delta}_{\mu+1\mu}\right] \\ &+ M^{\delta}_{\mu\mu+1}\left[-M^{\delta}_{\mu\mu} + M^{\delta}_{\mu+1\mu}\right] \\ &+ M^{\delta}_{\mu\mu}\left[M^{\delta}_{\mu\mu+1} - M^{\delta}_{\mu+1\mu+1}\right] \\ &+ M^{\delta}_{\mu\mu+1}\left[-M^{\delta}_{\mu\mu+1} + 2M^{\delta}_{\mu+1\mu+1} - M^{\delta}_{\mu+2\mu+1}\right] \\ &+ M^{\delta}_{\mu\mu+2}\left[-M^{\delta}_{\mu+1\mu+1} + M^{\delta}_{\mu+2\mu+1}\right] \\ &+ \cdots \Big\}\,. \end{aligned} \tag{F.7}$$

Note that if in (F.7) all the shown terms cancel, by symmetry, all the unshown terms also vanish. As $\mathbf{M}^{\delta}$ is as symmetric matrix, we have the following properties

$$\begin{aligned} M^{\delta}_{\mu\nu} &= M^{\delta}_{\nu\mu}\,, \\ M^{\delta}_{\mu\mu} &= M^{\delta}_{\nu\nu}\,, \end{aligned} \tag{F.8}$$

so that it is obvious that all the terms that appear in (F.7) vanish. Therefore, the gradient is identically equals to zero

$$\sum_{\nu}\frac{\partial D_{\mu\nu}}{\partial c_{\nu}} = 0\,. \tag{F.9}$$

# G

# List of Acronyms

| | |
|---|---|
| BD | Brownian Dynamics |
| CG | Coarse Grained (variable) |
| DDFT | Dynamic Density Functional Theory |
| FDT | Fluctuation-Dissipation Theorem |
| FFT | Fast Fourier Transform |
| FPE | Fokker-Planck Equation |
| GA | Gaussian |
| GL | Ginzburg-Landau |
| LLNS | Landau-Lifshitz Navier-Stokes |
| MD | Molecular Dynamics |
| ODE | Ordinary Differential Equation |
| PDE | Partial Differential Equation |
| SDE | Stochastic Differential Equation |
| SODE | Stochastic Ordinary Differential Equation |
| SPDE | Stochastic Partial Differential Equation |
| ToCG | Theory of Coarse-Graining |
| vdW | van der Waals |

# H
# List of Symbols

In general, **bold** shape refers to matrices (upper case) or vectors (lower case). *Italic* shape refers to scalars. $\mathcal{CALLIGRAPHIC}$ shape refers to operators.

## Physical parameters and variables

| | |
|---|---|
| $N$ | Number of particles |
| $M$ | Number of nodes |
| $k_{\mathrm{B}}$ | Boltzmann's constant |
| $T$ | Temperature |
| $\beta$ | $(k_{\mathrm{B}}T)^{-1}$ |
| $T_c$ | Critical temperature (vdW model, GL model) |
| $c(\mathbf{r},t)$ | Concentration field |
| $c_0$ | Average concentration field |
| $c_c$ | Critical concentration (vdW model, GL model) |
| $L$ | Total length of a $1D$ simulation box |
| $V_T$ | Total volume of a $D$ simulation box |
| $D$ | Diffusion coefficient |
| $\Gamma(c)$ | Mobility |
| $\mathbf{D}(\mathbf{c})$ | Dissipative matrix |
| $\mathcal{F}[c]$ | Free energy *functional* |
| $F(\mathbf{c})$ | Free energy *function* |

## Finite elements

| | |
|---|---|
| $V_\mu$ | Volume of node $\mu$ |
| $\psi_\mu(\mathbf{r})$ | Finite element with support on the Delaunay triangulation |
| $\delta_\mu(\mathbf{r})$ | (Conjugate) finite element of $\psi_\mu(\mathbf{r})$ |
| $\theta_{e_\mu}(\mathbf{r})$ | Characteristic function of the element $e_\mu$ |
| $\mathbf{b}_{e\to\mu}$ | Vector belonging to the element $e$ that points toward node $\mu$ |
| $\mathbf{M}^{\psi}$ | Mass matrix |
| $\mathbf{L}^{\psi}$ | Stiffness matrix |
| $\mathbf{M}^{\delta}$ | Inverse of the mass matrix $\mathbf{M}^{\psi}$ |
| $\mathbf{L}^{\delta}$ | Conjugate of the stiffness matrix $\mathbf{L}^{\psi}$ |

| | |
|---|---|
| $\mathbf{z}$ | Microscopic state |
| $\mathbf{z}_0$ | Initial microscopic state |
| $\rho(\mathbf{z})$ | Microscopic probability density |
| $\rho^{\mathrm{eq}}(\mathbf{z})$ | Equilibrium stationary microscopic probability density |
| $\overline{\rho}(\mathbf{z},t)$ | Microscopic *relevant* dynamics |
| $\delta\rho(\mathbf{z},t)$ | Microscopic *irrelevant* dynamics |
| $i\mathcal{L}$ | Liouville operator |
| $\mathcal{T}_t$ | Evolution operator |
| $\lambda(\mathbf{z}),\ \mu$ | Lagrange multipliers |
| $S[\rho(\mathbf{z})]$ | Gibbs-Jaynes Entropy functional |
| $\mathbf{X}(\mathbf{z})$ | Generic coarse-grained variable |
| $P(\mathbf{x})$ | Mesoscopic probability density |
| $P^{\mathrm{eq}}(\mathbf{x})$ | Equilibrium stationary mesoscopic probability density |
| $\mathcal{P}, \mathcal{P}^\dagger, \mathcal{Q}, \mathcal{Q}^\dagger$ | Projection operators |
| $\langle\cdots\rangle^{\mathbf{c}}$ | Conditional expectation |
| $v_\mu(\mathbf{z})$ | Drift |
| $K_{\mu\nu}(\mathbf{x},\mathbf{x}',\tau)$ | Memory kernel |


In partial fulfillment of the requeriments for the degree of Doctor of Science at the Universidad Nacional de Educación a Distancia, this dissertation was finished in Madrid, on May the Eighteenth, 2015.